1506
UNIVERSITÀ
DEGLI STUDI
DI URBINO
CARLO BO

DIPARTIMENTO DI SCIENZE PURE E APPLICATE
CORSO DI DOTTORATO DI RICERCA IN SCIENZE DI BASE E APPLICAZIONI
Curriculum SCIENZE CHIMICHE E SCIENZE FARMACEUTICHE
Ciclo XXX

SYNTHESIS, CHARACTERIZATION AND BIOLOGICAL EVALUATION OF NEW MATERIALS FOR PHARMACEUTICAL APPLICATIONS

Settore scientifico disciplinare: CHIM/09

RELATORE

Chiar.mo Prof. Gilberto Spadoni

Co-RELATORE

Prof. Luca Casettari

DOTTORANDO

Dott.ssa Laura Fagioli

Anno accademico 2016-2017

“Quando ti metterai in viaggio per Itaca
devi augurarti che la strada sia lunga,
fertile in avventure e in esperienze.
I Lestrigoni e i Ciclopi
o la furia di Nettuno non temere,
non sarà questo il genere di incontri
se il pensiero resta alto e un sentimento
fermo guida il tuo spirito e il tuo corpo…

…Devi augurarti che la strada sia lunga.
Che i mattini d’estate siano tanti
quando nei porti - finalmente e con che gioia -
toccherai terra tu per la prima volta:
negli empori fenici indugia e acquista
madreperle coralli ebano e ambre
tutta merce fina, anche profumi
penetranti d’ogni sorta; più profumi inebrianti che puoi,
va in molte città egizie
impara una quantità di cose dai dotti.

Sempre devi avere in mente Itaca -
raggiungerla sia il pensiero costante.
Soprattutto, non affrettare il viaggio;
fa che duri a lungo, per anni, e che da vecchio
metta piede sull’isola, tu, ricco
dei tesori accumulati per strada
senza aspettarti ricchezze da Itaca.
Itaca ti ha dato il bel viaggio,
senza di lei mai ti saresti messo
sulla strada: che cos’altro ti aspetti?

E se la trovi povera, non per questo Itaca ti avrà deluso.
Fatto ormai savio, con tutta la tua esperienza addosso
già tu avrai capito ciò che Itaca vuole significare.”

Itaca, Costantino Kavafis

Table of contents

Summary

The work described in this thesis was primarily focused on the synthesis, physicochemical characterization and biological evaluation of new materials for potential pharmaceutical applications. In this regard, biocompatible and biodegradable materials are strongly recommended to be used as pharmaceutical excipients, in order to limit related side effects, while increasing the potential benefits of the formulation.

The thesis consists of three parts, each of them related to a different research activity.
Part of the work has been dedicated to the study of innovative surfactants, such as sugar esters and biosurfactants produced by *Lactobacilli*, as attractive alternatives to the commonly employed surfactants. As regards sugar surfactants, a library of different lactose-based monoesters was designed, by employing lactose as polar head group, while varying the fatty acid chain length.
Surfactants were fully characterized for their physicochemical properties via nuclear magnetic resonance (NMR), high performance liquid chromatography-mass spectrometry (HPLC-MS), differential scanning calorimetry (DSC), dynamic light scattering (DLS) and surface tension measurements. Antimicrobial activity against different gram-positive and gram-negative bacteria was also investigated, while cytotoxicity and permeability enhancer ability were explored using Caco-2 and Calu-3 cell monolayers.
As part of the same project, biosurfactants produced by selected *Lactobacillus* spp. were also investigated for their surface properties, and anti-biofilm activity was finally evaluated against oral Streptococci.

In the second part, various polymeric materials were synthesized and used in the formulation of drug delivery systems (DDS) intended for the treatment of different diseases. More specifically, N-(2- benzoyloxypropyl) methacrylamide (HPMA-Bz)-based micelles were developed during my internship at the Department of Pharmaceutics of the Utrecht University, for targeted delivery to multiple myeloma cells, by exploiting a cyclic VLA-4 antagonist peptide.
Another work carried out in this field, has focused on the formulation and characterization of a Carbopol® hydrogel loaded with methoxy poly(ethylene glycol)-*block*-poly(lactide-*co*-glycolide) (mPEG-PLGA) nanoparticles for vaginal delivery with prophilaxis purposes.

The topic of the third project described in this thesis is the study of the rheological behaviour of selected polysaccharide dispersions, in function of various physiological parameters, such as concentration, pH and temperature. This rheological analysis provides really useful information, which can potentially help in selecting the polysaccharides with the desired characteristics to be applied in pharmaceutical or nutraceutical formulations.

SECTION ONE

BIOCOMPATIBLE SURFACTANTS FOR PHARMACEUTICAL APPLICATIONS

Chapter 1

General Introduction

1.1 General classification of surfactants

Surface-active agents, commonly referred to as surfactants, are amphiphilic molecules where two distinct regions coexist in the same structure, namely a polar head and a hydrophobic tail. Their peculiar structure is responsible for their ability to reduce surface and interfacial tension while promoting their miscibility or dispersion.

Surfactants have been widely employed in chemical, pharmaceutical, cosmetics and food industries and their production has hugely increased in the last decades. The list of available surfactants is updated annually and a useful technical reference to this regard is McCutcheon [1,2]. Surfactants are often classified based on their main use. Therefore, they are commonly labelled as emulsifiers, detergents, wetting agents, foaming agents, dispersants, detergents, stabilizers, etc. A more proper and scientifically recognized classification is based on the nature of the hydrophilic group. To this end, surfactants have been classified into four different groups: cationic, anionic, zwitterionic and non-ionic (Fig. 1).

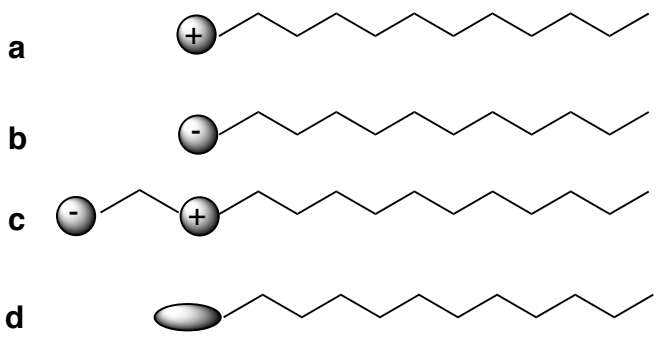

Fig. 1. Schematic representation of the different classes of surfactants: a) cationic surfactants; b) anionic surfactants: c) zwitterionic surfactants; d) non-ionic surfactants.

While cationic surfactants have a positive charge in the polar group, anionic surfactants have a negative charge; zwitterion molecules possess both positive and negative charge while non-ionic surfactants have no charges in their polar head. Some representative examples of the most widely employed surfactants and their traditional applications are reported below, in order to provide a general overview of the current status.

The most common employed cationic surfactants are the quaternary ammonium salts (e.g. benzalconium chloride) and long-chain amine salts, bringing one or more alkyl chains mostly derived from natural fatty acids [3,4]. They are mainly used for their recognized bactericidal

activity against a wide range of bacteria and due to this characteristic, they have been applied mostly in the treatment and cleaning of wounds.

Anionic surfactants have been intensively investigated for industrial applications and they are the most commonly employed surfactants, recommended for external use. They are characterized by a negatively charged polar head group, such as phosphate, sulphate, sulfonate and carboxylates [5]. As regard the latter, they are the earliest recognized surfactants to be employed in the classical soaps as detergents e.g. sodium stearate. Among the various sulphate surfactants, sodium dodecyl sulphate (SDS), also referred as sodium lauryl sulphate (SLS), is certainly the most commonly used. Anionic surfactants have been largely employed as detergents in soaps and shampoos but their use in personal care products is being progressively replaced versus more tolerated and less irritating agents.

Zwitterionic (amphoteric) surfactants contain both cationic and anionic groups in their polar head and based on the pH of the solution, they show different properties [6]. The most common zwitterionic surfactants are N-alkyl betaines and N-alkyl amino propionates. Natural products are also included in this class of surfactants, namely lecithins. Zwitterionic surfactants are recognized as safe and not irritating compounds due to their mild properties. For this reason, they have been included in many different cosmetic formulations and other personal care products.

The most interesting and actually employed class of surfactants comprises non-ionic surfactants, characterized by hydrophilic neutral groups as polar head. Non-ionic surfactants are widely employed in pharmaceutical, cosmetic and food industry as emulsifiers, detergents and wetting agents [7]. They are classified as polyol esters and polyoxyethylene derivatives, based on the hydrophilic group. Multihydroxy compounds, also known as polyol esters, include glycerol and sorbitan derivatives (Span). The hydrophilicity of ethoxylated surfactants is given by the presence of polyethylene oxide chains, obtained from the polycondensation of ethylene oxide. This class comprises alcohol ethoxylates, fatty acid ethoxylates, sorbitan esters ethoxylates, also known as Tween, and fatty amine ethoxylates. Block copolymers are also classified as non-ionic surfactants, with Poloxamers being the main representative. They are synthetic block copolymers made of two hydrophilic poly(oxyethylene) blocks and a hydrophobic poly(oxypropylene) portion in between.

Sugar based surfactants have emerged in the last decades as a promising alternative to the commonly used surfactants, being recognized as biocompatible and non-toxic compounds. They are classified as non-ionic surfactants where the hydrophilic group is a carbohydrate and

the hydrocarbon tails are derived from fatty acids or alcohols. This class will be extensively discussed in a dedicated section, focusing on the different derivatives and the potential applications.

1.2 Pharmaceutical applications of conventional surfactants

While there are several commercial surfactants available on the market, a relatively small percentage has been approved for pharmaceutical use, and have been included in the various pharmacopoeias (Ph. Eur., USP, BP). In fact, most of the commercially available surfactants are synthetic, mainly derived from petrochemicals with a consequent poor biocompatibility and high irritancy potential. It is also noteworthy that industrial surfactants exist as a mixture of molecules that differ for the length of the hydrophobic chain and the polar head units. This translates in non-pure compounds, where batch to batch properties variations are expected [8], thus resulting in a lack of a clear physicochemical characterization.

Surfactants employed as pharmaceutical excipients find application in a wide range of formulations [9]. They are commonly used as emulsifiers to stabilize emulsion systems intended for skin application and as solubilizers and stabilizers of different drugs in liquid formulations. Moreover, they are able to control flow properties of granulates in solid dosage forms as well as to influence textural properties and physicochemical stability of semisolid formulations [10]. Surfactants have also been widely employed as disintegrating agents and their permeation enhancers activity has been demonstrated for many drugs [11,12]. Surfactants play also a key role in the development of both conventional and innovative colloidal drug delivery systems such as micelles, nanoemulsions, vesicles and liquid crystal dispersions [9,13].

Among all the surfactants available for pharmaceutical applications, anionic sodium lauryl sulphate (SLS), non-ionic polyoxyethylated glycol monoethers, sorbitan esters and their ethoxylated derivatives (Span and Tween), have been the most commonly employed so far. However, their safety profile has been questioned as their irritation potential emerged as a limiting factor to their application.

1.3 Innovative natural surfactants: a general overview

The increasing demand for environmentally friendly and non-toxic compounds moved the attention of both industry and academia toward the use of more “natural surfactants”. Taken strictly, the definition is intended to include all that surface-active compounds derived from

natural raw sources, including both plants and animals. In line with this definition, no organic synthesis has to be involved and the surfactant has to be obtained by a separation technique. Lecithin, derived from eggs and soybean, is a representative example of a natural surfactant. Not many natural surfactants are available that fulfil the traditional requirements, mainly because of the high costs associated with the separation process and the relatively low yield.
For this reason the definition "natural surfactants" has been employed in a more general sense and includes all that surfactants chemically synthetized from natural starting material [14].
There are many advantages directly related with the use of natural compounds. First of all, these surfactants are expected to be less toxic and allergenic, resulting in a higher biocompatibility. Moreover, being derived from natural raw materials, they fully satisfy the growing need for environmentally friendly and biodegradable compounds. These characteristics, along with the cost-effectiveness and renewability, contributed to define these surfactants as promising candidates for future applications, leading to intensive scientific investigations. Natural surfactants can be classified into three main categories, according to the more general and accepted definition: biosurfactants produced by bacteria and yeast, amphipiles with a natural polar head (e.g. sugars and amino acids) and amphiphiles with a natural hydrocarbon chain [14]. Regarding the hydrophobic group, fatty acids and fatty alcohol as well as aromatic groups have been largely employed, while the most interesting hydrophilic moiety are amino acids and carbohydrates [15,16].

1.4 Sugar-based surfactants

In recent years increasing attention has been dedicated to sugar-based surfactants, recognized as promising candidates for a wide range of applications due to their attractive physicochemical properties. Sugar-based surfactants are non-ionic surface-active agents characterized by a carbohydrate as polar head group, linked to different alkyl or acyl chains [17]. Two main categories, namely alkyl glucosides (AGs) and sugar esters (SEs), have been particularly investigated for pharmaceutical, cosmetic and food applications [14]. Structures of these two main groups are schematically reported in Fig. 2. Sugar esters are synthetized by the esterification reaction of the sugar with the fatty acid while alkylglucosides are based on an ether bond not readily hydrolyzed in biological systems.

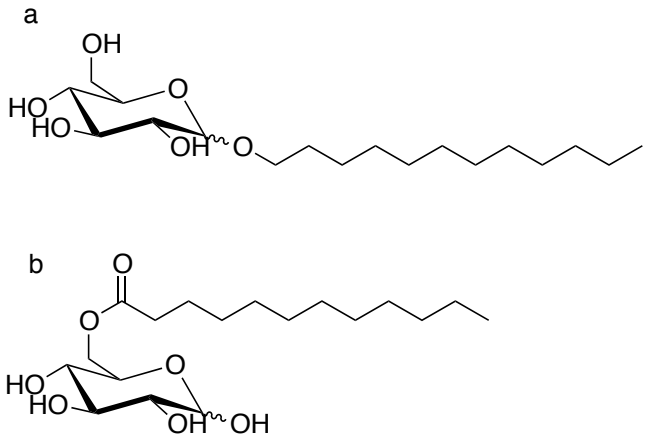

Fig. 2. Example of sugar-based surfactants: a) alkyl glucoside and b) sugar esters.

Physicochemical and biological properties of these compounds can be tailored by varying the polarity of the hydrophilic group and the length and degree of saturation of the hydrocarbon chain. In this regard, mono, di and tri-saccharides (e.g. glucose, fructose, sucrose, lactose, maltose, maltotriose, etc.) can be employed as polar heads, while saturated and unsaturated fatty acids and alcohols with different chain lengths (commonly C_8 - C_{18}) constitute the hydrophobic portion. Due to the high amount of hydroxyl groups available on the carbohydrate surface, surfactants with different degree of substitution can be obtained from the synthesis, often resulting in a mixture of non-pure products with different properties.

The following sections will review the class of sugar esters, mainly focusing on their physicochemical characterization and potential applications. A general overview of the different methods used for their production will also be given describing different the approaches employed so far (chemical and enzymatic synthesis).

1.5 Production of Sugar Esters: chemical versus enzymatic synthesis

Sugar esters can be synthetized by an esterification reaction between sugars and fatty acids. High substitution esters (HSEs), hexa, hepta and octa, and Low substitution esters (LSEs), mono, di and triesters can be obtained based on the degree of esterification.

A consistent number of research papers on sugar esters were published from the mid-50s, and culminated in the commercialization of LSE esters in the 60s. Dimethyl formamide (DMF) was initially chosen as solvent for the reaction [18]. Dai-Nippon Sugar Manufacturing Co., Ltd., first employed dimethyl formamide (DMF) to produce sucrose fatty acids esters as food additives in the late 60s [19] [20]. But this process was not approved in United States due to

safety concerns (odor and toxic materials present in the product). An alternative and safer process for the synthesis of sucrose esters, known as Nebraska-Snell process, was proposed from Osipow and Rosenblatt in 1967 [21]. Many studies have been focused in the optimization of the process to avoid the use of toxic solvents. Feuge et al. developed a solvent-free interesterification process using high temperatures but the drawback of this method was the degradation of the sugar at high temperatures [22].

In recent years research has been focused on the study of alternative synthetic routes that can avoid the low specificity and side reactions often associated with the chemical synthesis [23–25]. The use of enzymes as biocatalysts has emerged as a promising strategy to satisfy the growing demand for environmentally friendly processes. Enzymatic synthesis presents many advantages compared to the chemical one. Higher specificity and regioselectivity under milder conditions can be easily obtained using enzymes, thus resulting in products with the desired physicochemical properties. Moreover, due to the steric hindrance of the enzymes, only low substituted sugar esters are obtained, in particular pure sugar monoesters. Lipases and serine proteases are commonly used for the synthesis of sugar fatty acid esters [26,27]. Important factors that have to be considered when using the enzymatic synthesis are the stability of the enzyme and the solubility of the sugar substrate in the selected organic solvent. While better sugar solubility is obtained in water miscible organic solvents, including dimethylsulfoxide (DMSO) and dimethylformamide (DMF), many enzymes are denatured in the presence of polar solvents [28]. Immobilization and modification technologies have been widely exploited to stabilize enzymes avoiding the side effects of water. Ferrer et al. evaluated the effect of immobilization of *Thermomyces lanuginosus* lipase on the synthesis of 6-O-lauroyl sucrose [29]. Novozyme 435 (a lipase from *C. antartica* immobilized on a macropourus resin) was also employed as biocatalyst [30]. Enzymes from different sources present a high selectivity for fatty acids based on the chain length [23,31].

As regard the molar ratio, the conversion rate of lipase-mediated esterification reactions can be improved by using a molar excess of fatty acid when short chain fatty acids are involved. Conversely, if the reaction involves longer fatty acids, a lower molar ratio is required [32].

Ionic liquids (ILs) have recently emerged as a valid alternative to organic solvents in lipase mediated synthesis of sugar esters but the high costs have limited their use. Their favourable physicochemical properties, including the ability to dissolve both polar and non-polar molecules have been largely exploited for the synthesis of sugar esters [33–35].

1.6 Properties of sugar fatty acid esters

1.6.1 Physicochemical properties

Sugar esters have been extensively investigated for their special physicochemical properties. Sugar esters can exist as solids, waxy materials or liquids depending on the composition [17]. By varying the nature of the carbohydrate moiety, the length of the hydrocarbon chain and the degree of substitution, sugar esters with different surface-active properties can be obtained.

The HLB value is calculated based on the hydrophilic and lipophilic moieties of a surfactant molecule and it is useful to choose the proper surfactants for oil and water emulsions. Long chain fatty acid and high degree of substitution, contribute to a low HLB value. HLB scale ranges from 0 to 20. Surfactants with low HLB values are used in W/O emulsions while surfactants with higher HLB values are commonly employed in O/W emulsions [36].

Low substitution esters are able to reduce the surface tension of water. Neta et al. showed that fructose esters, synthetized using oleic acid and fructose, significantly reduce the surface tension to 35.8 mN/m^{-1} [37].

Most of the studies on the functional properties of sugar esters have been done using non-pure compounds which consist in a mixture of isomers, while pure monoesters have been less studied [38]. Ferrer et al. enzymatically synthetized a series of acyl sugar esters using sucrose, maltose, leucrose, maltotriose and β-D-dodecylmaltoside as carbohydrate moieties and C_8-C_{12} fatty acids. Either the influence of the hydrocarbon chain length, the sugar moiety and the degree of esterification were investigated for their ability to influence the surface properties. Both surface tension in water, critical micelle concentration and interfacial tension between water and xylene were evaluated. CMC was influenced by both the carbohydrate moiety and the hydrocarbon chain length. More specifically, medium to long chain fatty acid derivatives showed the lowest CMC. Moreover, di and trisaccharide-based surfactants displayed better surface properties compared to the respective monosaccharide esters [39]. Matsumura et al. studied surface properties of n-Alkyl α-and β-glucopyranosides, α-D-mannopyranosides and β-D-galactopyranosides with C_8-C_{12} alkyl chains. Alkyl glycosides containing C_8 to C_{12} carbon chains demonstrated surface activities. D-Glucoside, D-mannoside and D-galactoside with the same alkyl chain showed similar surface tension properties at lowering the CMC (γCMC) [40]. A similar relationship between chemical structure and surface properties was reported by Zhang et al. which studied the surface properties of a series of enzymatically prepared sugar medium-chain fatty acid monoesters [41]. Sugar monoester containing a C_8 to C_{12} carbon chain showed good surface activity and CMC values. However, the CMC and

surface tension of α-D-glucose monolaurate (GL) and methyl α-D-glucopyranoside monolaurate (MGL) could not be measured because of their low solubility in water, as previously reported by Matsumura et al. [40]. Ducret et al. summarized the CMC values of several sugar monoesters showing how a shorter alkyl chain gave a higher CMC value [42]. Moreover, oleate esters of glucose, fructose and sorbitol demonstrated a similar behaviour in reducing surface and interfacial tension. Di and trisaccharides derivatives are more soluble in water than monosaccharides-based fatty acid esters as a consequence of the increased hydrophilicity of the sugar head group.

This general overview on the surface-active properties of sugar esters clearly show the key role of the fatty acid chain length and the nature of the sugar head in defining the characteristics of the sugar-based surfactants.

Sugar esters have also been investigated for their thermal properties to evaluate their applicability in various technological processes. Carbohydrates present high melting points, while sugar esters have been reported to have lower melting points (40-79°C). Szűts et al. studied the thermal behaviour of various commercially available sucrose esters that consisted in a mixture of products with different degree of esterification. Sugar esters with high HLB values showed an amorphous behaviour with a glass transition temperature (Tg) instead a melting point upon heating. On the contrary, sugar esters with lower HLB melted [43].

The study of the thermal behaviour of sugar esters is really important to evaluate their potential use as excipients for different pharmaceutical applications, such as hot melt technology, and to predict their stability over time.

1.6.2 Biological properties of sugar fatty acid esters

Sugar fatty acid esters have been intensively investigated for their biological properties and their antimicrobial activity has been demonstrated against a wide range of microorganisms. In this regard, sucrose esters have found large application as preservative against food spoilage in canned beverages in Japan, and the US Food and Drug Administration (FDA) recently approved sucrose fatty acid esters as additives for certain processed food [44].

Furukawa et al. investigated the effect of food additives on the biofilm formation of food-borne pathogenic bacteria. Sucrose monomyristate and sucrose monopalmitate inhibited biofilm formation by *Staphylococcus aureus* and *Escherichia coli* at low concentration but bacterial growth was not affected at this concentration. The activity of sugar esters correlated with the increase of the alkyl chain length [45]. Zhao et al. studied the antibacterial activity of

various sugar esters against five common food-related bacteria. Glucose, fructose, sucrose and maltose were employed as carbohydrate moieties while the fatty acid chain length was chosen between C_{10} and C_{18}. Sucrose monocaprate showed the highest antimicrobial activity against the tested bacteria, especially Gram-positive bacteria. Results from SEM observations suggested an interaction of the surfactant with the cell membrane permeability [46].

Most of the studies conducted on the antimicrobial activity of sugar esters employed commercial derivatives [47,48]. The main disadvantage related with their use is that they are complex mixtures of mono, di and tri-esters containing different regioisomers. Ferrer et al. investigated the antimicrobial activity of pure sugar esters evaluating the influence of sugar type (glucose, sucrose and maltose), length of fatty acid (lauric and palmitic) and degree of substitution (mono and di-esters) on the final properties. Sucrose diesters and glucose monoesters showed low solubility in water, as a consequence of their higher hydrophobicity. 6-*O*-lauroylsucrose and 6'-*O*-lauroylmaltose inhibited the growth of *Bacillus* sp. and *E.coli* [23].

While the antibacterial activity of sucrose esters with lauric acid has been extensively studied, and efficacy against both Gram-positive and Gram-negative bacteria has been proved, different sugar esters have received less attention [49,50]. Fructose esters also showed antimicrobial activity and were demonstrated to be able to suppress the cell growth of *Streptococcus mutans*, responsible for the dental caries. Among the various sugar esters synthetized, galactose and fructose laurate were the most effective in inhibiting cell growth. Moreover the antimicrobial activity resulted to be affected by the configuration of hydroxyl groups [51].

Nobmann et al. studied the antimicrobial properties of a series of mono-substituted sugar esters and ethers against gram-positive and gram-negative bacteria focusing on *Listeria monocytogenes*. Sugar esters derivatives were generally more active against Gram positive bacteria than Gram negative. The study of both ethers and esters derivatives of the same sugar, in tandem with alpha and beta configuration of the sugar, showed that both the carbohydrate moiety and the nature of the bond affected the final activity. Ether bonds are not hydrolysed in biological systems as the ester derivatives. The authors found that not only the presence of free hydrophilic group in the carbohydrate moieties were important for the antimicrobial activity, but also the nature of the hydrophilic group per se. Moreover, it was found that sugar esters based on a monosaccharide unit showed a reduced activity, probably due to the poor water solubility [52].

Zhang et al. studied the antimicrobial activity of a series of sugar fatty acid monoesters containing different types of sugars (α-D-glucose, methyl α –D-glucopyranoside, sucrose, and raffinose) and C_8-C_{12} alkyl chains. The tested sugar monoesters were demonstrated to be more effective against Gram-positive than Gram-negative bacteria and yeast while a correlation between the structure of sugar esters and their biological properties was shown. Methyl glucopyranoside monoesters showed a higher antimicrobial activity compared to the other sugar monoesters while raffinose monoesters were not active against the tested colonies, probably because of the large hydrophilic group. Carbon chain length also influenced the final properties [41].

Results from antimicrobial studies suggest a more pronounced activity of sugar esters against Gram-positive than Gram-negative bacteria. Conley and Kabara determined the minimum inhibitory concentration using a broth dilution method of a series of sucrose fatty acid esters against different microorganisms. Their results showed that Gram-positive bacteria were inhibited while Gram-negative bacteria were not affected. Sucrose esters were more active than the respective free fatty acid, except for laurate [53]. The mechanism proposed is based on the interaction with the cell membrane of bacteria, resulting in autolysis. The lytic action is attributed to the stimulation of autolytic enzymes rather than to a direct solubilisation effect on cell membrane of bacteria [54,55].

Wagh et al. studied the antimicrobial activities of sucrose monolaurate and lactose monolaurate (LML) against Gram-positive and Gram-negative bacteria. Gram-positive bacteria were more susceptible than Gram-negative bacteria to both esters [56].

1.7 Surfactants as permeation enhancers

Non-invasive delivery of a broad range of protein, peptide and non-peptide drugs that can currently only be administered by injection, remain a big challenge in pharmaceutical research. The main reason has to be found in the difficulty for therapeutic macromolecules to cross the mucosal barriers. One option to improve the absorption of these molecules is the use of permeability enhancers. Several molecules have been studied so far for this purpose, including bile salts, chitosan, medium chain fatty acids (MCFAs) and medium chain fatty acids-based systems, such as sodium caprate, sodium caprylate and N-[8-(2-hydroxybenzoyl)amino]caprylate (SNAC) [57–60]. Their mechanism has been widely investigated and they have been recognised to act as absorption enhancers modulating both the transcellular and paracellular routes. While the transcellular route has been intensively

investigated and exploited, the paracellular route was not considered until the sixties, when for the first time it was reported that molecules of different size and hydrophilicity can cross the epithelium though the paracellular route [61]. Since then, many efforts have been focused to deeply understand the mechanism involved in the paracellular transport and tight junctions modulation.

Surfactants commonly employed in clinical have advantageous properties as absorption enhancers but their use has been often associated with unacceptable toxicity [62–64]. For this reason, there is a significant need for novel absorption enhancers agents with a safer profile, to be employed for transmucosal delivery of biotherapeutics.

Non-ionic surfactants have been intensively investigated for their permeability enhancer properties being recognized as less toxic and more tolerated compared to ionic surfactants [65].

Many drugs have been exploited for this purpose resulting in an increased absorption when formulated with surfactants [66–69]. Different mechanisms have been proposed to explain the increased permeability related to the use surfactants. A fundamental parameter to consider is the surfactant concentration, as it influences the surfactant colloidal state [70,71]. Moreover, structural factors such as chain length, degree of esterification, unsaturation, nature of the substituents can affect the ability of the surfactant to act as a permeation enhancer [72]. According to Dimitrijevic et al. the ideal chain length should be chosen in the range of C_8 to C_{12} [73]. Park et al. demonstrated that lauryl polyoxyethylene ether (C12) was an effective enhancer for ibuprofen, followed by the oleyl ether [74].

Sugar-based surfactants, including alkyl polyglucosides and sugar esters, have been recently investigated for their enhancer properties, toxicity profile and mode of action on different *in vitro* and *in vivo* models.

Alkylglucosides have received a great attention as permeation enhancers and various peptides and proteins have been formulated with these agents for transmucosal delivery [75,76]. Alkylmaltosides have been clinically advanced as transmucosal absorption enhancement agents for nasal delivery of peptide drugs (Intravail®) [77]. Due to their mild, non-irritating and nondenaturing properties, deeply investigated in many research papers, they have been recognized as GRAS (generally regarded as safe) for various applications [78–81]. Uchiyama et al. studied the enhanced permeability of insulin promoted by n-Lauryl-*β*-D-maltopyranoside in rat intestinal membranes. Results suggested a concentrations dependent mechanism with the paracellular pathway primarily involved at low concentration and the

transcellular route implicated at higher concentrations. TEER experiments showed that the transport of insulin increased when n-lauryl-*β*-D-maltopyranoside was co-administered [82].
Sugar esters have also been extensively applied as permeation enhancers for transmucosal absorption with sucrose esters resulting the most widely investigated [17,83–85].
In this regard Kis et al. studied the potential application of sucrose esters as oral permeation enhancers. Three different sucrose esters, namely sucrose laurate (C12), sucrose myristate (C14) and sucrose palmitate (C16) were tested for their toxicity and paracellular permeability on Caco-2 monolayers [86]. Their results showed increased drug permeability through a paracellular and transcellular mechanism without inhibiting P-gp. Similarly, Szűts et al. demonstrated that sucrose laurate was able to reduce transepithelial electrical resistence (TEER) and increased the paracellular transport of the marker molecules in Caco-2 cell monolayers [87].
While many studies have been carried out using *in vitro* models, relatively few *in vivo* studies have been reported and further investigations are needed to confirm the *in vitro* results.
An important aspect that has to be considered when studying absorption enhancers is the potential irritation and epithelial damage they can irreversibly cause when administered and the co-absorption of pathogenic bystander molecules and toxins. Moreover, it has to be carefully assessed if the membrane can sustain the repair mechanism, which should repeatedly undergo in case of a chronic therapy. For all these reasons, a careful assessment of the safety profile is required in order to limit the toxicity. Some of these permeation enhancers (e.g. sodium *N*-[8-(2-hydroxybenzoyl)amino] caprylate (SNAC), sodium caprate and caprylate) are in advanced clinical trials for selected oral peptide formulations and will be soon approved. Post marketing evaluation of the toxicological profile following a chronic exposure will be of fundamental importance in this context [88].

1.8 Aim of the present study

Natural surfactants have been intensively investigated in the last decades due to their attractive properties. They have been recognized as biodegradable and biocompatible compounds to be used for a wide range of applications, both in pharmaceutical, cosmetic and food industries. These characteristics, along with the cost-effectiveness and renewability of the raw materials, fully satisfy the growing demand for non-toxic and environmentally friendly compounds. Among all the natural surfactants, sugar-based surfactants have recently emerged as a valid alternative to the commonly employed non-ionic surfactants [14]. Alkylglucosides are obtained from the reaction of fatty alcohols with sugars and the resulting ether bonds are not hydrolysed in biological systems; on the other hand, sugar fatty acid esters are prepared from sugars and fatty acids through an esterification reaction. Despite the conspicuous literature available on the potential of sugar-based surfactants for pharmaceutical applications, limited studies focused on the investigation of lactose-based surfactants [89].

The work described in this thesis was primarily focused on the synthesis, physicochemical characterization and biological evaluation of a series of lactose fatty acid monoesters. A library of lactose-based surfactants was designed with the main aim of evaluating the influence of the hydrocarbon chain length on the final properties of the lactose ester derivatives. To this end, lactose was selected as polar head group due to its abundant availability and relatively low costs while two series of fatty acids with different chain lengths and degree of saturation were selected for the synthesis. Moreover, an enzymatic biocatalysis was explored to obtain relatively pure monoesters. This is an important aspect that deserve consideration. In fact, most of the sugar esters, both studied in literature and commercially available, are complex mixtures of mono, di and tri-esters containing different regioisomers, thus hindering a full comprehension of the relationship between the molecular structure and the physicochemical properties.

The obtained lactose-based surfactants were then characterized for their physicochemical properties via NMR, HPLC-MS, DSC, DLS and surface tension measurements. Antimicrobial activity against different gram-positive and gram-negative bacteria was also investigated while cytotoxicity and permeability enhancer ability were explored using Caco-2 and Calu-3 cell monolayers.

Chapter 2 focuses on the study of two innovative lactose monoesters derivatives based on unsaturated fatty acids. Palmitoleic acid (C16:1 ω7) and nervonic acid (C24:1 ω 9) were selected as long-chain fatty acids and reacted with lactose using a specific lipase as catalyst

(Lipozyme®, immobilized from *Mucormiehei*). Lactose palmitoleate and nervonate were studied for their physicochemical and biological properties showing promising results for future applications both as preservative and intestinal permeation enhancers.

Based on these encouraging results, oleic acid was then employed in **chapter 3** for the synthesis of lactose oleate. Oleic acid was selected as unsaturated fatty acid due to its intermediate acyl chain length (C18:1 ω 9) which lies in between the previously investigated palmitoleic and nervonic acids. Moreover, oleic acid is widely recognized as an ideal absorption enhancing agent. Lactose oleate was fully characterized for its physicochemical properties and evaluated for its toxicological profile. Further experiments were performed to evaluate its applicability as absorption enhancing agent (Transepithelial Electrical Resistance and permeability studies by employing fluorescent-labelled dextran 4kDa) and preservative.

Chapter 4 reports the synthesis, physicochemical characterization and toxicological evaluation of a library of saturated fatty acid lactose derivatives. To this end, decanoic (C10), lauric (C12), myristic (C14) and palmitic (C16) acids have been employed as medium and long chain fatty acids in order to investigate the correlation between the hydrocarbon chain length and the physicochemical and biological properties of the resulting lactose esters. The cytotoxicity profile was assessed by MTT and LDH assay on Calu-3 cell lines as model for the airway epithelium. Moreover, TEER experiments were also performed to evaluate their absorption enhancing properties.

In conclusion, the group of lactose-based surfactants deeply investigated in this work provides the class of sugar esters with two innovative products (lactose palmitoleate and lactose nervonate) and new information about physicochemical and biological properties of lactose ester derivatives. These information are really important since can guide in the selection of potential candidates for future applications.

Another important class of natural surfactants studied in the thesis are biosurfactants, surface-active agents produced by yeasts and bacteria. **Chapter 5** is focused on the characterization in terms of surface tension of biosurfactants produced by lactic acid bacteria. The crude excreted biosurfactants, consisting in complex biological mixtures, have been dialyzed using 1kDa and 6kDa molecular weight cut-off membranes before surface tension measurements.

References

[1] McCutcheon, Detergents and Emulsifiers, Allied Publishing Co, New Jersey, n.d.

[2] M.R. Porter, Handbook of surfactants, Blackie Academic & Professional, 1994.

[3] E. Jungerman, Cationic Surfactants, Marcel Dekker, New York, 1970.

[4] N. Rubingh, P.M. Holland, eds., Cationic Surfactants – Physical Chemistry, Marcel Dekker, New York, 1991.

[5] W.M. Linfield, W.M. Linfield, eds., Anionic Surfactants, Marcel Dekker, New York, 1967.

[6] B.R. Buestein, C. L. Hiliton, Amphoteric Surfactants, Marcel Dekker, New York, 1982.

[7] M. J. Schick, ed., Nonionic Surfactants, Marcel Dekker, New York, 1966.

[8] T.F. Tadros, Applied surfactants : principles and applications, Wiley-VCH, 2005.

[9] T.F. Tadros, Surfactants in Pharmaceutical Formulations, in: Appl. Surfactants, Wiley-VCH Verlag GmbH & Co. KGaA, Weinheim, FRG, 2005: pp. 433–501. doi:10.1002/3527604812.ch13.

[10] W. Musiał, E. Szewczyk, K. Karłowicz-Bodalska, S. Han, Surface Active Agents as Excipients in Semi-Solid Dosage Forms, Rom. Biotechnol. Lett. 20 (2015).

[11] J.O. Morales, J.I. Peters, R.O. Williams, Surfactants: their critical role in enhancing drug delivery to the lungs., Ther. Deliv. 2 (2011) 623–41.

[12] I. Som, K. Bhatia, M. Yasir, Status of surfactants as penetration enhancers in transdermal drug delivery., J. Pharm. Bioallied Sci. 4 (2012) 2–9. doi:10.4103/0975-7406.92724.

[13] G. Hema Sagar, M.A. Arunagirinathan, J.R. Bellare, Self-assembled surfactant nano-structures important in drug delivery: A review, Indian J. Exp. Biol. 45 (2007) 133–159.

[14] K. Holmberg, Natural surfactants, Curr. Opin. Colloid Interface Sci. 6 (2001) 148–159. doi:10.1016/S1359-0294(01)00074-7.

[15] M. Kjellin, I. Johansson, Surfactants from renewable resources, Wiley, 2010.

[16] I. Johansson, M. Svensson, Surfactants based on fatty acids and other natural hydrophobes, Curr. Opin. Colloid Interface Sci. 6 (2001) 178–188. doi:10.1016/S1359-0294(01)00076-0.

[17] A. Szuts, P. Szabó-Révész, Sucrose esters as natural surfactants in drug delivery systems - A mini-review, Int. J. Pharm. 433 (2012) 1–9. doi:10.1016/j.ijpharm.2012.04.076.

[18] L. Osipow, F.D. Snell, W.C. York, A. Finchler, Methods of Preparation Fatty Acid Esters of Sucrose, Ind. Eng. Chem. 48 (1956) 1459–1462. doi:10.1021/ie51400a026.

[19] Ryoto. Ryoto Sugar Ester Technical Information; Nonionic Surfactant/Sucrose Fatty Acid Ester/ Food Additive. Mitsubishi-Kasei Food Corporation: Tokyo, Japan, (1987) 8.

[20] T. Yamada, N. Kawase, K. Ogimoto, Sucrose Esters of Long-Chain Fatty Acids, J. Japan Oil Chem. Soc. 29 (1980) 543–553. doi:10.5650/jos1956.29.543.

[21] L.I. Osipow, W. Rosenblatt, Micro-emulsion process for the preparation of sucrose esters, J. Am. Oil Chem. Soc. 44 (1967) 307–309. doi:10.1007/BF02635621.

[22] R.O. Feuge, H.J. Zeringue, T.J. Weiss, M. Brown, Preparation of sucrose esters by interesterification, J. Am. Oil Chem. Soc. 47 (1970) 56–60. doi:10.1007/BF02541458.

[23] M. Ferrer, J. Soliveri, F.J. Plou, N. López-Cortés, D. Reyes-Duarte, M. Christensen, J.L. Copa-Patiño, A. Ballesteros, Synthesis of sugar esters in solvent mixtures by lipases from Thermomyces lanuginosus and Candida antarctica B, and their antimicrobial properties, Enzyme Microb. Technol. 36 (2005) 391–398. doi:10.1016/j.enzmictec.2004.02.009.

[24] N.R. Pedersen, R. Wimmer, R. Matthiesen, L.H. Pedersen, A. Gessesse, Synthesis of sucrose laurate using a new alkaline protease, Tetrahedron Asymmetry. 14 (2003) 667–673. doi:10.1016/S0957-4166(03)00086-7.

[25] F.J. Plou, M.A. Cruces, M. Ferrer, G. Fuentes, E. Pastor, M. Bernabé, M. Christensen, F. Comelles, J.L. Parra, A. Ballesteros, Enzymatic acylation of di- and trisaccharides with fatty acids: Choosing the appropriate enzyme, support and solvent, in: J. Biotechnol., Elsevier, 2002: pp. 55–66. doi:10.1016/S0168-1656(02)00037-8.

[26] L. Brady, A.M. Brzozowski, Z.S. Derewenda, E. Dodson, G. Dodson, S. Tolley, J.P. Turkenburg, L. Christiansen, B. Huge-Jensen, L. Norskov, L. Thim, U. Menge, A serine protease triad forms the catalytic centre of a triacylglycerol lipase, Nature. 343 (1990) 767–770. doi:10.1038/343767a0.

[27] M.K. Walsh, R.A. Bombyk, A. Wagh, A. Bingham, L.M. Berreau, Synthesis of lactose monolaurate as influenced by various lipases and solvents, J. Mol. Catal. B Enzym. 60 (2009) 171–177. doi:10.1016/j.molcatb.2009.05.003.

[28] N.R. Pedersen, R. Wimmer, J. Emmersen, P. Degn, L.H. Pedersen, Effect of fatty acid chain length on initial reaction rates and regioselectivity of lipase-catalysed esterification of disaccharides, Carbohydr. Res. 337 (2002) 1179–1184. doi:10.1016/S0008-6215(02)00112-X.

[29] M. Ferrer, F.J. Plou, G. Fuentes, M.A. Cruces, L. Andersen, O. Kirk, M. Christensen, A. Ballesteros, Effect of the Immobilization Method of Lipase from Thermomyces lanuginosus on Sucrose Acylation, Biocatal. Biotransformation. 20 (2002) 63–71. doi:10.1080/10242420210153.

[30] P. Degn, W. Zimmermann, Optimization of carbohydrate fatty acid ester synthesis in organic media by a lipase fromCandida antarctica, Biotechnol. Bioeng. 74 (2001) 483–491. doi:10.1002/bit.1139.

[31] R. Kumar, J. Modak, G. Madras, Effect of the chain length of the acid on the enzymatic synthesis of flavors in supercritical carbon dioxide, Biochem. Eng. J. 23 (2005) 199–202. doi:10.1016/j.bej.2005.01.007.

[32] A.M. Gumel, M.S.M. Annuar, T. Heidelberg, Y. Chisti, Lipase mediated synthesis of sugar fatty acid esters, Process Biochem. 46 (2011) 2079–2090. doi:10.1016/j.procbio.2011.07.021.

[33] Z. Findrik, G. Megyeri, L. Gubicza, K. Bélafi-Bakó, N. Nemestóthy, M. Sudar, Lipase catalyzed synthesis of glucose palmitate in ionic liquid, J. Clean. Prod. 112 (2016) 1106–1111. doi:10.1016/j.jclepro.2015.07.098.

[34] F. Ganske, U.T. Bornscheuer, Lipase-catalyzed glucose fatty acid ester synthesis in ionic liquids, Org. Lett. 7 (2005) 3097–3098. doi:10.1021/ol0511169.

[35] S.H. Lee, S.H. Ha, N.M. Hiep, W.J. Chang, Y.M. Koo, Lipase-catalyzed synthesis of glucose fatty acid ester using ionic liquids mixtures, J. Biotechnol. 133 (2008) 486–489. doi:10.1016/j.jbiotec.2007.11.001.

[36] W.C. Griffin, Classification of Surface-active Agents by "HLB, J. Soc. Cosm., Chem. 1 (1949) 311–326.

[37] N.S. Neta, A.M. Peres, J.A. Teixeira, L.R. Rodrigues, Maximization of fructose esters synthesis by response surface methodology, N. Biotechnol. 28 (2011) 349–355. doi:10.1016/j.nbt.2011.02.007.

[38] D.B. Sarney, M.J. Barnard, D.A. MacManus, E.N. Vulfson, Application of lipases to the regioselective synthesis of sucrose fatty acid monoesters, J. Am. Oil Chem. Soc. 73 (1996) 1481–1487. doi:10.1007/BF02523514.

[39] M. Ferrer, F. Comelles, F.J. Plou, M.A. Cruces, Gloria Fuentes, J.L. Parra, A. Ballesteros, Comparative Surface Activities of Di- and Trisaccharide Fatty Acid Esters, (2002). doi:10.1021/LA010727G.

[40] S. Matsumura, K. Imai, S. Yoshikawa, K. Kawada, T. Uchibor, Surface activities, biodegradability and antimicrobial properties of n-alkyl glucosides, mannosides and galactosides, J. Am. Oil Chem. Soc. 67 (1990) 996–1001. doi:10.1007/BF02541865.

[41] X. Zhang, W. Wei, X. Cao, F. Feng, Characterization of enzymatically prepared sugar medium-chain fatty acid monoesters, J. Sci. Food Agric. 95 (2015) 1631–1637. doi:10.1002/jsfa.6863.

[42] A. Ducret, A. Giroux, M. Trani, R. Lortie, Characterization of enzymatically prepared biosurfactants, J. Am. Oil Chem. Soc. 73 (1996) 109–113. doi:10.1007/BF02523456.

[43] A. Szuts, E. Pallagi, G. Regdon, Z. Aigner, P. Szabó-Révész, Study of thermal behaviour of sugar esters, Int. J. Pharm. 336 (2007) 199–207. doi:10.1016/j.ijpharm.2006.11.053.

[44] N. Suwa, H. Kubota, K. Takahashi, H. Machida, Studies on quality preservation of sterilized retort drinks during storage, 1: Effects of sucrose fatty acid esters on spoilage of canned coffee caused by thermophilic spore forming bacteria, J. Japanese Soc. Food Sci. Technol. (1986).

[45] S. Furukawa, Y. Akiyoshi, G.A. O'Toole, H. Ogihara, Y. Morinaga, Sugar fatty acid esters inhibit biofilm formation by food-borne pathogenic bacteria, Int. J. Food Microbiol. 138 (2010) 176–180. doi:10.1016/j.ijfoodmicro.2009.12.026.

[46] L. Zhao, H. Zhang, T. Hao, S. Li, In vitro antibacterial activities and mechanism of sugar fatty acid esters against five food-related bacteria, Food Chem. 187 (2015) 370–377. doi:10.1016/j.foodchem.2015.04.108.

[47] A.K. Hathcox, L.R. Beuchat, Inhibitory effects of sucrose fatty acid esters, alone and in combination with ethylenediaminetetraacetic acid and other organic acids, on viability of Escherichia coli O157:H7, Food Microbiol. 13 (1996) 213–225. doi:10.1006/fmic.1996.0027.

[48] D.L. Marshall, L.B. Bullerman, Antimicrobial properites of sucrose fatty acid esters, in: Carbohydr. Polyesters as Fat Substitutes, Marcel Dekker, Inc. (New York), 1994: pp. 149–167.

[49] S. Kato, H. Kobayashi, T. WAatanabe, Antimicrobial Action of Sucrose Monolaurate on Staphylococcus aureus, Food Hyg. Saf. Sci. (Shokuhin Eiseigaku Zasshi). 28 (1987) 261–266_1. doi:10.3358/shokueishi.28.261.

[50] A. Kato, K. Arima, Inhibitory effect of sucrose ester of lauric acid on the growth of Escherichia coli, Biochem. Biophys. Res. Commun. 42 (1971) 596–601. doi:10.1016/0006-291X(71)90529-8.

[51] T. Watanabe, R. Matsue, Y. Honda, M. Kuwahara, Differential activities of a lipase and a protease toward straight- and branched-chain acyl donors in transesterification to carbohydrates in an organic medium, Carbohydr. Res. 275 (1995) 215–220. doi:10.1016/0008-6215(95)00151-I.

[52] P. Nobmann, A. Smith, J. Dunne, G. Henehan, P. Bourke, The antimicrobial efficacy and structure activity relationship of novel carbohydrate fatty acid derivatives against Listeria spp. and food spoilage microorganisms, Int. J. Food Microbiol. 128 (2009) 440–445. doi:10.1016/j.ijfoodmicro.2008.10.008.

[53] A.J. Conley, J.J. Kabara, Antimicrobial action of esters of polyhydric alcohols., Antimicrob. Agents Chemother. 4 (1973) 501–6.

[54] Y.-J. Wang, Saccharides: Modifications and Applications, in: P. Tomasik (Ed.), Chem. Funct. Prop. Food Saccharides, Wang, Y P., CRC Press: New York, 2004: pp. 35–46.

[55] F. Marçon, V. Moreau, F. Helle, N. Thiebault, F. Djedaïni-Pilard, C. Mullié, β-Alkylated oligomaltosides as new alternative preservatives: antimicrobial activity, cytotoxicity and preliminary investigation of their mechanism of action, J. Appl. Microbiol. 115 (2013) 977-986. doi:10.1111/jam.12301.

[56] A. Wagh, S. Shen, F.A. Shen, C.D. Miller, M.K. Walsh, Effect of Lactose Monolaurate on Pathogenic and Nonpathogenic Bacteria, Appl. Environ. Microbiol. 78 (2012) 3465–3468. doi:10.1128/AEM.07701-11.

[57] B. Aungst, Fatty acids as skin permeation enhancers, in: E. Smith, H.I. Maibach (Eds.), Percutaneous Penetration Enhanc., CRC Press, New York, 1995: p. 277.

[58] D. Vllasaliu, L. Casettari, R. Fowler, R. Exposito-Harris, M. Garnett, L. Illum, S. Stolnik, Absorption-promoting effects of chitosan in airway and intestinal cell lines: A comparative study, Int. J. Pharm. 430 (2012) 151–160. doi:10.1016/j.ijpharm.2012.04.012.

[59] S.M. Krug, M. Amasheh, I. Dittmann, I. Christoffel, M. Fromm, S. Amasheh, Sodium caprate as an enhancer of macromolecule permeation across tricellular tight junctions of intestinal cells, Biomaterials. 34 (2013) 275–282. doi:10.1016/j.biomaterials.2012.09.051.

[60] Y. Takeuchi, H. Yasukawa, Y. Yamaoka, Y. Kato, Y. Morimoto, Y. Fukumori, T. Fukuda, Effects of fatty acids, fatty amines and propylene glycol on rat stratum corneum lipids and proteins in vitro measured by fourier transform infrared/attenuated total reflection (FT-IR/ATR) spectroscopy., Chem. Pharm. Bull. (Tokyo). 40 (1992) 1887–92.

[61] B. Lindemann, A.K. Solomon, Permeability of Luminal Surface of Intestinal Mucosal Cells, J. Gen. Physiol. 45 (1962) 801–810.

[62] M.A. Deli, Potential use of tight junction modulators to reversibly open membranous barriers and improve drug delivery, Biochim. Biophys. Acta - Biomembr. 1788 (2009) 892–910. doi:10.1016/j.bbamem.2008.09.016.

[63] B.J. Aungst, Absorption Enhancers: Applications and Advances, AAPS J. 14 (2012) 10–18. doi:10.1208/s12248-011-9307-4.

[64] L. Kiss, F.R. Walter, A. Bocsik, S. Veszelka, B. Ózsvári, L.G. Puskás, P. Szabó-Révész, M.A. Deli, Kinetic Analysis of the Toxicity of Pharmaceutical Excipients Cremophor EL and RH40 on Endothelial and Epithelial Cells, J. Pharm. Sci. 102 (2013) 1173–1181. doi:10.1002/jps.23458.

[65] B.D. Rege, L.X. Yu, A.S. Hussain, J.E. Polli, Effect of common excipients on Caco-2 transport of low-permeability drugs., J. Pharm. Sci. 90 (2001) 1776–86.

[66] P. Ashton, J. Hadgraft, K.A. Walters, Effects of surfactants in percutaneous absorption., Pharm. Acta Helv. 61 (1986) 228–35.

[67] P.P. Sarpotdar, J.L. Zatz, Evaluation of penetration enhancement of lidocaine by nonionic surfactants through hairless mouse skin in vitro., J. Pharm. Sci. 75 (1986) 176–81.

[68] P. P. Sarpotdar, J.L. Zatz, Percutaneous Absorption Enhancement by Nonionic Surfactants, Drug Dev. Ind. Pharm. 12 (1986) 1625–1647. doi:10.3109/03639048609042599.

[69] M.A. Thevenin, J.L. Grossiord, M.C. Poelman, Sucrose esters/cosurfactant microemulsion systems for transdermal delivery: Assessment of bicontinuous structures, Int. J. Pharm. 137 (1996) 177–186. doi:10.1016/0378-5173(96)04518-8.

[70] S. B. Ruddy, Surfactants, in: E.W. Smith, H.I. Maibach (Eds.), Percutaneous Penetration Enhanc., CRC Press, Inc., Florida, 1995: pp. 245–257.

[71] A. Ganem-Quintanar, Y.N. Kalia, F. Falson-Rieg, P. Buri, Mechanisms of oral permeation enhancement, Int. J. Pharm. 156 (1997) 127–142. doi:10.1016/S0378-5173(97)00193-2.

[72] H.A. Ayala-Bravo, D. Quintanar-Guerrero, A. Naik, Y.N. Kalia, J.M. Cornejo-Bravo, A. Ganem-Quintanar, Effects of sucrose oleate and sucrose laureate on in vivo human stratum corneum permeability, Pharm. Res. 20 (2003) 1267–1273. doi:10.1023/A:1025013401471.

[73] D. Dimitrijevic, A.J. Shaw, A.T. Florence, Effects of some non-ionic surfactants on transepithelial permeability in Caco-2 cells., J. Pharm. Pharmacol. 52 (2000) 157–62. doi: 10.1023/A:1025013401471

[74] E.S. Park, S.Y. Chang, M. Hahn, S.C. Chi, Enhancing effect of polyoxyethylene alkyl ethers on the skin permeation of ibuprofen., Int. J. Pharm. 209 (2000) 109–19.

[75] D.J. Pillion, J.A. Atchison, C. Gargiulo, R.X. Wang, P. Wang, E. Meezan, Insulin delivery in nosedrops: new formulations containing alkylglycosides, Endocrinology. 135 (1994) 2386–2391. doi:10.1210/en.135.6.2386.

[76] F. Ahsan, J. Arnold, E. Meezan, D.J. Pillion, Enhanced bioavailability of calcitonin formulated with alkylglycosides following nasal and ocular administration in rats., Pharm. Res. 18 (2001) 1742–6.

[77] L. Illum, Nasal drug delivery — Recent developments and future prospects, J. Control. Release. 161 (2012) 254–263. doi:10.1016/j.jconrel.2012.01.024.

[78] E.T. Maggio, Intravail^{TM}: highly effective intranasal delivery of peptide and protein drugs, Expert Opin. Drug Deliv. 3 (2006) 529–539. doi:10.1517/17425247.3.4.529.

[79] J.J. Arnold, F. Ahsan, E. Meezan, D.J. Pillion, Correlation of tetradecylmaltoside induced increases in nasal peptide drug delivery with morphological changes in nasal epithelial cells, J. Pharm. Sci. 93 (2004) 2205–2213. doi:10.1002/jps.20123.

[80] J.J. Arnold, M.D. Fyrberg, E. Meezan, D.J. Pillion, Reestablishment of the nasal permeability barrier to several peptides following exposure to the absorption enhancer tetradecyl-β-D-maltoside, J. Pharm. Sci. 99 (2010) 1912–1920. doi:10.1002/jps.21977.

[81] S.B. Petersen, G. Nolan, S. Maher, U.L. Rahbek, M. Guldbrandt, D.J. Brayden, Evaluation of alkylmaltosides as intestinal permeation enhancers: Comparison between rat intestinal mucosal sheets and Caco-2 monolayers, Eur. J. Pharm. Sci. 47 (2012) 701–712. doi:10.1016/j.ejps.2012.08.010.

[82] T. Uchiyama, T. Sugiyama, Y.S. Quan, A. Kotani, N. Okada, T. Fujita, S. Muranishi, A. Yamamoto, Enhanced permeability of insulin across the rat intestinal membrane by various absorption enhancers: their intestinal mucosal toxicity and absorption-enhancing mechanism of n-lauryl-beta-D-maltopyranoside., J. Pharm. Pharmacol. 51 (1999) 1241–50.

[83] A. Ganem-Quintanar, D. Quintanar-Guerrero, F. Falson-Rieg, P. Buri, Ex vivo oral mucosal permeation of lidocaine hydrochloride with sucrose fatty acid esters as absorption enhancers, Int. J. Pharm. 173 (1998) 203–210. doi:10.1016/S0378-5173(98)00226-9.

[84] S.B. Calderilla-Fajardo, J. Cázares-Delgadillo, R. Villalobos-García, D. Quintanar-Guerrero, A. Ganem-Quintanar, R. Robles, Influence of Sucrose Esters on the In Vivo Percutaneous Penetration of Octyl Methoxycinnamate Formulated in Nanocapsules, Nanoemulsion, and Emulsion, Drug Dev. Ind. Pharm. 32 (2006) 107–113. doi:10.1080/03639040500388540.

[85] G. Csóka, S. Marton, R. Zelko, N. Otomo, I. Antal, Application of sucrose fatty acid esters in transdermal therapeutic systems, Eur. J. Pharm. Biopharm. 65 (2007) 233–237. doi:10.1016/j.ejpb.2006.07.009.

[86] L. Kiss, É. Hellinger, A. Pilbat, Á. Kittel, Z. Török, A. Füredi, G. Szakács, S. Veszelka, P. Sipos, B. Ózsvári, L.G. Puskás, M. Vastag, P. Szabó-Révész, M.A. Deli, Sucrose Esters Increase Drug Penetration, But Do Not Inhibit P-Glycoprotein in Caco-2 Intestinal Epithelial Cells, J. Pharm. Sci. 103 (2014) 3107–3119. doi:10.1002/jps.24085.

[87] A. Szűts, P. Láng, R. Ambrus, L. Kiss, M.A. Deli, P. Szabó-Révész, Applicability of sucrose laurate as surfactant in solid dispersions prepared by melt technology, Int. J. Pharm. 410 (2011) 107–110. doi:10.1016/j.ijpharm.2011.03.033.

[88] F. McCartney, J.P. Gleeson, D.J. Brayden, Safety concerns over the use of intestinal permeation enhancers: A mini-review, Tissue Barriers. 4 (2016) e1176822. doi:10.1080/21688370.2016.1176822.

[89] J. Staroń, J.M. Dąbrowski, E. Cichoń, M. Guzik, Lactose esters: synthesis and biotechnological applications, Crit. Rev. Biotechnol. (2017) 1–14. doi:10.1080/07388551.2017.1332571.

Chapter 2

Unsaturated fatty acids lactose esters: biocompatibility, permeability enhancement and antimicrobial activity

Lucarini S, Fagioli L, Campana R, Cole H, Duranti A, Baffone W, Vllasaliu D, Casettari L. *European Journal of Pharmaceutics and Biopharmaceutics*. 2016; *107*: 88–96.

2.1 Introduction

Over the past few decades there has been a growing interest on sugar-based surfactants due to the large range of applications, from the biomedical field to cosmetics and food industries [1,2]. This class of molecules are generally classified as biocompatible and biodegradable non-ionic surfactants with emulsifying and antimicrobial abilities [3,4]. Their surface-active properties and applications are mainly influenced by the nature of the sugar headgroup (e.g. mono-, di- or polysaccharides), the carbon chain length and the degree of substitution [5].

The increasing demand for healthy and non-toxic additives has intensified the need for, and research on, novel compounds for food, medical and pharmaceutical applications. In this context, the development of sugar-fatty acid esters is becoming increasingly attractive. Among their possible applications, absorption-enhancing potential for biologics delivery has been recently evaluated [6,7].

Biological therapeutics (biologics) have and will continue to have a major impact on the management of a number of diseases. While their therapeutic potential is often unmatched by small drug molecules, biologics suffer from injection-only administration route. Non-invasive delivery of this class of therapeutics is highly attractive. However, drug delivery technologies, which offer the possibility to achieve safe and clinically relevant non-invasive delivery of biologics, are currently lacking. The key challenge to achieve this is a poor permeation of therapeutic macromolecules across the mucosal surfaces [8], which have evolved as biological structures presenting a barrier to the movement of material from the external environment into the systemic circulation.

The use of absorption enhancing agents is a common approach utilised to improve mucosal absorption (and hence the resulting bioavailability) of biologics following mucosal administration [8–11]. While the use of absorption enhancing agents offers significant potential in enabling non-invasive delivery of biologics, ‘absorption enhancers’, which are chemically diverse compounds exerting their absorption-enhancing effect through different mechanism(s), have often been associated with unacceptable toxicity profile [12]. Absorption enhancers that are capable of improving the mucosal absorption of biotherapeutics in a safe and therapeutically-effective manner are highly desirable, but the search for these continues [13–15].

In this study, we synthetized and characterized lactose palmitoleate and lactose nervonate, two new biodegradable lactose esters based on unsaturated fatty acids, namely palmitoleic (C16:1ω7) and nervonic (C24:1ω9) acids. The biocompatibility of these compounds was

evaluated *in vitro* and associated to the capacity to act as oral absorption enhancers of biotherapeutics as tested on the intestinal Caco-2 monolayers. Additionally, the compounds were also evaluated for antimicrobial activity by testing minimum inhibitory concentration (MIC) and effect on the growth inhibition of several pathogenic microorganisms.

2.2 Experimental section

2.2.1 Chemicals, materials and methods.

Palmitoleic acid and nervonic acid were purchased from TCI, lactose monohydrate from Carlo Erba, while Lipozyme® (immobilized from *Mucor miehei*), *p*-toluenesulfonic acid, 2,2-dimethoxypropane, tetrafluoroboric acid diethyl ether complex and all organic solvents used in this study were purchased from Sigma. Prior to use, acetonitrile was dried with molecular sieves with an effective pore diameter of 4 Å and toluene was saturated with water. Caco-2 cells were obtained from the European Collection of Cell Cultures. Dulbecco's Modified Eagles Medium (DMEM), Hank's Balanced Salt Solution (HBSS, with sodium bicarbonate and without phenol red), non-essential amino acids (100%), L-glutamine (200 mM), fetal bovine serum (FBS), antibiotic/antimycotic solution (10–12,000 U/mL penicillin, 10–12 mg/mL streptomycin, 25–30 μg/mL amphotericin B), trypsin–EDTA solution (2.5 mg/mL trypsin, 0.2 mg/mL EDTA) and fluorescein isothiocyanate-labelled ovalbumin (FITC-OVA) were supplied by Sigma (Poole, UK). MTS reagent, 3-(4,5-dimethylthiazol-2-yl)-5-(3-carboxymethoxyphenyl)-2-(4-sulfophenyl)-2*H*-tetrazolium (commercially known as CellTiter96® AQ_{ueous} One Solution Cell Proliferation Assay) was purchased from Promega (USA). Tissue culture flasks (75 cm^3 with ventilated caps), black 96-well plates and Transwell® inserts (12 mm diameter, 0.4 μm pore size, were purchased from Corning (USA). All other chemicals (reagent grade) were purchased from Sigma. Ultrapure chitosan chloride of 213 kDa average molecular weight ('Protasan UP CL 213') was obtained from Novamatrix (Denmark). Thermal analysis was carried out using differential scanning calorimetry (DSC). DSC analysis was performed using a DSC 8500 (Perkin-Elmer, Norwalk, USA) equipped with an intracooler (Intracooler 2, Perkin-Elmer, Norwalk, USA) and analyzed in an inert N_2 atmosphere. The structures of compounds were unambiguously assessed by MS, ^{1}H NMR, ^{13}C NMR, and IR. ESI-MS spectra were recorded with a Waters Micromass ZQ spectrometer in a negative or positive mode using a nebulizing nitrogen gas at 400 L/min and a temperature of 250 °C, cone flow 40 mL/min, capillary 3.5 Kvolts and cone voltage 60 V; only molecular ions $[M-H]^-$ or $[M+NH_4]^+$ are given. ^{1}H NMR and ^{13}C NMR spectra were recorded on a

Bruker AC 400 or 101, respectively, spectrometer and analyzed using the TopSpin software package. Chemical shifts were measured by using the central peak of the solvent. IR spectra were obtained on a Nicolet Atavar 360 FT spectrometer. Column chromatography purifications were performed under "flash" conditions using Merck 230–400 mesh silica gel. TLC was carried out on Merck silica gel 60 F254 plates, which were visualized by exposure to ultraviolet light and by exposure to an aqueous solution of ceric ammonium molibdate.

2.2.2 Synthesis of lactose-based surfactants

2.2.2.1 General procedure for the synthesis of lactose tetra acetate esters (*Z*)-6'-*O*-hexadec-9-enoyl- and (*Z*)-6'-*O*-tetracos-15-enoyl-4-*O*-(3',4'-*O*-isopropylidene-β-D-galactopyranosyl)-2,3:5,6-di-*O*-isopropylidene-1,1-di-*O*-methyl-D-glucopyranose (3a,b).

Lipozyme® (0.078 g) was added to a solution of palmitoleic acid (**1a**) or nervonic acid (**1b**) (0.79 mmol) and 4-*O*-(3',4'-*O*-isopropylidene-β-D-galactopyranosyl)-2,3:5,6-di-*O*-isopropylidene-1,1-di-*O*-methyl-D-glucopyranose (lactose tetra acetate, LTA) [16] (**2**) (0.401 g, 0.79 mmol) in water-satured toluene at 25 °C. The mixture was stirred at 75 °C for 12 h, cooled, diluted with acetone, then filtered, and the filtrate was concentrated. The purification of the residue by column chromatography (petroleum ether/EtOAc 7:3) gave **3a,b** as pale yellow oils.

3a. Yield: 70% (0.413 g). ESI-MS: *m/z* 744 $(M-H)^-$, 763 $(M+NH_4)^+$. ^{1}H NMR (CD_3OD) δ: 0.93 (t, 3H, J = 6.7 Hz, CH_3), 1.30–1.38 (m, 22H), 1.39 (s, 3H, CH_3), 1.41 (s, 3H, CH_3), 1.44 (s, 3H, CH_3), 1.49 (s, 3H, CH_3), 1.59–1.70 (m, 2H, CH_2CH_2COOR), 2.03–2.06 (m, 4H, $CH_2CH{=}CHCH_2$), 2.40 (t, 2H, J = 7.0 Hz, CH_2COOR), 3.45–3.47 (m, 6H, 2 -OCH_3), 3.47 (dd, 1H, $J_{8\text{-}9}$ = 7.1 Hz, $J_{8\text{-}7}$ = 8.0 Hz, H^8), 3.91 (dd, 1H, $J_{4\text{-}3}$ = 1.2 Hz, $J_{4\text{-}5}$ = 5.0 Hz, H^4), 4.04 (ddd, 1H, $J_{11\text{-}12a}$ = 1.5 Hz, $J_{11\text{-}10}$ = 2.2 Hz, $J_{11\text{-}12b}$ = 6.8 Hz, H^{11}), 4.05 (dd, 1H, $J_{6b\text{-}5}$ = 6.0 Hz, $J_{6b\text{-}6a}$ = 8.7 Hz, H^{6b}), 4.08 (dd, 1H, $J_{9\text{-}10}$ = 5.5 Hz, $J_{9\text{-}8}$ = 7.1 Hz, H^9), 4.14 (dd, 1H, $J_{3\text{-}4}$ = 1.2 Hz, $J_{3\text{-}2}$ = 7.5 Hz, H^3), 4.17 (dd, 1H, $J_{6a\text{-}5}$ = 6.0 Hz, $J_{6a\text{-}6b}$ = 8.7 Hz, H^{6a}), 4.22 (dd, 1H, $J_{10\text{-}11}$ = 2.2 Hz, $J_{10\text{-}9}$ = 5.5 Hz, H^{10}), 4.27 (dd, 1H, $J_{12b\text{-}11}$ = 6.8 Hz, $J_{12b\text{-}12a}$ = 11.5 Hz, H^{12b}), 4.30 (dd, 1H, $J_{12a\text{-}11}$ = 1.5 Hz, $J_{12a\text{-}12b}$ = 11.5 Hz, H^{12a}), 4.31 (ddd, $J_{5\text{-}4}$ = 5.0 Hz, $J_{5\text{-}6a} \cong J_{5\text{-}6b}$ = 6.0 Hz, H^5), 4.41 (d, 1H, $J_{1\text{-}2}$ = 6.2 Hz, H^1), 4.51 (d, 1H, $J_{7\text{-}8}$ = 8.0 Hz, H^7), 4.51 (dd, 1H, $J_{2\text{-}1}$ = 6.2 Hz, $J_{2\text{-}3}$ = 7.5 Hz, H^2), 5.35 (ddd, 1H, $J_{22\text{-}23a} \cong J_{22\text{-}23b}$ = 6.0 Hz, $J_{22\text{-}21}$ = 11.0 Hz, CH=CH), 5.39 (ddd, 1H, $J_{21\text{-}20a} \cong J_{21\text{-}20b}$ = 6.0 Hz, $J_{21\text{-}22}$ = 11.0 Hz, CH=CH) ppm. ^{13}C NMR (CD_3OD) δ: 13.0, 22.3, 24.2, 24.6, 25.1, 25.5, 25.7, 26.2, 26.7, 26.8, 27.0, 28.6, 28.76, 28.81, 28.9, 29.39, 29.43, 31.5,

33.5, 53.0, 55.1, 63.1, 65.5, 70.8, 73.3, 73.5, 75.4, 76.4, 76.8, 77.5, 79.4, 103.1, 105.7, 108.5, 109.7, 109.8, 129.4, 129.5, 173.8 ppm. IR (Nujol): 2952, 1729, 1712 cm^{-1}.

3b. Yield: 47% (0.222 g). ESI-MS: *m/z* 856 $(M-H)^-$, 875 $(M+NH_4)^+$. ^1H NMR (CD_3OD) δ: 0.93 (t, 3H, J= 6.7 Hz, CH_3), 1.30–1.38 (m, 38H), 1.39 (s, 3H, CH_3), 1.41 (s, 3H, CH_3), 1.44 (s, 3H, CH_3), 1.49 (s, 3H, CH_3), 1.59–1.70 (m, 2H, CH_2CH_2COOR), 2.03–2.08 (m, 4H, $CH_2CH{=}CHCH_2$), 2.40 (t, 2H, J= 7.0 Hz, CH_2COOR), 3.45–3.47 (m, 6H, 2 -OCH_3), 3.48 (dd, 1H, $J_{8\text{-}9}$= 7.1 Hz, $J_{8\text{-}7}$= 8.0 Hz, H^8), 3.91 (dd, 1H, $J_{4\text{-}3}$= 1.2 Hz, $J_{4\text{-}5}$= 5.0 Hz, H^4), 4.04 (ddd, 1H, $J_{11\text{-}12a}$= 1.5 Hz, $J_{11\text{-}10}$= 2.2 Hz, $J_{11\text{-}12b}$= 6.9 Hz, H^{11}), 4.05 (dd, 1H, $J_{6b\text{-}5}$= 6.0 Hz, $J_{6b\text{-}6a}$= 8.7 Hz, H^{6b}), 4.08 (dd, 1H, $J_{9\text{-}10}$= 5.6 Hz, $J_{9\text{-}8}$= 7.1 Hz, H^9), 4.14 (dd, 1H, $J_{3\text{-}4}$= 1.2 Hz, $J_{3\text{-}2}$= 7.5 Hz, H^3), 4.17 (dd, 1H, $J_{6a\text{-}5}$= 6.0 Hz, $J_{6a\text{-}6b}$= 8.7 Hz, H^{6a}), 4.21 (dd, 1H, $J_{10\text{-}11}$= 2.2 Hz, $J_{10\text{-}9}$= 5.5 Hz, H^{10}), 4.27 (dd, 1H, $J_{12b\text{-}11}$= 6.9 Hz, $J_{12b\text{-}12a}$= 11.5 Hz, H^{12b}), 4.29–4.33 (m, 2H, H^5, H^{12a}), 4.41 (d, 1H, $J_{1\text{-}2}$= 6.2 Hz, H^1), 4.51 (d, 1H, $J_{7\text{-}8}$= 8.0 Hz, H^7), 4.51 (dd, 1H, $J_{2\text{-}1}$= 6.2 Hz, $J_{2\text{-}3}$= 7.5 Hz, H^2), 5.35 (ddd, 1H, $J_{28\text{-}29a} \cong J_{28\text{-}29b}$= 6.0 Hz, $J_{28\text{-}27}$= 11.0 Hz, CH=CH), 5.39 (ddd, 1H, $J_{27\text{-}26a} \cong J_{27\text{-}26b}$= 6.0 Hz, $J_{27\text{-}28}$= 11.0 Hz, CH=CH) ppm. ^{13}C NMR (CD_3OD) δ: 13.1, 22.3, 24.2, 24.6, 25.1, 25.5, 25.7, 26.2, 26.7, 26.7, 26.9, 28.8, 28.9, 28.9, 29.0, 29.1, 29.20, 29.22, 29.33, 29.34, 29.35, 29.4, 29.4, 31.7, 33.5, 53.0, 55.1, 63.1, 65.5, 70.8, 73.3, 73.6, 75.4, 76.4, 76.9, 77.6, 79.4, 103.1, 105.7, 108.4, 109.7, 109.9, 129.5, 129.5, 173.8 ppm. IR (Nujol): 2965, 1731, 1713 cm^{-1}.

2.2.2.2 General procedure for the synthesis of lactose fatty acid esters (*Z*)-6'-*O*-hexadec-9-enoyl- and (*Z*)-6'-*O*-tetracos-15-enoyl-4-*O*-(β-D-galactopyranosyl)-D-glucopyranose (4a,b).

Compounds **3a** (0.320 g, 0.43 mmol) or **3b** (0.368g, 0.43 mmol) were dissolved in tetrafluoroboric diethylether/water/acetonitrile (3.5 mL, 1:5:500) and the mixture was stirred at 30 °C for 2 h. The products precipitated during the reaction as white solid were subsequently filtered, washed with acetonitrile, and then dried. The purification by crystallization from methanol gave the desired compounds as white solids.

4a [(*Z*)-6'-*O*-Hexadec-9-enoyl lactose, lactose palmitoleate]. Yield: 82% (0.305 g). Mp: modification of the physico-chemical state starting from 60 °C. ESI-MS: *m/z* 577 $(M-H)^-$, 596 $(M+NH_4)^+$. ^1H NMR (CD_3OD) δ: 0.91 (t, 3H, J= 7.0 Hz, CH_3), 1.25–1.45 [m, 16H, $(CH_2)_n$], 1.57–1.70 (m, 2H, CH_2CH_2COOR), 1.98–2.12 (m, 4H, $CH_2CH{=}CHCH_2$), 2.39 (t, 2H, J= 7.5 Hz, CH_2COOR), 3.42 (dd, 1H, $J_{2\text{-}1}$= 3.5 Hz, $J_{2\text{-}3}$= 9.5 Hz, H^2), 3.50 (dd, 1H, $J_{4\text{-}3} \cong J_{4\text{-}5}$= 9.5 Hz, H^4), 3.51 (dd, 1H, $J_{9\text{-}10}$= 3.0 Hz, $J_{9\text{-}8}$= 9.8 Hz, H^9), 3.58 (dd, 1H, $J_{8\text{-}7}$= 7.5 Hz, $J_{8\text{-}9}$= 9.8

Hz, H^8), 3.75–3.96 (m, 4H, H^5, H^{11}, H^{6a}, H^{6b}), 3.79 (dd, 1H, $J_{3\text{-}4} \cong J_{3\text{-}2}$ = 9.5 Hz, H^3), 3.80 (dd, 1H, $J_{10\text{-}9}$ = 3.0 Hz, $J_{10\text{-}11}$ = 5.0 Hz, H^{10}), 4.26 (dd, 1H, $J_{12b\text{-}11}$ = 5.0 Hz, $J_{12b\text{-}12a}$ = 11.5 Hz, H^{12b}), 4.29 (dd, 1H, $J_{12a\text{-}11}$ = 6.5 Hz, $J_{12a\text{-}12b}$ = 11.5 Hz, H^{12a}), 4.35 (d, 1H, $J_{7\text{-}8}$ = 7.5 Hz, H^7), 5.09 (d, 1H, $J_{1\text{-}2}$ = 3.5 Hz, H^1), 5.32 (ddd, 1H, $J_{22\text{-}23a} \cong J_{22\text{-}23b}$ = 6.0 Hz, $J_{22\text{-}21}$ = 11.0 Hz, CH=CH), 5.37 (ddd, 1H, $J_{21\text{-}20a} \cong J_{21\text{-}20b}$ = 6.0 Hz, $J_{21\text{-}22}$ = 11.0 Hz, CH=CH) ppm. ^{13}C NMR (CD_3OD) δ: 13.0, 22.3, 24.5, 26.7, 28.6, 28.8, 28.9, 29.4, 31.5, 33.4, 60.7, 63.2, 68.8, 69.8, 70.8, 71.8, 72.2, 72.9, 73.2, 80.8, 92.3, 103.9, 129.4, 129.5, 174.0 ppm. IR (Nujol): 3404, 2951, 1735, 1711 cm^{-1}.

4b [(*Z*)-6'-*O*-tetracos-15-enoyl lactose, lactose nervonate]. Yield: 93% (0.276 g). Mp: modification of the physico-chemical state starting from 60 °C. ESI-MS: *m/z* 690 $(M\text{-}H)^-$, 709 $(M+NH_4)^+$. ^{1}H NMR (DMSO) δ: 0.86 (t, 3H, *J* = 6.5 Hz, CH_3), 1.15–1.35 [m, 32H, $(CH_2)_n$], 1.47–1.58 (m, 2H, CH_2CH_2COOR), 1.94–2.04 (m, 4H, $CH_2CH{=}CHCH_2$), 2.30 (t, 2H, *J* = 7.5 Hz, CH_2COOR), 3.17 (ddd, 1H, $J_{2\text{-}1}$ = 4.0 Hz, $J_{2\text{-}OH2}$ = 7.0 Hz, $J_{2\text{-}3}$ = 9.5 Hz, H^2), 3.27 (dd, 1H, $J_{4\text{-}3} \cong J_{4\text{-}5}$ = 9.5 Hz, H^4), 3.33–3.37 (m, 2H, H^8, H^9), 3.57 (dd, 1H, $J_{3\text{-}2} \cong J_{3\text{-}4}$ = 9.5 Hz, H^3), 3.60–3.67 (m, 3H, H^{6a}, H^{6b}, H^{10}), 3.68–3.77 (m, 2H, H^5, H^{11}), 4.08 (dd, 1H, $J_{12b\text{-}11}$ = 4.5 Hz, $J_{12b\text{-}12a}$ = 11.5 Hz, H^{12b}), 4.16 (dd, 1H, $J_{12a\text{-}11}$ = 8.5 Hz, $J_{12a\text{-}12b}$ = 11.5 Hz, H^{12a}), 4.20–4.27 (m, 2H, H^7, OH^3), 4.41 (dd, 1H, $J_{OH6\text{-}6a} \cong J_{OH6\text{-}6b}$ = 6.0 Hz, OH^6), 4.54 (d, 1H, $J_{OH2\text{-}2}$ = 7.0 Hz, OH^2), 4.78 (d, 1H, $J_{OH10\text{-}10}$ = 5.0 Hz, OH^{10}), 4.85 (br s, 1H, OH), 4.90 (dd, 1H, $J_{1\text{-}OH1} \cong J_{1\text{-}2}$ = 4.0 Hz, H^1), 5.15 (br s, 1H, OH), 5.31 (ddd, 1H, $J_{28\text{-}29a} \cong J_{28\text{-}29b}$ = 6.0 Hz, $J_{28\text{-}27}$ = 11.0 Hz, CH=CH), 5.34 (ddd, 1H, $J_{27\text{-}26a} \cong J_{27\text{-}26b}$ = 6.0 Hz, $J_{27\text{-}28}$ = 11.0 Hz, CH=CH), 6.33 (d, 1H, $J_{OH1\text{-}1}$ = 4.0 Hz, OH^1) ppm. ^{13}C NMR (DMSO) δ: 14.4, 22.6, 24.8, 27.01, 27.02, 29.0, 29.02, 29.1, 29.2, 29.22, 29.29, 29.31, 29.4, 29.50, 29.52, 29.53, 29.6, 31.8, 33.8, 61.0, 63.7, 68.7, 70.2, 70.8, 71.7, 72.7, 72.9, 73.3, 81.6, 92.5, 104.0, 130.1, 130.1, 173.4 ppm. IR (Nujol): 3415, 2960, 1731, 1712 cm^{-1}.

2.2.3 Cell culture

Caco-2 cells were cultured to confluence in 75 cm^3 flasks at 5% CO_2 and 37 °C. Once confluent, they were detached from the flasks and seeded on filter inserts (Transwell®) at 100,000 cells/cm^2. Cells were maintained at 5% CO_2, 37 °C in DMEM supplemented with FBS (10%) antibiotic/antimycotic and L-glutamine, which was changed regularly (every other day). Cell growth and tight junction formation was assessed by transepitelial electrical

resistance (TEER) measurements. Cell layers were used for TEER and permeability experiments following 21 days culture on Transwell inserts.

2.2.4 MTS toxicity assay

The MTS colorimetric assay was performed to evaluate the effect of surfactants on cell viability. Caco-2 cells were seeded on 96-well plates at 10,000 cells per well and cultured in DMEM for 24 h. Prior to the assay, cell medium was removed and replaced with surfactant samples at the following concentrations: 0.00625 mg/mL, 0.0125 mg/mL, 0.025 mg/mL, 0.05 mg/mL, 0.1 mg/mL, 0.2 mg/mL, 0.4 mg/mL and 0.8 mg/mL in HBSS. Triton X-100 (0.1%, v/v in HBSS) and HBSS were used as a positive and negative control, respectively. Cells were incubated (at 37 °C, 5% CO_2) with samples and controls for a period of 3 h. Samples (and controls) were then removed and cells washed with phosphate-buffered saline (PBS). The MTS assay was subsequently conducted according to the manufacturer's instructions, with four repeats for each sample.

The relative cell viability (%) was calculated using the following equation:

$$\text{Relative Viability} = \frac{\text{S-T}}{H-T} \times 100 \quad \textbf{(Equation 1)}$$

Where: S is the absorbance of the tested samples, T is the absorbance of cells incubated with Triton X-100, and H is the absorbance of cells incubated with HBSS.

2.2.5 TEER experiments

Caco-2 cell monolayers with a TEER ≥800 Ωcm^2 were used in these experiments. Prior to the sample application, cell medium was removed and replaced with HBSS. Cells were equilibrated in HBSS (incubated at 37 ºC, 5% CO_2) for 30 min, following which TEER was measured; this was treated as the baseline TEER. Surfactants solutions at 0.0125-0.1 mg/mL concentration range were then applied to the apical side of the cell monolayers and cells were incubated with the samples for 3 hours. Chitosan solution at 0.1 mg/mL was employed for comparison as an example of a compound with well-documented ability to open epithelial tight junctions, and as a result, decrease TEER. TEER was measured every 30 min for 3 hours in the presence of the tested surfactant samples. The samples were removed after 3 hours and cells washed extensively with PBS. Cell medium was then added to both sides of the cell

monolayers and cells were incubated with the culture medium (DMEM) overnight. A further measurement of TEER was taken (with cells bathed in medium) 24 h following the exposure of the cells to surfactants to establish whether the changes in TEER (if any) were reversible. TEER was measured using an EVOM Voltohmmeter (World Precision Instruments, UK), equipped with a pair of chopstick electrodes. Background TEER due to the filter (~100 to 110 Ωcm^2) was deducted from the measurements in all cases. All experiments were performed in triplicates.

2.2.6 Permeability experiments

FITC-OVA was used as model of a protein drug. Caco-2 cells were cultured on filters as described above and only cell monolayers with TEER ≥800 Ωcm^2 were used for the purpose of this experiment. Prior to the sample application, culture medium was removed and the cell layers washed with PBS. Cells were then equilibrated in HBSS for 30-45 min. Surfactant solutions, at the final concentrations of 0.2, 0.1 and 0.05 mg/mL and FITC-OVA of 100 µg/mL, respectively, in HBSS, were then applied together to the apical side of the cells. Basolateral solution was sampled (100 µL volumes) at 30, 60, 90, 120, 150 and 180 min after sample application and the sampled volume replaced with fresh HBSS. Sampled FITC-OVA was quantified by fluorescence, using a Tecan M200 Pro plate reader. After the final sampling, the cell layers were then washed with PBS and TEER was measured in order to ensure that the cell layer integrity was not compromised during the permeability experiments and that cells recover. The permeability of FITC-OVA is expressed as the apparent permeability coefficient (P_{app}), calculated using the following equation:

$$P_{app} = \left(\frac{\Delta Q}{\Delta t}\right) \times \left(\frac{1}{A \times C_u}\right) \qquad \textbf{(Equation 2)}$$

P_{app}, apparent permeability (cm/s); $\Delta Q/\Delta t$, permeability rate (amount of FITC-OVA traversing the cell layers over time); A, diffusion area of the layer (cm_2); C_0, apically added FITC-OVA concentration. The experiment was conducted in triplicates.

2.2.7 Bacterial strains and culture conditions

Eight reference human pathogens were used in this study, *Escherichia coli* O157:H7 ATCC 35150, *Listeria monocytogenes* ATCC 7644, *Salmonella enteritidis* ATCC 13076, *Enterococcus fecalis* ATCC 29212, *Pseudomonas aeruginosa* ATCC 9027, *Staphylococcus*

aureus ATCC 43387, *Yersinia enterocolitica* ATCC 27729, and *Candida albicans* ATCC 14053. All the strains were routinely maintained in Tryptic Soy Agar (TSA, Oxoid, Milan, Italy) at 37 °C, while stock cultures were keep at -80 °C in Nutrient broth (Oxoid) with 15% of glycerol.

2.2.8 Determination of MICs

MICs determination of lactose palmitoleate and lactose nervonate was performed by microdilution method. For the tests, each compound (1.28 mg) was dissolved in DMSO (1 mL). Several colonies of each bacterial strain were picked and inoculated in sterilized Mueller-Hinton broth (MHB) (Oxoid) (10 mL) and incubated at 37 °C for 18–24 h. Bacterial suspensions were adjusted by spectrophotometer to a turbidity corresponding to 10^6 cfu/mL (OD_{610nm} 0.13-0.15) and each bacterial suspension (100 µL) was added in wells of the 96-well plate together with the appropriate volumes of the test solution to obtain final concentrations of 256, 128, 64, 32, 16, 8, 4, 2, 1, 0.5 µg/mL. Two rows of the 96-well plate were used for positive (bacteria alone) and negative controls (MHB alone), respectively. Gentamicin (128-0.125 µg/mL) and a standard preservative mixture (methylparaben and propylparaben, ratio 9:1) (1024-0.5 µg/mL) were added as internal controls. Preliminary assays with DMSO were performed to exclude its possible bacteriostatic and/or bactericidal activity; therefore, volumes of DMSO solutions added in each well never exceeded 5% (v/v) of the final total volume. MICs were defined as the lowest concentration of compound inhibiting the visible bacterial growth after 24 h of incubation. All the experiments were performed in duplicate.

2.2.9 Time kill experiments against food-borne pathogens

To evaluate the antimicrobial activity of lactose palmitoleate and lactose nervonate, time-kill experiments against food-borne pathogens, here represented by *E. coli* O157: H7 ATCC 35150, *L. monocytogenes* ATCC 7644, and *S. enteritidis* ATCC 13076, were performed. For this, pathogens strains were grown overnight in 20 mL of MHB at 37 °C and, after incubation, 500 µL (about 10^7 cfu/mL, as previously determined by spectrophotometer) of each pathogen suspension were incubated in 24-well culture plates with 500 µL of MBH with lactose palmitoleate or lactose nervonate at MIC and 2MIC concentrations. Several wells were inoculated with 500 µL of each pathogen suspension in 500 µL of MBH as controls.

At baseline, and after 3, 6 and 24 h of incubation, one aliquot of each sample was aseptically removed, serially diluted in physiological saline solution, and plated on TSA plates for colonies forming unit enumeration (cfu/mL). Volumes of DMSO solution added in each well

never exceeded 1% (v/v) of the final volume. All the experiments were performed in duplicate.

2.2.10 Statistical analysis

Statistical analysis was performed using Prism version 5.0 (GraphPad Inc., USA). The assumptions for parametric test were cheeked prior to carry out the analysis. To compare the numbers of bacteria recovered in time-kill experiments after exposure to lactose palmitoleate and lactose nervonate, one-way analysis of variance (ANOVA) with Bonferroni post-test was performed; when the assumptions for parametric test were not respected, Kruskall-Wallis non-parametric test with Dunn's multiple comparison test was applied. P values < 0.05 were considered to be statistically significant.

2.3 Results

2.3.1 Cell viability

Fig. 1 shows the effect of tested compounds, applied within a broad dose range, on Caco-2 cell viability. Lactose palmitoleate did not display notable toxicity to Caco-2 cells regardless of the applied concentration and no dose-dependent effect was apparent. Similarly, lactose nervonate did not show a concentration-dependent effect, but with this surfactant the majority of the tested concentrations were associated with a decrease in cell viability, which was most apparent with 0.05 mg/mL.

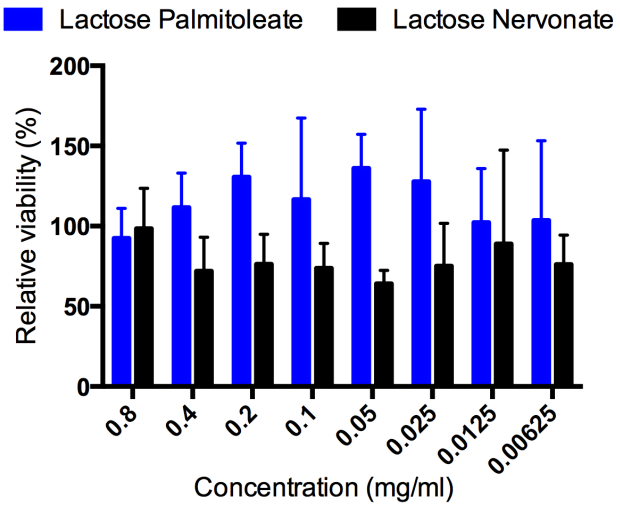

Fig. 1. Effect of lactose palmitoleate and lactose nervonate surfactants on relative Caco-2 cell viability, as determined by the MTS metabolic activity assay. Surfactants were applied at 0.00625 mg/mL, 0.0125 mg/mL, 0.025 mg/mL, 0.05 mg/mL, 0.1 mg/mL, 0.2 mg/mL, 0.4 mg/mL and 0.8 mg/mL. Relative viability calculated by normalising against negative control, Hank's Balanced Salt Solution (HBSS) and positive control, 0.1% v/v Triton X-100 in HBSS. Data shown as the mean ± SD (n=6).

2.3.2 TEER

Fig. 2 shows the effect of lactose palmitoleate and lactose nervonate surfactants on Caco-2 monolayer TEER. The concentration range tested for their impact on epithelial TEER was 0.0125-0.1 mg/mL, which is in fact well below 0.8 mg/mL, the dose found to be not toxic to Caco-2 cells (Figure 1). Chitosan was incorporated in this experiment as a TEER-lowering compound to provide a comparison.

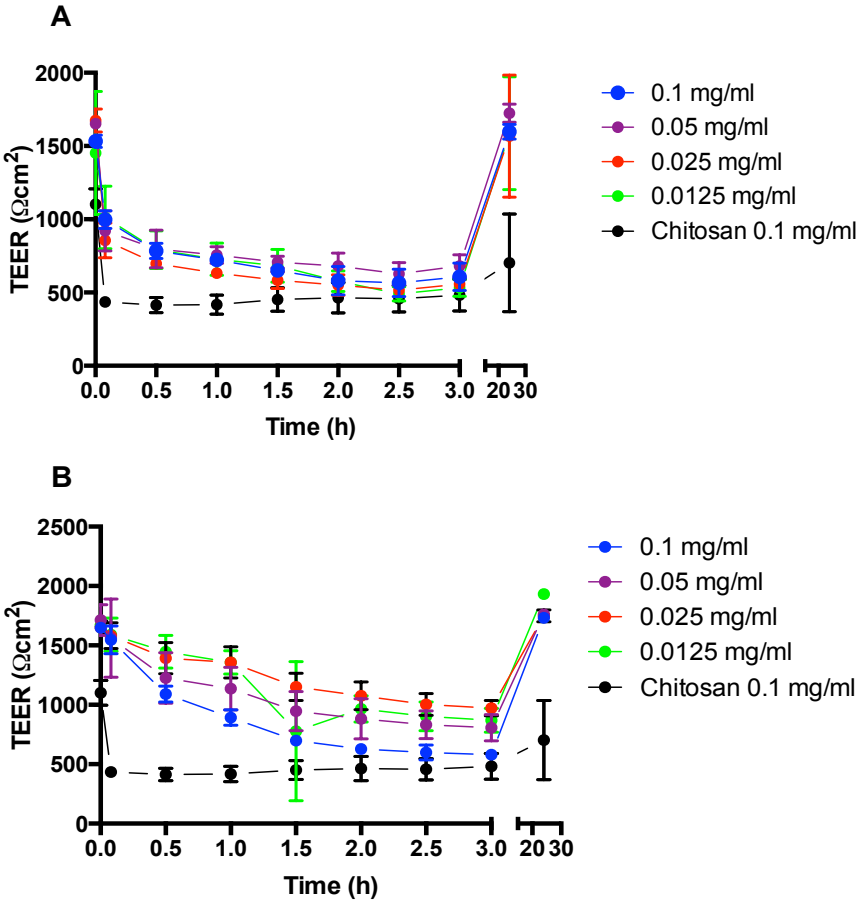

Fig. 2. Effect of lactose esters on Caco-2 cell monolayer transepithelial electrical resistance (TEER). A) Lactose palmitoleate and B) Lactose nervonate. Surfactants were applied to confluent cell monolayers at a concentration of 0.1, 0.05, 0.025 and 0.0125 mg/mL. Data are expressed as % of the baseline TEER and presented as the mean ± SD (n=3).

The data show that both lactose palmitoleate and lactose nervonate decreased Caco-2 monolayer TEER at all tested doses. For lactose palmitoleate, there is a sharp decrease in TEER, with maximal decrease by 62-68% of the baseline value (depending on the concentration), observed 2.5 h post application (Figure 2A). The maximal decrease amounted to 62% of the baseline value compared to chitosan, although a lower minimal TEER compared to the surfactants is apparent with chitosan. With lactose nervonate, a more gradual decrease in TEER was observed compared to both lactose palmitoleate and chitosan. TEER

reached a minimal value 3 h post application, which correspond to a drop of 41-65%, depending on the concentration (highest dose exerting the largest TEER decrease). With both surfactant compounds, TEER reversed to original (pre-application) values, confirming no long-lasting effect on cell toxicity, tight junctions and cell monolayer integrity, while the TEER of chitosan-treated cells showed partial TEER reversibility (to 64% of the baseline value).

2.3.3 Permeability studies

The effect of surfactants lactose palmitoleate and lactose nervonate on the permeability (apparent permeability coefficient) of a model protein, FITC-OVA (Mw ~45,000 Da), is shown in Fig. 3 (A and B, respectively). The compounds were applied to Caco-2 monolayers at 0.2 mg/mL, 0.1 mg/mL and 0.05 mg/mL. At 0.2 mg/mL concentration, lactose palmitoleate enhanced FITC-OVA permeability of 11.5-folds (Fig. 3A). The next lower dose (0.1 mg/mL) increased FITC-OVA permeability, but this increase was not found to be statistically siginficant. The lowest applied concentration of lactose palmitoleate did not influence FITC-OVA permeability.

With lactose nervonate (Fig. 3B), the highest and lowest used doses (0.2 and 0.05 mg/mL, respectively) did not induce a statistically significant effect on FITC-OVA permeability. The 0.1 mg/mL dose, however, led to a 2.5-fold enhancement of FITC-OVA permeability.

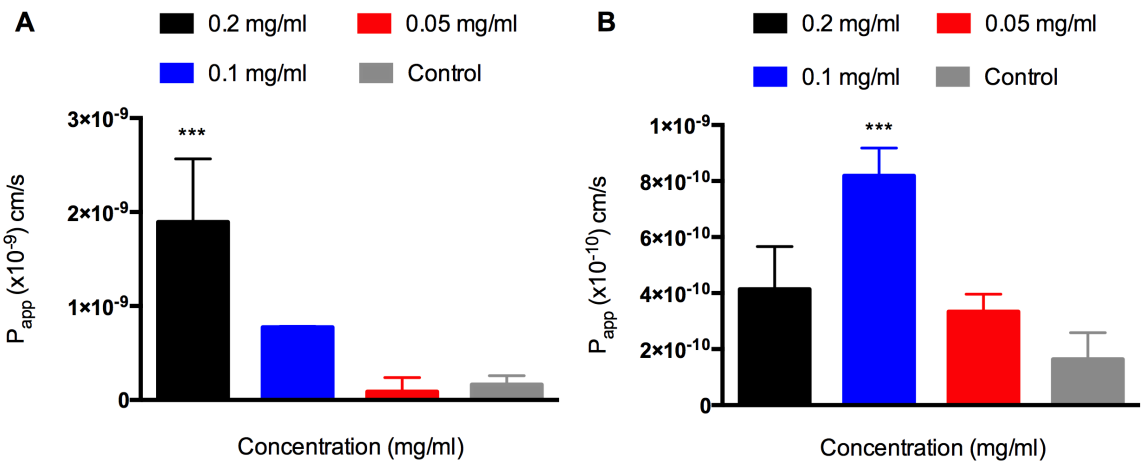

Fig. 3. Effect of lactose esters on ovalbumin permeability across Caco-2 cell monolayers. A) Lactose palmitoleate and B) Lactose nervonate. Surfactants were applied to confluent cell monolayers at 0.2 mg/ml, 0.1 mg/mL and 0.05 mg/mL. Data are expressed as apparent permeability coefficient (P_{app}) and presented as the mean ± SD (n=3).

2.3.4 Antimicrobial activities of lactose palmitoleate and lactose nervonate

The antimicrobial activities of lactose palmitoleate and lactose nervonate were evaluated by determining the MIC, and subsequently carrying out time-kill experiments against food-borne pathogens. MICs of lactose palmitoleate and lactose nervonate against *Escherichia coli* O157:H7 ATCC 35150, *Listeria monocytogenes* ATCC 7644, *Salmonella enteritidis* ATCC 13076, *Enterococcus fecalis* ATCC 29212, *Pseudomonas aeruginosa* ATCC 9027, *Staphylococcus aureus* ATCC 43387, *Yersinia enterocolitica* ATCC 27729 and *Candida albicans* ATCC 14053 were tested according to the National Committee for Clinical Laboratory Standards (NCCLS) document M100-S12 method. The relative data are shown in Table 1.

Lactose nervonate showed the greatest antimicrobial activity against the three food-borne pathogens included in this study, *Escherichia coli* O157:H7 ATCC 35150, *Listeria monocytogenes* ATCC 7644, and *Salmonella enteritidis* ATCC 13076*,* with MIC values of 64 μg/mL.

Lactose palmitoleate showed similar MIC values of 64 μg/mL toward *Escherichia coli* O157:H7 ATCC 35150 and *Listeria monocytogenes* ATCC 7644, and a higher MIC value (128 μg/mL) towards *Salmonella enteritidis* ATCC 13076. The MICs values of lactose palmitoleate and lactose nervonate against the others tested microorganisms were similar to those reported against the food-borne pathogens. With regards to internal controls, gentamicin inhibited microbial growth with the lowest MIC value of 4 μg/mL for *Salmonella enteritidis* ATCC 13076 and the highest MIC value of 128 μg/mL for *Escherichia coli* O157:H7 ATCC 35150, while parabens mixture showed MIC values >1024 μg/mL for all the examined bacterial species.

Table 1. MIC values (μg/mL) of the tested compounds against selected bacterial strains.

Target microrganisms	MICs (μg/mL)			
	Lactose palmitoleate	Lactose nervonate	Gentamicin	Parabens
E. coli O157:H7 ATCC 35150	64	64	128	>1024
L. monocytogenes ATCC 7644	64	64	8	>1024
S. enteritidis ATCC 13076	128	64	4	>1024
E. faecalis ATCC 29212	64	64	64	>1024
P. aeruginosa ATCC 9027	128	128	16	>1024
S. aureus ATCC 43387	128	128	16	>1024
Y. enterocolitica ATCC 27729	64	64	8	>1024
C. albicans ATCC 10231	64	64	NA	>1024

NA: not applicable

Results of time–kill experiments with lactose palmitoleate and lactose nervonate at their respective MIC and 2MIC concentrations against *E. coli* O157:H7 ATCC 35150, *L. monocytogenes* ATCC 7644, and *S. enteritidis* ATCC 13076 are summarized in Fig. 4.

In general, the antimicrobial effect of these compounds was confirmed on the tested food-borne pathogens with a cfu/mL reduction in all the samples containing lactose palmitoleate or lactose nervonate at different concentrations (MIC and 2MIC) in comparison to the relative control samples (Fig. 4a-c). In particular, the viability of *E. coli* O157:H7 ATCC 35150 decreased significantly to 7.70 log cfu/mL after 24 h of incubation with lactose palmitoleate at 2MIC, compared to 9.56 log cfu/mL of the control one (Fig. 4b). Similarly, the viability of *S. enteritidis* ATCC 13076 was significantly reduced after 24 h of incubation with lactose palmitoleate and lactose nervonate at 2MIC with 6.95 and 6.85 log cfu/mL, respectively, compared to 9.90 log cfu/mL of the relative control (Fig. 4c).

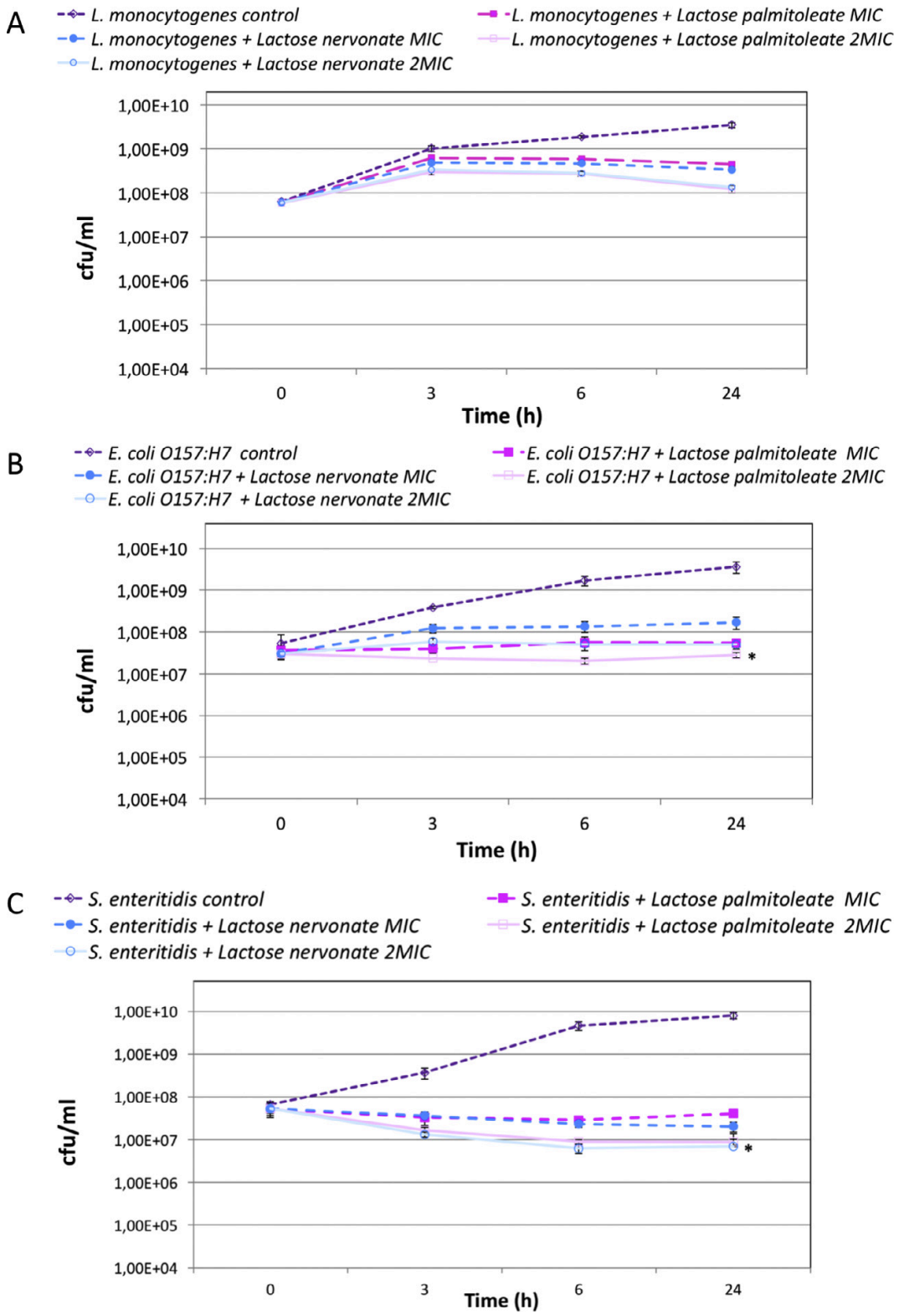

Figure 4. Antimicrobial activity of lactose palmitoleate and lactose nervonate at MIC and 2MIC concentration s in time-kill experiments against food-borne pathogens *L. monocytogenes* ATCC 7644 (A), *E. coli* O157:H7 ATCC 35150 (B), *S. enteritidis* ATCC 13076 (C). Data represent mean values of three independent experiments performed in duplicate and asterisks values statistically significant ($P < 0.05$, Kruskall-Wallis non-parametric test with Dunnett's multiple comparison test).

Both the tested substances induced a bacterial growth reduction during the entire incubation time, with an increased rate from 6 to 24 h. The highest values of growth inhibition, 30.88 and 29.84%, were obtained for *S. enteritidis* ATCC 13076 after 24 h of incubation with lactose palmitoleate and lactose nervonate at 2MIC concentration, respectively (Table 2).

Similar percentages of growth inhibition were also observed for *S. enteritidis* ATCC 13076 after 6 h incubation with lactose palmitoleate and lactose nervonate at MIC concentration (29.66 and 28.08%, respectively). With regard to *E. coli* O157:H7 ATCC 35150, growth inhibitions amounting to 22.08 and 19.47% were observed after 24 h incubation with lactose palmitoleate and lactose nervonate at 2MIC concentration, respectively. Lower percentages of growth inhibition were obtained with *L. monocytogenes* ATCC 7644, with 15.33 and 14.85% of growth inhibition after 24 h incubation in the presence of lactose palmitoleate and lactose nervonate at 2MIC concentration, respectively (Table 2).

Table 2. Percentages of growth inhibition induced by lactose palmitoleate and lactose nervonate, at their MIC and 2MIC concentrations, toward *E.coli* O157: H7 ATCC 35150, *L.monocytogenes* ATCC 7644 and *S. enteritidis* ATCC 13076, as assessed in time-kill experiments.

Food-borne pathogens:	**Growth inhibition by**			
	Lactose palmitoleate (μg/ml)		Lactose nervonate (μg/ml)	
	MIC	2MIC	MIC	2MIC
L. monocytogenes ATCC 7644				
3h	2.41%	5.99%	3.55%	5.38%
6h	5.40%	8.94%	6.49%	8.89%
24h	9.32%	15.33%	10.64%	14.85%
E. coli O157:H7 ATCC 35150				
3h	11.47%	14.20%	5.78%	9.51%
6h	16.00%	20.82%	11.88%	16.50%
24h	19.10%	22.08%	13.95%	19.47%
S. enteritidis ATCC 13076				
3h	12.16%	15.67%	11.68%	16.81%
6h	22.82%	28.08%	23.80%	29.66%
24h	23.13%	29.84%	26.20%	30.88%

2.4 Discussion

Different chemical or enzymatic synthetic strategies have been adopted to produce biodegradable, biocompatible and eco-friendly sugar-based materials with interesting properties, including ability to act as permeability enhancers and/or antimicrobial agents [2,17–21]. Among them, the enzymatic production of sucrose esters represent a route to obtain a promising class of compounds with multiple applications, already marketed in

different fields [22,23]. Lactose palmitoleate and lactose nervonate were synthesized from palmitoleic acid (**1a**) or nervonic acid (**1b**) following a literature procedure based on a specific lipase as a catalyst, namely Lipozyme® [19], and requiring a preventive step for the protection of disaccharide derivative lactose to obtain LTA (**2**) [19] (Scheme 1). The final step proceeded through the deprotection of the acetalic adducts **3a,b** to obtain the desired compounds **4a,b** (Scheme 1).

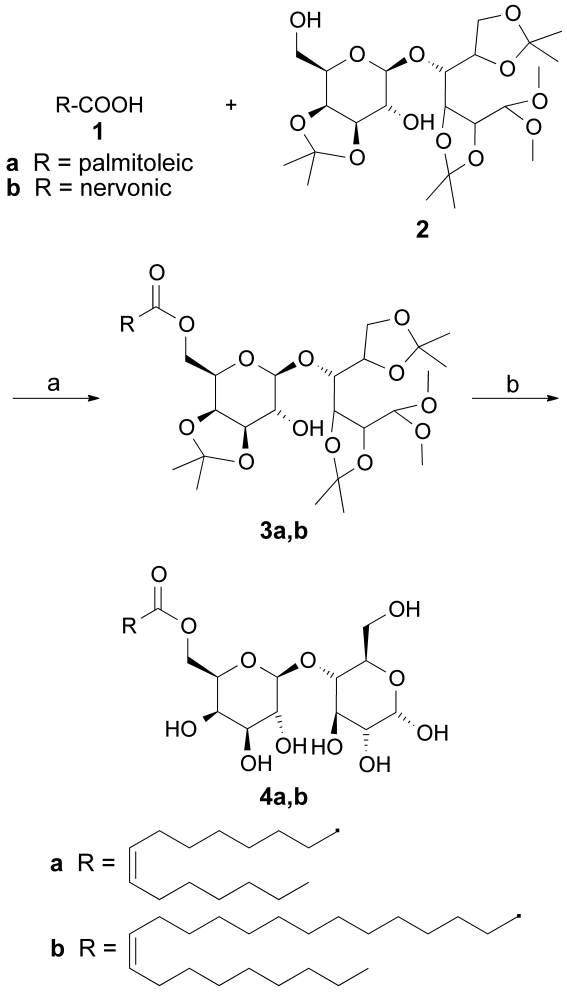

Scheme 1. Reagents and conditons: (a) toluene, 75 °C, 12 h; (b) $HBF_4{\cdot}Et_2O$, CH_3CN, 30 °C, 4 h.

The use of the surfactant described is of potential high value due to their biological effectiveness at low concentrations and metabolism in vivo. This situation leads to non-toxic metabolites, particularly when the molecules obtained by ester bond hydrolysis are sugar and fatty acid derivatives such as those studied here.

Regarding cell toxicity, it is interesting to consider that both lactose palmitoleate and lactose nervonate did not show marked toxicity to Caco-2 cells, even with a relatively high

application dose (0.8 mg/mL). Furthermore, no dose-dependency was apparent. The absence of significant cell toxicity with surfactant compounds, especially at doses used here, is rare. For example, Vllasaliu et al. previously evaluated alkylmaltosides (three sugar units and linear fatty chains from C12 to C14) for their absorption enhancing property [24]. Using a combination of methods, they demonstrated that these surfactants produced a significant level of toxicity in bronchial epithelial cells, Calu-3, with concentration of surfactant that caused 50% cell death (IC_{50}) values between 0.0031-0.0065% w/v for the three representative compounds tested. In another example, Warisnoicharoen et al. studied the toxicity of nonionic surfactants polyoxyethylene-10-oleyl ether (C18:1E10), polyoxyethylene-10-dodecyl ether, and *N*,*N*-dimethyldodecylamine-*N*-oxide in bronchial cells and obtained IC_{50} values ranging between 0.06-0.08 mg/mL [25].

Concerning the permeability enhancement activity, a wide range of ionic and non-ionic surfactants have been explored for their potential use as mucosal absorption enhancers. However, experience suggests that the use of surfactants as permeability enhancers is associated with cell toxicity [26–29], as discussed above, which severely limits their application. Of note is the emergence of alkylmaltosides, which have been clinically proposed for nasal delivery (e.g. Intravail®). They are being explored commercially due to evidence of increased systemic bioavailability of peptides and proteins when included in nasal or ocular formulations [7,30] or when evaluated on Caco-2 and rat intestinal mucosal tissue [31].

Studies exploring the use of surfactants as mucosal absorption enhancers predominantly employ relatively low molecular peptides and proteins. However, we were interested to determine whether the permeability of OVA, as a model protein of ~45 kDa, is improved in an intestinal model with the compounds synthesized here. A permeability enhancement ratio of 11.5 achieved with lactose palmitoleate is remarkable considering the molecular size of OVA. Perhaps even more remarkable is the fact that a clear permeability increasing effect is not mirrored by a notable change in TEER. The combination of findings therefore points to a transcellular rather than paracellular effect with lactose palmitoleate. These findings are in agreement with a recent study by Kiss et al. [22], which reported that non-toxic concentrations of sucrose esters significantly enhanced the permeability of atenolol and fluorescein across Caco-2 monolayers. In that study, however, the surfactants caused a reduction in TEER, but, interestingly, the morphology of tight junctions remained unaffected. The authors of this study concluded that sucrose ester surfactants act as absorption enhancers through an effect on both the transcellular and paracellular routes, with a clearly demonstrated effect on elevation of plasma membrane fluidity, which was suggested as a cause of increased

transcellular passage of molecules. Overall, the permeability data is important within the context of non-invasive delivery of peptide and protein therapeutics, as well as vaccine delivery (OVA is in fact a routinely used model vaccine antigen).

From the pharmaceutical to the cosmetic and food fields, the need of developing safe and efficient preservatives has been growing very rapidly, particularly to find alternatives to parabens. Different sugars derivatives have been proposed to achieve this goal, starting from monosaccharides to polysaccharides as glycosidic moieties. Among them, alkylated oligomaltosides (i.e. maltoside and maltotrioside) demonstrated a valuable alternative with good antimicrobial activity explained by the inhibition of the microbial enzymatic metabolism. Due to the low solubility of these compounds the authors conducted the experiments in DMSO and the results highlighted a higher microbial inhibition for di- and polysaccharide than monosaccharide derivatives [32].

In our study, the antibacterial activities of two sugar fatty acid esters, lactose palmitoleate and lactose nervonate, against several different human pathogens were evaluated. MICs of lactose palmitoleate and lactose nervonate, ranging from 64 to 128 μg/mL, highlighted a greater antibacterial property compared to the parabens mixture, with MIC values >1024 μg/mL. According to other authors who have tested the antibacterial efficacy of alkylated oligomaltosides [32], our findings highlighted the potential use of lactose palmitoleate and lactose nervonate sugar esters as alternative preservatives to the commonly employed ones, such as parabens.

Moreover, in time-kill experiments performed toward selected food-borne pathogens, higher concentrations (2MIC values) of lactose palmitoleate and lactose nervonate were able to inhibit the growth of these bacteria, with a variable degree of antibacterial activity. For both the tested compounds, a bacteriostatic effect toward *L. monocytogenes* ATCC 7644 at each time point was observed, while after 24 h of incubation with lactose palmitoleate and lactose nervonate the numbers of viable *E. coli* O157:H7 ATCC 35150 and *S. enteritidis* ATCC 13076 were noticeably lower than the initial values. These data are in agreement with those of other researchers [3], which report a strong antibacterial activity of sugar esters against food-borne pathogens. The results obtained here are interesting and encourage further studies in order to fully understand the antibacterial efficacy of lactose palmitoleate and lactose nervonate against other food-borne pathogens and their interactions with food ingredients, hence verifying their real application to control bacterial growth in food systems.

2.5 Conclusions

The study presented here reports novel sucrose ester-based surfactant compounds with a good toxicity profile, as determined by the MTS assay and evaluation of the effect on the epithelial barrier integrity (TEER investigations). The compounds were tested for and clearly shown to display a combination of macromolecular absorption enhancing and antimicrobial properties. This is important considering the toxicity profile of the compounds demonstrated here, as these properties are often associated with unacceptable toxicity. This work therefore clearly indicates that detailed evaluation of these compounds is warranted in the future.

Supporting Information

(*Z*)-6'-*O*-hexadec-9-enoyl-4-*O*-(β-D-galactopyranosyl)-D-glucopyranose (lactose palmitoleate).

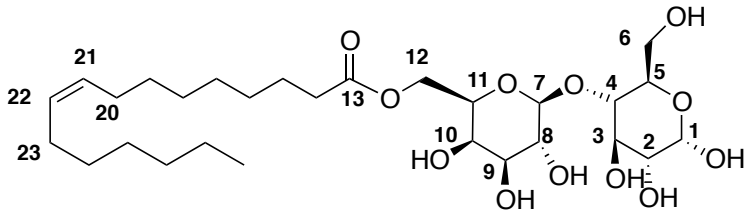

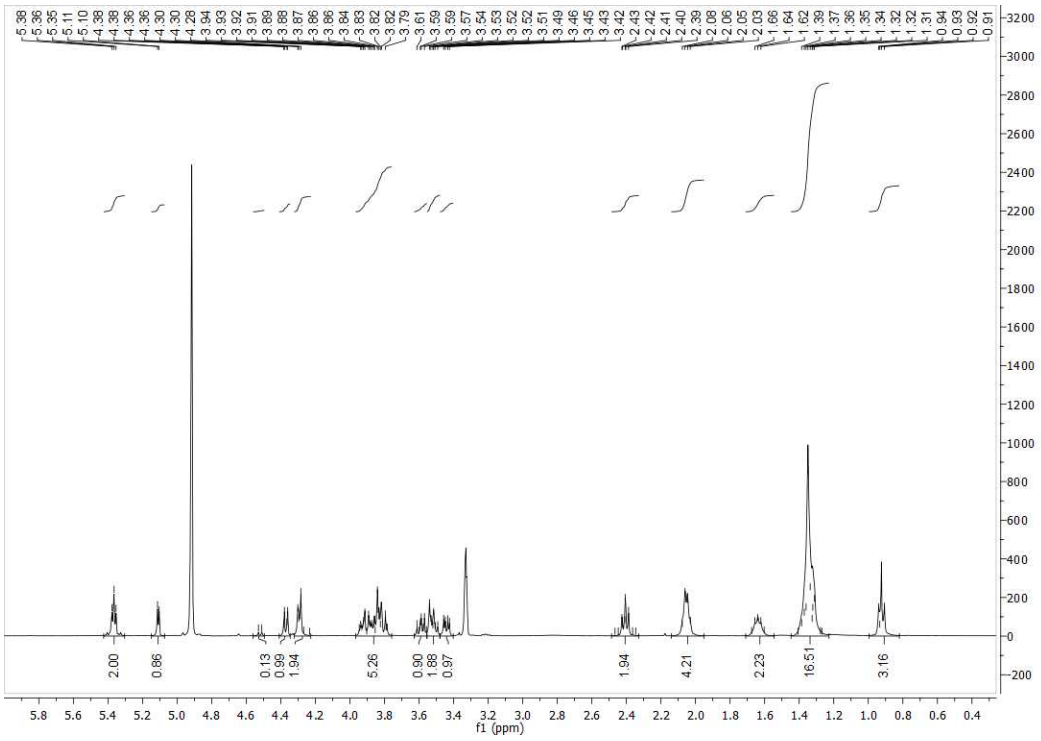

Fig. S1. ^{1}H NMR spectrum of (*Z*)-6'-*O*-hexadec-9-enoyl-4-*O*-(β-D-galactopyranosyl)-D-glucopyranose (lactose palmitoleate) in CD_3OD.

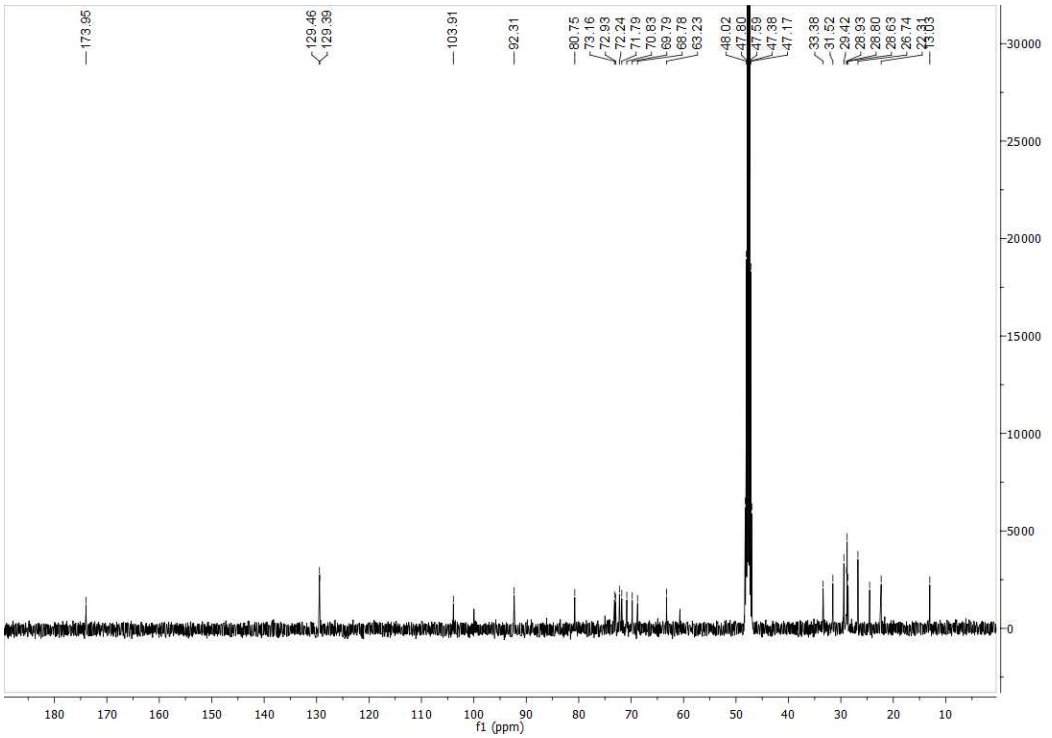

Fig. S2. ^{13}C NMR spectrum of (*Z*)-6'-*O*-hexadec-9-enoyl- -4-*O*-(β-D-galactopyranosyl)-D-glucopyranose (lactose palmitoleate) in CD_3OD.

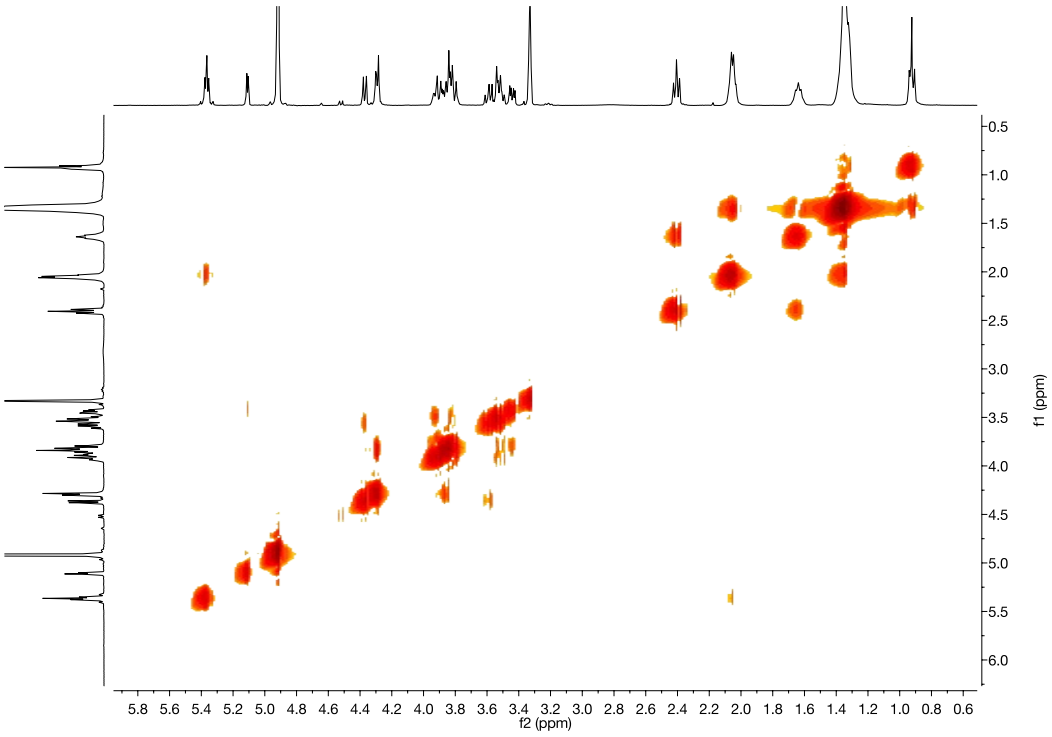

Fig. S3. COSY NMR spectrum of (*Z*)-6'-*O*-hexadec-9-enoyl- -4-*O*-(β-D-galactopyranosyl)-D-glucopyranose (lactose palmitoleate) in CD_3OD.

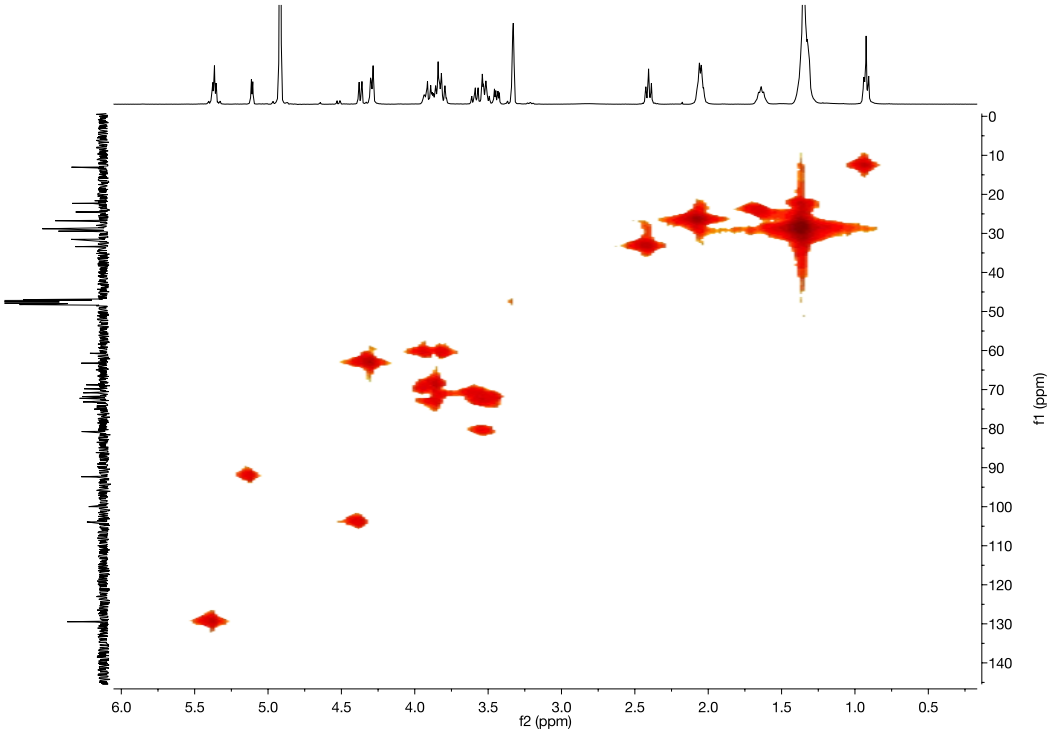

Fig. S4. HMQC NMR spectrum of (*Z*)-6'-*O*-hexadec-9-enoyl- -4-*O*-(β-D-galactopyranosyl)-D-glucopyranose (lactose palmitoleate) in CD_3OD.

(*Z*)-6'-*O*-tetracos-15-enoyl-4-*O*-(β-D-galactopyranosyl)-D-glucopyranose

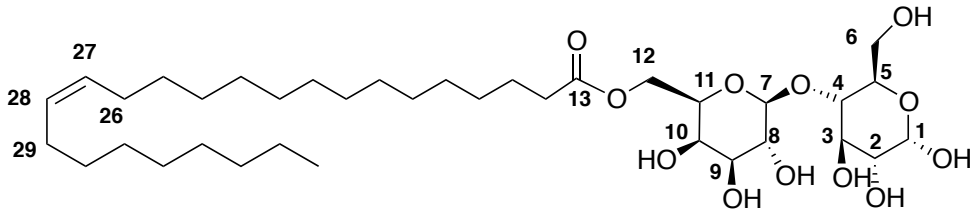

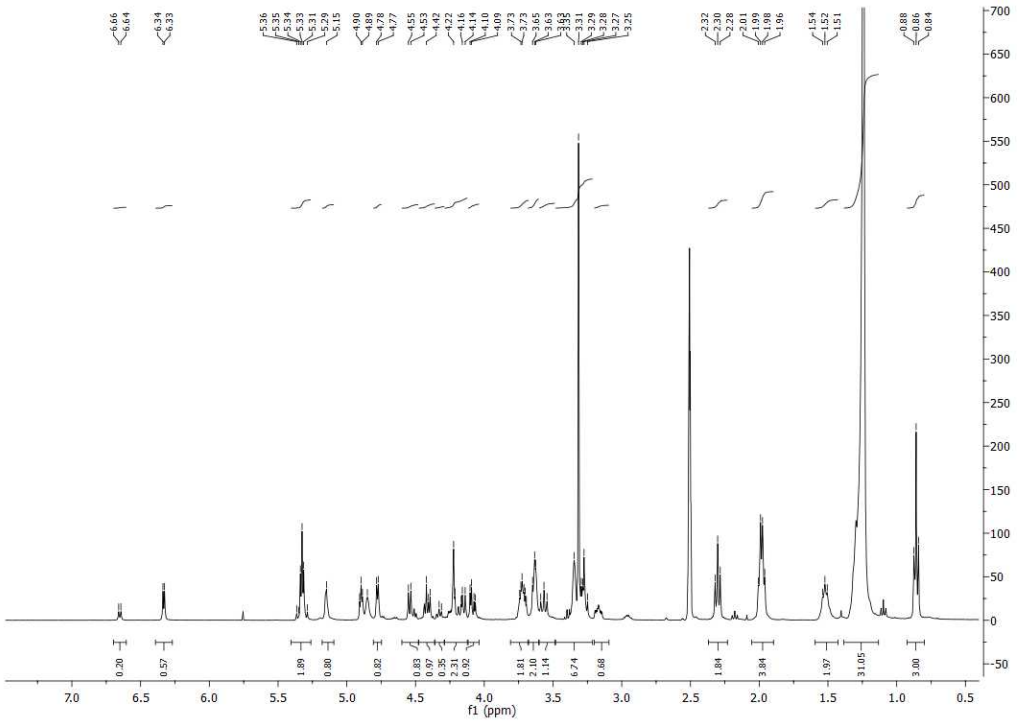

Fig S5. ^{1}H NMR spectrum of (*Z*)-6'-*O*-tetracos-15-enoyl-4-*O*-(β-D-galactopyranosyl)-D-glucopyranose in DMSO- d_6.

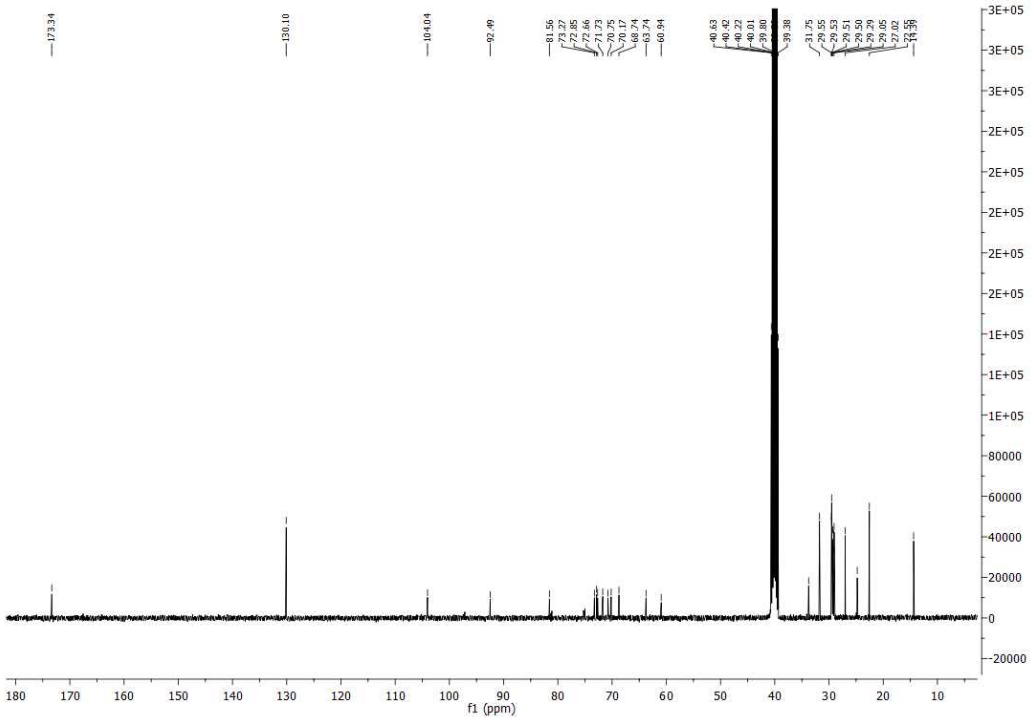

Fig S6. ^{13}C NMR spectrum of (*Z*)-6'-*O*-tetracos-15-enoyl-4-*O*-(β-D-galactopyranosyl)-D-glucopyranose in DMSO- d_6.

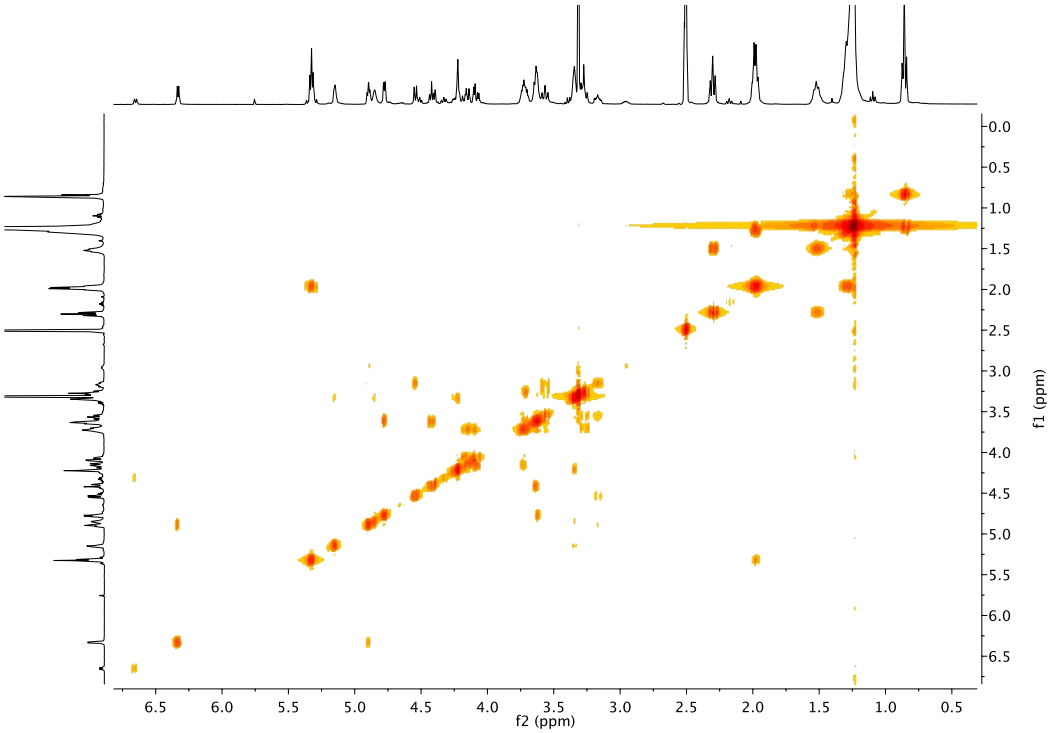

Fig. S7. COSY NMR spectrum of (*Z*)-6'-*O*-tetracos-15-enoyl-4-*O*-(β-D-galactopyranosyl)-D-glucopyranose in DMSO-d_6.

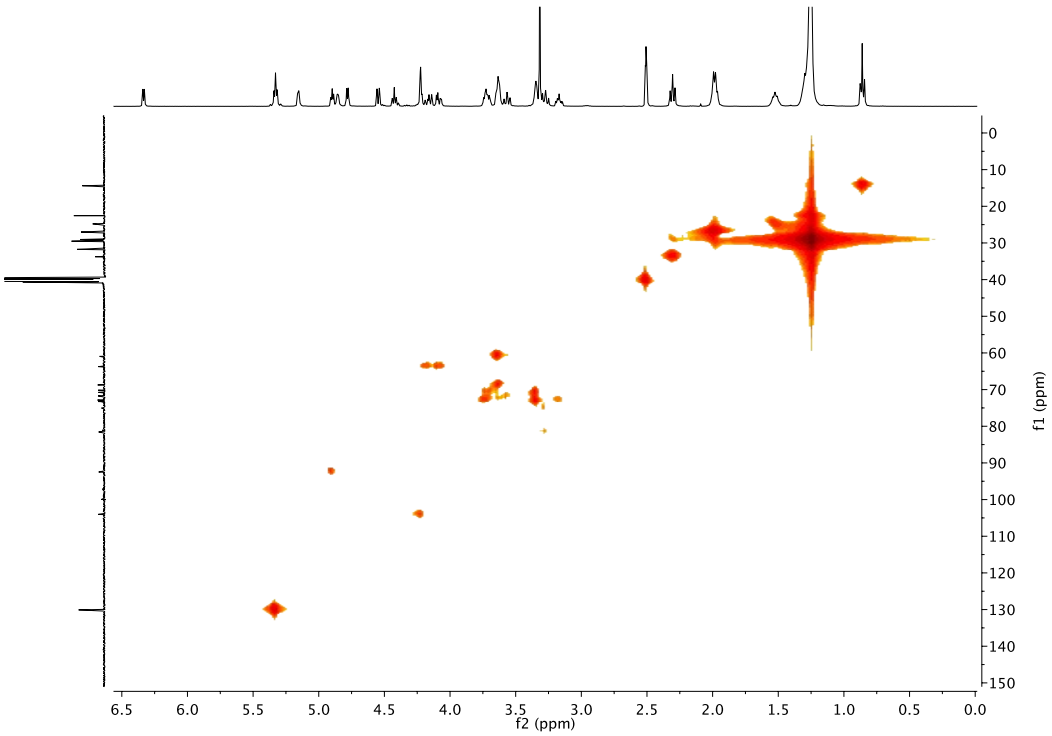

Fig. S8. HMQC NMR spectrum of (*Z*)-6'-*O*-tetracos-15-enoyl-4-*O*-(β-D-galactopyranosyl)-D-glucopyranose in DMSO- d_6.

References

[1] S. Savić, S. Tamburić, M.M. Savić, From conventional towards new natural surfactants in drug delivery systems design: Current status and perspectives, Expert Opin. Drug Deliv. 7 (2010) 353–369.doi:10.1517/17425240903535833.

[2] N.S. Neta, J.A. Teixeira, L.R. Rodrigues, Sugar Ester Surfactants: Enzymatic Synthesis and Applications in Food Industry, Crit. Rev. Food Sci. Nutr. 55 (2015) 595–610. doi:10.1080/10408398.2012.667461.

[3] L. Zhao, H. Zhang, T. Hao, S. Li, In vitro antibacterial activities and mechanism of sugar fatty acid esters against five food-related bacteria, Food Chem. 187 (2015) 370–377. doi:10.1016/j.foodchem.2015.04.108.

[4] P. Nobmann, A. Smith, J. Dunne, G. Henehan, P. Bourke, The antimicrobial efficacy and structure activity relationship of novel carbohydrate fatty acid derivatives against Listeria spp. and food spoilage microorganisms, Int. J. Food Microbiol. 128 (2009) 440–445. doi:10.1016/j.ijfoodmicro.2008.10.008.

[5] C. Stubenrauch, Sugar surfactants — aggregation, interfacial, and adsorption phenomena, Curr. Opin. Colloid Interface Sci. 6 (2001) 160–170. doi:10.1016/S1359-0294(01)00080-2.

[6] T. Uchiyama, T. Sugiyama, Y.-S. Quan, A. Kotani, N. Okada, T. Fujita, S. Muranishi, A. Yamamoto, Enhanced permeability of insulin across the rat intestinal membrane by various absorption enhancers: Their intestinal mucosal toxicity and absorption-enhancing mechanism of n-lauryl-β-D-maltopyranoside, J. Pharm. Pharmacol. 51 (1999) 1241–1250.

[7] F. Ahsan, J. Arnold, E. Meezan, D.J. Pillion, Enhanced bioavailability of calcitonin formulated with alkylglycosides following nasal and ocular administration in rats, Pharm. Res. 18 (2001) 1742–1746.doi:10.1023/A:1013330815253.

[8] D. Vllasaliu, L. Casettari, R. Fowler, R. Exposito-Harris, M. Garnett, L. Illum, S. Stolnik, Absorption-promoting effects of chitosan in airway and intestinal cell lines: A comparative study, Int. J. Pharm. 430 (2012) 151–160. doi:10.1016/j.ijpharm.2012.04.012.

[9] M. Thanou, J.C. Verhoef, H.E. Junginger, Chitosan and its derivatives as intestinal absorption enhancers, Adv. Drug Deliv. Rev. 50 (2001) S91–S101. doi:10.1016/S0169-409X(01)00180-6.

[10] G. Di Colo, Y. Zambito, C. Zaino, Polymeric enhancers of mucosal epithelia permeability: Synthesis, transepithelial penetration-enhancing properties, mechanism of action, safety issues, J. Pharm. Sci. 97 (2008) 1652–1680. doi:10.1002/jps.21043.

[11] D.S. Cox, S. Raje, H. Gao, N.N. Salama, N.D. Eddington, Enhanced permeability of molecular weight markers and poorly bioavailable compounds across Caco-2 cell monolayers using the absorption enhancer, zonula occludens toxin, Pharm. Res. 19 (2002) 1680–1688. doi:10.1023/A:1020709513562.

[12] B.J. Aungst, Absorption enhancers: Applications and advances, AAPS J. 14 (2012) 10–18. doi:10.1208/s12248-011-9307-4.

[13] L. Casettari, L. Illum, Chitosan in nasal delivery systems for therapeutic drugs, J. Controlled Release. 190 (2014) 189–200. doi:10.1016/j.jconrel.2014.05.003.

[14] D.R. Perinelli, L. Casettari, M. Cespi, F. Fini, D.K.W. Man, G. Giorgioni, S. Canala, J.K.W. Lam, G. Bonacucina, G.F. Palmieri, Chemical–physical properties and cytotoxicity of N-decanoyl amino acid-based surfactants: Effect of polar heads, Colloids Surf. Physicochem. Eng. Asp. 492 (2016) 38–46. doi:10.1016/j.colsurfa.2015.12.009.

[15] S. Shubber, D. Vllasaliu, C. Rauch, F. Jordan, L. Illum, S. Stolnik, Mechanism of mucosal permeability enhancement of CriticalSorb® (Solutol® HS15) investigated in vitro in cell cultures, Pharm. Res. 32 (2015) 516–527. doi:10.1007/s11095-014-1481-5.

[16] L.A.W. Thelwall, L. Hough, A.C. Richardson, Sugar acetals, their preparation and use, 1981. http://www.google.ch/patents/US4284763.

[17] J.H. Schwartz, E.A. Talley, Esters of glucose and lactose, J. Am. Chem. Soc. 73 (1951) 4490.

[18] F. Scholnick, M.K. Sucharski, W.M. Linfield, Lactose-derived surfactants (I) fatty esters of lactose, J. Am. Oil Chem. Soc. 51 (1974) 8–11. doi:10.1007/BF02545205.

[19] D.B. Sarney, H. Kapeller, G. Fregapane, E.N. Vulfson, Chemo-enzymatic synthesis of disaccharide fatty acid esters, J. Am. Oil Chem. Soc. 71 (1994) 711–714. doi:10.1007/BF02541426.

[20] M. Habulin, S. Šabeder, Ž. Knez, Enzymatic synthesis of sugar fatty acid esters in organic solvent and in supercritical carbon dioxide and their antimicrobial activity, J. Supercrit. Fluids. 45 (2008) 338–345. doi:10.1016/j.supflu.2008.01.002.

[21] T. Plat, R.J. Linhardt, Syntheses and applications of sucrose-based esters, J. Surfactants Deterg. 4 (2001) 415–421. doi:10.1007/s11743-001-0196-y.

[22] L. Kiss, É. Hellinger, A.-M. Pilbat, Á. Kittel, Z. Tö Rök, Furedi, G. Szakács, S. Veszelka, P. Sipos, B.É. Ózsvári, L.G. Puskás, M. Vastag, P. Szabó -Rèvèsz, M.A. Deli, Sucrose esters increase drug penetration, but do not inhibit P-glycoprotein in Caco-2 intestinal epithelial cells, J. Pharm. Sci. 103 (2014) 3107–3119. doi:10.1002/jps.24085.

[23] A. Szuts, P. Szabó-Révész, Sucrose esters as natural surfactants in drug delivery systems - A mini-review, Int. J. Pharm. 433 (2012) 1–9. doi:10.1016/j.ijpharm.2012.04.076.

[24] D. Vllasaliu, S. Shubber, R. Fowler, M. Garnett, C. Alexander, & S. Stolnik, Epithelial toxicity of alkylglycoside surfactants. *J. Pharm Sci*, *102*(1) (2013) 114-125.

[25] W. Warisnoicharoen, A.B. Lansley, M.J. Lawrence, Toxicological evaluation of mixtures of nonionic surfactants, alone and in combination with oil, J. Pharm. Sci. 92 (2003) 859–868. doi:10.1002/jps.10335.

[26] E.K. Anderberg, P. Artursson, Epithelial transport of drugs in cell culture. VIII: Effects of sodium dodecyl sulfate on cell membrane and tight junction permeability in human intestinal epithelial (Caco-2) cells, J. Pharm. Sci. 82 (1993) 392–398. doi:10.1002/jps.2600820412.

[27] E.K. Anderberg, C. Nyström, P. Artursson, Epithelial transport of drugs in cell culture. VII: Effects of pharmaceutical surfactant excipients and bile acids on transepithelial permeability in monolayers of human intestinal epithelial (Caco-2) cells, J. Pharm. Sci. 81 (1992) 879–887. doi:10.1002/jps.2600810908.

[28] E. Duizer, C. Van Der Wulp, C.H.M. Versantvoort, J.P. Groten, Absorption enhancement, structural changes in tight junctions and cytotoxicity caused by palmitoyl carnitine in Caco-2 and IEC-18 cells, J. Pharmacol. Exp. Ther. 287 (1998)395–402.

[29] S. Gizurarson, C. Marriott, G.P. Martin, E. Bechgaard, The influence of insulin and some excipients used in nasal insulin preparations on mucociliary clearance, Int. J. Pharm. 65 (1990) 243–247. doi:10.1016/0378-5173(90)90149-X.

[30] D.J. Pillion, J.A. Atchison, C. Gargiulo, R.-X. Wang, P. Wang, E. Meezan, Insulin delivery in nosedrops: New formulations containing alkylglycosides, Endocrinology. 135 (1994) 2386–2391 doi:10.1210/en.135.6.2386.

[31] S.B. Petersen, G. Nolan, S. Maher, U.L. Rahbek, M. Guldbrandt, D.J. Brayden, Evaluation of alkylmaltosides as intestinal permeation enhancers: Comparison between rat intestinal mucosal sheets and Caco-2 monolayers, Eur. J. Pharm. Sci. 47 (2012) 701–712. doi:10.1016/j.ejps.2012.08.010.

[32] F. Marçon, V. Moreau, F. Helle, N. Thiebault, F. Djedaïni-Pilard, C. Mullié, β-Alkylated oligomaltosides as new alternative preservatives: Antimicrobial activity, cytotoxicity and preliminary investigation of their mechanism of action, J. Appl. Microbiol. 115 (2013) 977–986. doi:10.1111/jam.12301.

Chapter 3

Lactose oleate as new biocompatible surfactant for pharmaceutical applications

Perinelli DR, Lucarini S, Fagioli L, Campana R, Vllasaliu D, Duranti A, Casettari L. *European Journal of Pharmaceutics and Biopharmaceutics*. March 2018; *124*: 55–62.

3.1 Introduction

Sugar-based surfactants are an emerging broad class of non-ionic amphiphiles characterized by a saccharide or polysaccharide polar moiety, linked to one or more hydrophobic alkyl or acyl chains of different lengths [1].

These surfactants have attracted a large attention in different fields thanks to their promising physico-chemical properties and desirable biodegradability and biocompatibility [2], [3]. Among all sugar-based surfactants, sucrose esters and alkyl glucosides are the most studied and utilised derivatives, particularly in the pharmaceutical, cosmetic and food formulations [4]–[7].

As regards the pharmaceutical perspective, this class of amphiphilic compounds can represent a suitable alternative to the commonly employed non-ionic surfactants (e.g. polysorbates).

For instance, alkyl glycosides have been proposed as replacers of polysorbates in biologics commercial formulations, because of their ability not to induce progressive protein degradation or increased immunogenicity, during manufacturing or storage time prior to administration [8]. Moreover, they may prevent biologics aggregation through the formation of a hydrophilic shield around the exposed hydrophobic sites of partially folded proteins or peptides [9].

Sugar-based surfactants have been also demonstrated to modify the bioavailability of drugs in different dosage forms by influencing the absorption, penetration and dissolution of the payload [10].

As such, new amphiphilic molecules (e.g. alkyl maltosides, sucrose esters) have been recently explored as permeation enhancers for biologics [11]. Their use as permeability enhancers, especially to improve the absorption of macromolecular drug across epithelia, seems to be a promising application of sugar-based surfactants [12].

Several molecules such as medium chain fatty acids (MCFAs), sodium *N*-[8-(2-hydroxybenzoyl)amino] caprylate (SNAC), carnitines, bile salts or polysaccharides like chitosan have been recognised to act as permeation enhancers either by facilitating transcellular transport or modulating the paracellular route through a reversible effect on tight junctions opening [13][14][15].

Among the biological properties, sugar-based surfactants also exhibit an interesting antimicrobial activity, mainly due to the interactions of the surfactants with cell membranes of bacteria [16]. An antiproliferative action has been also observed, which is also attributable to

the interaction/inhibition of these amphiphiles with enzymes involved in the mono/oligosaccharides microbial metabolism [17].

Despite the conspicuous evidences available in the literature about the potential use of sugar-based surfactants for pharmaceutical applications, a limited number of studies has been performed regarding lactose-based surfactants in this field [18].

Our group previously demonstrated the permeability enhancing effect and the antibacterial activity of novel unsaturated fatty acid monoesters based on lactose as polar moiety. Specifically, the synthesized lactose palmitoleate and lactose nervonate showed a marked effect on the permeability of fluorescein isothiocyanate-labeled ovalbumin across Caco-2 cell monolayer at not-toxic concentrations and resulted to be more effective than parabens as preservatives [19].

The work presented in this chapter reports, for the first time, the synthesis and characterization of a new lactose derivative obtained from the enzymatic mono-esterification of lactose with the oleic acid. The chemo- and regioselective mild esterification of lactose was ensured by Lipozyme®, an immobilized lipase obtained from Mucor miehei. The use of biocatalysts to promote ester formation is an example of achievable sustainable chemistry in the field of surfactants synthesis.

The oleic acid was selected as unsaturated fatty acid due to its well-characterized absorption enhancing properties [20]. Moreover, it has an intermediate hydrophobic chain length (C18) that lies between the previously investigate palmitoleic (C16) and nervonic (C24) acids [19].

Lactose oleate was successfully synthetized and widely characterized in terms of physicochemical properties (nuclear magnetic resonance, NMR; mass spectrometry, MS; infrared spectroscopy, IR; differential scanning calorimetry, DSC; circular dichroism, CD; dynamic light scattering, DLS).

Further experiments were performed to assess the cytotoxicity profile (MTS and LDH assays) of these lactose-based surfactants and to evaluate its possible use in pharmaceutical formulations as macromolecular absorption enhancer (Transepithelial Electrical Resistance measurements (TEER) and fluorescent-labelled dextran 4kDa permeability studies on Caco-2 cell monolayers) and preservative agent (minimum inhibitory concentration, MIC).

3.2 Material and methods

3.2.1 Materials

Oleic acid was purchased from TCI, lactose monohydrate from Carlo Erba, while Lipozyme® (immobilized from *Mucor miehei*), *p*-toluenesulfonic acid, 2,2-dimethoxypropane, tetrafluoroboric acid diethyl ether complex and all organic solvents used in the study were purchased from Sigma. Prior to use, acetonitrile was dried with molecular sieves with an effective pore diameter of 4 Å and toluene was saturated with water. Caco-2 cells were obtained from the European Collection of Cell Cultures. Dulbecco's Modified Eagles Medium (DMEM), Hank's Balanced Salt Solution (HBSS, with sodium bicarbonate and without phenol red), non-essential amino acids (100%), L-glutamine (200 mM), fetal bovine serum (FBS), antibiotic/antimycotic solution (10–12,000 U/mL penicillin, 10–12 mg/mL streptomycin, 25–30 μg/mL amphotericin B), trypsin–EDTA solution (2.5 mg/mL trypsin, 0.2 mg/mL EDTA) and fluorescein isothiocyanate-labelled dextran (FD-4) were supplied by Sigma (Poole, UK). MTS reagent, 3-(4,5-dimethylthiazol-2-yl)-5-(3-carboxymethoxyphenyl)-2-(4-sulfophenyl)-2*H*-tetrazolium (commercially known as CellTiter96® AQ_{ueous} One Solution Cell Proliferation Assay) was purchased from Promega (USA). Tissue culture flasks (75 cm^3 with ventilated caps), black 96-well plates and Transwell® inserts (12 mm diameter, 0.4 μm pore size, were purchased from Corning (USA).

3.2.2 Synthesis of (*Z*)-6'-*O*-octadec-9-enoyl-4-*O*-(3',4'-*O*-isopropylidene-β-D-galactopyranosyl)-2,3:5,6-di-*O*-isopropylidene-1,1-di-*O*-methyl-D-glucopyranose (3).

Lipozyme® (0.078 g) was added to a solution of oleic acid (**1**) (0.223 g, 0.79 mmol, 0.249 mL) and 4-*O*-(3',4'-*O*-isopropylidene-β-D-galactopyranosyl)-2,3:5,6-di-*O*-isopropylidene-1,1-di-*O*-methyl-D-glucopyranose (lactose tetra acetale, LTA, previously synthesized according to [21]) (**2**) (0.401 g, 0.79 mmol) in water-saturated toluene (50% v/w, 0.5 mL) at 25 °C [22][19]. The mixture was stirred at 75 °C for 12 h, cooled, diluted with acetone, then filtered, and the filtrate was concentrated. The purification of the residue by column chromatography (cyclohexane/ethyl acetale 8:2) gave **3** as a pale yellow oil. Yield: 62% (0.379 g). ^{1}H NMR (400 MHz, MeOD) δ: 0.92 (t, 3H, J = 7.0 Hz, CH_3), 1.29-1.38 (m, 26H), 1.39 (s, 3H, CH_3), 1.41 (s, 3H, CH_3), 1.44 (s, 3H, CH_3), 1.49 (s, 3H, CH_3),1.59-1.70 (m, 2H, CH_2CH_2COOR), 2.01-2.09 (m, 4H, $CH_2CH{=}CHCH_2$), 2.40 (t, 2H, J = 7.0 Hz, CH_2COOR), 3.30-3.47 (m, 6H, 2 -OCH_3), 3.47 (dd, 1H, $J_{8\text{-}9}$ = 7.0 Hz, $J_{8\text{-}7}$ = 8.0 Hz, H^8), 3.91 (dd, 1H, $J_{4\text{-}3}$ = 1.5 Hz, $J_{4\text{-}5}$ = 6.0 Hz, H^4), 4.04 (ddd, 1H, $J_{11\text{-}12a}$ = 1.5 Hz, $J_{11\text{-}10}$ = 2.5 Hz, $J_{11\text{-}12b}$ = 6.8 Hz,

H^{11}), 4.05 (dd, 1H, $J_{6b\text{-}5}$ = 6.0 Hz, $J_{6b\text{-}6a}$ = 8.5 Hz, H^{6b}),4.08 (dd, 1H, $J_{9\text{-}10}$ = 5.5 Hz, $J_{9\text{-}8}$ = 7.0 Hz, H^{9}), 4.14 (dd, 1H, $J_{3\text{-}4}$ = 1.5 Hz, $J_{3\text{-}2}$ = 7.6 Hz, H^{3}), 4.17 (dd, 1H, $J_{6a\text{-}5}$ = 6.0 Hz, $J_{6a\text{-}6b}$ = 8.5 Hz, H^{6a}), 4.21 (dd, 1H, $J_{10\text{-}11}$ = 2.5 Hz, $J_{10\text{-}9}$ = 5.5 Hz, H^{10}), 4.27 (dd, 1H, $J_{12b\text{-}11}$ = 6.8 Hz, $J_{12b\text{-}12a}$ = 11.5 Hz, H^{12b}), 4.30 (dd, 1H, $J_{12a\text{-}11}$ = 1.5 Hz, $J_{12a\text{-}12b}$ = 11.5 Hz, H^{12a}), 4.31 (ddd, $J_{5\text{-}4} \cong J_{5\text{-}6a} \cong J_{5\text{-}6b}$ = 6.0 Hz, H^{5}), 4.41 (d, 1H, $J_{1\text{-}2}$ = 6.4 Hz, H^{1}), 4.49 (d, 1H, $J_{7\text{-}8}$ = 8.0 Hz, H^{7}), 4.51 (dd, 1H, $J_{2\text{-}1}$ = 6.4 Hz, $J_{2\text{-}3}$ = 7.5 Hz, H^{2}), 5.35 (ddd, 1H, $J_{22\text{-}23a} \cong J_{22\text{-}23b}$ = 6.0 Hz, $J_{22\text{-}21}$ = 11.0 Hz, CH=CH), 5.39 (ddd, 1H, $J_{21\text{-}20a} \cong J_{21\text{-}20b}$ = 6.0 Hz, $J_{21\text{-}22}$ = 11.0 Hz, CH=CH) ppm. ^{13}C NMR (400 MHz, MeOD) δ: 13.0, 22.3, 24.2, 24.6, 25.1, 25.5, 25.6, 26.2, 26.7, 26.7, 27.0, 28.8, 28.8, 28.9, 28.9, 29.0,29.2, 29.4, 29.4, 31.7, 33.5, 53.0, 55.1, 63.0, 65.5, 70.8, 73.3, 73.5, 75.4, 76.4, 76.8, 77.6, 79.4, 103.1, 105.7, 108.4, 109.7, 109.8, 129.4, 129.5, 173.8 ppm. ESI-MS: *m/z* 772 $(M\text{-}H)^-$. IR (Nujol): 2955, 1730, 1711 cm^{-1}.

3.2.3 Synthesis of (*Z*)-6'-*O*-octadec-9-enoyl-4-*O*-(β-D-galactopyranosyl)-D-glucopyranose (4, lactose oleate).

3 (0.332 g, 0.43 mmol) was dissolved in tetrafluoroboric acid diethyl ether complex/water/acetonitrile (3.5 mL, 1:5:500) and the mixture was stirred at 30 °C for 4 h. The product precipitated during the reaction as white solid wa subsequently filtered, washed with acetonitrile, and then dried. The purification by recrystallization from methanol gave **4** (Scheme 1) as white solid. Yield: 30% (0.078 g). ^{1}H NMR (400 MHz, DMSO) δ: 0.86 (t, 3H, *J* = 6.5 Hz, CH_3), 1.16-1.36 (m, 20H, $(\text{-}CH_2\text{-})_n$), 1.47-1.57 (m, 2H, CH_2CH_2COOR), 1.94-2.04 (m, 4H, $CH_2CH{=}CHCH_2$), 2.30 (t, 2H, *J* = 7.5 Hz, CH_2COOR), 3.17 (ddd, 1H, $J_{2\text{-}1}$ = 4.0 Hz, $J_{2\text{-}OH2}$ = 7.0 Hz, $J_{2\text{-}3}$ = 9.5 Hz, H^{2}), 3.27 (dd, 1H, $J_{4\text{-}3} \cong J_{4\text{-}5}$ = 9.5 Hz, H^{4}), 3.32-3.38 (m, 2H, H^{8}, H^{9}), 3.57 (dd, 1H, $J_{3\text{-}2} \cong J_{3\text{-}4}$ = 9.5 Hz, H^{3}), 3.60-3.67 (m, 3 H, H^{6a}, H^{6b}, H^{10}), 3.67-3.76 (m, 2H, H^{5}, H^{11}), 4.08 (dd, 1H, $J_{12b\text{-}11}$ = 4.5 Hz, $J_{12b\text{-}12a}$ =11.5 Hz, H^{12b}), 4.16 (dd, 1H, $J_{12a\text{-}11}$ = 8.5 Hz, $J_{12a\text{-}12b}$ = 11.5 Hz, H^{12a}), 4.20-4.27 (m, 2H, H^{7}, OH^{3}), 4.42 (dd, 1H, $J_{OH6\text{-}6a} \cong J_{OH6\text{-}6b}$ = 6.0 Hz, OH^{6}), 4.55 (d, 1H, $J_{OH2\text{-}2}$ = 7.0 Hz, OH^{2}), 4.78 (d, 1H, $J_{OH10\text{-}10}$ = 5.0 Hz, OH^{10}), 4.86 (brs, 1H, OH), 4.90 (dd, 1H, $J_{1\text{-}OH1} \cong J_{1\text{-}2}$ = 4.0 Hz, H^{1}), 5.15 (brs, 1H, OH), 5.30 (ddd, 1H, $J_{22\text{-}23a} \cong J_{22\text{-}23b}$ = 6.0 Hz, $J_{22\text{-}21}$ = 11.0 Hz, CH=CH), 5.35 (ddd, 1H, $J_{21\text{-}20a} \cong J_{21\text{-}20b}$ = 6.0 Hz, $J_{21\text{-}22}$ = 11.0 Hz, CH=CH), 6.33 (d, 1H, $J_{OH1\text{-}1}$ = 4.0 Hz, OH^{1}) ppm. ^{13}C NMR (400 MHz, DMSO) δ: 14.4, 22.5, 24.8, 27.0, 27.1, 28.9, 29.0, 29.05, 29.06, 29.1, 29.3, 29.6, 31.7, 33.7, 60.9, 63.7, 68.7, 70.2, 70.8, 71.7, 72.7, 72.9, 73.3, 81.6, 92.5, 104.0, 130.1, 130.1, 173.4 ppm. ESI-MS: *m/z* 605 $(M\text{-}H)^-$. IR (Nujol): 3400, 2954, 1734, 1709 cm^{-1}.

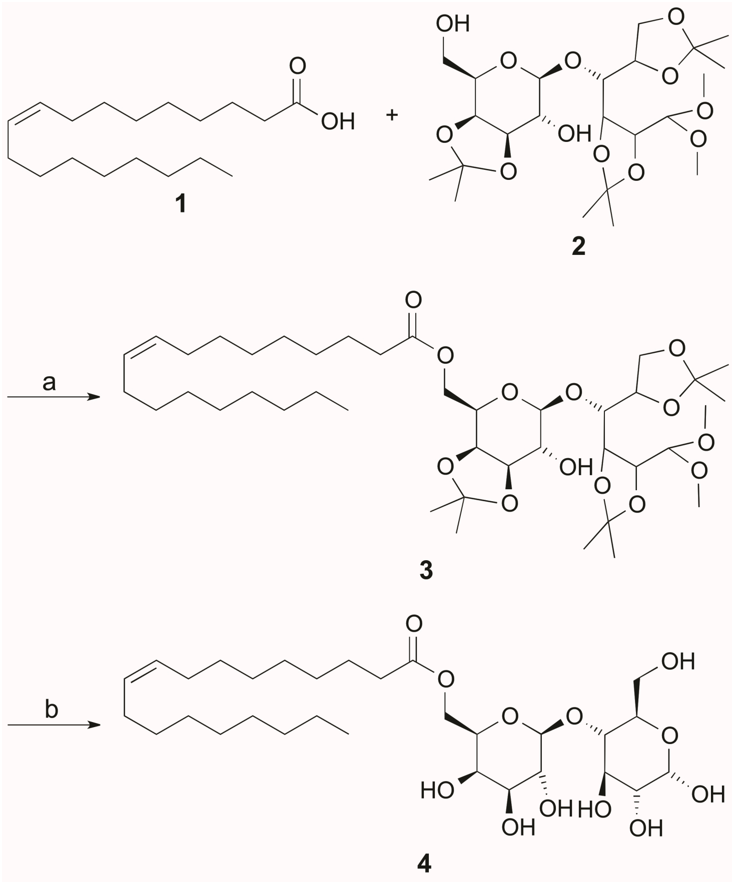

Scheme 1. Reagents and conditions: (a) toluene, 75 °C, 12 h; (b) $HBF_4{\cdot}Et_2O$, CH_3CN, 30 °C, 4 h.

3.2.4 Electronspray ionization mass spectrometry (ESI-MS), nuclear magnetic resonance (NMR) and infrared spectroscopy (IR)

The structures of compounds were unambiguously characterized by ESI-MS, ^{1}H NMR, ^{13}C NMR, and IR. ESI-MS spectra were recorded with a Waters Micromass ZQ spectrometer in a negative or positive mode using a nebulizing nitrogen gas at 400 L/min and a temperature of 250 °C, cone flow 40 mL/min, capillary 3.5 Kvolts and cone voltage 60 V. ^{1}H NMR and ^{13}C NMR spectra were recorded on a Bruker AC 400 or 101, respectively, spectrometer and analyzed using the TopSpin software package. Chemical shifts were measured by using the central peak of the solvent. IR spectra were obtained on a Nicolet Atavar 360 FT spectrometer. Column chromatography purifications were performed under "flash" conditions using Merck 230–400 mesh silica gel. TLC was carried out on Merck silica gel 60 F254 plates, which were visualized by exposure to ultraviolet light and by exposure to an aqueous solution of ceric ammonium molibdate.

3.2.5 Differential scanning calorimetry (DSC)

Thermal analysis was carried out in a DSC 8500 (PerkinElmer, USA), equipped with an intracooler (Intracooler 2, PerkinElmer, USA) under an inert nitrogen atmosphere (flow rate of 20 mL/min). A small amount (2–4 mg) of lactose oleate was placed in a sealed aluminium pan and analysed with respect to the reference.

For the analysis, the following thermal programme was applied: heating from 20 °C to 150 °C, cooling down to 20 °C, isotherm at 20 °C for 3 minutes and heating again to 150 °C. The heating/cooling rate was 10 °C/min. The instrument was calibrated following the manufacturer's procedure using indium and zinc as standards. Thermal parameters were calculated from the thermograms collected from the second heating scan. All runs were performed at least in triplicate.

3.2.6 Dynamic light scattering (DLS) measurement of the critical micelle concentration (CMC).

CMC and the hydrodynamic diameter of surfactant micelles and/or aggregates were determined by DLS technique using a Malvern Zetasizer Nano S (Malvern, Worcestershire, UK). Counts (Kcps), which are a measure of the scattering intensity to the detector, were recorded at different concentrations of lactose oleate solutions and the CMC value was determined by the straight-line interception method as previously reported [23]. Particle size and distribution of surfactants micelles and/or aggregates are expressed as hydrodynamic diameter (nm; from volume distribution %) and width (nm; width of the distribution at half height), respectively. All measurements were performed in triplicate.

3.2.7 Circular dichroism (CD)

Far UV CD spectra of lactose oleate at different concentrations (from 0.015 mg/mL to 1 mg/mL) were collected using a π*-180 step-flow spectrometer (Applied Photophysics, Leatherhead, UK). Spectra were recorded in the range 180-280 nm with a step of 0.1 nm and a bandwidth of 1 nm. The acquisition time was 2 s for each point. 1 mL of surfactant solution was inserted in a 10 mm path length quartz cuvette and measured at room temperature.

3.2.8 Caco-2 cell culture

Caco-2 were cultured in Dulbecco's Modified Eagle Medium (DMEM), supplemented with 10% v/v FBS, 1% v/v antibiotic-antimycotic solution and L-glutamine. Cells were grown to

confluence in T75 flasks at 5% CO_2 and 37 °C, detached from the flasks (using trypsin) and seeded on 96-well plates (for cytotoxicity assays) at 10,000 cells per well or on filter inserts (Transwell®, 0.4 μm pore size, 1.1 cm diameter) at 100,000 cells/cm^2. For transepithelial electrical resistance (TEER) and permeability studies, cells were cultured on Transwell® inserts for 21 days (typical requirement for Caco-2 differentiation) at the conditions detailed above prior to use. The culture medium was changed regularly (every other day). Cell growth, tight junction formation and cell monolayer integrity was ensured through measurement of TEER.

3.2.9 MTS toxicity assay

The effect of lactose oleate on cell viability was measured using the MTS colorimetric assay. Caco-2 cells were cultured on 96-well plates in DMEM for 24 h. Culture medium was replaced with lactose oleate at different concentrations in Hank's Balanced Salt Solution (HBSS). Triton X-100 (0.1% v/v, in HBSS) and HBSS were used as a positive and negative control assuming 0% and 100% cell death, respectively. Cells were incubated (at 37 °C, 5% CO_2) with lactose oleate for 3 h. Thereafter, the assay was performed according to the manufacturer's instructions, with four repeats for each sample.

Relative cell viability (%) was calculated using the following equation:

$$\text{Relative cell viability (\%)} = \frac{S-T}{H-T}\, x100 \qquad \textbf{(Equation 1)}$$

where S is the absorbance of the cells treated with the sample, T is the absorbance of cells treated with Triton X-100, and H is the absorbance of cells incubated with HBSS.

EC_{50} values were calculated by the non-linear regression analysis of the experimental data using a dose–response model (utilizing Prism version 6.0b, GraphPad Software).

3.2.10 LDH assay

LDH assay was used in the study to assess any potential membrane disruption effect exerted by lactose oleate. Caco-2 cells were cultured on 96-well plates. Lactose oleate solution in HBSS were added to the cells at the same concentrations as in MTS assay. Triton X-100 at 1% v/v and HBSS were used as controls. Cells were treated with lactose oleate at 37 °C for 3h. Thereafter, LDH release assay was carried out according to the manufacturer's instructions. LDH release was calculated relative to the controls following the assumption that

cells treated with Triton X-100 resulted in complete LHD release and HBSS-treated cells did not release LDH. The concentration of lactose oleate that induced 50% of LDH release (EC_{50}) was calculated by fitting the experimental data with dose–response model (Prism version 6.0b, GraphPad Software).

3.2.11 Transepithelial electrical resistance (TEER)

Differentiated Caco-2 cell monolayers with a TEER above 800 Ωcm^2 were used in these experiments. Prior to the application of lactose oleate to the cells, culture medium was replaced with HBSS and cells equilibrated in this (at 37 °C, 5% CO_2) for 45 min. An initial TEER recording was then conducted; this was treated as the baseline TEER. Lactose oleate solution at 0.015–0.25 mg/mL concentration range was applied to the apical side of the Caco-2 monolayers for 3 h and TEER measured every 30 min, taking care to ensure consistency in TEER measurement conditions (e.g. measurement time following removal from the incubator) at each interval. Lactose oleate solutions were removed from the cells after 3 h and cells washed with PBS. Culture medium was then added to both sides of the Caco-2 monolayers for overnight incubation. A further TEER recording was conducted 24 h following cell treatment with lactose oleate in order to establish TEER reversibility (if applicable). An EVOM Voltohmmeter (World Precision Instruments, UK), equipped with a pair of chopstick electrodes, was utilized for this study. Background TEER due to the filter (~100–110 Ω cm^2) was considered in all cases. All experiments were performed in triplicates.

3.2.12 Permeability experiments

FITC-Dextran 4 kDa (FD4) was used as model macromolecular drug in conjunction with differentiated Caco-2 cell monolayers with TEER above 800 Ω cm^2. Prior to the application of FD4 and lactose oleate, culture medium was removed and cells washed with PBS. Caco-2 monolayers were then equilibrated in HBSS for 45 min. Lactose oleate at 0.25, 0.12, 0.06 or 0.03 mg/mL and FD4 at 100 μg/mL (in HBSS) were then applied in combination to the apical side of the cell monolayers. Basolateral solution was thereafter sampled (100 μL volumes) at 30, 60, 90, 120, 150 and 180 min after sample application, with replenishment of sampled solution with fresh HBSS. FD4 was quantified by fluorescence, using a Tecan M200 Pro plate reader. After the final sampling, Caco-2 monolayers were washed with PBS and TEER measured to ensure that cell monolayer integrity remained intact during the permeability

experiments. The experiment was conducted in four replicates. FD4 permeability is expressed as apparent permeability coefficient (P_{app}), calculated using the following equation:

$$P_{app} = \left(\frac{\Delta Q}{\Delta t}\right) \times \left(\frac{1}{A \times C_o}\right) \qquad \textbf{(Equation 2)}$$

P_{app}, apparent permeability (cm/s); $\Delta Q/\Delta t$, permeability rate (amount of FD traversing cell monolayers over time); A, diffusion area of the cell monolayer (cm^2); C_0, apically added FD4 concentration.

3.2.13 Bacterial strains and culture conditions

Eight reference human pathogens were used in this study, namely *Escherichia coli* O157:H7 ATCC 35150, *Listeria monocytogenes* ATCC 7644, *Salmonella enteritidis* ATCC 13076, *Enterococcus faecalis* ATCC 29212, *Pseudomonas aeruginosa* ATCC 9027, *Staphylococcus aureus* ATCC 43387, *Yersinia enterocolitica* ATCC 27729 and *Candida albicans* ATCC 14053. All the strains were routinely maintained in Tryptic Soy Agar (TSA, Oxoid, Milan, Italy) at 37 °C, while stock cultures were kept at -80 °C in Nutrient broth (Oxoid) with 15% of glycerol.

3.2.14 Determination of minimum inhibitory concentration (MIC)

MIC determination of lactose oleate was performed by microdilution method. Briefly, 1.28 mg of the test compound was dissolved in DMSO (1 mL); several colonies of each bacterial strain were inoculated in 10 ml of Mueller-Hinton Broth (MHB) (Oxoid) and incubated at 37 °C for 18–24 h. Bacterial suspensions were adjusted to a turbidity (spectrophotometrically determined) corresponding to 10^6 cfu/mL (OD_{610nm} 0.13–0.15). Then, 100 µL of each bacterial suspension were added to a 96-well plate, together with the test solution to obtain final lactose oleate concentrations of 256, 128, 64, 32, 16, 8, 4, 2, 1, 0.5 µg/mL. Positive (bacteria alone) and negative (MHB alone) controls as well as gentamicin (128–0.125 µg/mL) and a standard preservative mixture (methylparaben and propylparaben, ratio 9:1) (1024–0.5 µg/mL) were added as controls. A preliminary assay with DMSO was performed to exclude its possible bacteriostatic and/or bactericidal activity. For this reason, the volume of DMSO never exceeded 5% (v/v) of the final total volume. MIC was defined as the lowest concentration of compound inhibiting the visible bacterial growth after 24 h incubation. All the experiments were performed in duplicate.

3.3 Results and discussion

3.3.1 Synthetic procedure to obtain lactose oleate

Lactose oleate was synthesized by a reaction coupling from oleic acid (**1**) and LTA (**2**) catalyzed by Lipozyme®. The deprotection of the acetalic adducts **3** was performed by using tetrafluoroboric acid diethyl ether complex to obtain the desired product **4** (Scheme 1).

3.3.2 Thermal analyses characterization by DSC

The thermal properties of sugar-based surfactants are very interesting to be investigated since sucrose esters have been demonstrated to act as promising hydrophilic carriers for the preparation of solid dispersions by hot-melt technology in order to increase the dissolution rate of hydrophobic drugs [24][25]. As such, lactose-based surfactants should display the same applicability in this field of technology. Moreover, several sugars surfactants, including lactose-based surfactants, have shown a thermotropic behaviour, thereby forming liquid crystalline phases by heating, thanks to the hydrogen bonding ability of the polyhydroxy polar heads [26].

According to the literature, sucrose esters with low HLB values (generally polyesters) are crystalline and have a melting points around 40-80 °C, while surfactants with high or moderate HLB value (generally monoesters) are amorphous and display a glass transition temperature (*T*g) [27][28].

Fig. 1 shows the thermogram obtained from lactose oleate from the second DSC heating ramp. The thermogram, clearly indicated a variation in the heat capacity (Cp) of the surfactant at the solid state over temperatures, denoting the amorphous state of lactose oleate. The calculated *T*g value from DSC was 62.49±1.45 °C with a ΔCp of 0.265±0.02 J/g °C.

The inset of the figure 1 reports the thermograms obtained from the starting materials as oleic acid and lactose monohydrate for comparison.

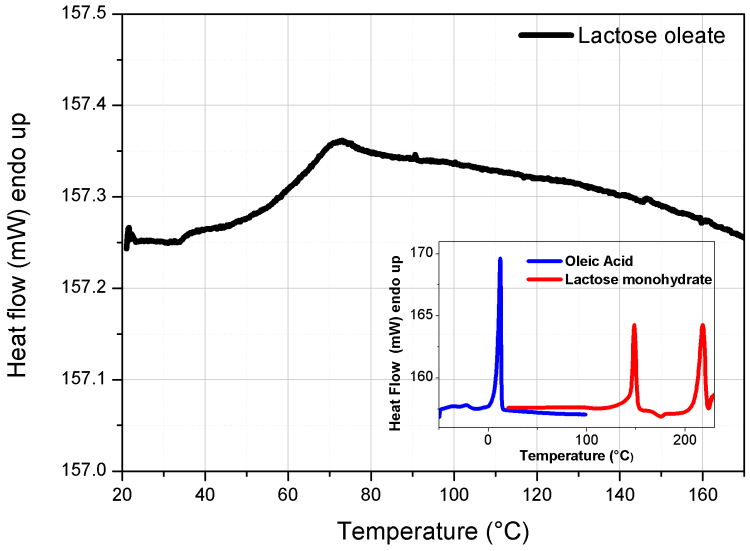

Fig. 1. DSC thermogram of lactose oleate recorded from the second heating ramp (10°C/min). The inset shows the thermograms of oleic acid and lactose monohydrate for comparison.

3.3.3 Determination of critical micelle concentration (CMC) by DLS

CMC is one of the main parameters describing the aggregation behaviour of surfactants, representing the concentration at which all interfaces are saturated and formation of micelles occurs. One of the methods by which CMC can be determined is through dynamic light scattering (DLS). Fig. 2 shows the variation of the scattering intensities to the detector (counts) as a function of surfactant concentration. This pattern has a typical profile. For surfactant concentration below CMC counts are low and comparable to those of HBSS. This is because the contribution to scattering intensity of surfactants as unimers is negligible. On the other hand, micelles formation is associated with a sudden increase in scattering intensity as a consequence of the modified optical properties of the solution. Thus, above CMC, counts are proportional to the number of the micelles in the samples. CMC can be determined by the sharp increase in counts (i.e. breakpoint of the plot in Fig. 2). For lactose oleate, the calculated CMC was 0.148±0.006 mg/mL (0.244±0.01 mM; MW 607.74), which is comparable with the value reported in the literature for sucrose oleate [29]. This denotes the major effect exerted by the nature of the hydrophobic tails (length, presence of unsaturation) with the respect to the hydrophilic heads in affecting the CMC values, as reported for other classes of surfactants [30] [31]. The size of micelles and/or aggregates above CMC was also calculated by DLS. A mean hydrodynamic diameter of 10.3±1.2 nm with a width of the size distribution of 3.09±0.04 nm was measured at a concentration of lactose oleate of 1.5 mg/mL (approximately 10-times CMC).

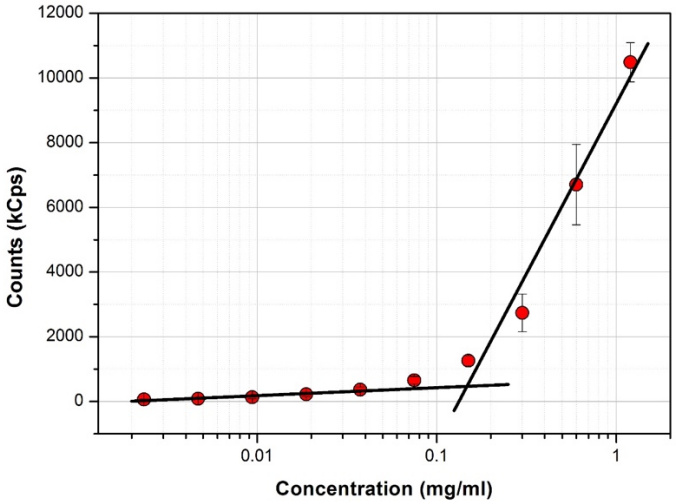

Fig. 2. Counts *vs* surfactant concentration (mg/mL) plot obtained from DLS measurements. The interception point of the two fitting lines represents the CMC value of lactose oleate.

3.3.4 Characterization by circular dichroism (CD)

Circular dichroism is a common technique to study the conformational state of macromolecules as proteins, peptides and nucleic acids [27][28], but sometimes neglected for the analysis of optically-active small molecules. Sugars, being chiral molecules, possess optical rotatory properties and their conformation state in aqueous solutions can be investigated by CD [29][30]. However, the characterization of sugar mono ester aqueous solution by CD at different concentrations has not been reported, to the best of our knowledge, in the literature. Fig. 3 shows the far-UV CD spectra of lactose oleate aqueous solutions at different concentrations. The spectra of lactose oleate in the range of concentration 1 mg/mL to 0.125 mg/mL displayed a broad negative band of ellipticity at around 232 nm. The intensity of this band decreased by lowering the concentration of the surfactant in solution. Interestingly, the disappearance of this signal corresponded at a concentration of surfactants comparable to the calculated CMC by DLS measurements and confirming a different conformation in aqueous solution of lactose oleate surfactant molecules as unimers or in the micellar state.

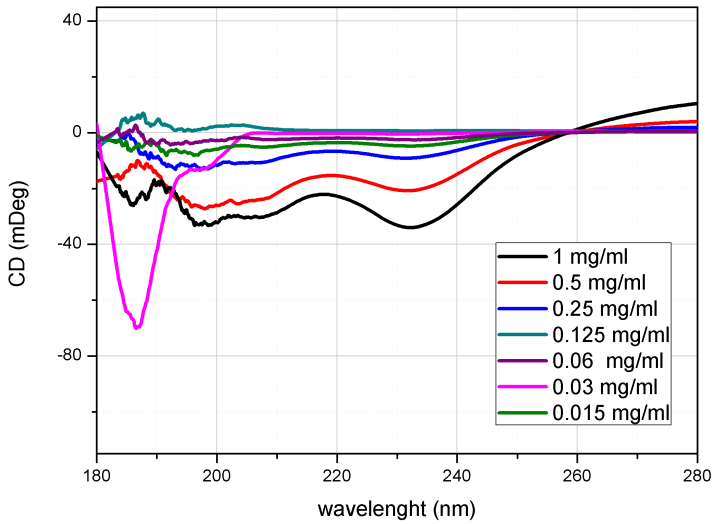

Fig. 3. Far UV circular dichroism spectra of lactose oleate at different concentrations (from 0.015 mg/mL to 1 mg/mL).

3.3.5 Biocompatibility evaluation on Caco-2 cell monolayer

Cytotoxicity of lactose oleate was assessed by MTS and LDH assays on the intestinal human cell line, Caco-2. The calculated EC_{50} values represent the concentration of surfactants causing 50% cell death for MTS and 50% release of the cytoplamatic enzyme lactate dehydrogenase for the LDH assay. The calculated EC_{50} values, based on the data from Fig. 4, were 0.138±0.03 mg/mL (0.227± 0.05 mM; MW 607.74) for MTS and 0.255±0.05 mg/mL (0.420±0.05 mM; MW 607.74) for the LDH assay. These values were found to be comparable (MTS assay) or slightly higher (LDH assay) than CMC, configuring lactose oleate as a relatively safe surfactant. In fact, surfactants, which generally display a high-level of cytotoxicity, showed EC_{50} values lower than CMC [23]. A limited number of studies have been performed to evaluate the cytotoxicity profiles of sugar ester surfactants (generally sucrose esters) on different cell lines [19][36][25][37],despite several data on animal model about their acute toxicity after oral administration or about their mild irritancy capacity on skin or mucosa are available [1].

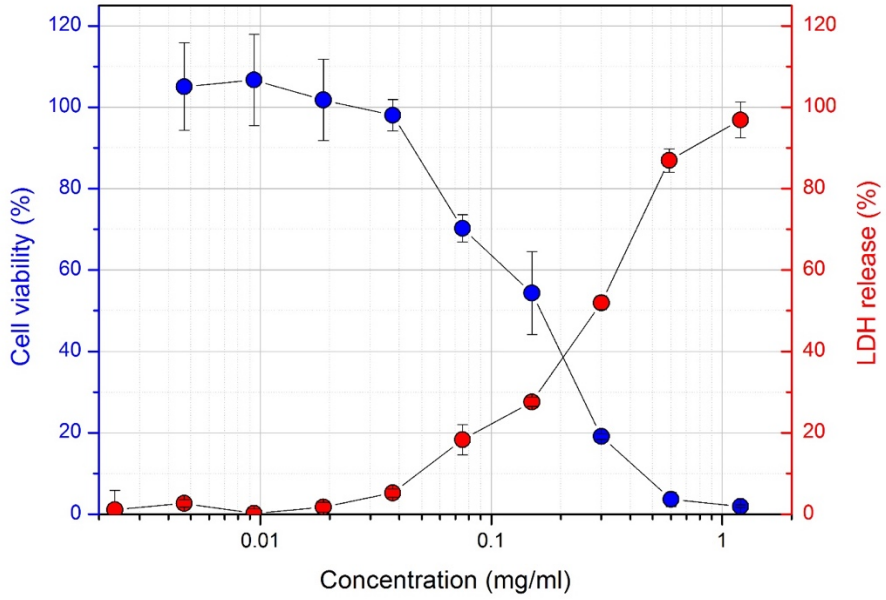

Fig. 4. Cytotoxicity assays results. The plot shows the cell viability (%; from MTS assay) and the LDH release (%; from LDH assay) values for different concentrations of lactose oleate using Caco-2 cells.

3.3.6 TEER experiments

TEER was measured to assess the ability of lactose oleate to open intercellular epithelial tight junctions in Caco-2 monolayer. Concentrations of lactose oleate selected from the cytotoxicity assays (0.015 mg/mL, 0.025 mM; 0.03 mg/mL, 0.05 mM; 0.6 mg/mL, 0.1 mM; 0.125 mg/mL, 0.21 mM; 0.25 mg/mL; 0.41 mM) up to the EC_{50} values, were tested. TEER was found to decrease as a function of lactose oleate concentration, particularly above 0.06 mg/mL (Fig. 5). The maximum decrease in TEER was observed after 120 min, with TEER remaining stable from that point and up to 180 min following the application of the surfactant. TEER values at 120 min were approximately 70%, 55% and 40% of the baseline value for lactose oleate concentrations of 0.06 mg/mL, 0.125mg/mL and 0.25 mg/mL, respectively. TEER recovered after 24 h with all the tested concentrations, indicating the reversible effect of lactose oleate on tight junction opening and no appreciable toxic effect on the cell monolayer.

A comparable effect in decreasing TEER at around 50% of the baseline values is reported for sucrose oleate (O-1570; composed of 70% monoester, 30% di-, tri-, poly-ester) on Caco-2 cell monolayers [11]. The results obtained from TEER measurements confirmed the ability of the unsaturated fatty acid mono ester of lactose to affect the electrical resistance of Caco-2 monolayer, at relatively not-toxic concentrations, by interacting with tight junctions [19].

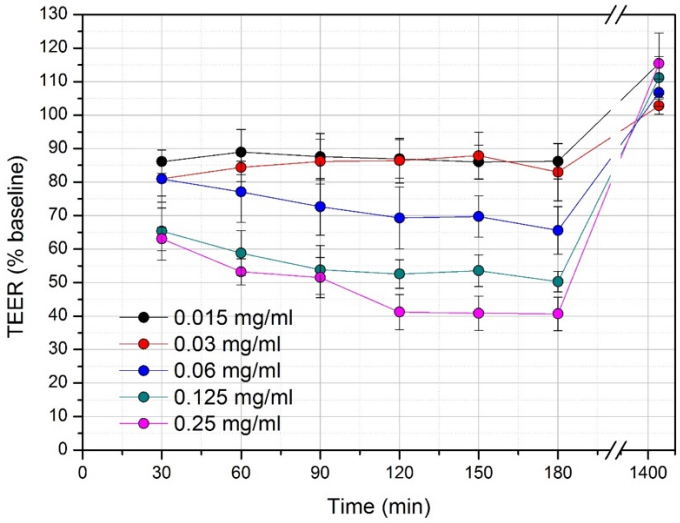

Fig. 5. Effect of different concentrations of lactose oleate (from 0.015 mg/mL; 0.025 mM to 0.25 mg/mL; 0.41 mM) on transepithelial electrical resistance (TEER) of Caco-2 monolayers. Data are presented as the mean ± SEM (n = 3).

3.3.7 Permeability study

The effect of sugar esters (generally sucrose esters) as mucosal enhancers has been only partially explored, since most of the available data are related to the increase in permeability of small molecular drugs. In this regard, the enhancement effect has been demonstrated *in vitro* using different cell lines (e.g. Caco-2, RPMI 2650) [38][37] but also *ex-vivo* and *in-vivo* [39][11].

On the other side, the non-invasive administration of biologic therapeutics (as pharmaceutically active proteins and peptides) have attracted a great interest, following the release in the market of several biotechnological products. In this context, sugar esters could represent a promising option, despite a limited number of studies, mainly focused on the permeability of insulin, has been conducted [40][41].

Lactose oleate, at the same concentrations used for TEER experiments, was subsequently tested for its ability to improve the *in vitro* permeability of FD-4, as model macromolecular drug. Results are expressed in terms of apparent permeability across Caco-2 monolayers (Fig. 6). The observed effect was found to be dependent on the applied surfactant concentration. In fact, FD-4 permeability in presence of the lowest tested concentration of lactose oleate (0.03 mg/mL, 0.05 mM) was comparable to the control (apparent permeabilities of 1.86×10^{-8} and 1.74×10^{-8} cm/s, respectively). On the other hand, the application of larger concentrations (from 0.06 mg/mL to 0.25 mg/mL) led to an increase in FD-4 permeability statistically

different from the control (ANOVA test followed by Dunnett test for multiple comparisons). Specifically, the calculated permeability enhancement was of 2.7-fold, 3.5-fold and 7.7-fold for surfactant concentrations of 0.06 mg/mL (0.1 mM), 0.125 mg/mL (0.21 mM) and 0.25 mg/mL (0.41 mM), respectively.

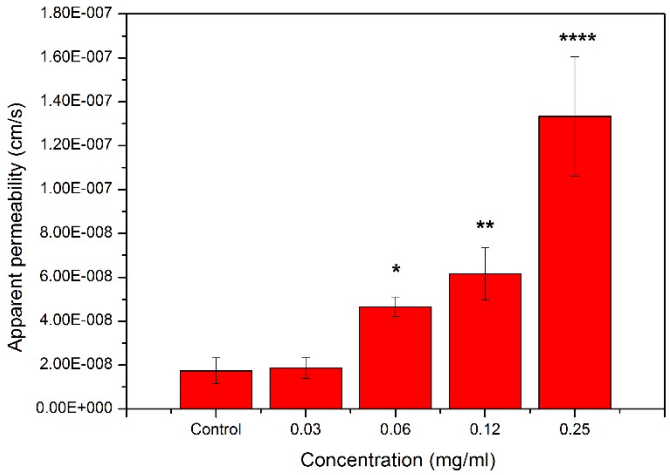

Fig. 6. Effect of different concentrations of lactose oleate (from 0.03 mg/mL, 0.05 mM to 0.25 mg/mL, 0.41 mM) on the apparent permeability of FITC-labelled dextran of 4kDa across Caco-2 cell monolayers. Data are presented as the mean ± SEM (n = 4). ****P<0.0001; ***0.0001<P <0.005; ** 0.005<P<0.01; *0.01<P<0.05.

Taken together, both TEER decrease and FD-4 permeability enhancement showed a trend, dependent on lactose oleate concentration. In fact, a statistically significant increase in FD-4 permeability was only evident at concentration of lactose oleate inducing at least a 30% drop in TEER. Moreover, the more pronounced enhancement in permeability was achieved with the higher tested concentration of lactose oleate (0.25 mg/mL, which also exerted the major observed effect on TEER (60% drop in TEER). These considerations point to a tight junction-related mechanism for the FD-4 absorption enhancing the effect of lactose oleate across Caco-2 cell (i.e. paracellular route), despite a possible involvement of the transcellular route cannot be excluded, as already proposed for other sugar-based surfactants [37].

3.3.8 Antimicrobial activity

Sugar esters have been shown to inhibit microbial growth, but there are conflicting data on the susceptibility of the tested microorganisms. In some studies, the inhibition of Gram-negative or Gram-positive bacteria, when tested alone, was reported [42][43], while in others the comparison regarding the inhibitory effect was performed only on a limited number of

bacterial species [44][45]. As regards lactose derivatives, they are increasingly of interest to the pharmaceutical and food industry since many compounds, such as lactose monolaurate, lactose monodecanoate and others lactose fatty acid esters, have shown a wide antimicrobial activity [45][46]. In the present work, the MICs of lactose oleate were determined against *E. coli* O157:H7 ATCC 35150, *L. monocytogenes* ATCC 7644, *S. enteritidis* AC 13076, *E. fecalis* ATCC 29212, *P. aeruginosa* ATCC 9027, *S. aureus* ATCC 43387, *Y. enterocolitica* ATCC 27729 and *C. albicans* ATCC 14053 according to the National Committee for Clinical Laboratory Standards (NCCLS) document M100-S12 method. The data are summarized in Table 1. As shown, lactose oleate demonstrated a similar antimicrobial activity against the tested food-borne pathogens with MIC values of 0.128 mg/mL, except for *L. monocytogenes* ATCC 7644 (MIC 0.256 mg/mL). This different antimicrobial activity is not clearly understood, but it is supposed to be related to the sugar group attached to the ester, the number and type of fatty acids esterified, and the degree of esterification, as referred by other authors [44][47].

As regards the internal controls, gentamicin showed the lowest MIC value for *S. enteritidis* ATCC 13076 (0.004 mg/mL) and the highest MIC value for *E. coli* O157:H7 ATCC 35150 (0.128 mg/mL), while the used parabens mixture determined MIC values >1.024 mg/mL for all the examined bacterial species.

It is worth to underline that these amphiphiles showed an antibacterial effect (according to the calculated MIC values) over a panel of Gram-negative and Gram-positive bacteria at concentrations comparable to those they are able to exert an *in vitro* permeability enhancer effect on Caco-2 cells. This consideration encourages further studies aimed to clarify the molecular mechanism upon the interesting properties of lactose oleate surfactant.

Table 1. MIC values (mg/mL) of the lactose oleate against selected bacterial strains. Gentamicin and parabens mixture were used as internal controls.

Specie target	MICs (µg/ml)		
	Lactose oleate	Gentamicin	Paraben mix
E. coli O157:H7 ATCC 35150	128	128	>1024
E. faecalis ATCC 29212	128	64	>1024
L. monocytogenes ATCC 7644	256	8	>1024
P. aeruginosa ATCC 9027	128	16	>1024
S. aureus ATCC 43387	128	16	>1024
S. enteritidis ATCC 13076	128	4	>1024
Y. enterocolitica ATCC 27729	128	8	>1024
C. albicans ATCC 10231	128	nd	>1024

3.4 Conclusions

This work reports the synthesis and a comprehensive physicochemical characterization (NMR, ESI-MS, DSC, CD and DLS) of a new sugar-based surfactant, namely lactose oleate, obtained from the enzymatic mono-esterification of lactose and oleic acid. Lactose oleate displayed an acceptable cytotoxicity profile (EC_{50} comparable or higher than CMC) and a concentration-dependent absorption enhancing effect on intestinal Caco-2 monolayers using FD-4 as model for macromolecular drugs. The permeability effect was most pronounced at the highest tested surfactant concentration (0.25 mg/mL, 0.41 mM), which also determined the most remarkable decrease in TEER value. The obtained results suggest the involvement of the intercellular tight junction opening (paracellular route) in the increased permeability of FD-4 in presence of lactose oleate, although a combined effect, correlated to other mechanisms (e.g. transcytosis) cannot be excluded. Moreover, this work also introduces lactose oleate as antimicrobial agent (MIC values) intermediate between those of some antibiotics and common preservatives (i.d. parabens). Overall, this study highlights the potential use of lactose oleate in pharmaceutical formulations as an absorption enhancer and/or an alternative preservative.

Supporting Information

(*Z*)-6'-*O*-octadec-9-enoyl-4-*O*-(β-D-galactopyranosyl)-D-glucopyranose

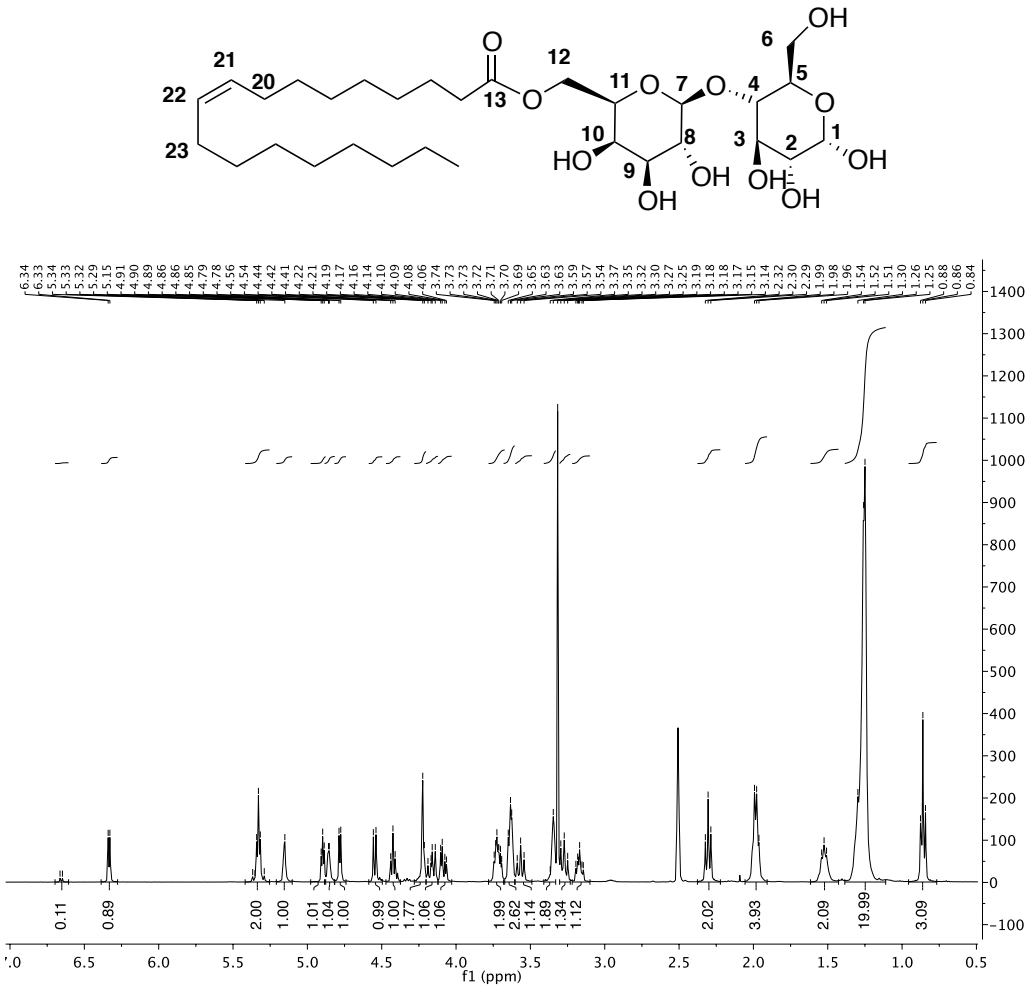

Fig. S1. [1]H NMR spectrum of (*Z*)-6'-*O*-octadec-9-enoyl-4-*O*-(β-D-galactopyranosyl)-D-glucopyranose in d_6 DMSO- d_6.

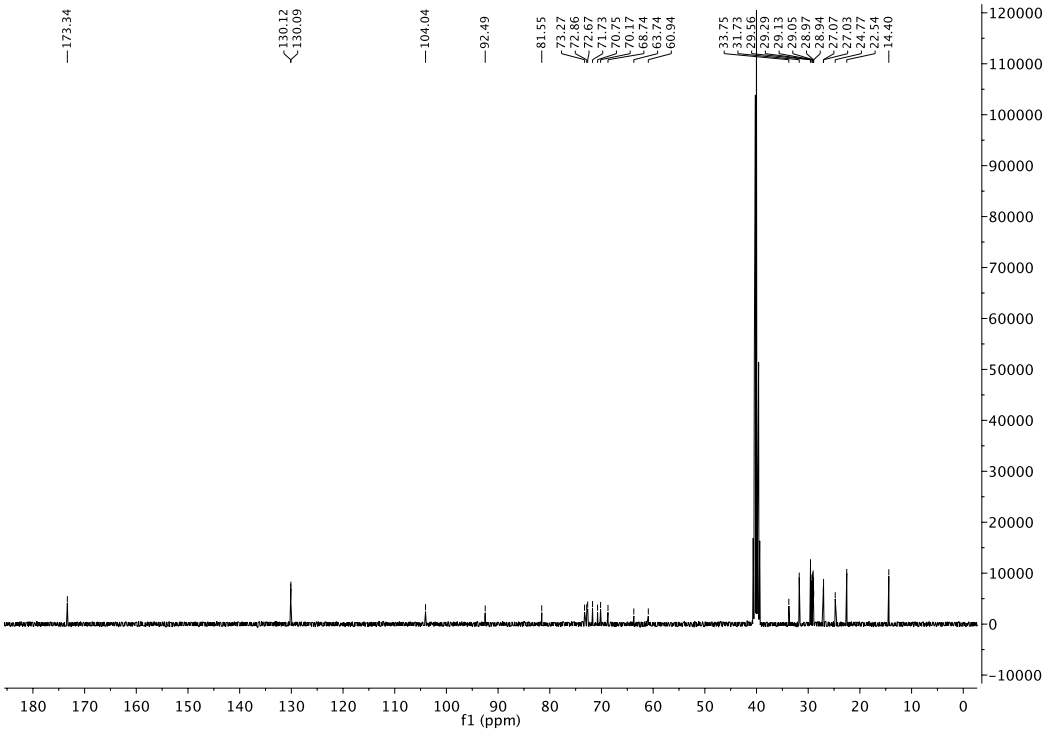

Fig. S2. ^{13}C NMR spectrum of (*Z*)-6'-*O*-octadec-9-enoyl-4-*O*-(β-D-galactopyranosyl)-D-glucopyranose in DMSO- d_6.

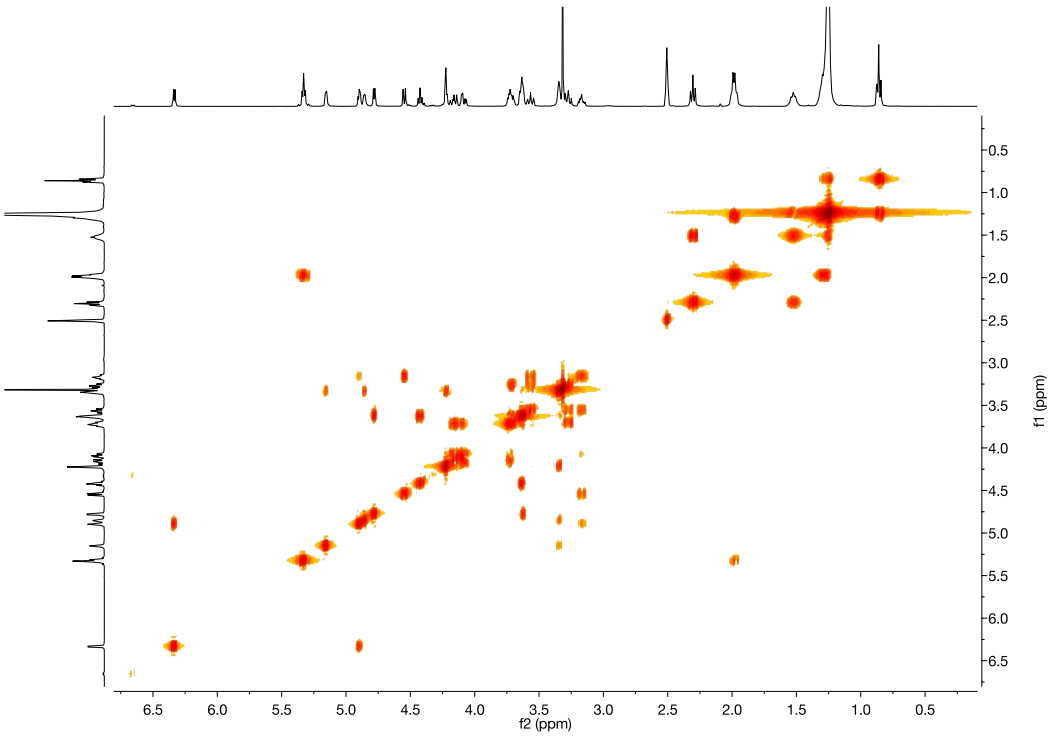

Fig. S3. COSY NMR spectrum of (*Z*)-6'-*O*-octadec-9-enoyl-4-*O*-(β-D-galactopyranosyl)-D-glucopyranose in DMSO- d_6.

References

[1] A. Szűts, P. Szabó-Révész, Sucrose esters as natural surfactants in drug delivery systems—A mini-review, Int. J. Pharm. 433 (2012) 1–9. doi:10.1016/j.ijpharm.2012.04.076.

[2] I.J.A. Baker, B. Matthews, H. Suares, I. Krodkiewska, D.N. Furlong, F. Grieser, C.I. Drummond, Sugar fatty acid ester surfactants: Structure and ultimate aerobic biodegradability, J. Surfactants Deterg. 3 (2000) 1–11. doi:10.1007/s11743-000-0107-2.

[3] I. Söderberg, C.J. Drummond, D. Neil Furlong, S. Godkin, B. Matthews, Non-ionic sugar-based surfactants: Self assembly and air/water interfacial activity, Colloids Surfaces A Physicochem. Eng. Asp. 102 (1995) 91–97. doi:10.1016/0927-7757(95)03250-H.

[4] T.A.S. Aguirre, M. Rosa, S.S. Guterres, A.R. Pohlmann, I. Coulter, D.J. Brayden, Investigation of coco-glucoside as a novel intestinal permeation enhancer in rat models, Eur. J. Pharm. Biopharm. 88 (2014) 856–865. doi:10.1016/j.ejpb.2014.10.013.

[5] F. Ahsan, J. Arnold, E. Meezan, D.J. Pillion, Enhanced bioavailability of calcitonin formulated with alkylglycosides following nasal and ocular administration in rats., Pharm. Res. 18 (2001) 1742–6.

[6] K. Hill, O. Rhode, Sugar-based surfactants for consumer products and technical applications, Lipid - Fett. 101 (1999) 25–33. doi:10.1002/(SICI)1521-4133(19991)101:1<25::AID-LIPI25>3.0.CO;2-N.

[7] N.S. Neta, J.A. Teixeira, L.R. Rodrigues, Sugar Ester Surfactants: Enzymatic Synthesis and Applications in Food Industry, Crit. Rev. Food Sci. Nutr. 55 (2015) 595–610. doi:10.1080/10408398.2012.667461.

[8] E.T. Maggio, Alkylsaccharides: circumventing oxidative damage to biotherapeutics caused by polyoxyethylene-based surfactants, Ther. Deliv. 4 (2013) 567–572. doi:10.4155/tde.13.19.

[9] H. Hamada, T. Arakawa, K. Shiraki, Effect of additives on protein aggregation., Curr. Pharm. Biotechnol. 10 (2009) 400–7.

[10] S. Maher, R.J. Mrsny, D.J. Brayden, Intestinal permeation enhancers for oral peptide delivery, Oral Deliv. Pept. Issues Transl. 106, Part (2016) 277–319. doi:10.1016/j.addr.2016.06.005.

[11] T. Alama, H. Katayama, S. Hirai, S. Ono, A. Kajiyama, K. Kusamori, H. Katsumi, T. Sakane, A. Yamamoto, Enhanced oral delivery of alendronate by sucrose fatty acids esters in rats and their absorption-enhancing mechanisms, Int. J. Pharm. 515 (2016) 476–489. doi:10.1016/j.ijpharm.2016.10.046.

[12] S.B. Petersen, G. Nolan, S. Maher, U.L. Rahbek, M. Guldbrandt, D.J. Brayden, Evaluation of alkylmaltosides as intestinal permeation enhancers: Comparison between rat intestinal mucosal sheets and Caco-2 monolayers, Eur. J. Pharm. Sci. 47 (2012) 701–712. doi:10.1016/j.ejps.2012.08.010.

[13] S.M. Krug, M. Amasheh, I. Dittmann, I. Christoffel, M. Fromm, S. Amasheh, Sodium caprate as an enhancer of macromolecule permeation across tricellular tight junctions of intestinal cells, Biomaterials. 34 (2013) 275–282. doi:10.1016/j.biomaterials.2012.09.051.

[14] S. Maher, R.J. Mrsny, D.J. Brayden, Intestinal permeation enhancers for oral peptide delivery, Adv. Drug Deliv. Rev. 106 (2016) 277–319. doi:10.1016/j.addr.2016.06.005.

[15] D. Vllasaliu, L. Casettari, R. Fowler, R. Exposito-Harris, M. Garnett, L. Illum, S. Stolnik, Absorption-promoting effects of chitosan in airway and intestinal cell lines: A comparative study, Int. J. Pharm. 430 (2012) 151–160. doi:10.1016/j.ijpharm.2012.04.012.

[16] M. le Maire, P. Champeil, J. V Moller, Interaction of membrane proteins and lipids with solubilizing detergents., Biochim. Biophys. Acta. 1508 (2000) 86–111.

[17] F. Marçon, V. Moreau, F. Helle, N. Thiebault, F. Djedaïni-Pilard, C. Mullié, β-Alkylated oligomaltosides as new alternative preservatives: antimicrobial activity, cytotoxicity and preliminary investigation of their mechanism of action, J. Appl. Microbiol. 115 (2013) n/a-n/a. doi:10.1111/jam.12301.

[18] J. Staroń, J.M. Dąbrowski, E. Cichoń, M. Guzik, Lactose esters: synthesis and biotechnological applications, Crit. Rev. Biotechnol. (2017) 1–14. doi:10.1080/07388551.2017.1332571.

[19] S. Lucarini, L. Fagioli, R. Campana, H. Cole, A. Duranti, W. Baffone, D. Vllasaliu, L. Casettari, Unsaturated fatty acids lactose esters: cytotoxicity, permeability enhancement and antimicrobial activity, Eur. J. Pharm. Biopharm. 107 (2016) 88–96. doi:10.1016/j.ejpb.2016.06.022.

[20] M.A. Deli, Potential use of tight junction modulators to reversibly open membranous barriers and improve drug delivery, Biochim. Biophys. Acta - Biomembr. 1788 (2009) 892–910. doi:10.1016/j.bbamem.2008.09.016.

[21] L.A.W. Thelwall, L. Hough, A.C. Richardson, Sugar acetals, their preparation and use, US4284763 A, 1980.

[22] D.B. Sarney, H. Kapeller, G. Fregapane, E.N. Vulfson, Chemo-enzymatic synthesis of disaccharide fatty acid esters, J. Am. Oil Chem. Soc. 71 (1994) 711–714. doi:10.1007/BF02541426.

[23] D.R. Perinelli, L. Casettari, M. Cespi, F. Fini, D.K.W. Man, G. Giorgioni, S. Canala, J.K.W. Lam, G. Bonacucina, G.F. Palmieri, Chemical–physical properties and cytotoxicity of N-decanoyl amino acid-based surfactants: Effect of polar heads, Colloids Surfaces A Physicochem. Eng. Asp. 492 (2016) 38–46. doi:10.1016/j.colsurfa.2015.12.009.

[24] A. Szűts, Z. Makai, R. Rajkó, P. Szabó-Révész, Study of the effects of drugs on the structures of sucrose esters and the effects of solid-state interactions on drug release, J. Pharm. Biomed. Anal. 48 (2008) 1136–1142. doi:10.1016/j.jpba.2008.08.028.

[25] A. Szűts, P. Láng, R. Ambrus, L. Kiss, M.A. Deli, P. Szabó-Révész, Applicability of sucrose laurate as surfactant in solid dispersions prepared by melt technology, Int. J. Pharm. 410 (2011) 107–110. doi:10.1016/j.ijpharm.2011.03.033.

[26] C.J. Drummond, D. Wells, Nonionic lactose and lactitol based surfactants: comparison of some physico-chemical properties, Colloids Surfaces A Physicochem. Eng. Asp. 141 (1998) 131–142. doi:10.1016/S0927-7757(98)00209-X.

[27] A. Szűts, E. Pallagi, G. Regdon, Z. Aigner, P. Szabó-Révész, Study of thermal behaviour of sugar esters, Int. J. Pharm. 336 (2007) 199–207. doi:10.1016/j.ijpharm.2006.11.053.

[28] S. Ogawa, K. Asakura, S. Osanai, V. Rodriguez-Mora, M.A. Ramos, R. Luckhurst, T. Benvegnu, P. Boullanger, D. Lafont, Y. Queneau, S. Chambert, J. Fitremann, Thermotropic and glass transition behaviors of n-alkyl β-d-glucosides, RSC Adv. 3 (2013) 21439. doi:10.1039/c3ra43187h.

[29] H.A. Ayala-Bravo, D. Quintanar-Guerrero, A. Naik, Y.N. Kalia, J.M. Cornejo-Bravo, A. Ganem-Quintanar, Effects of Sucrose Oleate and Sucrose Laureate on in Vivo Human Stratum Corneum Permeability, Pharm. Res. 20 (2003) 1267–1273. doi:10.1023/A:1025013401471.

[30] D. Romano Perinelli, M. Cespi, L. Casettari, D. Vllasaliu, M. Cangiotti, M.F. Ottaviani, G. Giorgioni, G. Bonacucina, G.F. Palmieri, Correlation among chemical structure, surface properties and cytotoxicity of N-acyl alanine and serine surfactants, (2016). doi:10.1016/j.ejpb.2016.09.015.

[31] T. Zhang, R.E. Marchant, Novel Polysaccharide Surfactants: The Effect of Hydrophobic and Hydrophilic Chain Length on Surface Active Properties, J. Colloid Interface Sci. 177 (1996) 419–426. doi:10.1006/jcis.1996.0054.

[32] K. Bakshi, M.R. Liyanage, D.B. Volkin, C.R. Middaugh, Circular Dichroism of Peptides, in: A.E. Nixon (Ed.), Ther. Pept. Methods Protoc., Humana Press, Totowa, NJ, 2014: pp. 247–253.

[33] N.J. Greenfield, Using circular dichroism spectra to estimate protein secondary structure, Nat. Protoc. 1 (2007) 2876–2890. doi:10.1038/nprot.2006.202.

[34] E.A. Kabat, K.O. Lloyd, S. Beychok, Optical activity and conformation of carbohydrates. II. Optical rotatory dispersion and circular dichroism studies on immunochemically reactive oligo- and polysaccharides containing amino sugars and their derivatives, Biochemistry. 8 (1969) 747–756. doi:10.1021/bi00831a001.

[35] T. Taniguchi, K. Monde, Vibrational circular dichroism (VCD) studies on disaccharides in the CH region: toward discrimination of the glycosidic linkage position, Org. Biomol. Chem. 5 (2007) 1104–1110. doi:10.1039/B618841A.

[36] K. Valdés, M.J. Morilla, E. Romero, J. Chávez, Physicochemical characterization and cytotoxic studies of nonionic surfactant vesicles using sucrose esters as oral delivery systems, Colloids Surfaces B Biointerfaces. 117 (2014) 1–6. doi:10.1016/j.colsurfb.2014.01.029.

[37] L. Kiss, É. Hellinger, A.-M. Pilbat, Á. Kittel, Z. Török, A. Füredi, G. Szakács, S. Veszelka, P. Sipos, B. Ózsvári, L.G. Puskás, M. Vastag, P. Szabó-Révész, M.A. Deli, J. Mönkkönen, C. O'Driscoll, H.M. Oppers-Tiemissen, E.G. Ragnarsson, M. Rooseboom, A.L. Ungell, Sucrose esters increase drug penetration, but do not inhibit p-glycoprotein in caco-2 intestinal epithelial cells., J. Pharm. Sci. 103 (2014) 3107–19. doi:10.1002/jps.24085.

[38] L. Kürti, S. Veszelka, A. Bocsik, N.T.K. Dung, B. Ózsvári, L.G. Puskás, Á. Kittel, P. Szabó-Révész, M.A. Deli, The effect of sucrose esters on a culture model of the nasal barrier, Toxicol. Vitr. 26 (2012) 445–454. doi:10.1016/j.tiv.2012.01.015.

[39] A. Ganem-Quintanar, D. Quintanar-Guerrero, F. Falson-Rieg, P. Buri, Ex vivo oral mucosal permeation of lidocaine hydrochloride with sucrose fatty acid esters as absorption enhancers, Int. J. Pharm. 173 (1998) 203–210. doi:10.1016/S0378-5173(98)00226-9.

[40] D.J. Pillion, F. Ahsan, J.J. Arnold, B.M. Balusubramanian, O. Piraner, E. Meezan, Synthetic long-chain alkyl maltosides and alkyl sucrose esters as enhancers of nasal insulin absorption, J. Pharm. Sci. 91 (2002) 1456–1462. doi:10.1002/jps.10150.

[41] F. Ahsan, J.J. Arnold, E. Meezan, D.J. Pillion, Sucrose cocoate, a component of cosmetic preparations, enhances nasal and ocular peptide absorption, Int. J. Pharm. 251 (2003) 195–203. doi:10.1016/S0378-5173(02)00597-5.

[42] D. Xiao, R. Ye, P.M. Davidson, D.G. Hayes, D.A. Golden, Q. Zhong, Sucrose monolaurate improves the efficacy of sodium hypochlorite against Escherichia coli O157:H7 on spinach, Int. J. Food Microbiol. 145 (2011) 64–68. doi:10.1016/j.ijfoodmicro.2010.11.029.

[43] T. Watanabe, S. Katayama, M. Matsubara, Y. Honda, M. Kuwahara, Antibacterial carbohydrate monoesters suppressing cell growth of Streptococcus mutans in the presence of sucrose., Curr. Microbiol. 41 (2000) 210–3.

[44] P. Nobmann, A. Smith, J. Dunne, G. Henehan, P. Bourke, The antimicrobial efficacy and structure activity relationship of novel carbohydrate fatty acid derivatives against Listeria spp. and food spoilage microorganisms, Int. J. Food Microbiol. 128 (2009) 440–445. doi:10.1016/j.ijfoodmicro.2008.10.008.

[45] A. Wagh, S. Shen, F.A. Shen, C.D. Miller, M.K. Walsh, Effect of Lactose Monolaurate on Pathogenic and Nonpathogenic Bacteria, Appl. Environ. Microbiol. 78 (2012) 3465–3468. doi:10.1128/AEM.07701-11.

[46] S.-M. Lee, G. Sandhu, M.K. Walsh, Growth inhibitory properties of lactose fatty acid esters, Saudi J. Biol. Sci. (2015). doi:10.1016/j.sjbs.2015.10.013.

[47] A. Smith, P. Nobmann, G. Henehan, P. Bourke, J. Dunne, Synthesis and antimicrobial evaluation of carbohydrate and polyhydroxylated non-carbohydrate fatty acid ester and ether derivatives, Carbohydr. Res. 343 (2008) 2557–2566. doi:10.1016/j.carres.2008.07.012.

Chapter 4

Synthesis, physicochemical characterization and cytotoxicity studies of a series of saturated fatty acids lactose monoesters applied as drug permeability enhancers

Manuscript in preparation

4.1 Introduction

A major concern related to the use of traditional surfactants is their unacceptable toxicological profile that highly limited their application over the years. Moreover, recent evidences have demonstrated the environmental effects associated with their prolonged use, mainly derived from their non-biodegradability [1]. Therefore, many efforts have been made to develop innovative surfactants with an increased biocompatibility and a higher environmental sustainability. In this regard, sugar-based surfactants have recently emerged as a promising alternative due to their attractive characteristics. They are non-ionic surfactants constituted by a carbohydrate as polar head group, linked to a fatty acid or alcohol as alkyl chain. By varying the carbohydrate moiety and the alkyl chain, various sugar surfactants can be easily obtained, while at the same time different degree of substitution can be achieved. As result, surfactants with various hydrophilic lipophilic balance (HLB) have been designed and then tested for physicochemical and biological properties.

Made up of natural substrates, easily available and therefore inexpensive and renewable, sugar-based surfactants are considered ideal materials to employ in cosmetics, food, detergent and pharmaceutical fields for their excellent surface and antimicrobial properties [2–4]. Sugar surfactants are receiving growing attention as strict requirements for non toxic, non irritant and highly biocompatible and biodegradable compounds increases [5,6].

Although toxicity has been demonstrated to be mainly dependent on the hydrocarbon chain length of the surfactant, studies are still required in order to further investigate the relationship between the physicochemical properties and the biocompatibility of different classes of surfactants [7] [8].

Among the various sugar-based surfactants, sugar esters (SEs) are a relatively new class of non-ionic surfactants that possess attractive characteristics suitable for different applications. In this regard, sucrose esters have received a particular attention and are actually employed as innovative surfactants both in food, cosmetic and pharmaceutical industries, as alternatives to the traditional surfactants.

Our research interest has been focused on lactose-based surfactants, monoesterified with different fatty acids. Previous studies were dedicated to the investigation of a series of novel unsaturated fatty acid lactose monoesters [9]. Lactose palmitoleate, lactose oleate and lactose nervonate were fully characterized for their physicochemical properties and studied for their biocompatibility, antimicrobial activity and absorption enhancing properties.

The aim of this work was to systematically investigate the structure-activity relationship and toxicological profile (MTT and LDH) of a series of saturated lactose esters derivatives. Lactose-based surfactants monoesterified with various fatty acids (C10, C12, C14 and C16) were successfully synthetized and characterized for their surface tension and critical micelle concentration (CMC) in order to establish a correlation between the hydrophobic chain length and critical micelles concentration (CMC).

Moreover, absorption enhancing properties have been studied by measuring the trans epithelial electrical resistance (TEER) on Calu-3 cells as model for the human airway epithelium.

4.2 Experimental section

4.2.1 Materials and methods

Decanoic acid, lauric acid, myristic acid and palmitic acid were purchased from TCI, lactose monohydrate from Carlo Erba, while Lipozyme® (immobilized from Mucor miehei), p-toluenesulfonic acid, 2,2-dimethoxypropane, tetrafluoroboric acid diethyl ether complex and all organic solvents used in this study were purchased from Sigma. Prior to use, acetonitrile was dried with molecular sieves with an effective pore diameter of 4 Å and toluene was saturated with water.

Calu-3 cells were obtained from American Type Culture Collection (Manassas, VA, USA).

Calu-3 cells were cultured in Dulbecco's Modified Eagles Medium: Nutrient Mixture F-12 (DMEM F-12) supplemented with 10% fetal bovine serum (FBS) and 1% antibiotics-antimycotic solution. All cell lines were maintained at a 5% CO2 in a humidified incubator at 37 °C.

The structures of compounds were unambiguously assessed by ^{1}H NMR and ^{13}C NMR recorded on a Bruker AC 400 or 101, respectively, spectrometer and analyzed using the TopSpin software package. Chemical shifts were measured by using the central peak of the solvent. Column chromatography purifications were performed under "flash" conditions using Merck 230-400 mesh silica gel. TLC was carried out on Merck silica gel 60 F254 plates, which were visualized by exposure to an aqueous solution of ceric ammonium molibdate.

4.2.2 Synthesis of lactose-based surfactants

4.2.2.1 General procedure for the synthesis of lactose tetra acetal monoesters (3a-3d).

Lipozyme® (0.078 g) was added to a solution of fatty acid (**1a-d**) (0.79 mmol) and 4-*O*-(3',4'-*O*-isopropylidene-β-D-galactopyranosyl)-2,3:5,6-di-*O*-isopropylidene-1,1-di-*O*-methyl-D-glucopyranose (lactose tetra acetate, LTA, previously synthetized according to Thelwall et al. [10]) (**2**) (0.401 g, 0.79 mmol) in water-satured toluene at 25 °C [11,12] . The mixture was stirred at 75 °C for 12 h, cooled and diluted with acetone, then the enzyme was filtered and the filtrate was concentrated. The resulting crude products were purified by column flash chromatography on silica gel (cyclohexan/ EtOAc 8:2 as eluent) to give compound **3a-d** (Scheme 1) as pale yellow oils.

3a [6'-*O*-decanoyl-4-*O*-(3',4'-*O*-isopropylidene-β-D-galactopyranosyl)-2,3:5,6-di-*O*-isopropylidene -1,1-di-*O*-methyl-D-glucopyranose]. Yield: 53% (0.275 g). ^{1}H NMR (400 MHZ, MeOD) δ: 0.92 (t, 3H, J = 6.7 Hz, CH_3),1.32 (s, 6H, 2 CH_3), 1.33-1.37 (m, 12 H, (-CH_2-)$_n$), 1.39 (s, 3H, CH_3), 1.41 (s, 3H, CH_3), 1.44 (s, 3H, CH_3), 1.49 (s, 3H, CH_3),1.62-1.67 (m, 2H, $CH_2$$CH_2$COOR), 2.40 (t, 2H, J = 7.0 Hz, CH_2COOR), 3.46 (s, 6H, 2 OCH_3), 3.47 (dd, 1H, $J_{8\text{-}9}$ = 7.0 Hz, $J_{8\text{-}7}$ = 8.0 Hz, H^8), 3.91 (dd, 1H, $J_{4\text{-}3}$ = 1.2 Hz, $J_{4\text{-}5}$ = 5.0 Hz, H^4), 4.04 (ddd, 1H, $J_{11\text{-}12a}$ = 1.5 Hz, $J_{11\text{-}10}$ = 2.1 Hz, $J_{11\text{-}12b}$ = 6.8 Hz, H^{11}), 4.05 (dd, 1H, $J_{6b\text{-}5}$ = 6.0 Hz, $J_{6b\text{-}6a}$ = 8.7 Hz, H^{6b}),4.08 (dd, 1H, $J_{9\text{-}10}$ = 5.5 Hz, $J_{9\text{-}8}$ = 7.0 Hz, H^9), 4.14 (dd, 1H, $J_{3\text{-}4}$ = 1.2 Hz, $J_{3\text{-}2}$ = 7.5 Hz, H^3), 4.17 (dd, 1H, $J_{6a\text{-}5}$ = 6.0 Hz, $J_{6a\text{-}6b}$ = 8.7 Hz, H^{6a}), 4.22 (dd, 1H, $J_{10\text{-}11}$ = 2.1 Hz, $J_{10\text{-}9}$ = 5.5 Hz, H^{10}), 4.27 (dd, 1H, $J_{12b\text{-}11}$ = 6.8 Hz, $J_{12b\text{-}12a}$ = 11.5 Hz, H^{12b}), 4.30 (dd, 1H, $J_{12a\text{-}11}$ = 1.5 Hz, $J_{12a\text{-}12b}$ = 11.5 Hz, H^{12a}), 4.31 (ddd, 1H, $J_{5\text{-}4}$ = 5.0 Hz, $J_{5\text{-}6a} \cong J_{5\text{-}6b}$ = 6.0 Hz, H^5), 4.41 (d, 1H, $J_{1\text{-}2}$ = 6.2 Hz, H^1), 4.51 (d, 1H, $J_{7\text{-}8}$ = 8.0 Hz, H^7), 4.51 (dd, 1H, $J_{2\text{-}1}$ = 6.2 Hz, $J_{2\text{-}3}$ = 7.5 Hz, H^2) ppm. ^{13}C NMR (400 MHz, MeOD) δ: 13.0, 22.3, 24.2, 24.6, 25.1, 25.5, 25.6, 26.2, 27.0, 28.8, 29.00,29.02, 29.2, 31.6, 33.5, 53.0, 55.1, 63.0, 65.5, 70.8, 73.3, 73.5, 75.4, 76.4, 76.8, 77.6, 79.4, 103.1, 105.7, 108.5, 109.7, 109.9, 173.8 ppm.

3b [6'-*O*-dodecanoyl-4-*O*-(3',4'-*O*-isopropylidene-β-D-galactopyranosyl)-2,3:5,6-di-*O*-isopropylidene-1,1-di-*O*-methyl-D-glucopyranose]. Yield: 50% (0.274 g)**.** ^{1}H NMR (400 MHZ, MeOD) δ: 0.92 (t, 3H, J = 6.7 Hz, CH_3), 1.32 (s, 6H, 2 CH_3), 1.33-1.37 (m, 16 H, (-CH_2-)$_n$), 1.39 (s, 3H, CH_3), 1.41 (s, 3H, CH_3), 1.44 (s, 3H, CH_3), 1.49 (s, 3H, CH_3), 1.62-1.67 (m, 2H, CH_2CH_2COOR), 2.40 (t, 2H, J = 7.0 Hz, CH_2COOR), 3.45-3.46 (m, 6H, 2 -OCH_3), 3.47 (dd, 1H, $J_{8\text{-}9}$ = 7.1 Hz, $J_{8\text{-}7}$ = 8.0 Hz, H^8), 3.91 (dd, 1H, $J_{4\text{-}3}$ = 1.2 Hz, $J_{4\text{-}5}$ = 5.0 Hz, H^4), 4.05 (ddd, 1H, $J_{11\text{-}12a}$ = 1.2 Hz, $J_{11\text{-}10}$ = 2.1 Hz, $J_{11\text{-}12b}$ = 6.8 Hz, H^{11}), 4.05 (dd, 1H, $J_{6b\text{-}5}$ = 6.0

Hz, $J_{6b\text{-}6a}$ = 8.7 Hz, H^{6b}),4.08 (dd, 1H, $J_{9\text{-}10}$ = 5.6 Hz, $J_{9\text{-}8}$ = 7.1 Hz, H^{9}), 4.14 (dd, 1H, $J_{3\text{-}4}$ = 1.2 Hz, $J_{3\text{-}2}$ = 7.5 Hz, H^{3}), 4.17 (dd, 1H, $J_{6a\text{-}5}$ = 6.0 Hz, $J_{6a\text{-}6b}$ = 8.7 Hz, H^{6a}), 4.22 (dd, 1H, $J_{10\text{-}11}$ = 2.1 Hz, $J_{10\text{-}9}$ = 5.6 Hz, H^{10}), 4.27 (dd, 1H, $J_{12b\text{-}11}$ = 6.8 Hz, $J_{12b\text{-}12a}$ = 11.5 Hz, H^{12b}), 4.30 (dd, 1H, $J_{12a\text{-}11}$ = 1.2 Hz, $J_{12a\text{-}12b}$ = 11.5 Hz, H^{12a}), 4.31 (ddd, 1H, $J_{5\text{-}4}$ = 5.0 Hz, $J_{5\text{-}6a} \cong J_{5\text{-}6b}$ = 6.0 Hz, H^{5}), 4.41 (d, 1H, $J_{1\text{-}2}$ = 6.2 Hz, H^{1}), 4.51 (d, 1H, $J_{7\text{-}8}$ = 8.0 Hz, H^{7}), 4.51 (dd, 1H, $J_{2\text{-}1}$ = 6.2 Hz, $J_{2\text{-}3}$ = 7.5 Hz, H^{2}) ppm. ^{13}C NMR (400 MHz, MeOD) δ: 13.0, 22.3, 24.2, 24.6, 25.1, 25.5, 25.7, 26.2, 27.0, 28.8, 29.0, 29.1, 29.2, 29.3, 31.7, 33.5, 53.0, 55.1, 63.1, 65.5, 70.8, 73.3, 73.5, 75.4, 76.4, 76.8, 77.7, 79.4, 103.1, 105.7, 108.5, 109.7, 109.9, 173.8 ppm.

3c [6'-*O*-tetradecanoyl-4-*O*-(3',4'-*O*-isopropylidene-β-D-galactopyranosyl)-2,3:5,6-di-*O*-isopropylidene-1,1-di-*O*-methyl-D-glucopyranose]. Yield: 44% (0.248 g). ^{1}H NMR (400 MHZ, MeOD) δ: 0.92 (t, 3H, J = 6.7 Hz, CH_3), 1.31 (s, 6H, 2 CH_3), 1.33-1.37 (m, 20 H, (-CH_2-)$_n$), 1.39 (s, 3H, CH_3), 1.41 (s, 3H, CH_3), 1.44 (s, 3H, CH_3), 1.49 (s, 3H, CH_3), 1.61-1.67 (m, 2H, CH_2CH_2COOR), 2.40 (t, 2H, J = 7.0 Hz, CH_2COOR), 3.45-3.47 (m, 6H, 2 -OCH_3), 3.47 (dd, 1H, $J_{8\text{-}9}$ = 7.1 Hz, $J_{8\text{-}7}$ = 8.0 Hz, H^{8}), 3.91 (dd, 1H, $J_{4\text{-}3}$ = 1.0 Hz, $J_{4\text{-}5}$ = 5.0 Hz, H^{4}), 4.04 (ddd, 1H, $J_{11\text{-}12a}$ = 1.0 Hz, $J_{11\text{-}10}$ = 2.2 Hz, $J_{11\text{-}12b}$ = 6.8 Hz, H^{11}), 4.05 (dd, 1H, $J_{6b\text{-}5}$ = 6.0 Hz, $J_{6b\text{-}6a}$ = 8.7 Hz, H^{6b}),4.08 (dd, 1H, $J_{9\text{-}10}$ = 5.6 Hz, $J_{9\text{-}8}$ = 7.1 Hz, H^{9}), 4.15 (dd, 1H, $J_{3\text{-}4}$ = 1.0 Hz, $J_{3\text{-}2}$ = 7.5 Hz, H^{3}), 4.17 (dd, 1H, $J_{6a\text{-}5}$ = 6.0 Hz, $J_{6a\text{-}6b}$ = 8.7 Hz, H^{6a}), 4.22 (dd, 1H, $J_{10\text{-}11}$ = 2.2 Hz, $J_{10\text{-}9}$ = 5.6 Hz, H^{10}), 4.27 (dd, 1H, $J_{12b\text{-}11}$ = 6.8 Hz, $J_{12b\text{-}12a}$ = 11.5 Hz, H^{12b}), 4.30 (dd, 1H, $J_{12a\text{-}11}$ = 1.0 Hz, $J_{12a\text{-}12b}$ = 11.5 Hz, H^{12a}), 4.30 (ddd, $J_{5\text{-}4}$ = 5.0 Hz, $J_{5\text{-}6a} \cong J_{5\text{-}6b}$ = 6.0 Hz, H^{5}), 4.41 (d, 1H, $J_{1\text{-}2}$ = 6.2 Hz, H^{1}), 4.51 (d, 1H, $J_{7\text{-}8}$ = 8.0 Hz, H^{7}), 4.51 (dd, 1H, $J_{2\text{-}1}$ = 6.2 Hz, $J_{2\text{-}3}$ = 7.5 Hz, H^{2}) ppm. ^{13}C NMR (400 MHz, MeOD) δ: 13.0, 22.3, 24.2, 24.6, 25.1, 25.5, 25.6, 26.2, 27.0, 28.8, 29.0, 29.1, 29.2, 29.31, 29.34, 29.4, 31.7, 33.5, 53.0, 55.1, 63.1, 65.5, 70.8, 73.3, 73.6, 75.4, 76.4, 76.8, 77.6, 79.4, 103.1, 105.7, 108.5, 109.7, 109.9, 173.8 ppm.

3d [6'-*O*-palmitoyl-4-*O*-(3',4'-*O*-isopropylidene-β-D-galactopyranosyl)-2,3:5,6-di-*O*-isopropylidene-1,1-di-*O*-methyl-D-glucopyranose]. Yield: 34% (0.200 g) **.** ^{1}H NMR (400 MHZ, MeOD) δ: 0.92 (t, 3H, J = 6.7 Hz, CH_3), 1.31 (s, 6H, 2 CH_3), 1.33-1.37 (m, 24 H, (-CH_2-)$_n$), 1.39 (s, 3H, CH_3), 1.41 (s, 3H, CH_3), 1.44 (s, 3H, CH_3), 1.49 (s, 3H, CH_3), 1.60-1.67 (m, 2H, CH_2CH_2COOR), 2.40 (t, 2H, J = 7.4 Hz, CH_2COOR), 3.45-3.47 (m, 6H, 2 -OCH_3), 3.47 (dd, 1H, $J_{8\text{-}9}$ = 7.1 Hz, $J_{8\text{-}7}$ = 8.0 Hz, H^{8}), 3.91 (dd, 1H, $J_{4\text{-}3}$ = 1.0 Hz, $J_{4\text{-}5}$ = 5.0 Hz, H^{4}), 4.04 (ddd, 1H, $J_{11\text{-}12a}$ = 1.5 Hz, $J_{11\text{-}10}$ = 2.2 Hz, $J_{11\text{-}12b}$ = 6.8 Hz, H^{11}), 4.05 (dd, 1H, $J_{6b\text{-}5}$ = 6.0 Hz, $J_{6b\text{-}6a}$ = 8.7 Hz, H^{6b}),4.08 (dd, 1H, $J_{9\text{-}10}$ = 5.5 Hz, $J_{9\text{-}8}$ = 7.1 Hz, H^{9}), 4.14 (dd, 1H, $J_{3\text{-}4}$ = 1.0

Hz, $J_{3\text{-}2}$ = 7.5 Hz, H^3), 4.17 (dd, 1H, $J_{6a\text{-}5}$ = 6.0 Hz, $J_{6a\text{-}6b}$ = 8.7 Hz, H^{6a}), 4.22 (dd, 1H, $J_{10\text{-}11}$ = 2.2 Hz, $J_{10\text{-}9}$ = 5.5 Hz, H^{10}), 4.27 (dd, 1H, $J_{12b\text{-}11}$ = 6.8 Hz, $J_{12b\text{-}12a}$ = 11.5 Hz, H^{12b}), 4.30 (dd, 1H, $J_{12a\text{-}11}$ = 1.5 Hz, $J_{12a\text{-}12b}$ = 11.5 Hz, H^{12a}), 4.31 (ddd, $J_{5\text{-}4}$ = 5.0 Hz, $J_{5\text{-}6a} \cong J_{5\text{-}6b}$ = 6.0 Hz, H^5), 4.41 (d, 1H, $J_{1\text{-}2}$ = 6.2 Hz, H^1), 4.51 (d, 1H, $J_{7\text{-}8}$ = 8.0 Hz, H^7), 4.51 (dd, 1H, $J_{2\text{-}1}$ = 6.2 Hz, $J_{2\text{-}3}$ = 7.5 Hz, H^2) ppm. ^{13}C NMR (400 MHz, MeOD) δ: 13.0, 22.3, 24.2, 24.6, 25.1, 25.7, 26.2, 27.0, 29.0, 29.1, 29.2, 29.4, 31.7, 33.5, 53.0, 55.1, 63.1, 65.5, 70.8, 73.3, 73.6, 75.4, 76.4, 76.9, 77.8, 79.4, 103.1, 105.7, 108.5, 109.7, 109.9, 173.9 ppm.

4.2.2.2 General procedure for the synthesis of lactose fatty acid monoesters (4a-4d).

Compounds **3a-d** (0.30 mmol) were dissolved in tetrafluoroboric acid diethyl ether complex/water/acetonitrile (2.5 ml,1:5:500) and the mixture was stirred at 30 °C for 3 h. The products precipitated during the reaction as white solids were subsequently filtered, washed with acetonitrile and dried. The purification by recrystallization from methanol gave **4a-d** (Scheme 1) as white solids.

4a [6'-*O*-decanoyl-4-*O*-(β-D-galactopyranosyl)-D-glucopyranose]. Yield: 75% (0.112 g). The physicochemical data are in agreement to those previously reported [11]. ^{1}H NMR (400 MHZ, DMSO) δ: 0.86 (t, 3H, *J* = 6.5 Hz, CH_3), 1.20-1.32 (m, 12H, $(\text{-}CH_2\text{-})_n$), 1.49-1.57 (m, 2H, CH_2CH_2COOR), 2.27 (t, 2H, *J* = 7.5 Hz, CH_2COOR), 3.17 (ddd, 1H, $J_{2\text{-}1}$ = 4.0 Hz, $J_{2\text{-}OH2}$ = 7.0 Hz, $J_{2\text{-}3}$ = 9.5 Hz, H^2), 3.27 (dd, 1H, $J_{4\text{-}3} \cong J_{4\text{-}5}$ = 9.5 Hz, H^4), 3.33-3.38 (m, 2H, H^8, H^9), 3.57 (dd, 1H, $J_{3\text{-}2} \cong J_{3\text{-}4}$ = 9.5 Hz, H^3), 3.60-3.67 (m, 3 H, H^{6a}, H^{6b}, H^{10}), 3.68-3.76 (m, 2H, H^5, H^{11}), 4.09 (dd, 1H, $J_{12b\text{-}11}$ = 4.5 Hz, $J_{12b\text{-}12a}$ =11.5 Hz, H^{6a}), 4.17 (dd, 1H, $J_{12a\text{-}11}$ = 8.5 Hz, $J_{12a\text{-}12b}$ = 11.5 Hz, H^{6b}), 4.20-4.25 (m, 2H, H^7, OH^3), 4.43 (dd, 1H, $J_{OH6\text{-}6a} \cong J_{OH6\text{-}6b}$ = 6.0 Hz, OH^6), 4.55 (d, 1H, $J_{OH2\text{-}2}$ = 7.0 Hz, OH^2), 4.78 (d, 1H, $J_{OH10\text{-}10}$ = 5.0 Hz, OH^{10}), 4.86 (d, 1H, *J* = 3.0 Hz, OH), 4.90 (dd, 1H, $J_{1\text{-}OH1} \cong J_{1\text{-}2}$ = 4.0 Hz, H^1), 5.15 (d, 1H, *J* = 3.0 Hz, OH), 6.33 (d, 1H, $J_{OH1\text{-}1}$ = 4.0 Hz, OH^1) ppm. ^{13}C NMR (400 MHz, DMSO) δ: 14.4, 22.6, 24.8, 29.0, 29.1, 29.2, 29.3, 31.7, 33.8, 61.0, 63.8, 68.7, 70.2, 70.8, 71.7, 72.7, 72.9, 73.3, 81.6, 92.5, 104.0, 173.4 ppm.

4b [6'-*O*-dodecanoyl-4-*O*-(β-D-galactopyranosyl)-D-glucopyranose]. Yield: 44% (0.692 g)**.** The physicochemical data are in agreement to those previously reported [11]. ^{1}H NMR (400 MHZ, DMSO) δ: 0.86 (t, 3H, *J* = 6.6 Hz, CH_3), 1.19-1.32 (m, 16H, $(\text{-}CH_2\text{-})_n$), 1.49-1.57 (m, 2H, CH_2CH_2COOR), 2.31 (t, 2H, *J* = 7.5 Hz, CH_2COOR), 3.17 (ddd, 1H, $J_{2\text{-}1}$ = 4.0 Hz, $J_{2\text{-}OH2}$ = 7.0 Hz, $J_{2\text{-}3}$ = 9.5 Hz, H^2), 3.27 (dd, 1H, $J_{4\text{-}3} \cong J_{4\text{-}5}$ = 9.5 Hz, H^4), 3.33-3.38 (m, 2H, H^8 and

H^9), 3.56 (dd, 1H, $J_{3\text{-}2} \cong J_{3\text{-}4}$ = 9.5 Hz, H^3), 3.60-3.67 (m, 3 H, H^{6a}, H^{6b}, H^{10}), 3.68-3.76 (m, 2H, H^5, H^{11}), 4.09 (dd, 1H, $J_{12b\text{-}11}$ = 4.5 Hz, $J_{12b\text{-}12a}$ =11.5 Hz, H^{6a}), 4.17 (dd, 1H, $J_{12a\text{-}11}$ = 8.5 Hz, $J_{12a\text{-}12b}$ = 11.5 Hz, H^{6b}), 4.20-4.24 (m, 2H, H^7, OH^3), 4.43 (dd, 1H, $J_{OH6\text{-}6a} \cong J_{OH6\text{-}6b}$ = 6.0 Hz, OH^6), 4.55 (d, 1H, $J_{OH2\text{-}2}$ = 7.0 Hz, OH^2), 4.78 (d, 1H, $J_{OH10\text{-}10}$ = 5.0 Hz, OH^{10}), 4.86 (d, 1H, J = 3.0 Hz, OH), 4.90 (dd, 1H, $J_{1\text{-}OH1} \cong J_{1\text{-}2}$ = 4.0 Hz, H^1), 5.16 (d, 1H, J = 4.0 Hz, OH), 6.34 (d, 1H, $J_{OH1\text{-}1}$ = 4.0 Hz, OH^1) ppm. ^{13}C NMR (400 MHz, DMSO) δ: 14.4, 22.6, 24.8, 28.9, 29.2, 29.4, 29.46, 29.48, 31.8, 33.8, 60.9, 63.8, 68.7, 70.2, 70.7, 71.7, 72.7, 72.9, 73.3, 81.6, 92.5, 104.0, 173.4 ppm.

4c [6'-*O*-tetradecanoyl-4-*O*-(β-D-galactopyranosyl)-D-glucopyranose]. Yield: 65% (0.107g)**.** The physicochemical data are in agreement to those previously reported [11]. ^{1}H NMR (400 MHZ, DMSO) δ: 0.86 (t, 3H, J = 6.6 Hz, CH_3), 1.17-1.32 (m, 20H, $(\text{-}CH_2\text{-})_n$), 1.48-1.57 (m, 2H, CH_2CH_2COOR), 2.31 (t, 2H, J = 7.5 Hz, CH_2COOR), 3.16 (ddd, 1H, $J_{2\text{-}1}$ = 4.0 Hz, $J_{2\text{-}OH2}$ = 7.0 Hz, $J_{2\text{-}3}$ = 9.5 Hz, H^2), 3.27 (dd, 1H, $J_{4\text{-}3} \cong J_{4\text{-}5}$ = 9.5 Hz, H^4), 3.31-3.37 (m, 2H, H^8 and H^9), 3.56 (dd, 1H, $J_{3\text{-}2} \cong J_{3\text{-}4}$ = 9.5 Hz, H^3), 3.60-3.66 (m, 3 H, H^{6a}, H^{6b}, H^{10}), 3.67-3.76 (m, 2H, H^5, H^{11}), 4.08 (dd, 1H, $J_{12b\text{-}11}$ = 4.5 Hz, $J_{12b\text{-}12a}$ =11.5 Hz, H^{6a}), 4.16 (dd, 1H, $J_{12a\text{-}11}$ = 8.5 Hz, $J_{12a\text{-}12b}$ = 11.5 Hz, H^{6b}), 4.20-4.25 (m, 2H, H^7, OH^3), 4.47 (dd, 1H, $J_{OH6\text{-}6a} \cong J_{OH6\text{-}6b}$ = 6.0 Hz, OH^6), 4.60 (d, 1H, $J_{OH2\text{-}2}$ = 7.0 Hz, OH^2), 4.82 (d, 1H, $J_{OH10\text{-}10}$ = 5.0 Hz, OH^{10}), 4.89 (d, 1H, J = 4.0 Hz, OH), 4.90 (dd, 1H, $J_{1\text{-}OH1} \cong J_{1\text{-}2}$ = 4.0 Hz, H^1), 5.19 (d, 1H, J = 4.0 Hz, OH), 6.37 (d, 1H, $J_{OH1\text{-}1}$ = 4.0 Hz, OH^1) ppm. ^{13}C NMR (400 MHz, DMSO) δ: 14.4, 22.6, 24.8, 29.0, 29.18, 29.19, 29.4, 29.48, 29.51, 29.53, 31.8, 33.8, 60.9, 63.8, 68.7, 70.2, 70.7, 71.7, 72.7, 72.9, 73.3, 81.6, 92.5, 104.0, 173.4 ppm.

4d [6'-*O*- palmitoyl-4-*O*-(β-D-galactopyranosyl)-D-glucopyranose]. Yield: 80% (0.139 g). The physicochemical data are in agreement to those previously reported [11]. ^{1}H NMR (400 MHZ, DMSO) δ: 0.86 (t, 3H, J = 6.6 Hz, CH_3), 1.18-1.32 (m, 24H, $(\text{-}CH_2\text{-})_n$), 1.49-1.58 (m, 2H, CH_2CH_2COOR), 2.31 (t, 2H, J = 7.5 Hz, CH_2COOR), 3.17 (ddd, 1H, $J_{2\text{-}1}$ = 4.0 Hz, $J_{2\text{-}OH2}$ = 7.0 Hz, $J_{2\text{-}3}$ = 9.5 Hz, H^2), 3.27 (dd, 1H, $J_{4\text{-}3} \cong J_{4\text{-}5}$ = 9.5 Hz, H^4), 3.32-3.38 (m, 2H, H^8, H^9), 3.57 (dd, 1H, $J_{3\text{-}2} \cong J_{3\text{-}4}$ = 9.5 Hz, H^3), 3.61-3.67 (m, 3 H, H^{6a}, H^{6b}, H^{10}), 3.68-3.76 (m, 2H, H^5, H^{11}), 4.09 (dd, 1H, $J_{12b\text{-}11}$ = 4.5 Hz, $J_{12b\text{-}12a}$ =11.5 Hz, H^{12b}), 4.17 (dd, 1H, $J_{12a\text{-}11}$ = 8.5 Hz, $J_{12a\text{-}12b}$ = 11.5 Hz, H^{12a}), 4.20-4.28 (m, 2H, H^7, OH^3), 4.39 (dd, 1H, $J_{OH6\text{-}6a} \cong J_{OH6\text{-}6b}$ = 6.0 Hz, OH^6), 4.50 (d, 1H, $J_{OH2\text{-}2}$ = 7.0 Hz, OH^2), 4.75 (d, 1H, $J_{OH10\text{-}10}$ = 5.0 Hz, OH^{10}), 4.82 (brs, 1H,

OH), 4.89 (dd, 1H, $J_{1\text{-}OH1} \cong J_{1\text{-}2} = 4.0$ Hz, H^1), 5.12 (brs, 1H, OH), 6.30 (d, 1H, $J_{OH1\text{-}1} = 4.0$ Hz, OH^1) ppm. ^{13}C NMR (400 MHz, DMSO) δ: 14.4, 22.5, 24.8, 28.9, 29.1, 29.2, 29.44, 29.46, 29.50, 31.7, 33.8, 61.0, 63.7, 68.7, 70.2, 70.8, 71.7, 72.7, 72.9, 73.3, 81.6, 92.5, 104.0, 173.4 ppm.

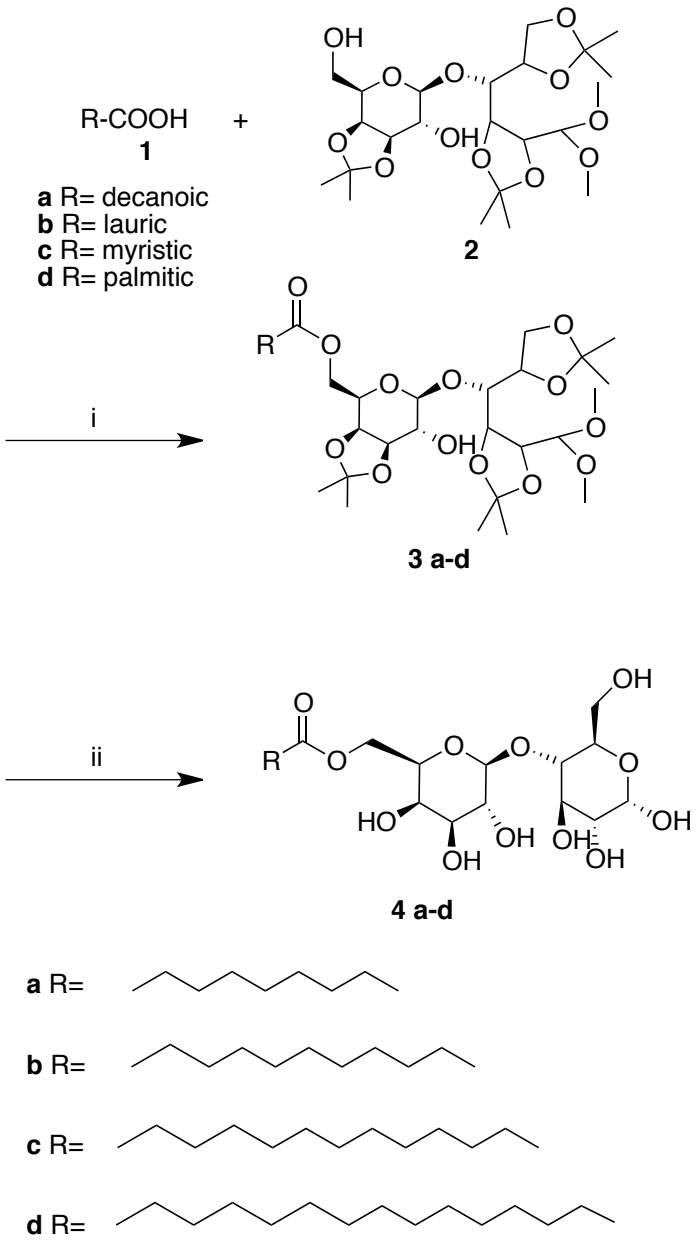

Scheme 1. Reagents and conditions: (a) toluene, 75°C, 12h; (b) HBF_4 Et_2O, CH_3CN, 30°C, 3 h.

4.2.3 Surface tension measurements

Surface tension of different concentrations of surfactant solutions in water was measured using a platinum cylindrical rod probe with wetted length of 1.6 mm (K100-Krüss force tensiometer). Approximately 1 ml of each surfactant solution was placed onto a teflon plate

and the surface of the liquid was aspirated in order to remove any remaining impurities. Then, the rod probe was immersed 2 mm into the liquid. Data are expressed as the mean of three repeated measurements performed at room temperature. The critical micelle concentration and the surface tension at the CMC (γCMC) were calculated through the straight-line interception method, while the Gibbs surface excess (Γ_{max}) was calculated from the following equation:

$$\Gamma_{max} = \frac{1}{2.303 \times \mathrm{n} \times \mathrm{R} \times \mathrm{T}} \left(\frac{\delta_\gamma}{\delta log C} \right) \quad \textbf{(Equation 1)}$$

where T is the absolute temperature, R is the gas constant (8.314 J/mol K), C is the surfactant concentration, n =1 for a non-ionic candidate. $\delta_\gamma / \delta \log C$ was calculated from the maximum slope of the plot surface tension vs surfactant concentration in the linear region before CMC (REF).

The minimum area per surfactant molecule at the air-water interface (A_{min}) was determined as follow:

$$A_{min} = \frac{10^{18}}{N \times \Gamma_{max}} \quad \textbf{(Equation 2)}$$

where *N* is the Avogadro number.

4.2.4 MTT assay

Calu-3 cells were seeded in sterile 96-well culture plates at a density of 3×10^4 cells per well. The cells were incubated to attain at least 80% confluence before the experiment. Surfactant solutions were prepared in isotonic buffer at various concentrations (from 1 to 0.0078 mg/ml) and were added to the cells. Complete culture media were used as control. The cytotoxic effect of each surfactant was evaluated using the MTT cell viability assay. After 24 h of incubation, surfactant solution was discarded and replaced by MTT solution (0.8 mg/ml in PBS). The cells were subjected to MTT treatment for 2 h. Formazan crystals formed were then dissolved in absolute isopropanol and incubated with gentle shaking at room temperature for 15 min. Absorbance was measured at 595 nm using a microplate reader (Multiskan™ GO Microplate Spectrophotometer Thermo Scientific, USA). Percentage of viable cells was calculated using untreated cells as control with 100% cell viability. The percentage of viable cells was plotted against log concentration of the surfactants. EC50 (mg/ml), the concentration of surfactant that caused a 50% reduction in cell viability was calculated by

fitting the experimental data with dose–response model (Prism 6, Version 6.0b, GraphPad Software).

4.2.5 LDH assay

LDH assay was used to evaluate the membrane disruption effect exhibited by the surfactants. Calu-3 cells were seeded in sterile 96-well culture plates at a density of 3×10^4 cells per well. Surfactant solutions (at the same concentration as in MTT assay described above) were added to the cells and incubated at 37 °C for 24 h. 1% Triton X-100 was used as positive control. The LDH release assay was conducted according to the manufacturer's protocol. The percentage of released LDH was calculated relative to the controls by taking samples treated with Triton X-100 as complete LHD release and untreated cells as nil LDH release.

EC50 (mg/ml), the concentration of surfactant that caused a 50% release of LDH, was calculated by fitting the experimental data with dose–response model (Prism 6, Version 6.0b, GraphPad Software).

4.2.6 TEER

Calu-3 cells were seeded at a density of 2×10^5 cells per well on filter inserts (Transwell® Permeable Support 12 mm Insert, Life Sciences, USA) and cultured to confluence under an air-liquid interface (ALI) microenvironment. Culture media on the apical and baso-lateral sides of the cells were changed every 24 h. For TEER measurements, culture medium was discarded from the cell layer and replaced with KBSS on both the apical and baso-lateral sides of the monolayers. Cell layers were allowed equilibrating in KBSS at 37 °C, 5% CO_2 for 45 min prior to sample application. Baseline TEER was measured before the treatment with surfactants. For each surfactant, concentrations that caused 50 % cell viability, and the highest concentration that maintained 100% cell viability (according to the MTT assay) were added to the apical sides of the cell layers and incubated for 2 h. TEER was then measured at 5, 30, 60, 90 and 120 min after surfactant addition. Between TEER measurements, cells were incubated at normal cell culture conditions. After 120 min, surfactant was removed and culture media were added to both sides of the filter inserts. TEER measurement was conducted again after 24 h in order to evaluate the recovery of cell monolayers. A voltohmmeter (Millcell® ERS-2 Voltohmmeter, Millipore, USA) equipped with a pair of electrodes was used for TEER measurement. Baseline TEER measured from cell layers incubated in KBSS was used as control and the change in TEER was presented as a percentage relative to baseline value. Three independent experiments were performed in duplicates.

4.3 Results and discussion

4.3.1 Surface tension measurements

Fig. 1 shows the surface properties of each lactose fatty acid monoester. From the plotted curves it is possible to observe the significant influence of the carbon chain length on the molecules surface properties.

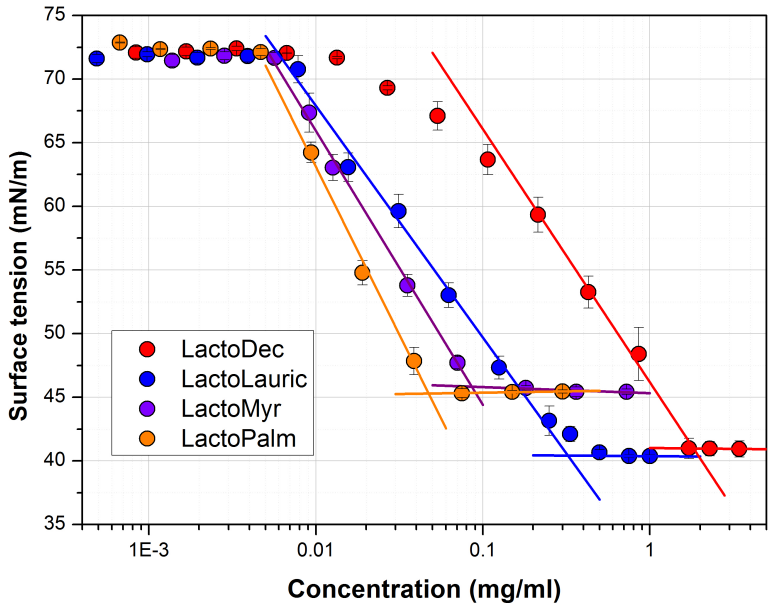

Fig. 1. Surface tension (mN/N) vs surfactant concentration plot (mg/ml) for the lactose fatty acid monoesters. Surface tension data are the mean of three repeated measurements (n = 3) performed at room temperature. The CMC is calculated from the straight-line interception method.

A clear correlation between the calculated CMC values (Table 1) and the carbon chain length can be established. Indeed, lactose esters with longer carbon chains show a lower CMC as results from the higher hydrophobicity. This translates in lower water solubility and micellization reasonably occurs at lower concentrations. These results are in agreement with those previously reported by Becerra et al. and Garofalakis et al. [13,14].

Table 1. Surface parameters of the synthetized lactose fatty acid monoesters.

	CMC (mg/ml)	γCMC (mN/m)	$10^{-6}\Gamma_{max}$ (mol/m^2)	A_{min} (Å^2)
LactoDec	1.28±0.16	40.6±0.04	9.52±0.11	17.46±0.25
LactoLauric	0.29±0.01	40.4±0.02	9.52±0.05	17.45±0.09
LactoMyr	0.08±0.03	45.6±0.19	8.37±0.46	19.86±0.80
LactoPalm	0.05±0.02	45.1±0.33	6.46±0.11	25.69±0.43

The surface tension at the CMC (γCMC) was calculated to be around 40mN/m for all the tested lactose esters, demonstrating the potential application of these compounds as surface active agents.

The Absorption of the surfactants at the interface is described by the maximum surface excess concentration (Γ_{max}), according to the Gibbs isotherm.

The packing ability of surfactants at the interface is influenced by both the hydrocarbon chain length and polar head group. Surfactants with the bulkiest organization are generally characterized by a lower area per surfactants (A_{min}). In fact, as previously reported, A_{min} depends not only on the hydrophilic head group dimensions (number of hydroxyl group), but also on packing and stereochemistry of the whole structure [14].

According to Becerra et al., the surface excess is inversely dependent on the hydrocarbon chain length, therefore as the carbon chain length increase, the $\Gamma_{max.}$ decreases. Conversely, the area occupied by each molecule of surfactant increases as the carbon chain length increases [13]. In this regard, 6'-*O*-decanoyl-4-*O*-(β-D-galactopyranosyl)-D-glucopyranose and 6'-*O*-dodecanoyl-4-*O*-(β-D-galactopyranosyl)-D-glucopyranose, characterized by short hydrocarbon chain lengths, showed the highest Γ_{max}, suggesting the organization in a more packed monolayer as indicated by the lower area per molecule.

4.3.2 Toxicological studies: MTT and LDH assays

MTT and LDH assays have been carried out to assess the cytotoxicity of various concentration of lactose esters on Calu-3 cells after 24 h exposure. Results showed in Fig. 2 clearly suggest that cell viability is influenced by both carbon chain length and surfactant concentration. As the carbon chain length is increased, the EC_{50} decreases (Table 2).

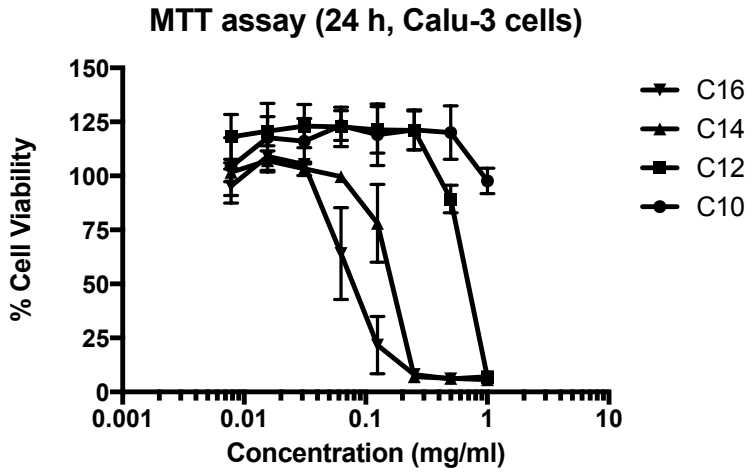

Fig. 2. MTT assay on saturated lactose esters derivatives. Cell viability (%) of Calu-3 after 24 h exposure to different concentrations of lactose surfactants. Data are expressed as the mean ± S.E.M. for three independent experiments.

LDH assay was performed to evaluate the influence of surfactants on the membrane integrity (Fig. 3). The toxicological profile obtained from LDH assay confirmed the influence of the carbon chain length on the surfactant cytotoxicity.

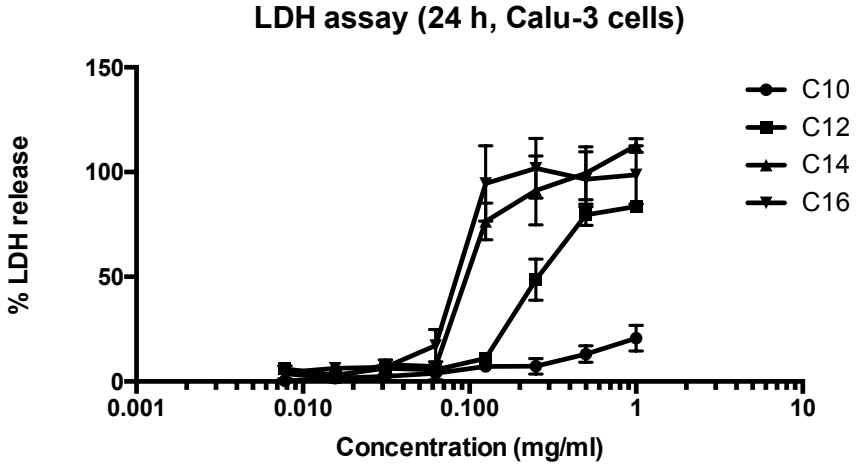

Fig. 3. LDH assay on saturated lactose esters derivatives. Cell viability (%) of Calu-3 after 24 h exposure to different concentrations of lactose surfactants. Data are expressed as the mean ± S.E.M. for three independent experiments.

EC_{50} calculated from the MTT assay was demonstrated to be slightly higher than those derived from LDH. While MTT assay refers to the inactivation of enzymes that regulate cellular metabolism, LDH assays evaluates the integrity of the plasma membrane. Based on this consideration, it is reasonable to hypothesize a toxicological mechanism mainly related to the permeabilisation of the plasma membrane, likely due the surfactant interaction and incorporation into the phospholipid bilayer.

Interestingly, previous studies demonstrated the correlation between the hydrocarbon chain length and the cytotoxicity of surfactants. Surfactants with longer hydrocarbon chains, showed higher cytotoxicity [15,16]. In this regard, Perinelli et al. recently investigated the correlation between the CMC and the cytotoxicity of N-decanoyl amino acid-based surfactants with different polar head groups. The authors demonstrated that the toxicity is affected by both the polar head and the hydrocarbon chain length, with the latter parameter causing the main effect [8,17].

Additionally, surfactants with longer chains are characterized by a lower CMC. As a result, it is reasonable to correlate cytotoxicity to CMC. In this regard, 6'-*O*-palmitoyl-4-*O*-(β-D-galactopyranosyl)-D-glucopyranose, which is characterized by the lowest CMC (0.05 mg/ml), demonstrated the highest cytotoxicity in Calu-3 cells (0.0708 mg/ml).

Moreover, EC_{50} values were compared to the CMC values, since it has already been demonstrated that surfactants with high cytotoxicity, show EC_{50} values lower than the CMC [17]. All the surfactants demonstrated EC_{50} values higher or comparable to the CMC in both MTT and LDH assay on Calu-3 cells, thus showing an acceptable toxicological profile.

Table 2. MTT and LDH cytotoxicity studies of lactose surfactants on Calu-3 cells. EC_{50} is the concentration of surfactant that causes 50% reduction of viable cells (MTT assay) or 50% release of LDH (LDH assay).

Surfactant	MTT assay EC_{50} (mg/ml)	LDH assay EC_{50} (mg/ml)
	Calu-3	
C10	n.d.	n.d.
C12	0.5611	0.2370
C14	0.1441	0.1048
C16	0.0708	0.0823

4.3.3 TEER on Calu-3 cells

TEER is used to measure the ability of surfactants to transiently open the tight junctions, thus acting as absorption enhancers for various biopharmaceutics suffering of poor mucosal permeation. Moreover, TEER can be used as indirect method to study the interaction of exogenous molecules with the plasma membrane [18]. A transient opening of tight junctions

translates in a reversible modification of the TEER, while irreversible effect on the TEER indicates a damage to the cell membrane.

TEER measurements were performed on Calu-3 cell monolayer as model for the airway epithelium, since these cells are able to form a monolayer. Two concentrations of lactose surfactants were selected for TEER studies, namely the IC_{50} calculated from the MTT assay and the highest concentration that show 100% viability, as reported in Fig. 4.

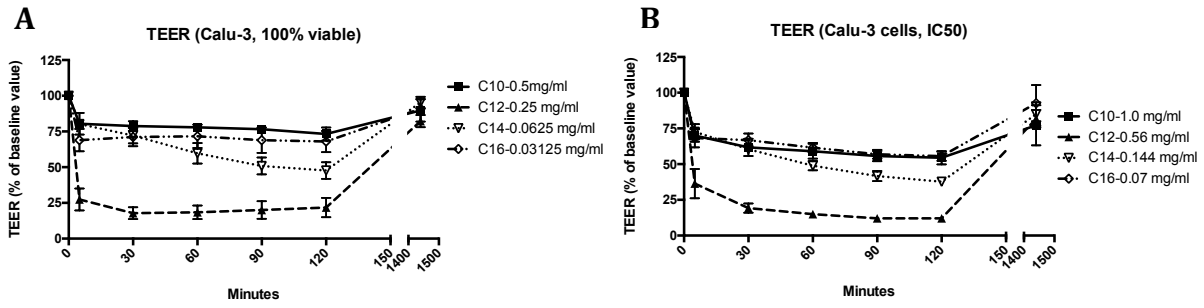

Fig. 4. TEER studies on Calu-3 cell layers. TEER was measured at two different concentration of lactose surfactants, namely IC_{50} (from the MTT assay) and highest concentration that shows 100% viability. Data represent the mean and standard error (n= 2).

6'-*O*-dodecanoyl-4-*O*-(β-D-galactopyranosyl)-D-glucopyranose was found to be the most effective surfactant in decreasing the TEER at both tested concentrations, while all the other surfactants showed a moderate decreased in the TEER. Interestingly, TEER reversed to the initial value after 25h, suggesting a reversible effect on tight junction opening and cell toxicity.

4.4 Conclusions

This work reported the physicochemical characterization and toxicological evaluation of a series of saturated lactose-fatty acids monoesters. The series was designed by varying the fatty acid chain lengtht, while lactose was employed as polar head group. The resulting lactose fatty acid monoesters demonstrated interesting surface-active properties

Cytotoxicity was found to be related to the hydrocarbon chain length. Indeed, higher EC_{50} values were observed in presence of more hydrophilic compounds (shorter hydrocarbon chain length). Moreover, when these values were compared to the CMC values, they resulted lower or similar, thus showing an acceptable toxicological profile. Interestingly, 6'-*O*-dodecanoyl-4-*O*-(β-D-galactopyranosyl)-D-glucopyranose showed the highest ability to decrease the TEER

on Calu-3 cell monolayers, while all the surfactants demonstrated a no-long lasting effect on cell toxicity and tight junction opening. Based on these promising results, further studies will be focused on the comprehension of the toxicological mechanism of these surfactants and TEER studies on different cell lines will be conducted.

Acknowledgments

I would like to thank Dr. Robert Cavanagh, Dr. Wanling Liang, Dr. Diego Romano Perinelli, Dr. Mario Campana, Professor Snjezana Stolnik, Professor Jenny K. W. Lam for the precious collaboration in the collection and analysis of the data.

References

[1] U. Tsoler, Handbook of detergents. Part B, Environmental impact, M. Dekker, 2004.

[2] G. Garofalakis, B. Murray, D. Sarney, Surface Activity and Critical Aggregation Concentration of Pure Sugar Esters with Different Sugar Headgroups., J. Colloid Interface Sci. 229 (2000) 391–398. doi:10.1006/jcis.2000.7035.

[3] G.J. Puterka, W. Farone, T. Palmer, A. Barrington, Structure-function relationships affecting the insecticidal and miticidal activity of sugar esters., J. Econ. Entomol. 96 (2003) 636–44.

[4] P. Nobmann, A. Smith, J. Dunne, G. Henehan, P. Bourke, The antimicrobial efficacy and structure activity relationship of novel carbohydrate fatty acid derivatives against Listeria spp. and food spoilage microorganisms, Int. J. Food Microbiol. 128 (2009) 440–445. doi:10.1016/j.ijfoodmicro.2008.10.008.

[5] K. Hill, O. Rhode, Sugar-based surfactants for consumer products and technical applications, Lipid - Fett. 101 (1999) 25–33. doi:10.1002/(SICI)1521-4133(19991)101:1<25::AID-LIPI25>3.0.CO;2-N.

[6] T. Watanabe, S. Katayama, M. Matsubara, Y. Honda, M. Kuwahara, Antibacterial carbohydrate monoesters suppressing cell growth of Streptococcus mutans in the presence of sucrose., Curr. Microbiol. 41 (2000) 210–3.

[7] D.W. Roberts, S.J. Marshall, Application of Hydrophobicity Parameters to Prediction of the Acute Aquatic Toxicity of Commercial Surfactant Mixtures, SAR QSAR Environ. Res. 4 (1995) 167–176. doi:10.1080/10629369508029914.

[8] D. R. Perinelli, M. Cespi, L. Casettari, D. Vllasaliu, M. Cangiotti, M.F. Ottaviani, G. Giorgioni, G. Bonacucina, G.F. Palmieri, Correlation among chemical structure, surface properties and cytotoxicity of N-acyl alanine and serine surfactants, (2016). doi:10.1016/j.ejpb.2016.09.015.

[9] S. Lucarini, L. Fagioli, R. Campana, H. Cole, A. Duranti, W. Baffone, D. Vllasaliu, L. Casettari, Unsaturated fatty acids lactose esters: cytotoxicity, permeability enhancement and antimicrobial activity, (2016). doi:10.1016/j.ejpb.2016.06.022.

[10] L.A.W. Thelwall, L. Hough, A.C. Richardson, U.S. Patent 4,284,763, 1981.

[11] D.B. Sarney, H. Kapeller, G. Fregapane, E.N. Vulfson, Chemo-enzymatic synthesis of disaccharide fatty acid esters, J. Am. Oil Chem. Soc. 71 (1994) 711–714. doi:10.1007/BF02541426.

[12] S. Lucarini, L. Fagioli, R. Campana, H. Cole, A. Duranti, W. Baffone, D. Vllasaliu, L. Casettari, Unsaturated fatty acids lactose esters: cytotoxicity, permeability enhancement and antimicrobial activity, Eur. J. Pharm. Biopharm. 107 (2016) 88–96. doi:10.1016/j.ejpb.2016.06.022.

[13] N. Becerra, C. Toro, A.L. Zanocco, E. Lemp, G. Günther, Characterization of micelles formed by sucrose 6-O-monoesters, Aspects. 327 (2008) 134–139. doi:10.1016/j.colsurfa.2008.06.012.

[14] G. Garofalakis, B.S. Murray, D.B. Sarney, Surface Activity and Critical Aggregation Concentration of Pure Sugar Esters with Different Sugar Headgroups, J. Colloid Interface Sci. 229 (2000) 391–398. doi:10.1006.

[15] B. Lu, M. Vayssade, Y. Miao, V. Chagnault, E. Grand, A. Wadouachi, D. Postel, A. Drelich, C. Egles, I. Pezron, Physico-chemical properties and cytotoxic effects of sugar-based surfactants: Impact of structural variations, Colloids Surfaces B Biointerfaces. 145 (2016) 79–86. doi:10.1016/j.colsurfb.2016.04.044.

[16] X. Li, J. Turánek, P. Knötigová, H. Kudláčková, J. Mašek, S. Parkin, S.E. Rankin, B.L. Knutson, H.-J. Lehmler, Hydrophobic tail length, degree of fluorination and headgroup stereochemistry are determinants of the biocompatibility of (fluorinated) carbohydrate surfactants, Colloids Surfaces B Biointerfaces. 73 (2009) 65–74. doi:10.1016/j.colsurfb.2009.04.023.

[17] D.R. Perinelli, L. Casettari, M. Cespi, F. Fini, D.K.W. Man, G. Giorgioni, S. Canala, J.K.W. Lam, G. Bonacucina, G.F. Palmieri, Chemical–physical properties and cytotoxicity of N-decanoyl amino acid-based surfactants: Effect of polar heads, Aspects. 492 (2016) 38–46. doi:10.1016/j.colsurfa.2015.12.009.

[18] D. Vllasaliu, L. Casettari, R. Fowler, R. Exposito-Harris, M. Garnett, L. Illum, S. Stolnik, Absorption-promoting effects of chitosan in airway and intestinal cell lines: A comparative study, Int. J. Pharm. 430 (2012) 151–160. doi:10.1016/j.ijpharm.2012.04.012.

Chapter 5

Characterization of biosurfactants produced by *Lactobacillus* spp.

Characterization of biosurfactants produced by *Lactobacillus* spp. and their activity against oral streptococci biofilm. *Applied Microbiology and Biotechnology*. 2016; *100*: 6767-6777.

5.1 Introduction

Biosurfactants (BSFs) are surface-active agents synthesized by various classes of microorganisms, which includes a wide variety of chemical compounds, such as fatty acids, neutral lipids, phospholipds, glycolipids and lipopeptides. Biosurfactants have been initially employed in late 60s as dissolution agents [1]. Later, they have attracted an increasing attention from both academic and industrial field, being proposed as a valid alternative to synthetic surfactants (e.g. carboxylates, sulphonates and sulphate acid esters), due to their peculiar characteristics which includes low toxicity, high biodegradability and effectiveness at a wide range of temperatures, pH and salinity[2,3].

The most commonly isolated biosurfactants are represented by glycolipids and lipopeptides, while rhamnolipids, sophorolipids, surfactin and iturin have also been studied in recent years. These biosurfactants have been intensively investigated for their ability to reduce water surface tension to values below 30 mN/m [4–6].

Moreover, biosurfactants were found to be released by different species of lactic acid bacteria (LAB), also known as lactobacilli. They are commensal microorganism, classified as GRAS (Generally Recognized As Safe) bacteria. Lactobacilli produce biosurfactants in low amounts (20-100 mg/l) compared to the 2-10 g/l production from other microorganisms and are generally less effective to lower the air-water surface tension (around 36-40 mN/m) [7]. Such biosurfactants have been characterized as complex mixtures, whose composition has been only partially identified. However, many studies reported the attractive properties of biosurfactants produced by lactobacilli and their ability to inhibit the adhesion of pathogens to biomaterial and/or cell surfaces, highlighting their key role in the biofilm formation process [8–11].

A biofilm is a thin layer of microorganisms adhering to the surface of an organic or inorganic structure, together with their secreted “extracellular polymeric substances” (EPS). In this regard, biofilm formation by oral pathogens, such as *Streptococci* spp., on the solid surface of the enamel or the root of the teeth is considered to play a major role in the pathogenesis of dental caries [12]. The application of antimicrobial agents seems to be a useful tool for controlling the formation and growth of oral biofilms [13]. In recent years the attention has been focused on the use of new antimicrobial agents as alternative to traditional antibiotics, while new strategies to control biofilm formation have also been developed [14]. A field particularly explored is represented by lactobacilli and their ability to interfere with the adhesion of oral pathogens to abiotic surfaces [15–17].

Data in literature are mostly referred to the so called "cell-bound biosurfactants", which are commonly extracted at the end of the fermentation [7,9,18]. Conversely, few data are available for the so called "excreted biosurfactants", which are released in the culture media during the fermentation process [19].

The aim of the present study was to characterize "excreted biosurfactants" (BSF), produced by selected *Lactobacillus* spp., in terms of surface tension reduction and emulsifying activity. Since crude excreted biosurfactants produced by lactobacilli are complex biological mixtures, they were initially purified through a dialysis method, using membranes with two different molecular weight cut-off (1 and 6 kDa). Finally, both fractions of dialyzed biosurfactants, were studied for their anti-biofilm properties against oral Streptococci.

5.2 Materials and methods

5.2.1 Materials, culture conditions and antimicrobial activity of the excreted biosurfactants

Seven *Lactobacillus* spp. were used in this study, *Lactobacillus reuteri* DSM 17938 (Reuflor, Italchimici, Italy), *Lactobacillus acidophilus* DDS-1 (Nutratec, Urbino, Italy), *Lactobacillus paracasei* B21060 (Floratec, Bracco, Italy), *Lactobacillus rhamnosus* ATCC 53103, *Lactobacillus rhamnosus* ATCC 7469*, Lactobacillus casei* ATCC 15008*, Lactobacillus salivarius* ATCC 11741. All these strains were grown in Man Rogosa and Shape agar (MRS) (Oxoid, UK) at 37°C for 24-48h under microaerophilic conditions (5% O_2; 10% CO_2; 85% N_2).

In addition, *Streptococcus mutans* ATCC 25175 and *Streptococcus oralis* ATCC 9811, two reference human oral pathogens, were used as pathogen bacteria model. These strains were routinely grown on Sheep blood agar base (Oxoid, UK) with 5% of Sheep blood (Oxoid, UK) at 37°C for 24h.

Stock cultures of each strain were keep at -80°C in Nutrient broth (Oxoid, UK) with 15% of glycerol.

LAB strains overnight cultures (15 ml) were inoculated to 600 ml of MRS broth (Oxoid, UK) and incubated at 37°C for 48h under microaerophilic conditions. For the recovery of the crude excreted biosurfactants (BSF), bacterial cultures were centrifuged at 17.000 rpm for 15 min at 4 °C and the supernatants were filtered through a 0.22 μm pore size filter (Millipore).

To test the antimicrobial effect of the crude excreted biosurfactants, *S. mutans* ATCC 25175 and *S. oralis* ATCC 9811 were grown in Brain Heart Infusion broth (BHI) (Oxoid, UK)

supplemented with 1% yeast extract at 37°C for 18 h. Then, 500 µl of each bacterial culture (about 10^8 cfu/ml) and 500 µl of each biosurfactant were combined in 24 well-polystyrene plates and incubated at 37°C. At the baseline time (0 h) and after 3, 6 and 24h, different aliquots were aseptically removed, serially diluted in physiological saline solution and plated on Sheep agar base with 5% sheep blood at 37°C for 24-48 h. At the end of incubation, plates were observed to calculate the colony-forming unit (cfu/ml). Each experiment was performed in duplicate.

5.2.2 Dialysis of biosurfactants

Four *Lactobacillus* spp. (*L. reuteri* DSM 17938, *L. acidophilus* DDS-1, *L. rhamnosus* ATCC 53103 and *L. paracasei* B21060) were selected on the basis of the antimicrobial activity determined by time-killing studies and their excreted biosurfactants were purified through dialysis. The dialyses were performed against demineralized water at room temperature using Spectra/Por® membranes at two different molecular weight cut-off, 1 and 6 kDa (Spectrum® Laboratories, Inc.). The solutions containing the biosurfactants were finally freeze-dried.

5.2.3 Characterization of dialyzed biosurfactant surface properties

The following experiments were conducted to determine biosurfactant activities of dialyzed/freeze-dried biosurfactants in terms of reduction in air-water surface tension and oil-water emulsion ability.

The reduction in air-water surface tension (ST) of biosurfactants was determined by the Ring method [20] using a tensiometer (DCA-100 Contact Angle Tensiometer - First Ten Angstroms, Inc., USA) equipped with a 1.9 cm De Noüy platinum ring at room temperature. About 15 mL of each sample was withdrawn and surface tension was measured at 0.5, 1, 2.5, 5 and 10 mg/ml. MRS broth was also analyzed at the same concentrations for comparison.

The emulsification activity of biosurfactants is expressed as emulsification index (E24) [21]. Equal volumes of the aqueous phase containing the dialyzed biosurfactant (1mg/ml and 10 mg/ml) and paraffin oil were vigorously mixed with a vortex for 2 min, and allowed 24 h to settle. The emulsification index was calculated by the following equation:

$$E24 = \frac{\text{height of an emulsion layer}}{\text{total height}} \text{ x } 100 \qquad \textbf{(Equation 1)}$$

Each test was performed in duplicate.

5.2.4 Anti-biofilm activity of dialyzed biosurfactants

Biofilm formation on titanium surface of *S. mutans* ATCC 25175 and *S. oralis* ATCC 9811 was obtained following a procedure already reported by Ciandrini et al. with some modification [22].

Each dialyzed biosurfactant (1 kDa and 6 kDa) was then tested for its anti-biofilm activity against *S. mutans* ATCC 25175 and *S. oralis* ATCC 9811 during biofilm formation on titanium surface.

To this end, saliva-conditioned titanium discs, were positioned into a 24-wells polystyrene cell culture plate, covered with 200 µl (10^6 cell/ml) of *S. mutans* ATCC 25175 and *S. oralis* ATCC 9811 cultures and 1 ml of each dialyzed biosurfactant, at two concentrations (1 mg/ml and 10 mg/ml). Wells inoculated with 200 µl (10^6 cell/ml) of *S. mutans* ATCC 25175 and *S. oralis* ATCC 9811 in BHI broth were used as controls for each microorganism. Plates were incubated at 37°C for 24 h to allow biofilm formation. At the end of the incubation, bacteria adherent to titanium disks were harvested by vigorous vortexing for 2 min in physiological saline solution, then serially diluted and plated on Sheep agar base with 5% sheep blood (Oxoid, UK). The plates were incubated at 37°C under the adequate conditions for 24-48 h and the colony forming units per milliliter (cfu/ml) were counted.

Flow cytometry (FCM) was also performed. For this purpose, an additional series of 24-wells polystyrene cell culture plates was prepared, using the same procedure described above. The titanium adherent bacteria were harvested by vigorous vortexing for 2 min in physiological saline solution. Each sample, diluted in the same buffer, was labeled with SYBR Green I (1/10.000 v/v) and Propidium Iodide (PI) (10 µg/ml), incubated in the dark for 15 min at room temperature and immediately processed by FACS Calibur flow cytometer (BD Biosciences, USA) equipped with a 488 nm laser [23]. All experiments were performed in triplicates. Multi-parametric analyses were performed on both scattering signals as forward-scattered light (FSC) and side-scattered light (SSC) and fluorescence emission in FL1/FL3 channels. In particular, the green fluorescence of SYBR Green I was detected in the FL1 (530/30) channel while PI red fluorescence in the FL3 (>670) channel. Threshold levels were set on FSC in order to eliminate noise, due to the presence of cellular debris which contribute much smaller than intact cells to the overall signal. Bacterial cells were gated according to FSC/SSC parameters. The data were analyzed using CellQuest™ Pro software (BD Biosciences, USA).

5.2.5 Statistical analysis

Statistical analysis was performed using Prism version 5.0 (GraphPad Inc., USA). All experiments were performed in duplicate and the standard error of the mean was calculated from the combined measurements. Data points were analyzed through one-way analysis of variance (ANOVA) with Bonferroni post-hoc test unless the assumptions for the parametric test was not respected. In this case, Kruskall-Wallis non-parametric test with Dunnett's multiple comparison test was applied. P values < 0.05 were considered to be statistically significant.

5.3 Results

5.3.1 Antimicrobial activity of crude excreted biosurfactants in killing studies

The antimicrobial activities of all *Lactobacillus* spp. crude excreted biosurfactants against oral streptococci were determined by time-kill assays (Fig. 1).

In general, the results show that BSFs were able to reduce the growth of both *S. mutans* ATCC 25175 and *S. oralis* ATCC 9811 up to 24h with variable ability depending on the specific LAB strain.

As regards *S. mutans* ATCC 25175, biosurfactants produced by *L. acidophilus* DDS-1, *L. paracasei* B21060 and *L. rhamnosus* ATCC 53103, induced 1-log reduction in cfu/ml values after 3h of incubation, reaching 2-log reduction after 24h of incubation. Biosurfactant from *L. reuteri* DSM 17938 showed the greatest antimicrobial activity against *S. mutans* ATCC 25175, with a cfu /ml reduction of 2- log after 3h and 8-log after 24h (Fig. 1a).

Similarly, a reduction of cfu/ml values was also observed towards *S. oralis* ATCC 9811. Biosurfactants produced by *L. acidophilus* DDS-1, *L. paracasei* B21060 and *L. rhamnosus* ATCC 53103 induced a reduction of 2-log after 3h and 6h of incubation, reaching 5.4-log after 24 h. The biosurfactant of *L. reuteri* DSM 17938 showed the greatest antimicrobial activity, with a decrease of 3-, 4- and 8- log after 3h, 6h and 24h, respectively (Fig. 1b). Biosurfactants excreted by *L. rhamnosus* ATCC 7469*, L. casei* ATCC 15008 *and L. salivarius* ATCC 11741 showed the lowest antimicrobial activity against *S. mutans* ATCC 25175 and *S. oralis* ATCC 9811.

Based on these results, four *Lactyobacilli* spp. (*L. reuteri* DSM 17938, *L. acidophilus* DDS-1, *L. paracasei* B21060 and *L. rhamnosus* ATCC 53103) and their excreted biosurfactants were selected for the following dialysis procedure.

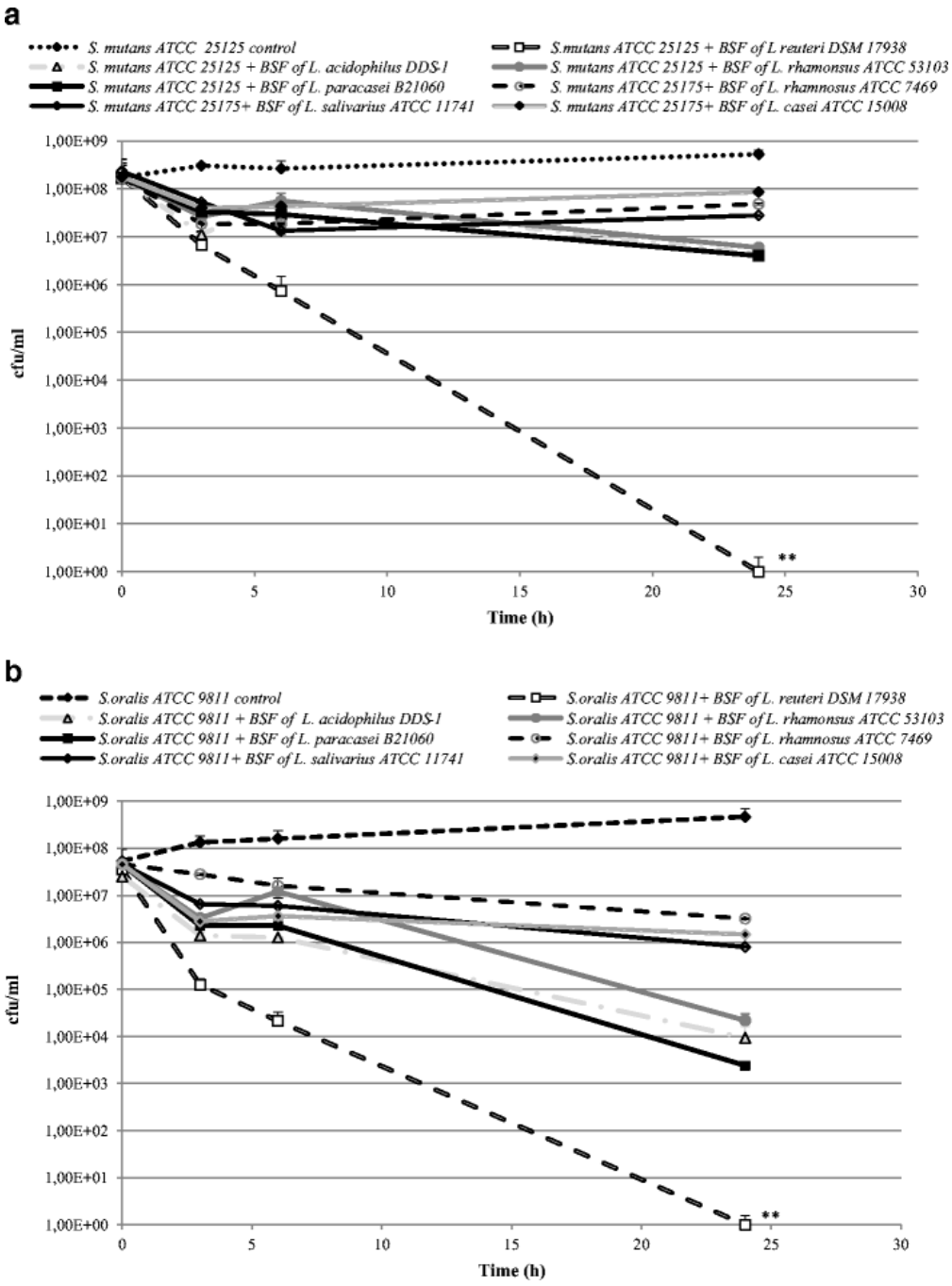

Fig.1. Antimicrobial activity of biosurfactants produced by *L. reuteri* DSM 17938, *L. acidophilus* DDS-1, *L. paracasei* B21060 and *L. rhamnosus* ATCC 53103 against a *S. mutans* ATCC 25175 and b *S. oralis* ATCC 9811 assessed by time-kill studies.

5.3.2 Characterization of dialyzed biosurfactant surface properties

Biosurfactants produced from *L. reuteri* DSM 17938, *L. acidophilus* DDS-1, *L. paracasei* and *L. rhamnosus* ATCC 53103 B21060 were dialyzed (1kDa and 6kDa cut-off) and then characterized in terms of surface tension reduction and emulsifying ability.

All dialyzed biosurfactants (1kDa and 6kDa) were able to decrease air-water surface tension over the entire range of tested concentrations (1-10 mg/ml) (Fig. 2). The reduction in surface tension was quite linear and clearly more pronounced for the biosurfactants with respect to the growth medium (MRS broth), analyzed for comparison. In fact, the measured surface tension for MRS broth was 48 mN/m at 10 mg/ml, different from the bisurfactants, which showed lower values (35-40 mN/m). In general, no marked differences among biosurfactants are evident, although a slightly higher surface activity was observed for the 1kDa dialyzed compounds. These data are in agreement with those reported by Sharma and Saharan, showing similar values of ST for excreted biosurfactants produced by a different *Lattobacillus* strains, with a surface tension reduction of the production media to 40.8 mN/m from the initial value of 53 mN/m [19].

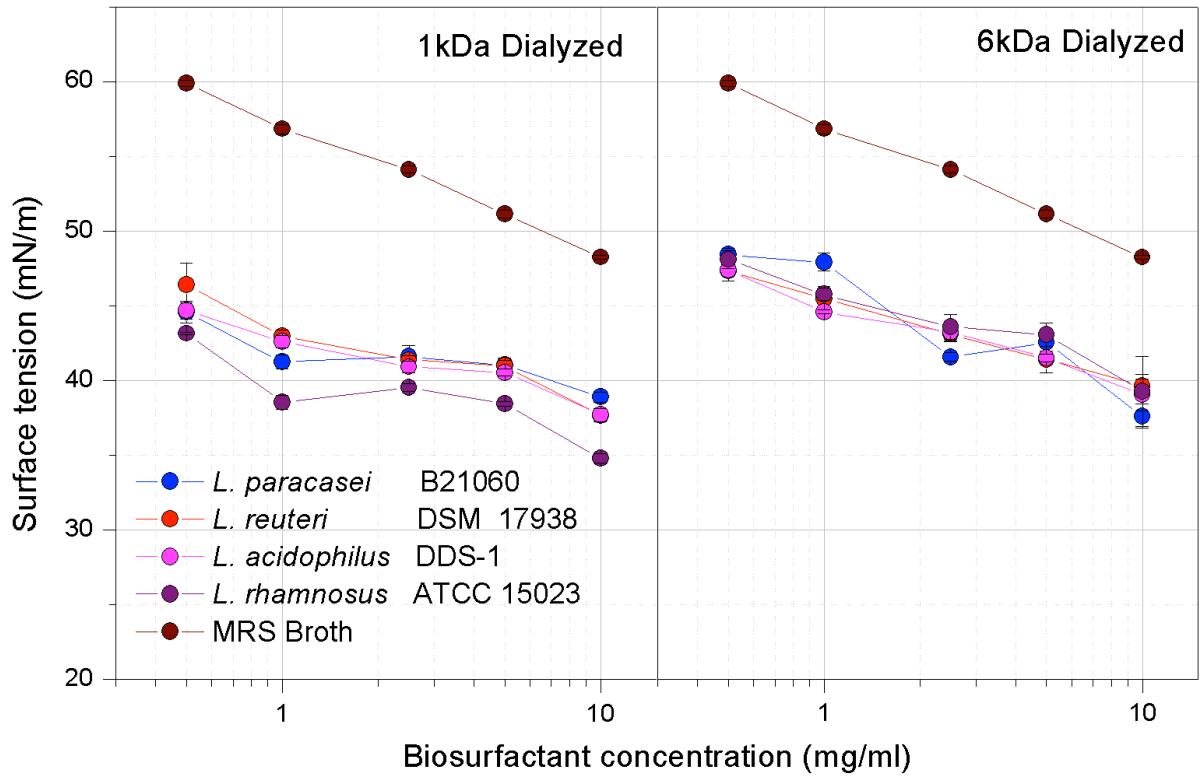

Fig. 2. Effect of dialyzed (1kDa and 6kDa) biosurfactants on their air/water surface tension (mN/m) at different concentrations, obtained from *L. reuteri* DSM 17938, *L. acidophilus* DDS-1, *L. rhamnosus* ATCC 53103, *L. paracasei* B21060, and the starting MRS broth used. The reference surface tension value was 72.2 mN/m. Results represent the average of three independent measurements, and *error bars* represent standard deviations of the mean values.

The estimation of emulsification activity (E24) against paraffin oil was also employed to assess the biosurfactant activity. Data obtained from the differently dialyzed biosurfactants

(Table 1) were compared with those of distilled water, as negative control, and 1% SDS, a common chemical surfactant, as positive control. All the dialyzed biosurfactants showed dose-dependent emulsifying activities, with the highest E24 index of 50% and 61.11% for the 1kDa and 6kDa dialyzed biosurfactants from *L. paracasei* B21060, respectively, comparable with 58% and 57% referred by referred by Sharma and Saharan [19]. However, all the 6kDa dialyzed biosurfactants, with the exception of that from *L. paracasei* B21060, showed E24 values higher than those of the correspondent 1kDa dialyzed biosurfactants.

Table 1. Surface tension and emulsification activity against paraffin oil of dialyzed biosurfactants (1 and 6 kDa) produced by selected Lactobacillus spp.

	Surface tension[a]				Percent of emulsification (E24 index)[b]			
	Dialyzed 1 kDa		Dialyzed 6 kDa		Dialyzed 1 kDa		Dialyzed 6 kDa	
Strains	10 mg/ml	1 mg/ml	10 mg/ml	1 mg/ml	10 mg/ml	1 mg/ml	10 mg/ml	1 mg/ml
L. reuteri DSM 17938	37.67 ± 0.33	42.98 ± 0.40	39.65 ± 0.75	45.38 ± 0.80	42.86	46.67	58.82	35.29
L.acidophilus DDS-1	37.71 ± 0.44	42.61 ± 0.41	39.04 ± 1.08	44.59 ± 0.13	46.67	37.50	53.33	47.06
L. rhamnosus ATCC 15023	34.81 ± 0.31	38.53 ± 0.48	39.27 ± 2.36	45.75 ± 0.42	43.75	37.50	58.82	52.94
L. paracasei B21060	38.90 ± 0.34	41.24 ± 0.45	37.62 ± 0.82	47.92 ± 0.58	50.00	41.18	61.11	41.17

[a] Surface tension of MRS broth was 53.0 mN/m; surface tension of water was 72.2 mN/m
[b] Emulsification index of 1 % SDS was 65.52 % and that of distilled water was 1.72 %

5.3.3 Anti-biofilm effect of dialyzed biosurfactants

The anti-biofilm activity of dialyzed biosurfactants (1kDa and 6kDa) against streptococci was assessed by the plate counts agar. As shown in Fig.3, all 1kDa and 6kDa dialyzed BSFs were effective to inhibit the biofilm growth of *S. mutants* ATCC 25175 and *S. oralis* ATCC 9811. As regards *S. mutans* ATCC 25175, 1kDa dialyzed biosurfactants produced by *L. acidophilus* DDS-1, *L. paracasei* B21060 and *L. rhamnosus* ATCC 53103, induced a cfu/ml reduction of 3-log when tested at 10 mg/ml, while that from *L. reuteri* DSM 17938 determined a reduction less than 2-log. Moreover, a lower logarithmic decrease of the cfu/ml values of *S. mutans* ATCC 25175 was observed when treated with 1kDa dialyzed BSFs at the concentration of 1

mg/ml, thus highlighting their dose-dependent effect (Fig. 3a). Moreover, the 1kDa dialyzed BSF from *L. acidophilus* DDS-1 (10 mg /ml) was the most effective against *S. oralis* ATCC 9811 biofilm formation, showing a cfu/ml reduction of 3-log. On the other hand, BSFs produced by *L. reuteri* DSM17938*, L. rhamnosus* ATCC 53103 and *L. paracasei* B21060 caused a moderate decrease of cfu /ml values in *S. oralis* ATCC 9811 (Fig. 3a). As regards 6 kDa dialyzed BSFs produced by *L. reuteri* DSM17938, *L. acidophilus* DDS-1 and *L. paracasei* B21060 and tested at 10 mg/ml, a 1-log reduction in cfu/ml values of *S. mutans* ATCC 25175 was observed, while that of *L. rhamnosus* ATCC53103 determined 3-log reduction (Fig. 3b). Moreover, the BSFs 6kDa of L. *acidophilus* DDS-1 and *L. rhamnosus* ATCC53103 (10 mg/ml) exhibited good antimicrobial activity against *S. oralis* ATCC 9811, with a 3-log reduction, while those of *L. reuteri* DSM 17938 and *L. paracasei* B21060, at the same concentration, induced only 1 log reduction in cfu /ml values (Fig. 3b). A dose-dependent effect was also confirmed for the 6kDa BSFs against *S. mutans* ATCC 25175 and *S. oralis* ATCC 9811.

FCM analysis, assessed by double staining with SYBR Green I and PI, showed a remarkable biofilm inhibition percentage in term of total viable cells in each treated sample. In particular, all the 1kDa dialyzed biosurfactants 10 mg/ml showed the higher inhibition percentages of biofilm formation against *S. mutans* ATCC 25175, with values ranging from 98.25% with BSF from *L. acidophilus* DDS-1 to 99.18% with that from *L. reuteri* DSM 17938. In the case of *S. oralis* ATCC 9811, the percentages of biofilm formation inhibition ranged from 92.32% with BSF from *L. paracasei* B21060 to 98.19% with BSF from *L. reuteri* DSM 17938. As regards 6kDa biosufactants, biofilm inhibition percentages against *S. mutans* ATCC 25175 ranged from 92.52% with BSF from *L. rhamnosus* ATCC 53103 to 96.43% with BSF from *L. acidophilus* DDS-1. Similarly, biofilm inhibition percentages toward *S. oralis* ATCC 9811 varied from 94.79% with BSF from *L. reuteri* DSM 17938 to 95.52% with that from *L. acidophilus* DDS-1. FCM analysis also registered the dose-dependent effect of 1kDa and 6kDa dialyzed biosurfactants with less activity at 1 mg/ml concentration against *S. mutans* ATCC 25175 and *S. oralis* ATCC 9811.

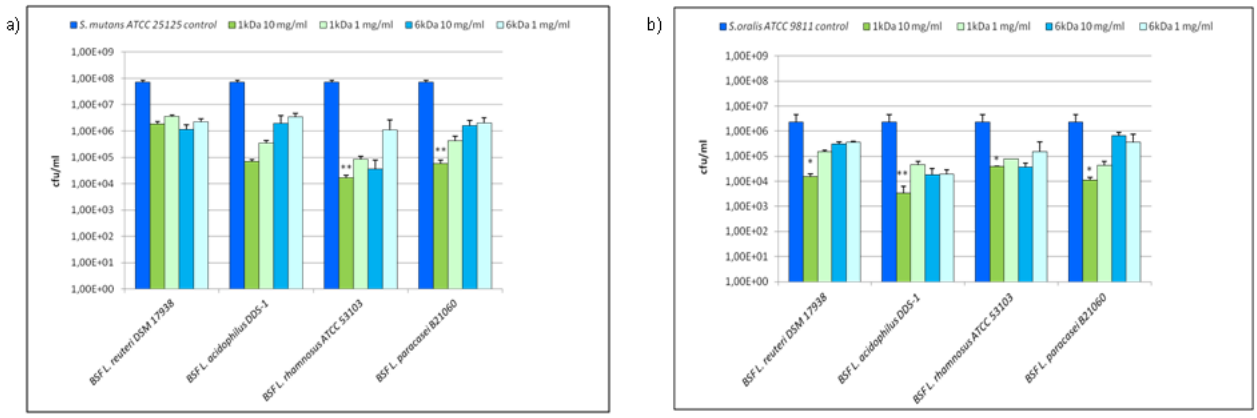

Fig. 3. Activity of dialyzed biosurfactants (1kDa and 6kDa) produced by *L. reuteri* DSM 17938, *L. acidophilus* DDS-1, *L. rhamnosus* ATCC 53103 and *L. paracasei* B21060 at two concentrations (10 mg/ml and 1 mg/ml) against *S. mutans* ATCC 25175 **(a)** and *S. oralis* ATCC 9811**(b)** biofilm formation assessed by counts agar.

5.4 Discussion

Several studies have shown the beneficial properties of lactobacilli for humans in various anatomic districts, including the gastrointestinal and the genito-urinary tracts [24]. In addition, these bacteria have been recognized as fundamental in the maintenance of homeostasis in the oral cavity [25]. The ability showed by streptococci to steadily adhere to the surfaces of salivary protein-coated teeth and to dental implants, and to create a biofilm, is fundamental for the promotion of the oral lesion development leading, at least, to dental or implant loss.

An important protective role was demonstrated by lactobacilli in the biofilm process [16,25]. Lactobacilli were able to reduce the growth in the oral cavity of pathogens, such as streptococci, and to inhibit the biofilm formation [26–28]. Lactobacilli are also involved in the process of biofilm formation on oral surfaces, by exerting an anti-microbial and anti-adhesive effect against pathogen bacteria through the production of specific substances, such as bacteriocins and biosurfactants and, at the same time, by competing with them for the colonization [15].

In the present study, the antimicrobial activity of crude excreted biosurfactants derived from different *Lactobacillus* spp. toward *S. mutans* ATCC 25175 and *S. oralis* ATCC 9811 was initially studied.

Since crude excreted biosurfactants are complex biological mixtures released in the culture media, a dialysis method was initially employed to collect different molecular weight purified fractions. The two obtained fractions (1kDa and 6kDa cut-off) after freeze-drying, were then characterized in terms of surface tension reduction and emulsifying ability. In fact, according

to the literature, bacteria with high surface activity and emulsifying properties represent promising microbial candidates for biosurfactants production [29].

As regards the surface tension, a reduction of the interfacial tension from 47.92 to 34.81 mN/m was observed for all 1kDa and 6kDa dialyzed fractions after 48 h of incubation, when compared to the surface tension of MRS broth (53.0 mN/m), with a slight higher surface activity in the 1kDa fractions. This decrease of surface tension confirmed the production of biosurfactants by the isolates and accumulation within the media.

Another characteristic of a biosurfactants is their ability to reduce pathogen adhesion and subsequent biofilm formation on different surfaces, such as plastic materials or glass [9,24,30,18]. Therefore, biosurfactants, fully characterized for their surface properties, have been then evaluated for their antimicrobial activity against *S. mutans* ATCC 25175 and *S. oralis* ATCC 9811 on titanium surface. The results reported in the present study indicate an anti-biofilm activity of the dialyzed BSFs when added in the culture medium, as demonstrated by decrease of cfu/ml and FCM values. The inhibitory effect showed a dose-dependence for both the 1kDa and 6kDa BSFs against *S. mutans* ATCC 25175 and *S. oralis* ATCC 9811.

5.5 Conclusions

Surface interactions are mediated by the amphiphilic nature of surfactants characterized by an hydrophilic portion and an hydrophobic regions, allowing them to act as surfactants at the interfaces [31,32]. Biosurfactants can be excreted in the culture broth or remain attached to the cell wall of bacteria, but most data in literature are referred to cell-bound biosurfactants [10,11], and few reports are available on biosurfactants contained in culture media [33]. This study represents the first work in which the excreted biosurfactants of different LAB strains were dialyzed and characterized for their surface ability prior to be tested for their antimicrobial activity. Moreover, we have demonstrated that active biosurfactant molecules are released by LAB in the culture media, from which can be separated by a simple dialysis method, and, the obtained dialyzed fractions, in particular those with 6kDa molecular weight, possess surface properties, antimicrobial and anti-biofilm activities against oral streptococci.

Our results confirm that LAB strains are biosurfactant producers and, since these microrganisms are considered as GRAS, their biosurfactants are safe for human consumption and biomedical applications. In particular, biosurfactants of LAB origin, reducing the ability of streptococci to adhere and develop biofilm on oral surfaces, may contribute to prevent oral diseases. These findings are encouraging and could suggest the application of lactobacilli

excreted biosurfactants as surface active agents in oral hygiene formulations, or as suitable alternative to conventional antimicrobials. Further studies are undergoing to better understand the chemical structural characterization of these excreted biosurfactants.

References

[1] D.S. Francy, J.M. Thomas, R.L. Raymond, C.H. Ward, Emulsification of hydrocarbons by subsurface bacteria, J. Ind. Microbiol. 8 (1991) 237–245. doi:10.1007/BF01576061.

[2] L. Rodrigues, I.M. Banat, J. Teixeira, R. Oliveira, Biosurfactants: potential applications in medicine, J. Antimicrob. Chemother. 57 (2006) 609–618. doi:10.1093/jac/dkl024.

[3] B. Saharan, R. Sahu, D. Sharma, A Review on Biosurfactants: Fermentation, Current Developments and Perspectives, Genet. Eng. Biotechnol. J. 2011 (2011).

[4] F. Ahimou, P. Jacques, M. Deleu, Surfactin and iturin A effects on Bacillus subtilis surface hydrophobicity, (n.d.).

[5] M. Nitschke, S.G.V.A.O. Costa, J. Contiero, Rhamnolipid Surfactants: An Update on the General Aspects of These Remarkable Biomolecules, (n.d.). doi:10.1021/bp050239p.

[6] A. Daverey, K. Pakshirajan, Production, Characterization, and Properties of Sophorolipids from the Yeast Candida bombicola using a Low-cost Fermentative Medium, Appl. Biochem. Biotechnol. 158 (2009) 663–674. doi:10.1007/s12010-008-8449-z.

[7] L.R. Rodrigues, J.A. Teixeira, H.C. Van Der Mei, R. Oliveira, Isolation and partial characterization of a biosurfactant produced by Streptococcus thermophilus A, Colloids Surfaces B Biointerfaces. 53 (2006) 105–112. doi:10.1016/j.colsurfb.2006.08.009.

[8] P. Saravanakumari, K. Mani, Structural characterization of a novel xylolipid biosurfactant from Lactococcus lactis and analysis of antibacterial activity against multi-drug resistant pathogens, Bioresour. Technol. 101 (2010) 8851–8854. doi:10.1016/j.biortech.2010.06.104.

[9] E.J. Gudiña, J.A. Teixeira, L.R. Rodrigues, Isolation and functional characterization of a biosurfactant produced by Lactobacillus paracasei, Colloids Surfaces B Biointerfaces. 76 (2010) 298–304. doi:10.1016/j.colsurfb.2009.11.008.

[10] D. Sharma, B.S. Saharan, N. Chauhan, S. Procha, S. Lal, Isolation and functional characterization of novel biosurfactant produced by Enterococcus faecium., Springerplus. 4 (2015) 4. doi:10.1186/2193-1801-4-4.

[11] D. Sharma, B.S. Saharan, N. Chauhan, A. Bansal, S. Procha, Production and structural characterization of Lactobacillus helveticus derived biosurfactant, Sci. World J. 2014 (2014) 1–9. doi:10.1155/2014/493548.

[12] S.S. Socransky, A.D. Haffajee, Dental biofilms: difficult therapeutic targets., Periodontol. 2000. 28 (2002) 12–55.

[13] V.I. Ntrouka, D.E. Slot, A. Louropoulou, F. Van der Weijden, The effect of chemotherapeutic agents on contaminated titanium surfaces: a systematic review, Clin. Oral Implants Res. 22 (2011) 681–690. doi:10.1111/j.1600-0501.2010.02037.x.

[14] J.G. Jeon, P.L. Rosalen, M.L. Falsetta, H. Koo, Natural products in caries research: Current (limited) knowledge, challenges and future perspective, Caries Res. 45 (2011) 243–263. doi:10.1159/000327250.

[15] E.M. Söderling, A.M. Marttinen, A.L. Haukioja, Probiotic Lactobacilli Interfere with Streptococcus mutans Biofilm Formation In Vitro, Curr. Microbiol. 62 (2011) 618–622. doi:10.1007/s00284-010-9752-9.

[16] R. Teanpaisan, S. Piwat, G. Dahlén, Inhibitory effect of oral Lactobacillus against oral pathogens, Lett. Appl. Microbiol. 53 (2011) 452–459. doi:10.1111/j.1472-765X.2011.03132.x.

[17] A.M. Marttinen, A.L. Haukioja, M. Keskin, E.M. Söderling, Effects of Lactobacillus reuteri PTA 5289 and L. paracasei DSMZ16671 on the Adhesion and Biofilm Formation of Streptococcus mutans, Curr. Microbiol. 67 (2013) 193–199. doi:10.1007/s00284-013-0352-3.

[18] A. Tahmourespour, R. Salehi, R.K. Kermanshahi, Lactobacillus acidophilus-derived biosurfactant effect on gtfB and gtfC expression level in Streptococcus mutans biofilm cells, Brazilian J. Microbiol. 42 (2011) 330–339. doi:10.1590/S1517-83822011000100042.

[19] D. Sharma, B. Singh Saharan, Simultaneous Production of Biosurfactants and Bacteriocins by Probiotic *Lactobacillus casei* MRTL3, Int. J. Microbiol. (2014) 1–7. doi:10.1155/2014/698713.

[20] S.H. Kim, E.J. Lim, S.O. Lee, J.D. Lee, T.H. Lee, Purification and characterization of biosurfactants from Nocardia sp. L-417, Biotechnol. Appl. Biochem. 31 (2000) 249–253. doi:10.1042/BA19990111.

[21] I. Kuiper, E.L. Lagendijk, R. Pickford, J.P. Derrick, G.E.M. Lamers, J.E. Thomas-Oates, B.J.J. Lugtenberg, G. V Bloemberg, Characterization of two Pseudomonas putida lipopeptide biosurfactants, putisolvin I and II, which inhibit biofilm formation and break down existing biofilms., Mol. Microbiol. 51 (2004) 97–113.

[22] E. Ciandrini, R. Campana, S. Federici, A. Manti, M. Battistelli, E. Falcieri, S. Papa, W. Baffone, In vitro activity of Carvacrol against titanium-adherent oral biofilms and planktonic cultures, Clin. Oral Investig. 18 (2014) 2001–2013. doi:10.1007/s00784-013-1179-9.

[23] S. Barbesti, S. Citterio, M. Labra, M.D. Baroni, M.G. Neri, S. Sgorbati, Two and three-color fluorescence flow cytometric analysis of immunoidentified viable bacteria, Cytometry. 40 (2000) 214–218. doi:10.1002/1097-0320(20000701)40:3<214::AID-CYTO6>3.0.CO;2-M.

[24] E.Z. Gomaa, Antimicrobial and anti-adhesive properties of biosurfactant produced by lactobacilli isolates, biofilm formation and aggregation ability, J. Gen. Appl. Microbiol. 59 (2013) 425–436. doi:10.2323/jgam.59.425.

[25] J. Meurman, Stamatova I, Lactic acid bacteria in oral health, in: Lact. Acid Bact. Microbiol. Funct. Asp., CRC press, 2011: pp. 403–422.

[26] E. Çaglar, S. Kavaloglu Cildir, S. Ergeneli, N. Sandalli, S. Twetman, Salivary mutans streptococci and lactobacilli levels after ingestion of the probiotic bacterium *Lactobacillus reuteri* ATCC 55730 by straws or tablets, Acta Odontol. Scand. 64 (2006) 314–318. doi:10.1080/00016350600801709.

[27] E. Çaglar, O.O. Kuscu, S.K. Cildir, S.S. Kuvvetli, N. Sandalli, A probiotic lozenge administered medical device and its effect on salivary mutans streptococci and lactobacilli, Int. J. Paediatr. Dent. 18 (2008) 35–39. doi:10.1111/j.1365-263X.2007.00866.x.

[28] H. Jalasvuori, A. Haukioja, J. Tenovuo, Probiotic Lactobacillus reuteri strains ATCC PTA 5289 and ATCC 55730 differ in their cariogenic properties in vitro, Arch. Oral Biol. 57 (2012) 1633–1638. doi:10.1016/j.archoralbio.2012.07.014.

[29] I.M. Banat, R.S. Makkar, S.S. Cameotra, Potential commercial applications of microbial surfactants., Appl. Microbiol. Biotechnol. 53 (2000) 495–508.

[30] L. Rodrigues, I.M. Banat, J. Teixeira, R. Oliveira, Biosurfactants: Potential applications in medicine, J. Antimicrob. Chemother. 57 (2006) 609–618. doi:10.1093/jac/dkl024.

[31] D. Myers, Surfactant science and technology, J. Wiley, 2006.

[32] I.M. Banat, A. Franzetti, I. Gandolfi, G. Bestetti, M.G. Martinotti, L. Fracchia, T.J. Smyth, R. Marchant, Microbial biosurfactants production, applications and future potential, Appl. Microbiol. Biotechnol. 87 (2010) 427–444. doi:10.1007/s00253-010-2589-0.

[33] D. Sharma, B.S. Saharan, Simultaneous production of biosurfactants and bacteriocins by probiotic lactobacillus casei MRTL3, Int. J. Microbiol. 2014 (2014). doi:10.1155/2014/698713.

SECTION TWO

POLYMERIC NANOCARRIERS: THEORY AND APPLICATIONS AS INNOVATIVE DRUG DELIVERY SYSTEMS

Chapter 6

General Introduction

6.1 A historical overview of nanoparticles development

In his talk "There's Plenty of Room at the bottom", the physician Richard Feynman laid the foundations for the field nowadays known as "nanotechnology", imaging a day when things could be miniaturized and machines could be made smaller. He asked the audience:" I don't know how to do this on a small scale in a practical way, but I do know that computing machines are very large; they fill rooms. Why can't we make them very small, make them of little wires, little elements, and by little, I mean little?"[1]. It was 1960 when Feyman gave his talk, and today, over fifty years after, the nanotechnology field has grown exponentially, gaining a central role in tissue engineering, electronic, nanobiotechnology, medicine and drug delivery. Both academia and industry are actively working on the development of nanoscale systems (1-1000 nm) intended for different applications, and research on this field has achieved considerable progress.

Among the several applications of nanomaterials, many efforts have been made during the last decades in drug delivery systems and research on the "nano" field resulted in the advent of innovative nanopharmaceuticals, also reported as "nanodrugs" or "nanomedicines". Nanopharmaceuticals have been defined by Rivera et al. as " *Pharmaceuticals engineered on the nanoscale, ie, pharmaceuticals where the nanomaterial plays the pivotal therapeutic role or adds additional functionality to the previous compound"* [2].

The term "nanomedicine" define the application of nanotechnology to medicine. It employs nanoscale systems for prevention, diagnosis and treatment of a specific disease, with the final aim of improving the quality of life of patients in treatment. The need for improved drug delivery systems motivated the significant efforts made over the last years in the nanomedicine field.

The concept of nanoparticles and targeted delivery was for the first time introduced by the Nobel Prize winner Paul Ehrlich, in the early twentieth century. As reported by Greiling, Ehrlich was inspired in this concept by the opera "Der Freischütz", where so-called "Freikugeln" always hit their goal nevertheless the rifleman or the goal [3,4]. Ehrlich, who had been working for a long time on the bacteriology and immunology field, immediately readapted this thought to drug delivery, certain that it would greatly improve drug therapy. That is how the famous concept of "magic bullet" was born.

One of the pioneers of nanoparticles application in controlled drug release was Professor Peter Paul Pseiser, who developed in the late 1960s at the ETH (Zürich), the first nanoparticles for vaccination purposes[5,6] . Nanomedicines can provide many advantages

compared to the conventional delivery systems. More specifically they can simultaneously protect the body from the drug and the drug from the body, avoiding both accumulation in healthy non-target tissues (site-avoidance drug delivery) and inactivation or metabolism of the drug once administered. Drugs can be physically entrapped or chemically bound to the nanocarrier system and depending on the nanocarrier system both hydrophobic and hydrophilic drugs can be transported. Moreover, a more precise targeting with a controlled drug release can be achieved by designing nanoparticles with specific functionalities, especially for those drugs that suffer of poor water solubility and low bioavailability (Fig. 1).

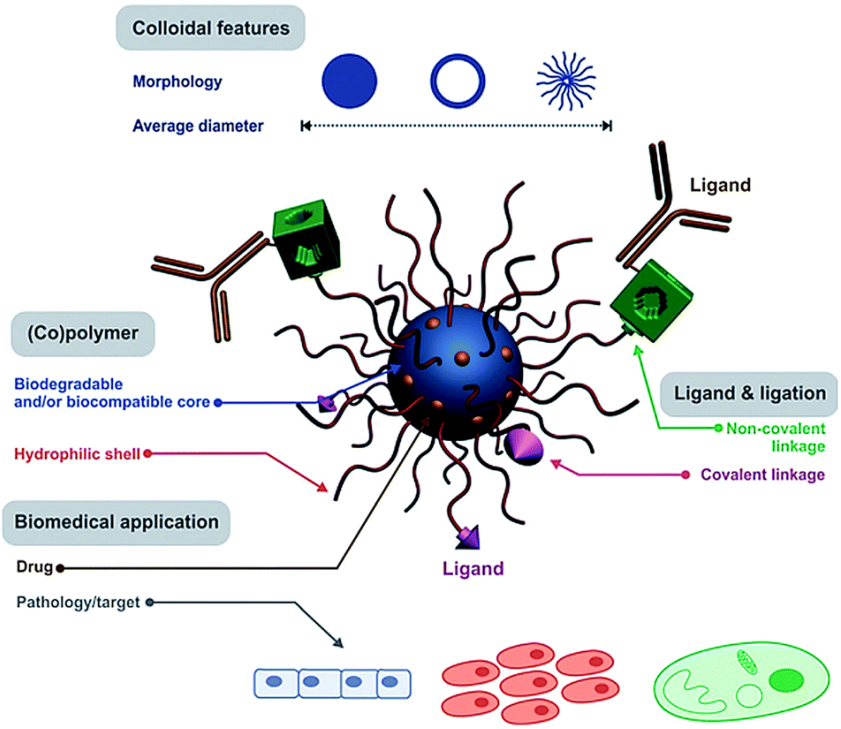

Fig. 1. Design of a nanomedicine-based drug delivery systems. Reproduced from ref. [25]

6.2 Nanomedicines: general classification and approved products

A comprehensive analysis of the state of art on nanomedicine was provided in 2013 by Etheridge et al. in "*The big picture on nanomedicine: the state of investigational and approved nanomedicine products*" [7]. Later, in 2014, Wessing et al. exhaustively reviewed the nanopharmaceutical products on the market, discussing all the 43 approved drug formulations [8].

Many different nanomedicines have been designed and evaluated over the years, including liposomes, drug conjugates, nanocrystals, dendrimers, polymeric micelles, organic and polymeric nanoparticles (Fig. 2).

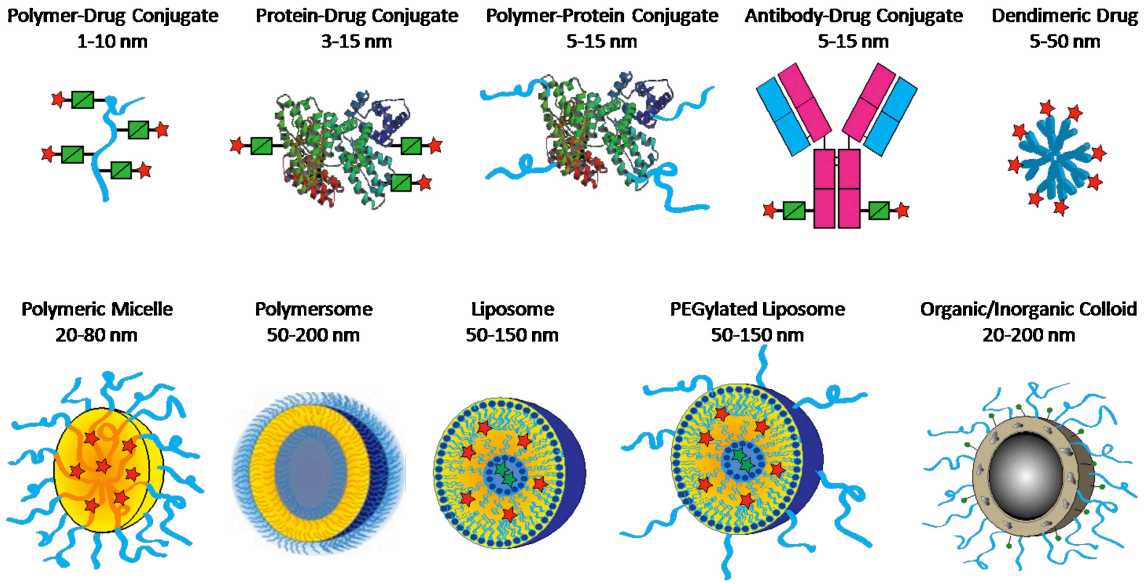

Fig. 2. Main nanoparticulate systems used for drug targeting. Image reproduced from ref. [9].

Among the nanocarrier systems developed so far, liposomes are frontrunners [10–12]. Liposomes are self-assembling lipid vehicles (typically 50-200 nm) constituted by a phospholipid bilayer surrounding an inner aqueous compartment. Due to their structure, they can load both hydrophilic and hydrophobic drugs in either the aqueous compartment or in the lipid bilayer, respectively. Stealth liposomes have also been designed by the addition of poly(ethylene glycol) (PEG) on the surface of the nanosystem, in order to increase the circulation time by reducing the recognition by the reticuloendothelial system (RES), also known as mononuclear phagocytic system (MPS) [13].

Research in the liposome field date back to early 1980s, when liposomes were first used by Forssen and Tökès to decrease the cardiotoxicity of doxorubicin [14] . In the same years, Gregoriadis reported the promising potential of liposomes as novel delivery system for traditional drugs [11]. Later, during the 1980s, three US start-up companies working on liposomes, competed in the development of three different doxorubicin liposomal formulations (The Liposome Company in Princeton, NJ, USA, Vestar in Pasadena, CA, USA, and Liposome Technology Inc., in Menlo Park, CA, USA) [8]. Research on liposome culminated in 1995 when the US Food and Drug Administration (FDA) approved Doxil®, "the first FDA-approved nanodrug ", for the treatment of AIDS-related Kaposi Sarcoma, multiple myeloma and ovarian cancer [15]. The benefit provided by the liposomal formulation are evident: while the free doxorubicin was characterized by an elimination half-

life time of 0.2 h and an AUC (area under the curve) of 4 μg h ml^{-1}, Doxil® demonstrated an elimination half-life of 55 h and an AUC of 900 μg h ml^{-1} [16].

Another interesting class of nanopharmaceuticals that have already reached the market, are PEGylated proteins and polypeptides. Generally, therapeutic agents such as enzymes, polypeptides and proteins would be classified as nanopharmaceuticals due to their size. Nevertheless, research in nanotechnology was focused on the improvement of the properties of these compounds, mainly by PEGylation. PEGylation is now recognized as a promising technique to increase circulation and retention time, decrease renal excretion and reduce immonogenicity of biological therapeutics [17] [18].

Protein-drug conjugates are also recognized as nanopharmaceuticals. In this regard, albumin has gained an increasing attention as a promising candidate to improve the pharmacokinetic profile of free drugs, and various albumin-based nanotherapeutics are currently in clinical trials [19]. Abraxane®, which is constituted by nanoparticles formed by albumin-paclitaxel conjugates, has received FDA approval in 2005 for the treatment of metastatic breast cancer and non-small lung cancer.

Inorganic nanoparticles have been extensively studied for their potential application in therapy, diagnosis and imaging and different formulations have reached the market so far. Feridex® received FDA approval in 1996 for magnetic resonance imaging (MRI). Feridex® is constituted by superparamagnetic iron oxide particles (SPION), surface modified with dextran.

Research in the nanoparticles field has recently been focused on polymer-based nanostructures, as promising platform for various pharmaceutical applications. In the following section a general overview of the various polymer-based nanocarriers is given, mainly focusing on polymeric micelles. Moreover, the main polymers employed for nanoparticles formulations is also listed.

6.3 Polymer-based nanocarriers

Among the various materials employed for biomedical applications, polymers have attracted a great attention in recent years due to their high flexibility, low toxicity and biocompatibility.

Polymers-based materials have been employed both in regenerative medicine and in the design of innovative drug delivery systems, such as nanocarriers. Biocompatibility and biodegradability are highly recommended to minimize toxicity and undesirable side effects [20].

Both synthetic and natural polymers have been employed in the formulation of nanosystems for drug delivery [21]. Initially natural polymers have been preferred, due to their abundance in nature and biocompatibility. However, they present some drawbacks that progressively limited their application, such as high batch to batch variability and risk of infections.

On the other hand, synthetic polymers, are really promising materials for biomedical applications due to their reproducibility and high flexibility of the final structure [22].

Several monomers, initiators and catalysts are available and various synthetic procedures can be employed such as ring opening polymerization (ROP), polycondensation, free radical polymerization, atomic transfer radical polymerization (ATRP) and reversible addition-fragmentation chain transfer (RAFT). Among the large variety of polymers available, only a limited number obtained regulatory approval for biomedical application. Among them, poly(ethylene glycol) (PEG), poly(ethylene oxide) (PEO)/poly(propylene oxide) (PPO)/ polyethylene oxide (PEO) (PEO-PPO-PEO; poloxamer); cellulose derivatives, poly(vinyl alcohol) (PVA); poly(DL-lactic acid) (PDLLA), poly(lactic-*co*-glycolic acid) (PLGA), polycaprolactone (PCL), polyacrilates, and polymethacrylates have been approved by the US Food and Drug Administration (FDA) and others authorities [20,21,23].

An important aspect that has to be deeply investigated is the toxicity related to the nanomaterials, which is often overgeneralized and underanappreciated. In fact, carrier systems tend to stay in the body much longer than the conventional low-molecular weight drugs. Thus biodegradation and biodistribution studies are necessarily required to better understand the toxicological profile [20,24].

Properties of nanoparticles can be easily tailored by selecting the polymer with the desired characteristics and based on the nature, physicochemical properties and composition, a great variety of nanostructures (comprising pH and temperature responsive) can be obtained [25].

Different polymer-based nanosystems have been designed so far, comprising nanoparticles (kinetically “frozen” state and their aggregation is not governed by a thermodynamic equilibrium), polymersomes (artificial vehicles resulting from the self-assembling of amphiphilic block copolymers into a bilayer membrane, surrounding an aqueous core) and polymeric micelles (PMs).

PMs have been extensively investigated in the last few years, especially for cancer treatment. PM are based on the spontaneous self-assembling of amphiphilic block copolymers into well-defined core-shell structures at a concentration exceeding their critical micelles concentration (CMC). The core segregation that occurs in an aqueous medium represents the driving force for micelles formation. Polymeric micelles were first proposed as drug nanocarriers by Bader

et al. due to their reduced size, they have been often compared to natural carrier systems, e.g. viruses and lipoproteins [26,27]. Polymeric micelles are characterized by a lower CMC compared to surfactants micelles, which ideally translates into a higher stability, prolonged circulation times and improved therapeutic index [28–30].

However, despite the pharmaceutical potential of polymeric micelles, when applied *in vivo* they suffer of poor stability and premature disintegration in the bloodstream, as their concentration decrease below the CMC. In this regard, different strategies have been employed so far to enhance micelles stability, including core and shell crosslinking. Thus, micelles can be stabilized via the formation of covalent bonds, hydrogen bonding or Π-Π stacking interactions. Drug retention into the micellar core can be increased by the covalent attachment of pro-drug molecules, employing for example stimuli-responsive drug linkers.

As regards the clinical translation, only one polymeric micelles-based formulation (Genexol-PM®) has been approved so far, while many others are currently under clinical trials [31]. Genexol-PM® is a paclitaxel PEG-PLLA based micellar formulation approved in South Korea in 2001 for the treatment of metastatic breast cancer and pancreatic cancer [32].

Overall, this section provides a general overview of the polymers used for biomedical applications and of the main classes of polymer-based nanoparticles. The properties of the nanocarrier can be tailored by changing the polymer and the operative conditions, thus affecting the final structure and biological properties of the nanosystem.

6.4 Long-circulating nanoparticles (PEGylation)

Many efforts have recently been made to develop nanopharmaceuticals that are able to circulate for a prolonged time, thus avoiding the mononuclear phagocyte system (MPS) recognition and uptake. The MPS is the main body defence line against the introduction of foreign biomaterials and particulate nanostructures. Circulating nanoparticles can interact with serum proteins, also known as opsonin proteins, and based on their physicochemical properties they can undergo opsonisation and consequently MPS uptake. Moreover, liver, spleen and kidneys represent anatomical barriers for circulating nanoparticles due to their fenestrated vasculature responsible for filtration and elimination of foreign compounds [33]. Nanoparticles uptake, filtration and elimination are highly dependent on their physicochemical characteristics such as hydrophobicity, size and surface charge.

Thus, engineered long-circulating nanoparticles have been designed with the purpose of limiting particles clearance from blood circulation [34]. Moreover, PEGylation have been

demonstrated to be really useful in cancer nanomedicine, to increase the circulation kinetic, as will be discussed later. A common strategy employed to overcome these limitation, is represented by surface modification with PEG, a highly flexible and hydrophilic polymer considered a successful strategy to avoid protein adhesion. PEGylation commonly refers to the decoration of the particles surface with PEG chains, which are able to induce a steric repulsion, thus preventing opsonisation [33].

PEGylated stealth nanoparticles can therefore remain invisible to phagocytic cells since they do not bind opsonin proteins, thus increasing their circulation half-life.

6.5 Biomedical applications of nanoparticles

Over the past decades significant advances have been made in the nanomedicine fields and nanoparticles-based formulations have been extensively studied for therapeutic, diagnostic and theranostic applications [35].

Nanoparticles have been initially proposed as promising drug delivery systems to improve the therapeutic efficacy of conventional drugs. The adverse pharmacokinetic and biodistribution of such compounds have been mainly referred to their low stability and low solubility in aqueous media. At the same time the reduced selectivity often related to the administration route, causes accumulation in healthy tissues, which translates in reduced efficacy and unexpected toxicity. Another problem faced by low-molecular weight drugs, is their renal excretion and hepatic degradation upon administration. Nanocarrier systems have been developed in order to overcome such limitations and increase the therapeutic efficacy of the loaded drug decreasing at the same time the associated toxicity to non-target organs.

Since the approval of Doxil®, significant investments have been made in the nanomedicine field and several advanced drug delivery systems have been developed to target different diseases. Several nanocarriers have been designed to address systemic, oral and local administration.

Small hydrophobic drugs, proteins and nucleic acids have been formulated using nanoparticles to overcome limitations, often associated to their traditional delivery.

As regards proteins, their oral availability is limited by the enzymatic degradation that occurs in the gastrointestinal tract and by the biological barrier that hinders intestinal absorption. Due to these issues, proteins have been commonly administered by invasive routes (e.g. subcutaneous). Therefore, formulation in nanoparticles is intended to reduce rapid

degradation and elimination of protein therapeutics, increasing at the same time their availability [36].

Polymer-based nanoparticles have been extensively employed as an attractive alternative to viral delivery systems for nucleic acids, whose transfection efficiency is limited by their negative charge and large size [37]. Nanoparticles have been used in vaccines formulations to provide a prolonged release of antigens (e.g. proteins, peptides, viruses or plasmid DNA, while targeting at the same time the immune system) [38–42] . Nanomedicine has been also widely applied to the treatment of inflammatory diseases, such as bowel diseases and rheumatoid arthritis [43–47]. Kreuter extensively revised the use of nanoparticles for drug delivery to brain, that represent a challenging organ for drug delivery mainly due to the presence of the blood brain barrier (BBB) [48].

Nanotechnology has been largely applied to the treatment of cardiovascular diseases, both for therapeutic, diagnostic and nanoengineering purposes [49–52].

As regards the administration route, a considerable research has been focused on the development of nanoparticles for oral delivery [53]. Oral administration has been largely exploited as an attractive alternative to the intravenous administration. Formulation into nanoparticles can be really useful in increasing drug stability and bioavailability when passing the gastrointestinal tract, where pH and digestive enzymes can dramatically influence the fate of the free drug [54].

Local drug delivery of nanoparticles provides many advantages compared to the systemic administration, including increased drug concentration and reduced systemic toxicity. The vaginal route is receiving an increasing interest for the mucosal administration of nanoparticles intended for both local and systemic application. Many advantages can ideally be provided by nanocarriers, such as protection of the active molecules from the pH of the vaginal tract, higher stability and solubility, increased retention time in the vaginal lumen and active targeting. For these purposes, microbiocides and antimicrobial drugs have been loaded into nanoparticles for the prevention of sexually transmitted infections and bacterial vaginosis.

6.6 Nanomedicine in cancer therapy: passive and active drug targeting

The vast majority of nanomedicine have been developed for cancer treatment. Traditional chemotherapeutic agents are characterized by a reduced solubility in aqueous systems due to their high hydrophobicity and low molecular weight, which translates in reduced therapeutic

efficacy, rapid clearance from the systemic circulation and accumulation in healthy tissues. Nanocarriers have been proposed as promising vehicles to increase "site-specific drug delivery", thus increasing the therapeutic index of the drug while decreasing side effects. Moreover, nanomedicines have been designed to assist traditional anti-cancer agents to overcome various biological barriers before reaching the target site [55,56]. Different mechanisms have been described to assist drug delivery to tumors, namely passive and active targeting (Fig. 3).

Nanoparticles application to cancer treatment was greatly motivated by the so-called enhanced permeability and retention (EPR) effect, first proposed by Maeda and colleagues [57,58]. Solids tumors are characterized by a leaky vasculature, which allow extravasation and accumulation of nanocarrier systems, with size up to 400 nm, at the target tissue. In addition, the reduced lymphatic drainage decreases the removal of extravasated nanoparticles from the tissue, thus increasing their retention time. To this end, long-circulating nanoparticles have been designed, to achieve extravasation and accumulation at the tumor site. This explains the key role of PEGylation in the development of long-circulating nanoparticles.

This mechanism is referred as "passive drug targeting", since it exploits the pathophysiological properties of the tissue to selectively promote drug accumulation. Although passive targeting constitutes the basis of clinical application of nanomedicine, it presents some evident limitations. Recent papers have exhaustively revised the EPR effect, often oversold and misinterpreted. Animal models are often inappropriate leading to an overestimation of the EPR effect. In fact, tumors grow much faster in animals and as results, blood vessels do not develop properly. Moreover the EPR effect is a really heterogeneous mechanism and a variability in vessels permeability between different tumors and patients has been observed [59,60]. Kaposi sarcoma is a prototype of tumor where the EPR effect can be largely exploited, due to abundant vasculature and to the presence of leaky vessels. In addition, it is possible to observe an intra tumor variability in vessel permeability.

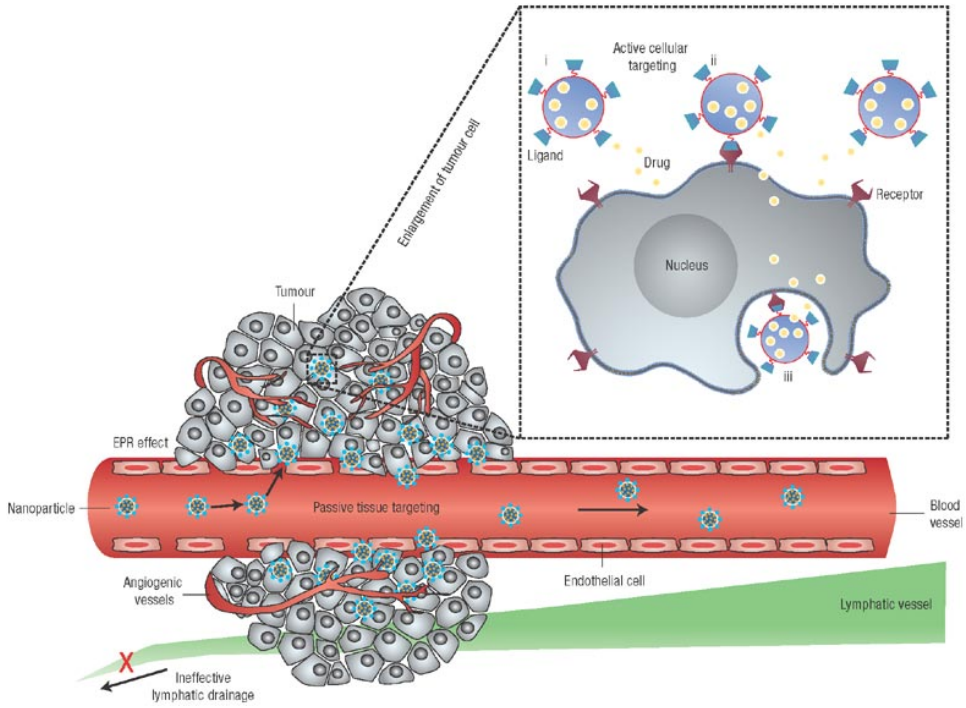

Fig. 3. Schematic representation of the different mechanisms involved in drug delivery to tumors. Passive targeting is achieved by extravasation from the leaky vasculature and reduced lymphatic drainage (EPR effect). Active targeting is achieved by surface functionalization of nanoparticles with specific ligands. Reproduced from ref. [61].

Another mechanism more recently investigated is represented by "Active drug targeting", which relies on the use of targeting ligands to facilitate target cells recognition and uptake, without influencing the overall tumor accumulation. Nanoparticles surface can be specifically functionalized using small molecules, antibodies, peptides and sugar moieties which specifically bind to overexpressed functionalities on the target cells, as extensively revised by Couvrer et al. [25]. Examples of the most investigated targeting ligands are folate, RGD peptide, transferrin and galactosamine [62,63]. Actively targeted nanoparticles can be really useful carrier systems for specific molecules, such as nucleic acids, which are unable themselves to enters cancer cells. Moreover, in the case of circulating cells, such as leukemia and lymphoma, an actively targeted nanomedicine represents a promising strategy for drug targeting to malignant cells.

A considerable benefit of actively targeted nanomedicine, over the conventional formulations designed for passive targeting, is represented by the potential longer retention time within the tumor tissue. Another big advantage over the untargeted nanomedicine, is the more efficient uptake of actively targeted nanomedicine by cancer cells.

Nanomedicines have been recently considered for diagnostic purposes. Labeling nanomedicines with contrast agents would be really useful for non-invasive imaging. The

application of nanomedicine in theranostic has also been proposed according to the "see and treat modalities". Thus, various formulations containing both drug and imaging agent have been developed and evaluated, resulting in the so-called "nanotheranostics" [64,65].

6.7 Into the future

Even if we are still far from the "magic bullet" proposed by the Nobel Prize Paul Ehrlich, nanomedicine achieved significant advances and several nanopharmaceuticals have been approved on the market, while many others are currently under clinical evaluation. Nanocarriers can provide many advantages in terms of drug solubility, biodistribution, circulation time, toxicity and therapeutic efficacy. Despite the recent advances in the nanomedicine field, their efficacy in cancer treatment has been questioned. In recently published controversial analysis of 10 years literature on nanoparticles, Wilhelm and colleagues came out with an impressive finding. In preclinical model only 0.7 % (median) of the intravenously administered nanoparticles was found to be delivered to the tumor [66]. This result, even if questionable, has to encourage scientists toward innovative applications of nanomedicines, intended to enable a more rapid and reliable clinical translation. The use of nanoparticles for theranostic purposes has been recently proposed as a promising strategy to rationally combine non-invasive imaging and tumor-targeted drug delivery. Patients can be selected based on the observed tumor accumulation for the treatment with the nanomedicine. Only patients showing high accumulation levels in tumors are then treated with nanoparticles and non-invasive imaging is used to identify patients responding well to the therapy. Based on these promising strategy, personalized therapies can be potentially developed so that only patients showing a significant EPR effect are treated with nanomedicines.

References

[1] R. Faeyman, There's plenty of room at the bottom, Eng.Sci (CalTech). 23 (1960) 22–36.

[2] P. Rivera Gil, D. Hühn, L.L. del Mercato, D. Sasse, W.J. Parak, Nanopharmacy: Inorganic nanoscale devices as vectors and active compounds, Pharmacol. Res. 62 (2010) 115–125. doi:10.1016/j.phrs.2010.01.009.

[3] J. Kreuter, Nanoparticles—a historical perspective, Int. J. Pharm. 331 (2007) 1–10. doi:10.1016/j.ijpharm.2006.10.021.

[4] W. Greiling, Paul Ehrlich, in: Econ Verlag, Düsseldorf, Ger., 1954: p. 48.

[5] S.C. Khanna, P. Speiser, Epoxy resin beads as a pharmaceutical dosage form I: Method of preparation, J. Pharm. Sci. 58 (1969) 1114–1117. doi:10.1002/jps.2600580916.

[6] S.C. Khanna, T. Jecklin, P. Speiser, Bead Polymerization Technique for Sustained-Release Dosage Form, J. Pharm. Sci. 59 (1970) 614–618. doi:10.1002/jps.2600590508.

[7] M.L. Etheridge, S.A. Campbell, A.G. Erdman, C.L. Haynes, S.M. Wolf, J. McCullough, The big picture on nanomedicine: the state of investigational and approved nanomedicine products, Nanomedicine Nanotechnology, Biol. Med. 9 (2013) 1–14. doi:10.1016/j.nano.2012.05.013.

[8] V. Weissig, T. Pettinger, N. Murdock, Nanopharmaceuticals (part 1): products on the market, Int. J. Nanomedicine. 9 (2014) 4357. doi:10.2147/IJN.S46900.

[9] M. Talelli, M. Barz, C.J.F. Rijcken, F. Kiessling, W.E. Hennink, T. Lammers, Core-crosslinked polymeric micelles: Principles, preparation, biomedical applications and clinical translation, Nano Today. 10 (2015) 93–117. doi:10.1016/j.nantod.2015.01.005.

[10] A.D. Bangham, M.M. Standish, J.C. Watkins, Diffusion of univalent ions across the lamellae of swollen phospholipids., J. Mol. Biol. 13 (1965) 238–52.

[11] G. Gregoriadis, The Carrier Potential of Liposomes in Biology and Medicine, N. Engl. J. Med. 295 (1976) 765–770. doi:10.1056/NEJM197609302951406.

[12] T. Lammers, W.E. Hennink, G. Storm, Tumour-targeted nanomedicines: principles and practice., Br. J. Cancer. 99 (2008) 392–7. doi:10.1038/sj.bjc.6604483.

[13] V.P. Torchilin, Recent advances with liposomes as pharmaceutical carriers, Nat. Rev. Drug Discov. 4 (2005) 145–160. doi:10.1038/nrd1632.

[14] E.A. Forssen, Z.A. Tökès, Use of anionic liposomes for the reduction of chronic doxorubicin-induced cardiotoxicity., Proc. Natl. Acad. Sci. U. S. A. 78 (1981) 1873–7.

[15] Y. (Chezy) Barenholz, Doxil® — The first FDA-approved nano-drug: Lessons learned, J. Control. Release. 160 (2012) 117–134. doi:10.1016/j.jconrel.2012.03.020.

[16] R.-D. Hofheinz, S.U. Gnad-Vogt, U. Beyer, A. Hochhaus, Liposomal encapsulated anti-cancer drugs, Anticancer. Drugs. 16 (2005).

[17] N.C.P. Frank F. Davis, Theodorus Van Es, Non-immunogenic polypeptides, 1977.

[18] F.F. Davis, The origin of pegnology, Adv. Drug Deliv. Rev. 54 (2002) 457–458. doi:10.1016/S0169-409X(02)00021-2.

[19] B. Elsadek, F. Kratz, Impact of albumin on drug delivery — New applications on the horizon, J. Control. Release. 157 (2012) 4–28. doi:10.1016/j.jconrel.2011.09.069.

[20] E. Marin, M.I. Briceño, C. Caballero-George, Critical evaluation of biodegradable polymers used in nanodrugs., Int. J. Nanomedicine. 8 (2013) 3071–90. doi:10.2147/IJN.S47186.

[21] B.D. Ulery, L.S. Nair, C.T. Laurencin, Biomedical Applications of Biodegradable Polymers., J. Polym. Sci. B. Polym. Phys. 49 (2011) 832–864. doi:10.1002/polb.22259.

[22] J.-M. Lü, X. Wang, C. Marin-Muller, H. Wang, P.H. Lin, Q. Yao, C. Chen, Current advances in research and clinical applications of PLGA-based nanotechnology, Expert Rev. Mol. Diagn. 9 (2009) 325–341. doi:10.1586/erm.09.15.

[23] R.C. Rowe, P.J. Sheskey, M.E. Quinn, Handbook of Pharmaceutical Excipients, 6 th, Pharmaceutical Press & American Pharmacists Association, London, UK & Grayslake, IL, USA, 2009.

[24] W.H. De Jong, P.J.A. Borm, Drug delivery and nanoparticles:applications and hazards., Int. J. Nanomedicine. 3 (2008) 133–49.

[25] J. Nicolas, S. Mura, D. Brambilla, N. Mackiewicz, P. Couvreur, Design, functionalization strategies and biomedical applications of targeted biodegradable/biocompatible polymer-based nanocarriers for drug delivery., Chem. Soc. Rev. 42 (2013) 1147–235. doi:10.1039/c2cs35265f.

[26] H. Bader, H. Ringsdorf, B. Schmidt, Watersoluble polymers in medicine, Angew. Makromol. Chemie. 123 (1984) 457–485. doi:10.1002/apmc.1984.051230121.

[27] M. Jones, J. Leroux, Polymeric micelles - a new generation of colloidal drug carriers., Eur. J. Pharm. Biopharm. 48 (1999) 101–11.

[28] G.S. Kwon, T. Okano, Polymeric micelles as new drug carriers, Adv. Drug Deliv. Rev. 21 (1996) 107–116. doi:10.1016/S0169-409X(96)00401-2.

[29] V.P. Torchilin, Targeted polymeric micelles for delivery of poorly soluble drugs, Cell. Mol. Life Sci. 61 (2004) 2549–2559. doi:10.1007/s00018-004-4153-5.

[30] K. Kazunori, K. Glenn S., Y. Masayuki, O. Teruo, S. Yasuhisa, Block copolymer micelles as vehicles for drug delivery, J. Control. Release. 24 (1993) 119–132. doi:10.1016/0168-3659(93)90172-2.

[31] A. Varela-Moreira, Y. Shi, M.H.A.M. Fens, T. Lammers, W.E. Hennink, R.M. Schiffelers, Clinical application of polymeric micelles for the treatment of cancer, Mater. Chem. Front. 1 (2017) 1485–1501. doi:10.1039/C6QM00289G.

[32] H. Cabral, K. Kataoka, Progress of drug-loaded polymeric micelles into clinical studies, J. Control. Release. 190 (2014) 465–476. doi:10.1016/j.jconrel.2014.06.042.

[33] D. Owens, N. Peppas, Opsonization, biodistribution, and pharmacokinetics of polymeric nanoparticles, Int. J. Pharm. 307 (2006) 93–102. doi:10.1016/j.ijpharm.2005.10.010.

[34] M.N. V. Ravi Kumar, Handbook of Polyester Drug Delivery Systems, n.d.

[35] F. Danhier, E. Ansorena, J.M. Silva, R. Coco, A. Le Breton, V. Préat, PLGA-based nanoparticles: An overview of biomedical applications, J. Control. Release. 161 (2012) 505–522. doi:10.1016/j.jconrel.2012.01.043.

[36] J.E. Talmadge, The pharmaceutics and delivery of therapeutic polypeptides and proteins, Adv. Drug Deliv. Rev. 10 (1993) 247–299. doi:10.1016/0169-409X(93)90049-A.

[37] S. Ribeiro, N. Hussain, A.T. Florence, Release of DNA from dendriplexes encapsulated in PLGA nanoparticles, Int. J. Pharm. 298 (2005) 354–360. doi:10.1016/j.ijpharm.2005.03.036.

[38] A. des Rieux, V. Fievez, M. Garinot, Y.-J. Schneider, V. Préat, Nanoparticles as potential oral delivery systems of proteins and vaccines: A mechanistic approach, J. Control. Release. 116 (2006) 1–27. doi:10.1016/j.jconrel.2006.08.013.

[39] M. Diwan, P. Elamanchili, H. Lane, A. Gainer, J. Samuel, Biodegradable nanoparticle mediated antigen delivery to human cord blood derived dendritic cells for induction of primary T cell responses, J. Drug Target. 11 (2003) 495–507. doi:10.1080/10611860410001670026.

[40] C. Clawson, C.-T. Huang, D. Futalan, D. Martin Seible, R. Saenz, M. Larsson, W. Ma, B. Minev, F. Zhang, M. Ozkan, C. Ozkan, S. Esener, D. Messmer, Delivery of a peptide via poly(d,l-lactic-co-glycolic) acid nanoparticles enhances its dendritic cell–stimulatory capacity, Nanomedicine Nanotechnology, Biol. Med. 6 (2010) 651–661. doi:10.1016/j.nano.2010.03.001.

[41] V. Manolova, A. Flace, M. Bauer, K. Schwarz, P. Saudan, M.F. Bachmann, Nanoparticles target distinct dendritic cell populations according to their size, Eur. J. Immunol. 38 (2008) 1404–1413. doi:10.1002/eji.200737984.

[42] J. Panyam, V. Labhasetwar, Biodegradable nanoparticles for drug and gene delivery to cells and tissue., Adv. Drug Deliv. Rev. 55 (2003) 329–47.

[43] A. Lamprecht, N. Ubrich, H. Yamamoto, U. Schäfer, H. Takeuchi, P. Maincent, Y. Kawashima, C.M. Lehr, Biodegradable nanoparticles for targeted drug delivery in treatment of inflammatory bowel disease., J. Pharmacol. Exp. Ther. 299 (2001) 775–81.

[44] A. Lamprecht, H. Yamamoto, H. Takeuchi, Y. Kawashima, Nanoparticles Enhance Therapeutic Efficiency by Selectively Increased Local Drug Dose in Experimental Colitis in Rats, J. Pharmacol. Exp. Ther. 315 (2005) 196–202. doi:10.1124/jpet.105.088146.

[45] M. Higaki, T. Ishihara, N. Izumo, M. Takatsu, Y. Mizushima, Treatment of experimental arthritis with poly(D, L-lactic/glycolic acid) nanoparticles encapsulating betamethasone sodium phosphate, Ann. Rheum. Dis. 64 (2005) 1132–1136. doi:10.1136/ard.2004.030759.

[46] E. Horisawa, K. Kubota, I. Tuboi, K. Sato, H. Yamamoto, H. Takeuchi, Y. Kawashima, Size-dependency of DL-lactide/glycolide copolymer particulates for intra-articular delivery system on phagocytosis in rat synovium., Pharm. Res. 19 (2002) 132–9.

[47] Y. Meissner, Y. Pellequer, A. Lamprecht, Nanoparticles in inflammatory bowel disease: Particle targeting versus pH-sensitive delivery, Int. J. Pharm. 316 (2006) 138–143. doi:10.1016/j.ijpharm.2006.01.032.

[48] J. Kreuter, Nanoparticulate systems for brain delivery of drugs., Adv. Drug Deliv. Rev. 47 (2001) 65–81.

[49] K. Donaldson, R. Duffin, J.P. Langrish, M.R. Miller, N.L. Mills, C.A. Poland, J. Raftis, A. Shah, C.A. Shaw, D.E. Newby, Nanoparticles and the cardiovascular system: a critical review, Nanomedicine. 8 (2013) 403–423. doi:10.2217/nnm.13.16.

[50] J.R. McCarthy, Nanomedicine and Cardiovascular Disease., Curr. Cardiovasc. Imaging Rep. 3 (2010) 42–49. doi:10.1007/s12410-009-9002-3.

[51] W.J.M. Mulder, Z.A. Fayad, Nanomedicine captures cardiovascular disease., Arterioscler. Thromb. Vasc. Biol. 28 (2008) 801–2. doi:10.1161/ATVBAHA.108.165332.

[52] S. Suarez, A. Almutairi, K.L. Christman, Micro- and nanoparticles for treating cardiovascular disease, Biomater. Sci. 3 (2015) 564–580. doi:10.1039/C4BM00441H.

[53] A.A. Date, J. Hanes, L.M. Ensign, Nanoparticles for oral delivery: Design, evaluation and state-of-the-art, J. Control. Release. 240 (2016) 504–526. doi:10.1016/j.jconrel.2016.06.016.

[54] T. Jung, W. Kamm, A. Breitenbach, E. Kaiserling, J.X. Xiao, T. Kissel, Biodegradable nanoparticles for oral delivery of peptides: is there a role for polymers to affect mucosal uptake?, Eur. J. Pharm. Biopharm. 50 (2000) 147–60.

[55] L.Y. Rizzo, B. Theek, G. Storm, F. Kiessling, T. Lammers, Recent progress in nanomedicine: therapeutic, diagnostic and theranostic applications, Curr. Opin. Biotechnol. 24 (2013) 1159–1166. doi:10.1016/j.copbio.2013.02.020.

[56] T. Lammers, Improving the efficacy of combined modality anticancer therapy using HPMA copolymer-based nanomedicine formulations☆, Adv. Drug Deliv. Rev. 62 (2010) 203–230. doi:10.1016/j.addr.2009.11.028.

[57] Y. Matsumura, H. Maeda, A new concept for macromolecular therapeutics in cancer chemotherapy: mechanism of tumoritropic accumulation of proteins and the antitumor agent smancs., Cancer Res. 46 (1986) 6387–92.

[58] H. Maeda, J. Wu, T. Sawa, Y. Matsumura, K. Hori, Tumor vascular permeability and the EPR effect in macromolecular therapeutics: a review., J. Control. Release. 65 (2000) 271–84.

[59] Y.H. Bae, K. Park, Targeted drug delivery to tumors: Myths, reality and possibility, J. Control. Release. 153 (2011) 198–205. doi:10.1016/j.jconrel.2011.06.001.

[60] R.K. Jain, T. Stylianopoulos, Delivering nanomedicine to solid tumors, Nat. Rev. Clin. Oncol. 7 (2010) 653–664. doi:10.1038/nrclinonc.2010.139.

[61] D. Peer, J.M. Karp, S. Hong, O.C. Farokhzad, R. Margalit, R. Langer, Nanocarriers as an emerging platform for cancer therapy, Nat. Nanotechnol. 2 (2007) 751–760. doi:10.1038/nnano.2007.387.

[62] S. Wang, P.S. Low, Folate-mediated targeting of antineoplastic drugs, imaging agents, and nucleic acids to cancer cells., J. Control. Release. 53 (1998) 39–48.

[63] Z.M. Qian, H. Li, H. Sun, K. Ho, Targeted drug delivery via the transferrin receptor-mediated endocytosis pathway., Pharmacol. Rev. 54 (2002) 561–87.

[64] T. Lammers, F. Kiessling, W.E. Hennink, G. Storm, Drug targeting to tumors: Principles, pitfalls and (pre-) clinical progress, J. Control. Release. 161 (2012) 175–187. doi:10.1016/j.jconrel.2011.09.063.

[65] T. Lammers, S. Aime, W.E. Hennink, G. Storm, F. Kiessling, Theranostic Nanomedicine, Acc. Chem. Res. 44 (2011) 1029–1038. doi:10.1021/ar200019c.

[66] S. Wilhelm, A.J. Tavares, Q. Dai, S. Ohta, J. Audet, H.F. Dvorak, W.C.W. Chan, Analysis of nanoparticle delivery to tumours, Nat. Rev. Mater. 1 (2016) 16014. doi:10.1038/natrevmats.2016.14.

Chapter 7

Toward the formulation of VLA-4 targeted polymeric micelles

I had the pleasure to work on this project as an exchange PhD student at the Department of Pharmaceutics, Utrecht University, under the supervision of Prof Dr. W.E. Hennink.

Acknowledgements

Prof. Dr. W.E. Hennink, Dr C.F. van Nostrum, Prof. Dr. R.M. Schiffelers, Dr. M.H.A Fens, A.A. Varela Moreira MSc, A.K. Deshantri MSc, M.J. van Steenbergen.

7.1 Introduction

Many of the clinically approved therapeutic agents for cancer treatment suffer of poor water solubility, systemic toxicity and rapid clearance, resulting in a reduced applicability and efficacy.

Different strategies have been exploited in order to overcome these issues, including development of innovative drug delivery systems (DDSs). Drug delivery systems are designed to deliver loaded drugs to the target site with the final aim of increasing the therapeutic efficacy while decreasing the associated systemic toxicity. In cancer, increased target site accumulation of DDSs has been attributed to the so-called enhanced permeability and retention (EPR) effect, first proposed by Maeda and co-workers in the mid-80s [1,2]. As a result of the EPR effect, nanocarrier systems are able to spontaneously and preferentially accumulate in tumors due to the leaky angiogenic vasculature and reduced lymphatic drainage. To this end, prolonged circulation kinetic of the system is required for the drug loaded nanoparticles to extravasate and accumulate into the targeted tissue.

Polymeric micelles have been recognized in the last decades as promising delivery systems for hydrophobic drugs. In 2007 the first micellar formulation Genexol^{TM}-PM, a paclitaxel-loaded methoxy poly(ethylene glycol)-block-poly(D,L-lactide) (mPEG-PDLLA) based system, was approved in South Korea for the treatment of various cancers [3,4]. Genexol™ showed a significant decrease in the associated toxicity and a maximum tolerated dose 2-3 times higher than the Taxol® formulation [3,5,6]. Since then, different polymeric micelles have entered clinical trials [7,8].

Polymeric micelles are nanoparticles with a defined size range of 10-200 nm, based on the self-assembly of amphiphilic block copolymers in aqueous media. They present many advantages compared to surfactant micelles as they are characterized by a lower critical micellar concentration (CMC) with consequent higher stability. A typical core-shell structure is formed in solution, with the hydrophobic block representing the inner core and the hydrophilic part oriented at the micelles surface. As a result, poor water-soluble drugs can be loaded into the hydrophobic core and can be retained for sufficient time by different mechanisms, such as physical or chemical attachment. Moreover polyethylene glycols (PEG) of different molecular weights have often been employed as hydrophilic corona, resulting in a stealthy surface that decreases the binding of plasma proteins during circulation [9,10].

Although a great interest has been focused on the development of innovative drug delivery systems, and research on micelles has considerably advanced [11–13], a significant limitation

is represented by the premature disintegration of polymeric micelles *in vivo* [14,15]. A lot of efforts have been made in the last decades on the development of more stable micellar systems, exploiting both chemical and physical cross-linking strategies.

While chemical crosslinking has been widely investigated, including shell and core covalent cross-linking [16–19], physical interactions have recently emerged as a promising strategy to increase micellar stability. In this regard, Shi et al. developed an amphiphilic block copolymer, exploiting Π-Π interactions to increase both the micellar stability and drug retention inside the micellar core, resulting in an improved pharmacokinetic profile and decelerated systemic drug release [20]. Methoxy poly(ethylene glycol)-b-(N-(2-benzoyloxypropyl) methacrylamide)) (mPEG-*b*-p-HPMA-Bz) block copolymer was synthetized by free radical polymerization using a macroinitiator route[21]. Additionally, aromatic benzoyl groups were introduced into the polymer structure to provide stronger hydrophobic interactions. Paclitaxel loaded polymeric micelles stabilized via Π-Π stacking, showed high tumor accumulation, and *in vivo* efficacy studies demonstrated complete tumor regression in murine xenograft models of human epidermoid carcinoma (A431) and human breast adenocarcinoma (MDA-MB-468). Based on these promising results, it is reasonable to consider mPEG-*b*-p-HPMA-Bz micelles as an attractive nanomedicine for the loading and delivery of different hydrophobic drugs.

Interestingly, recent evidences have shown the important role of angiogenesis in haematological malignancies, such as multiple myeloma (MM), to develop and grow [22–26]. Multiple myeloma is a kind of haematological malignancy characterized by uncontrolled proliferation of plasma cells in the bone marrow (BM) of patients. In this kind of malignancy, a major role is recognized to the BM microenvironment, which is responsible for the interaction with MM cells. This multiple myeloma-stroma alliance is also held responsible for cell-adhesion-mediated drug resistance (CAM-DR).

Targeting MM cells with specific ligands that bind to overexpressed receptors on MM cells could be useful tools to further steer target cell delivery. The therapeutic agent is delivered to malignant target cells and at the same time the adhesion of MM cells with BM stroma is inhibited [27,28]. This results in a reduced CAM-DR and increased therapeutic efficacy.

Very late antigen-4 (VLA-4) also known as $\alpha_4\beta_1$ integrin or CD49d/CD29, is an integrin dimer composed of the CD49d (α_4) and the CD29 (β_1) units, expressed on the surface of cancer cells of haematological origin. It is responsible for the adhesion of MM cells to BM stroma, and therefore it plays a major role in CAM-DR [29]. Particles functionalized with VLA- 4 antagonist will be able to both increase the cellular uptake and inhibit the cross-talk

between cancer cells and the BM microenvironment [30]. A schematic representation of the mechanisms involved is resumed in Fig. 1.

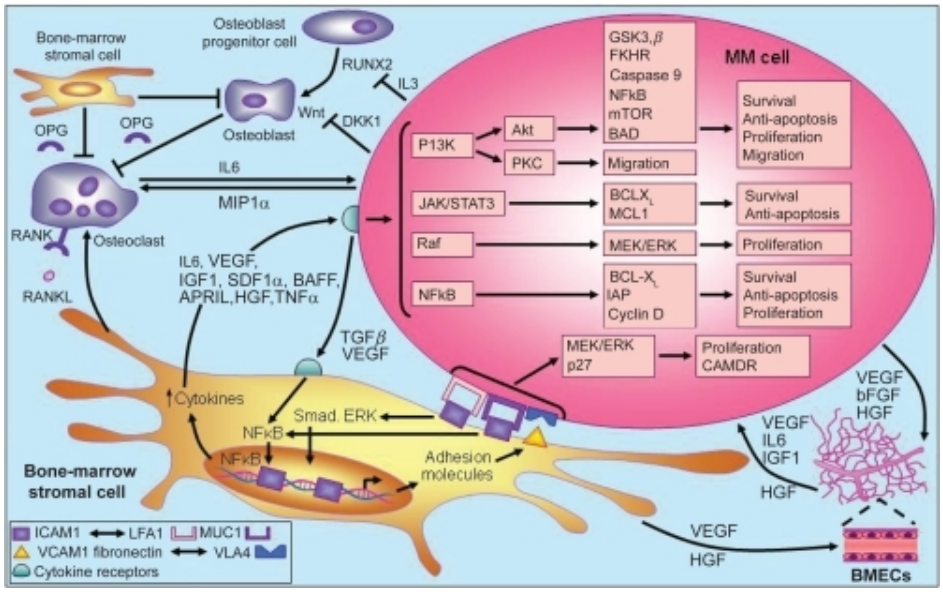

Fig. 1. Schematic representation of MM cells microenvironment and pathway involved in the pathogenesis of multiple myeloma. Image reproduced from ref [31].

The work reported in this chapter is part of a project that aims to employ polymeric micelles based on mPEG-*b*-p-HPMA-Bz as a dynamic self-assembly nanocarrier system to actively target MM cells using a specific VLA-4 antagonist peptide. A cyclic VLA-4 antagonist peptide (Tyr-Cys-Asp-Pro-Cys) protected with a SATA group was designed based on the results obtained from Kizilpete et al. [30]. The SATA functionalization was introduced to get a sulphydryl group available for coupling with the polymer (Fig. 2).

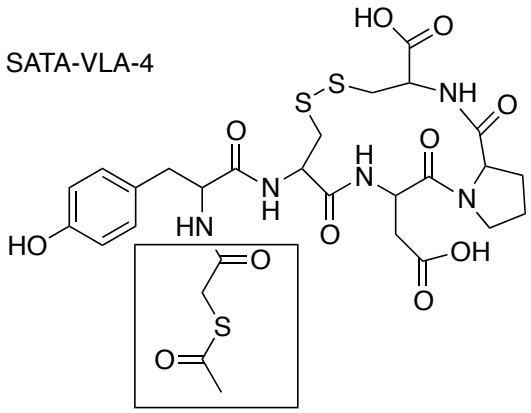

Fig. 2. Structure of SATA-VLA-4 peptide.

In the first step of the work, two different conjugation techniques (Fig. 3) have been exploited to functionalize the block copolymer with an appropriate linker for coupling with the targeting peptide.

In particular, maleimide poly(ethylene glycol) (Mal-PEG) and 3-(2-pyridyldithio) propionate poly(ethylene glycol) (PDP-PEG) (M_n 5000 g mol^{-1}) have been employed as hydrophilic blocks to create specific functionalities on the polymer structure, by exploiting the chemistry of these two reactive groups [32]. Unfortunately, the Mal-PEG strategy has proven to be difficult due to many factors that will be discussed later. Therefore, additional efforts were made to investigate a different strategy and an amine poly(ethylene glycol) (NH_2PEG-OH), functionalized with a heterobifunctional N-succinimidyl-3-(2-pyridyldithio)-propionate (SPDP) crosslinker, was finally used for the macroinitiator synthesis. SPDP is one of the most popular heterobifunctional crosslinking agents. The NHS ester end is available for reactions with amine groups while the 2-pyridylthiol group on the opposite side can undergo a disulphide exchange reaction with a sulphydryl groups [33]. SPDP is in fact a valid and largely exploited strategy for coupling sulphydryl containing molecules to liposomes [34].

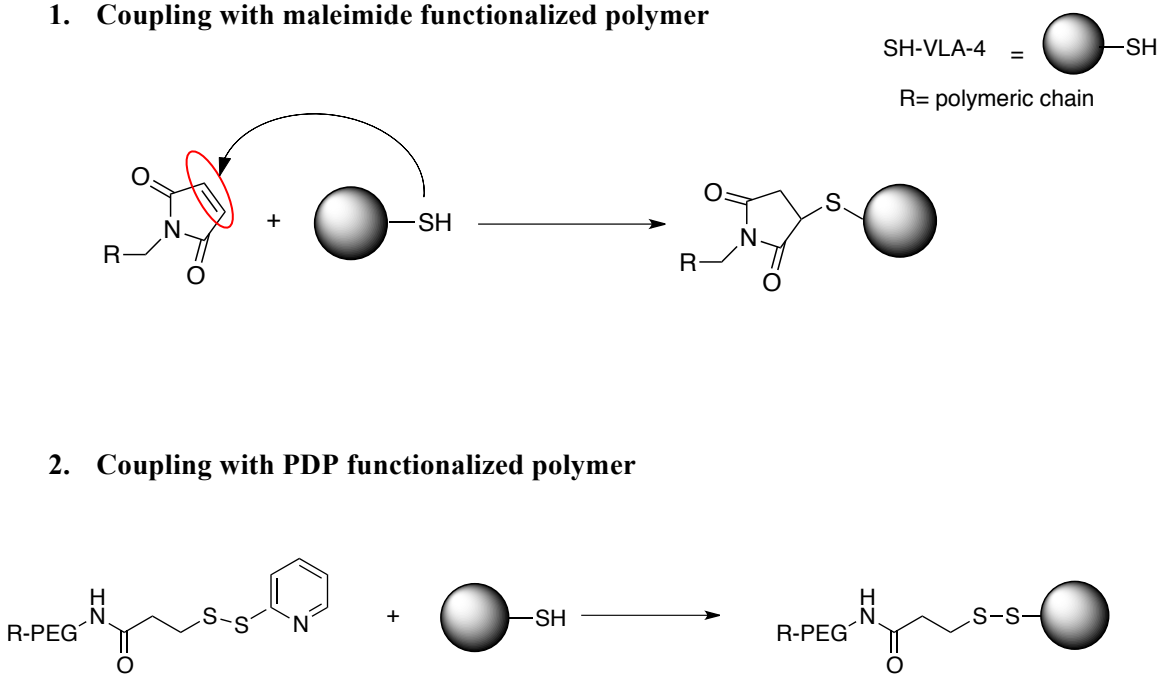

Fig. 3. Schematic representation of the conjugation techniques exploited in the present work. a) Expected VLA-4 coupling with mal-PEG functionalized polymer; b) VLA-4 coupling with PDP functionalized polymer.

In the second step, PDP surface modified micelles were formulated by using different amounts of mPEG-HPMA-Bz and PDP-PEG-*b*-p-(HPMA-Bz) block copolymers. The functionalized nanocarrier systems combines the novelty of Π–Π Stacking stabilized polymeric micelles with the advantages related to actively targeting systems. Micelles were formed by self-assembly to finally get the classical micellar core-shell structure. The prepared micelles were characterized for their properties by dynamic light scattering (DLS) and dithiothreitol (DTT) assay, to assess their size distribution and the amount of PDP exposed on the micelles surface and therefore available for conjugation with VLA-4 peptide, respectively. 5% PDP-PEG-*b*-p-(HPMA-Bz) micelles were finally selected as the most promising system for the next step.

A post micellar modification strategy was chosen for the coupling of VLA-4 to PDP-PEG-*b*-p-(HPMA-Bz) (Fig. 4). Preliminary experiments to efficiently couple VLA-4 peptide to the micelles surface and to determine the coupling efficiency were conducted and future studies will focus on the optimization of the formulation to then test *in vitro* models.

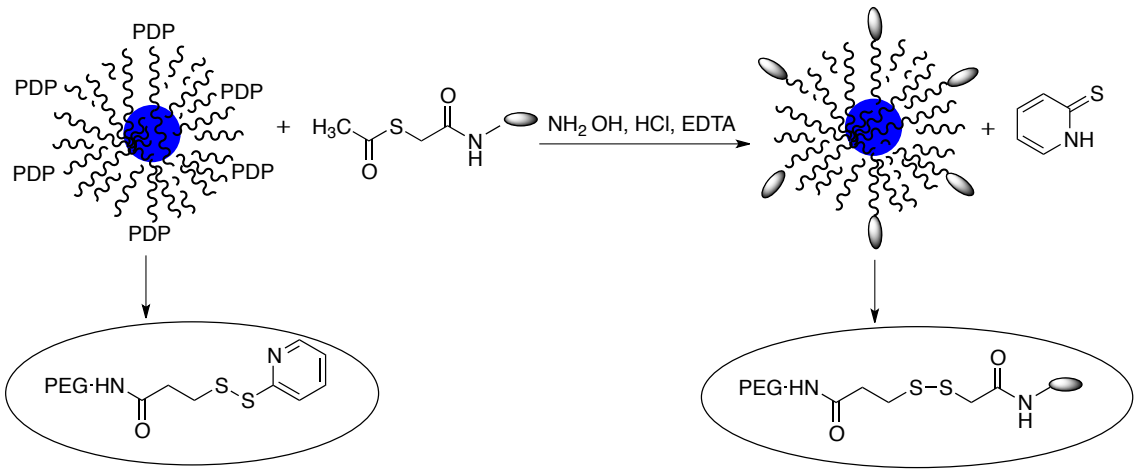

Fig. 4. Deprotection of SATA-VLA-4 peptide and subsequent coupling to PDP-PEG-*b*-p-(HPMA-Bz) functionalized micelles.

7.2 Materials and methods

7.2.1 Materials

NH_2-PEG_{5000}-OH was purchased from NOF (Kyoto, Japan) while mal-PEG_{5000}-OH was a product of JenKem Technology (Beijing, China). SATA-VLA-4 peptide was supplied by DgPeptides (Zhejiang province, China).

N-succinimidyl-3-(2-pyridyldithio)-propionate (SPDP), N-(2-Hydroxypropyl)methacrylamide (HPMAm), benzoyl chloride, magnesium sulphate ($MgSO_4$), triethylamine (TEA), 4,4-azobis(4-cyanopentanoic acid) (ABCPA), N,N'- dicyclohexyl carbodiimide (DCC), hydroxylamine hydrochloride (NH_2OH HCl), ethylenediaminetetraacetic acid disodium salt dihydrate (EDTA Na_2), HEPES and dithiothreitol (DTT) were purchased from Sigma-Aldrich (Zwijndrecht, The Netherlands). Dimethylaminopyridinium toluene sulfonate (DPTS) was synthetized using a previously reported procedure [35]. 4-methoxyphenol was a product of Fluka.

Acetonitrile (ACN), dimethylformamide (DMF), diethylether, dichloromethane (DCM) were supplied by Biosolve Ltd. (Valkenswaard, the Netherldans). ACN and DCM were dried using 4Å molecular sieves and all buffers were filterd through a 0.22 μm filter prior to use.

PEGs for GPC calibration were obtained from Polymer Standards Service-USA Inc. Syringe filters with Nylon membrane (size of 0.45 μm) were ordered from Pall Corporation. PD-10 column were from GE Healthcare, Europe GmbH).

7.2.2 Modification of NH_2-PEG_{5000}-OH with N-succinimidyl 3-(2-pyrydyldithio)-propionate

N-succinimidyl 3-(2-pyrydyldithio)-propionate (SPDP) is one of the most popular heterobifunctional crosslinking agents. The NHS ester end is available for reactions with amine groups while the 2-pyridylthiol group on the opposite side can undergo a disulphide exchange reaction with a sulphydryl group [34].

The amine group of NH_2-PEG-OH was modified with SPDP as follow (Fig. 5). SPDP (60 mg) was added in a molar ratio of 2:1 to a 10 ml solution of NH_2-PEG-OH (500 mg) in ACN and the reaction was conducted overnight at room temperature, according to a method described earlier. The solvent was evaporated and the crude product was purified from the unreacted SPDP by PD-10 column after re-suspending in water [36].

DTT assay was performed in order to assess the degree of functionalization of PEG with PDP. Briefly 10 μl DTT (15mg/ml in PBS) was added to 1ml sample in PBS (0.5mg/ml) and

the mixture was incubated 15 minutes before the Absorbance measurement. The disulfide bond of OH-PEG-PDP is cleaved by the reducing reagent DTT and the released pyridine-2-thione group has unique spectral properties at 343 nm, allowing the quantification by UV spectrophotometric analysis [37], based on the equation:

$$\frac{\Delta A}{\varepsilon l}\frac{M_w\, OH-PEG-PDP}{[OH-PEG-PDP]} = moles\ of\ SPDP\ per\ mole\ of\ HO-PEG-NH_2$$

where:

ΔA: difference registered in the Absorbance after and before the addition of TAIC

ε: molar extinction coefficient of pyridine-2thyone at 343 nm 8,080 M^{-1} cm^{-1} as reported in literature [37].

l: path lenght of the cuvette

M_w OH-PEG-PDP= 5230 g mol^{-1}

[OH-PEG-PDP]= 0.5mg/ml

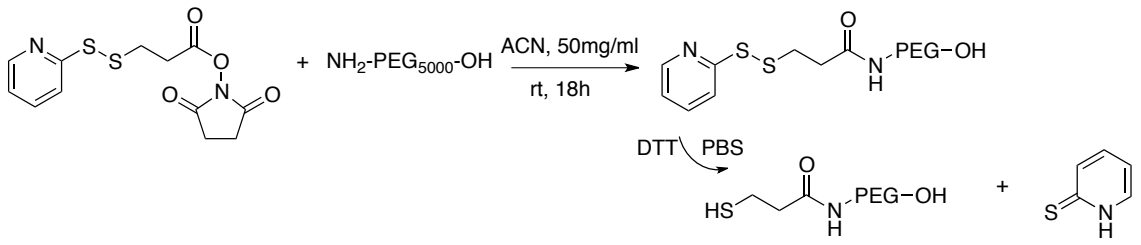

Fig. 5. Schematic representation of PDP-PEG-OH synthesis and DTT assay.

7.2.3 Synthesis of PDP-PEG_2-ABCPA and mPEG_2-ABCPA macroinitiators

The PDP-PEG_2-ABCPA was synthetized by slightly modifying and scaling down a procedure previously reported by Neradovic et al. and Talelli et al. (Fig. 6) [21,36] . Briefly 300 mg of PDP-PEG-OH (0.058 mmol, number average molecular weight M_n=5230 g mol^{-1}), 8.2 mg of ABCPA (0.029 mmol) and 2.8 mg of DPTS (0.009 mmol) were dissolved in 1.5 ml of dried DCM (4Å molecular sieves) and the mixture was stirred at 0°C. DCC (18.5mg, 0.09 mmol) was dissolved in 1.5 ml of dried DCM and added dropwise to the mixture at 0°C under nitrogen atmosphere. The reaction was conducted overnight at room temperature and then filtered to remove the precipitated dicyclourea (DCU); the organic solvent was removed by rotary evaporation and the final product was characterized by ^{1}H NMR and GPC.

The same procedure was employed for the mPEG_2-ABCPA macroinitiator synthesis (number average molecular weight of mPEG-OH M_n= 5000 g mol^{-1}). In this case 10 g of mPEG

(2mmol), 0.28 g of ABCPA (1mmol), 0.094 g of DPTS and 0.619g of DCC (3 mmol) were used for the reaction and the product, after solvent evaporation, was dialyzed at 10mg/ml against water for 72h at 4°C (MWCO 6-8 kDa) before final characterization.

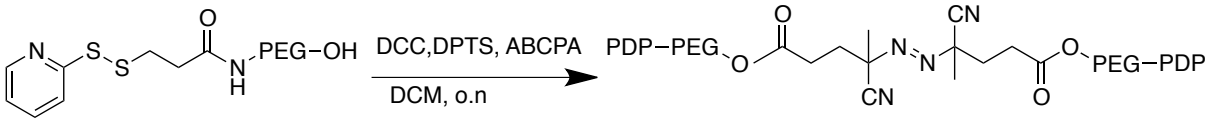

Fig. 6. Synthesis of PDP-PEG_2-ABCPA.

7.2.4 Synthesis of PDP-PEG_{5kDa}-*b*-p(HPMA-Bz) mPEG_{5kDa}-*b*-p(HPMA-Bz) polymers

The block copolymers PDP-PEG_{5KDa}-*b*-p(HPMAm-Bz) and mPEG_{5KDa}-*b*-p(HPMAm-Bz) were synthetized by free radical polymerization of the monomer HPMA-Bz using a macroinitiator route according to a method previously described [38,39]. A schematic representation of the synthetic procedure is reported in Fig. 7.

mHPMA-Bz and, PDP-PEG_2-ABCPA or mPEG_2-ABCPA (final concentration 0.3g/ml) respectively, were dissolved in dried ACN at a molar ratio of 200:1 (monomer to macroinitiator). The solution was flushed with nitrogen for 30 min while stirring and then let react overnight at 70°C under constant stirring. The polymers were purified by precipitation in an excess of diethyl ether and dried under vacuum at room temperature for 24h to remove residual solvents. The polymers were finally characterized by ^{1}H NMR DMSO-d_6 and GPC.

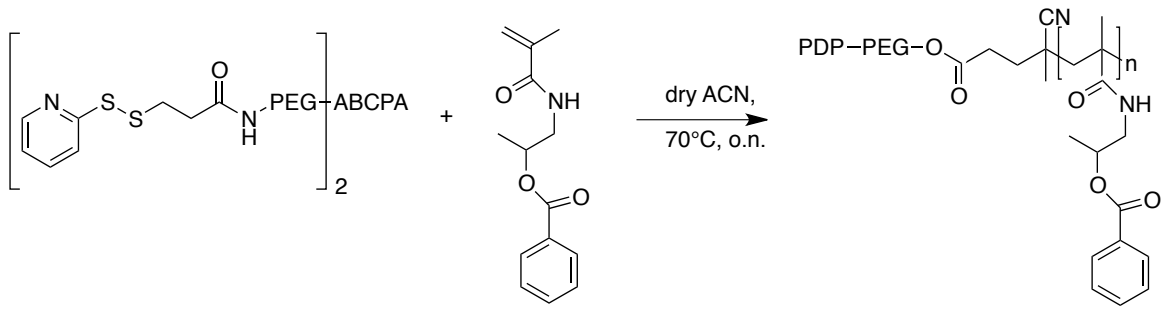

Fig. 7. Synthesis of PDP-PEG_{5kDa}-*b*-p(HPMA-Bz)

7.2.5 Mal-PEG_2-ABCPA macroinitiator synthesis

Mal-PEG_2 –ABCPA (number average molecular weight of mal-PEG-OH M_n = 5000 g mol^{-1}) was synthetized following the same procedure used for the mPEG_2-ABCPA synthesis, as above reported, but scaling down 20 times the synthesis. Due to the low volume of the

reaction (5ml), the precipitated DCU in the reaction was filtered off by using a 0.2 μm filter. The final product was characterized by ^{1}H NMR and GPC. The presence of the maleimide group after DCC coupling was confirmed by ^{1}H NMR, where the typical signal at 6.7 ppm referred to the maleimide protons is visible (Fig. 8).

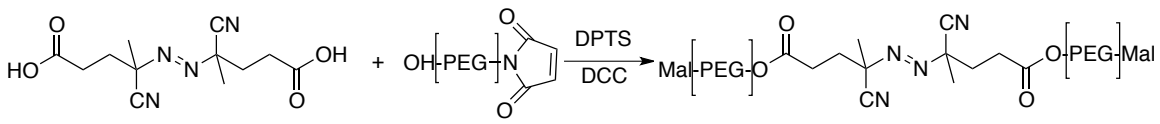

Fig. 8. Mal-PEG$_2$-ABCPA synthesis

7.2.6 Synthesis of mal-PEG$_{5kDa}$-*b*-p(HPMA-Bz)

A slightly modified procedure than the one reported above for PDP-PEG$_{5kDa}$-*b*-p(HPMA-Bz) was followed to synthetize mal-PEG$_{5kDa}$-*b*-p(HPMA-Bz). Many papers have been published on maleimide functionalized polymers to employ in actively targeted nanocarrier systems [40–43]. The temperature is a key factor to be controlled when using the maleimide group due to the thermal susceptibility of maleimide. In this regard, Nasonglka et al. reported the opening polymerization reaction (ROP) of maleimide-poly(ethylene glycol)-poly(ε-caprolactone) using 68°C to reduce the thermal degradation of maleimide to negligible levels [44].

The degradation kinetic of maleimide in ACN at 70°C was studied prior free radical polymerization to assess maleimide preservation and after 4h 64% of maleimide resulted still active (supporting data). Based on the decomposition half-life ($t_{1/2}$) of mPEG$_2$-ABCPA macroinitiator ($t_{½}$= 5.1 h in ACN) reported by Shi et al. [39], it was reasonable to conduct the polymerization with mal-PEG$_2$-ABCPA macroinitiator for 4h in order to preserve the maleimide functionality for the coupling with the peptide. Therefore, Mal-PEG$_{5kDa}$-*b*-p(HPMA-Bz) polymerization was conducted for 4h, expecting 64% of the maleimide function still active.

A schematic representation of the expected product is reported in Fig. 9. Unfortunately, the synthesis was not successful and a cross-linked polymer was obtained, with maleimide probably involved in a co-polymerization reaction. To prove this hypothesis, mal-PEG$_2$-ABCPA macroinitiator was polymerized under the same conditions; a cross-linked polymer was obtained with the double bond of the maleimide involved in the polymerization.

Our finding was then confirmed with literature where maleimide polymerization was reported [45–47]. Moreover maleimide group has been intensively investigated in Michael-type

addition reactions to create cross-linked polymer networks for pharmaceutical application [48].

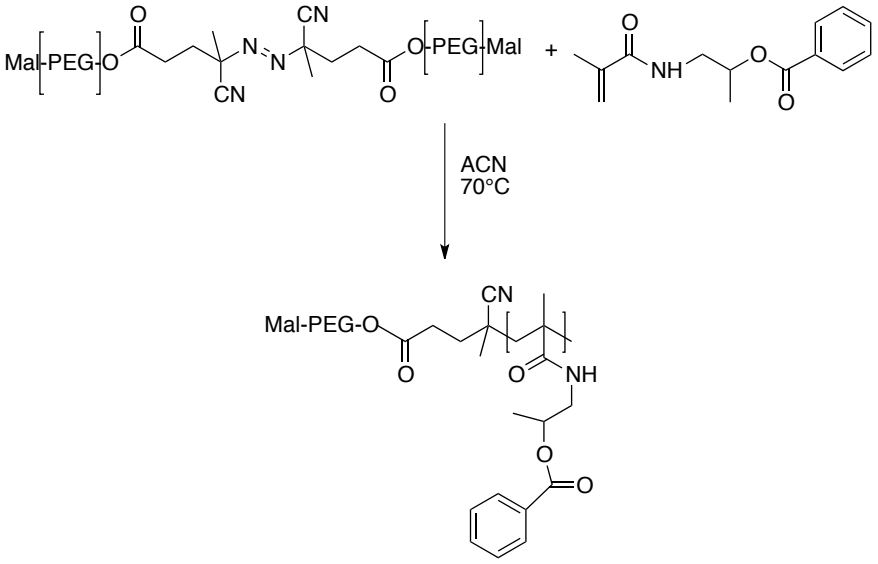

Fig. 9. Proposed mechanism for Mal-PEG$_{5kDa}$-*b*-p(HPMA-Bz) synthesis.

7.2.7 ^{1}HNMR Spectroscopy

^{1}H NMR spectra were recorded on a Gemini 300 MHz spectrometer (Varian Associates Inc. NMR Instruments, Palo Alto, CA) using $CDCl_3$ and DMSO-d_6 as solvents. Chemical shifts were referred to the solvent peak (7.26 ppm and 2.50 ppm respectively) and resulted in agreement with those previously reported [20].

^{1}H NMR was used to calculate the number average molecular weight of the final block copolymers PDP-PEG$_{5KDa}$-*b*-p(HPMAm-Bz) and mPEG$_{5KDa}$-*b*-p(HPMAm-Bz) as follows:

$$\mathrm{Mn} = \frac{(\text{integral of aromatic protons of HPMA} - \text{Bz at 8.0 ppm} / 2\ ) \text{ x molar mass of HPMA} - \text{Bz}}{(\text{integral at } 3.4 - 3.6 \text{ ppm}/448)} + 5000$$

where:

- molar mass of HPMA-Bz is 247
- integral at 3.4-3.6 ppm = methylene proton of PDP-PEG or mPEG chains
- 448 is the average number of protons per PEG chain with M_n=5000 g/mol
- 5000 Mn of PDP-PEG or mPEG chain

Moreover ^{1}H NMR was used to determine the ratio HPMA-Bz/PDP-PEG and HPMA-Bz/mPEG in the final PDP-PEG$_{5KDa}$-*b*-p(HPMAm-Bz) and mPEG5KDa-*b*-p(HPMAm-Bz) polymers respectively, referring to the follow equation:

$$\frac{\text{HPMA} - \text{Bz}}{\text{PDP} - \text{PEG (or mPEG) based on the synthetized polymer}} = \frac{\text{integral at 8.0 ppm}/2}{(\text{integral at } 3.4 - 3.6 \text{ ppm})/448}$$

7.2.8 Gel Permeation Chromatography

GPC was performed to determine the number average molecular weight (M_n), weight average molecular weight (M_w) and the polydispersity index (M_w/M_n = PDI) of the polymers using two serial PLgel 5 μm MIXED-D columns (Polymer Laboratories) and PEGs with defined molecular weight as standards for the calibration curve. The column temperature was 65°C, DMF containing 10mM LiCl was used as eluent, the flow rate was 1ml/min and refractive index was used as detection method. Samples were prepared at 5mg/ml in 10mM LiCl DMF and allow to dissolve at 37°C for 30 min.

7.2.9 Preparation and characterization of polymeric micelles

PDP-PEG$_{5KDa}$-*b*-p(HPMAm-Bz) polymeric micelles were prepared by a solvent evaporation method and different amounts of mPEG$_{5KDa}$-*b*-p(HPMAm-Bz) were co-introduced in the micellar structure to control the density of PDP at the micelles surface. mPEG$_{5KDa}$-*b*-p(HPMAm-Bz) micelles were also prepared as control. The final polymer concentration was 30mg/ml.

THF was used as anti-solvent where the block copolymer was dispersed and then 1 ml of the polymer solution was added dropwise to 1 ml of reverse osmosis water or HBS buffer (pH 7.2) while stirring. The THF was allowed to evaporate overnight under a fume hood before micelles characterization.

The Z-average particle size (Z_{ave}) and the polydispersity index of the micelles were measured by dynamic light scattering (DLS), using a Malvern CGS-3 multiangle goniometer with a 22mW He-Ne laser source operating at 632 nm with an angle of 90° (Malvern Instruments, Malvern, UK). The zeta-potential (ZP) was measured using a Malvern Zetasizer Nano-Z (Malvern Instruments, Malvern, UK) and samples were dispersed in 10mM Hepes buffer (pH 7.4) at a polymer concentration of 3 mg/ml.

DTT assay was performed on PDP-PEG$_{5KDa}$-*b*-p(HPMAm-Bz) polymeric micelles in order to assess the presence of PDP groups on the micelles surface, following the same procedure

described above in section 7.2.2. ^{1}H NMR spectrum of the PDP-PEG$_{5KDa}$-*b*-p(HPMAm-Bz) micelles prepared in D_2O was performed to investigate the core-shell structure.

7.2.10 Conjugation of VLA-4 peptide to PDP/mPEG$_{5KDa}$-*b*-p(HPMAm-Bz)

Preliminary experiments were performed to conjugate the VLA-4 peptide on the micelles surface. For this purpose, a post micellar modification strategy was designed [44]. Peptide deacetylation and coupling to the micelles surface were performed simultaneously in order to preserve VLA-4 functionality, as above described and avoid disulphide formation. Actively targeted polymeric micelles were prepared as follow:

SATA-VLA-4 peptide (1mg/ml in HBS) was added to one volume of 5% PDP functionalized micelles (30mg/ml in HBS pH=7.2) to a final molar ratio SATA-PDP of 2:1. 0.1 volume of deacetylation buffer (0.5 M HEPES/0.5 M hydroxyl amine-HCl/ 25 mM EDTA, pH 7.0) was added to allow SATA-VLA-4 deacetylation before the coupling reaction [49]. Next the mixture was incubated overnight at 4°C in a roller bench.

The mean particle size and zeta potential of the conjugated micelles were measured as described above and the results compared to the uncoupled PDP/mPEG micelles, in order to evaluate eventual changes in the micelles properties due to the conjugated peptide.

The conjugation reaction was investigated by measuring the Absorbance of pyridine thione released during the coupling reaction and the percentage of coupling was determined as the ratio of pyridine thione released to the pyridine thione released after addition of DTT to PDP micelles.

The formulation was desalted and purified from the unbounded peptide by gel permeation chromatography over a PD-10 column (Pharmacia, Uppsala, Sweden) using HBS as eluent.

UPLC analysis was explored as technique to assess the coupling efficiency, by indirectly measuring the unbounded peptide fractions recovered from the PD-10 washing using a Waters Acquity system equipped with a ACQUITY UPLC BEH 300 column (C18 1.7 µm, 2.1x 50 mm). The following method was developed: eluent A: water/ACN 95/5 (v/v) with 0.1% trifluoroacetic acid. Eluent B: ACN 100 with 0.1% trifluoroacetic acid. A gradient was run with the volume fraction of eluent B increasing from 5 to 40% in 3 minutes Between each sample measurement the column was flushed for 1.5 minutes with 95% eluent A. The flow rate was set to 0.250 ml/min and injection volume was 7.5 µl. Unbounded VLA-4 was detected by measuring the UV absorbance at 220 nm and by using a calibration curve derived from the integration of the peaks referred to the deacetylated VLA-4 (supplementary data).

7.3 Results

7.3.1 Characterization of NH_2-PEG_{5000}-OH with N-succinimidyl 3-(2-pyrydyldithio)-propionate

N-succinimidyl-3-(2-pyridyldithio)-propionate (SPDP) was successfully coupled to NH_2-PEG_{5000}-OH (80% yield) as shown by the ^{1}H NMR spectrum, where the peaks of the pyridine thione were visible in the aromatic region at 8.6, 8.0 and 7.4 ppm. The degree of modification was assessed by DTT assay resulting in 90% functionalization.

7.3.2 Synthesis of PDP-PEG_2-ABCPA and mPEG_2-ABCPA macroinitiators

PDP-PEG_2-ABCPA and mPEG_2-ABCPA macroinitiators were synthetized by DCC coupling reaction using DPTS as catalyst, from PDP-PEG-OH/mPEG-OH (number average molecular weight M_n=5000 g mol^{-1}) and ABCPA. mPEG_2-ABCPA macroinitiator was synthetized with high yield (90%) and high conversion and characterized by ^{1}H NMR and GPC (data not shown).

PDP function was preserved during the macroinitiator synthesis, as shown in the ^{1}H NMR spectrum (Fig. 10).The obtained data are in agreement with those previously reported [36,50]. GPC chromatogram of PDP-PEG_2-ABCPA shows 78% conversion, while the presence of a second peak (rt 15 min) indicates either the mono-substituted PDP-PEG_2-ABCPA or unreacted PDP-PEG-OH (Fig. 11). This is probably due to the low scale synthesis that involves a stronger interference of water with the coupling reaction.

7.3.3 Synthesis of PDP-PEG_{5kDa}-*b*-p(HPMA-Bz) and mPEG_{5kDa}-*b*-p(HPMA-Bz) polymers

PDP-PEG_{5kDa}-*b*-p(HPMA-Bz) block copolymer was synthetized by free radical polymerization, using PDP-PEG_2-ABCPA as macroinitiator, with a yield of around 60%.^{1}H NMR spectrum showed a number average molecular weight of 18,500 Da and a HPMA-Bz/ PDP-PEG ratio of 56 [36]. Moreover, the pyridine protons were still visible in the ^{1}H NMR spectrum confirming the presence of PDP group in the final block copolymer (Fig. 12). GPC results showed a M_n of ≅22,000 Da and a PDI of 1.6. Moreover, GPC chromatogram (Figure 11) indicates the presence of two small peaks with the same retention time of PDP-PEG-OH 5kDa and PDP-PEG_2-ABCPA 10kDa. They are most likely referable to unreacted PDP-PEG-OH originated from the macroinitiator synthesis (shoulder of 5kDa) and homopolymer p(HPMA-Bz) derived from the polymerization of PDP-PEG-ABCPA (macroinitiator coupled

to one PEG molecule) or combination of two PDP-PEG-macroinitiator. This theory has been extensively discussed by Shi et al. [39]. Since the PDP-PEG_{5kDa}-*b*-p(HPMA-Bz) block copolymer will be used in a small amount to prepare micelles, the presence of a small amount of homopolymer will be negligible and will not interfere with the final loading capacity of the micelles.

On the other hand, $mPEG_{5kDa}$-*b*-p(HPMA-Bz) copolymer showed a similar number average molecular weight (Mn ≅ 22,000 Da) and a PDI of 1.7. Table 1 summarizes the properties of PDP-PEG_{5kDa}-*b*-p(HPMA-Bz) and m-PEG_{5kDa}-*b*-p(HPMA-Bz) as obtained from ^{1}H NMR and GPC.

^{1}H NMR (DMSO-d_6, 300 MHz) δ: 7.9 (b, 2H, aromatic -CH), 7.5 (b, 1H, aromatic –CH), 7.4 (b, 2H, aromatic –CH), 4.9 (b, NH-CH_2-*CH*-(CH_3)-O-(Bz)), 3.4-3.6 (b, O-*CH_2*-*CH_2*-methylene protons of PEG), 3.1 (b, NH-*CH_2*-CH), 0.4-2.0 (b, main chain protons and -CH_3) ppm. PDP polymer also showed chemical shifts at 7.0-8.5 ppm referred to the protons of the pyridine thione group.

These data suggest in principle a good exposure of the PDP-PEG_{5kDa}-*b*-p(HPMA-Bz) block copolymer on the micelles surfaces, since it exhibits a similar Mn compared to $mPEG_{5kDa}$-*b*-p(HPMA-Bz) block copolymer. As a consequence, a higher theoretical conjugation with VLA-4 peptide could be achieved.

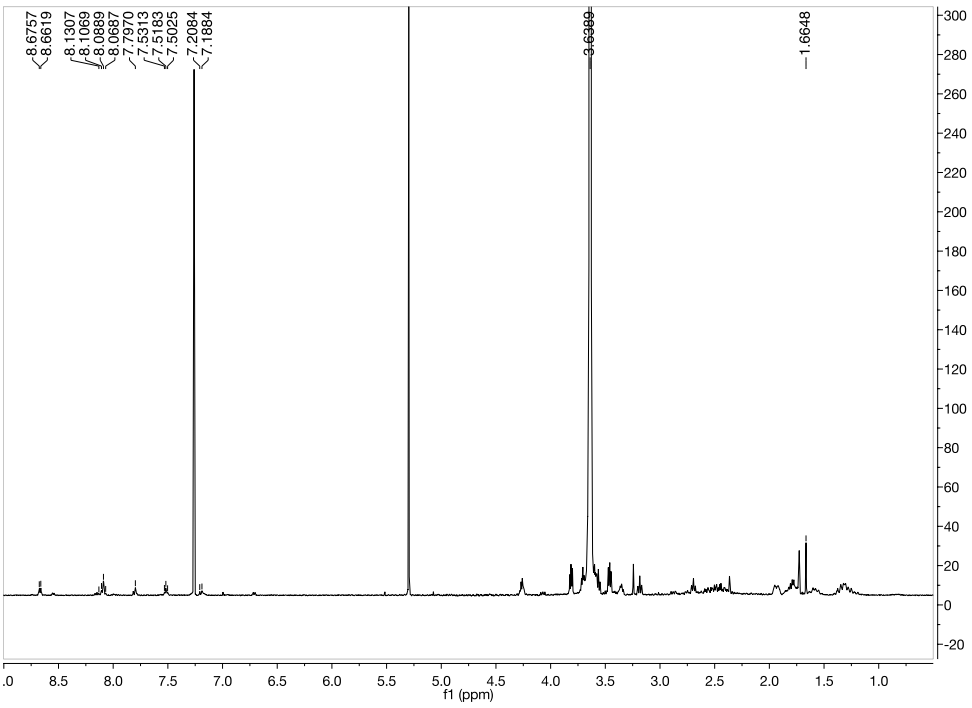

Fig. 10. NMR spectrum of PDP-PEG macroinitiator in $CDCl_3$.

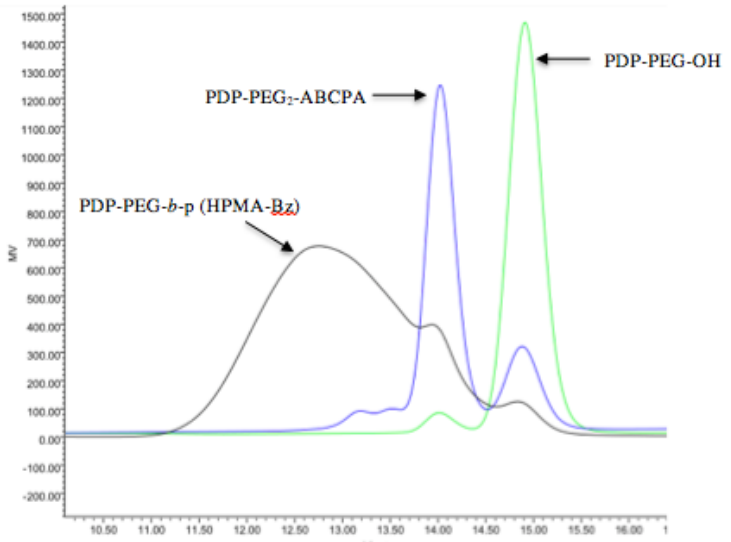

Fig. 11. GPC chromatogram of PDP-PEG-OH, PDP-PEG$_2$-ABCPA and PDP-PEG-*b*-p(HPMA-Bz) block copolymer.

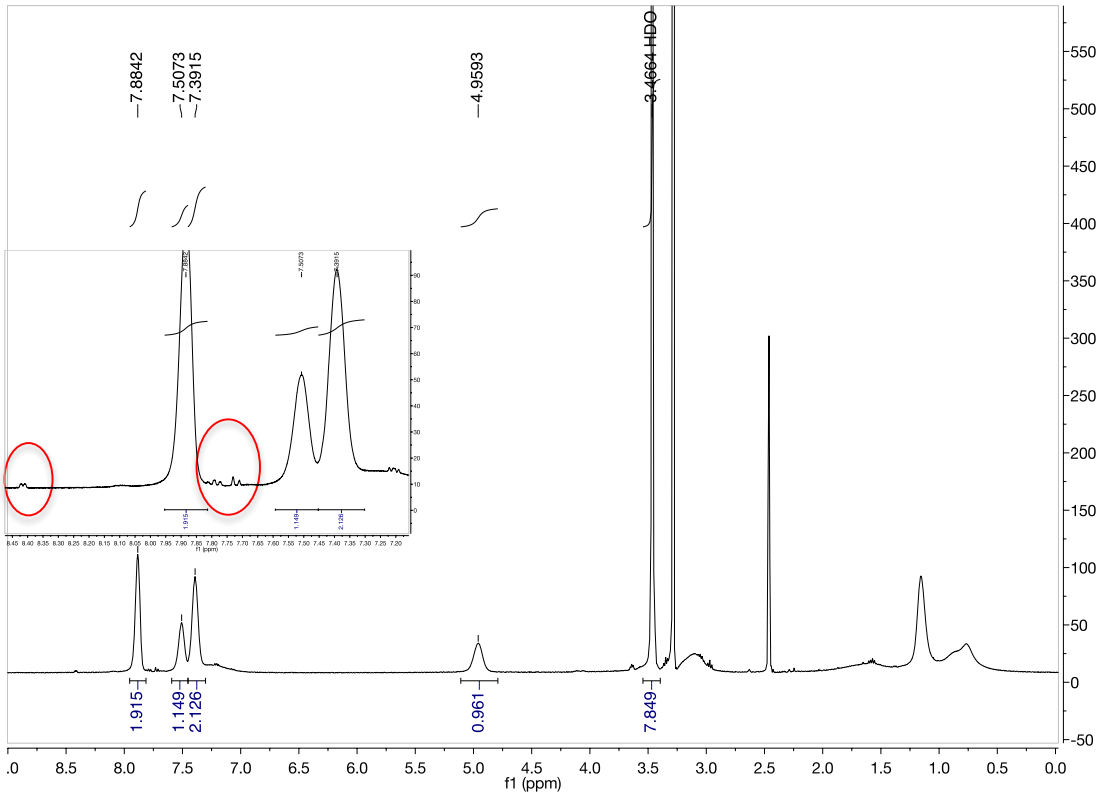

Fig. 12. ^{1}H NMR of PDP-PEG-*b*-p(HPMA-Bz) in DMSO-d$_6$. The zoomed region of the spectrum shows the aromatic protons of the PDP groups preserved in the polymerization reaction.

Table 1. Characterization of PDP-PEG-*b*-p(HPMA-Bz) and mPEG-*b*-p(HPMA-Bz) copolymers based on GPC and ^{1}H NMR.

entry	Mn [a]	Mn [b]	Mw [b]	PDI [b]	Ratio mHPMA-Bz/ PEG [a]
PDP-PEG-*b*-p(HPMA-Bz)	18500	22038	36928	1.6	56
mPEG-*b*-p(HPMA-Bz)	16660	22170	36960	1.7	47

a - based on ^{1}H NMR spectra

b - based on GPC chromatograms

7.3.4 Mal-PEG functionalized block copolymer: synthesis and discussion

Mal-PEG-$_2$-ABCPA macroinitiator was synthetized using the DCC coupling reaction starting from mal-PEG (Mw 5000 g/mol) and ABCPA. Since the reaction was performed in a low scale, a partial conversion (58%) was obtained (Table. 2 and Fig. 13). This result is comparable with PDP-PEG$_2$-ABCPA synthesis, where however a higher conversion was observed (78%). ^{1}H NMR showed the preservation of the maleimide function with a typical signal at 6.7 ppm referred to the maleimide protons (Fig 14).

The degradation kinetics of maleimide in ACN at 70°C was studied prior to free radical polymerization and taking into account the decomposition half life ($t_{1/2}$) of mPEG$_2$-ABCPA macroinitiator ($t_{½}$= 5.1 h in ACN) reported by Shi et al., mal-PEG$_{5kDa}$-*b*-p(HPMA-Bz) polymerization was conducted for 4h in order to preserve the maleimide functionalities [39]. The reaction, as exhaustively discussed in section 2.2.5, was not successful and an unexpected cross-linked product was obtained, as demonstrated by the GPC chromatogram, where a broad peak with a categorically high PDI and molecular weight were observed.

Table 2. Characteristics of mal-PEG macroinitiator based on GPC.

entry	Ret. Time (min.)	Mn	Mw	Area%
Peak 1	11.25	12875	13240	41
Peak 2	12.28	5192	5286	58

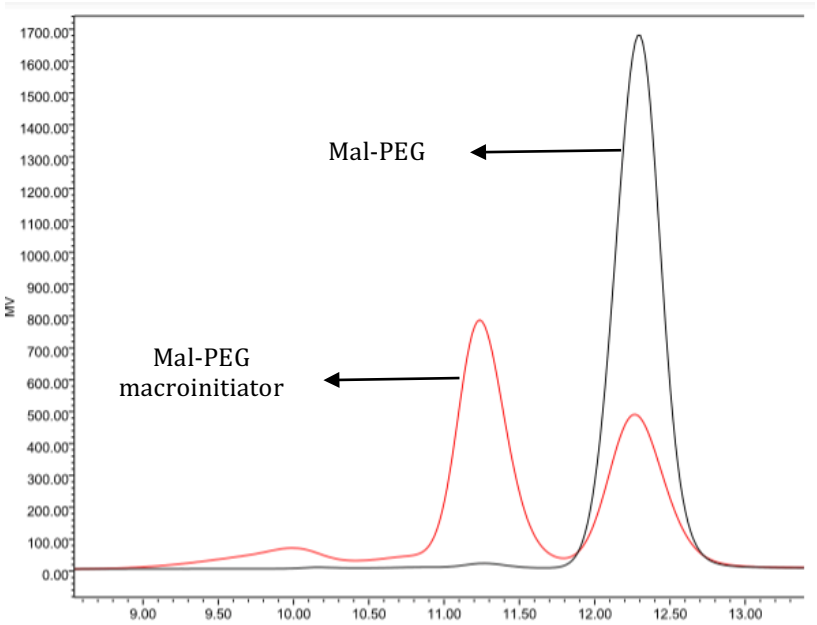

Fig. 13. GPC chromatogram of mal-PEG macroinitiator.

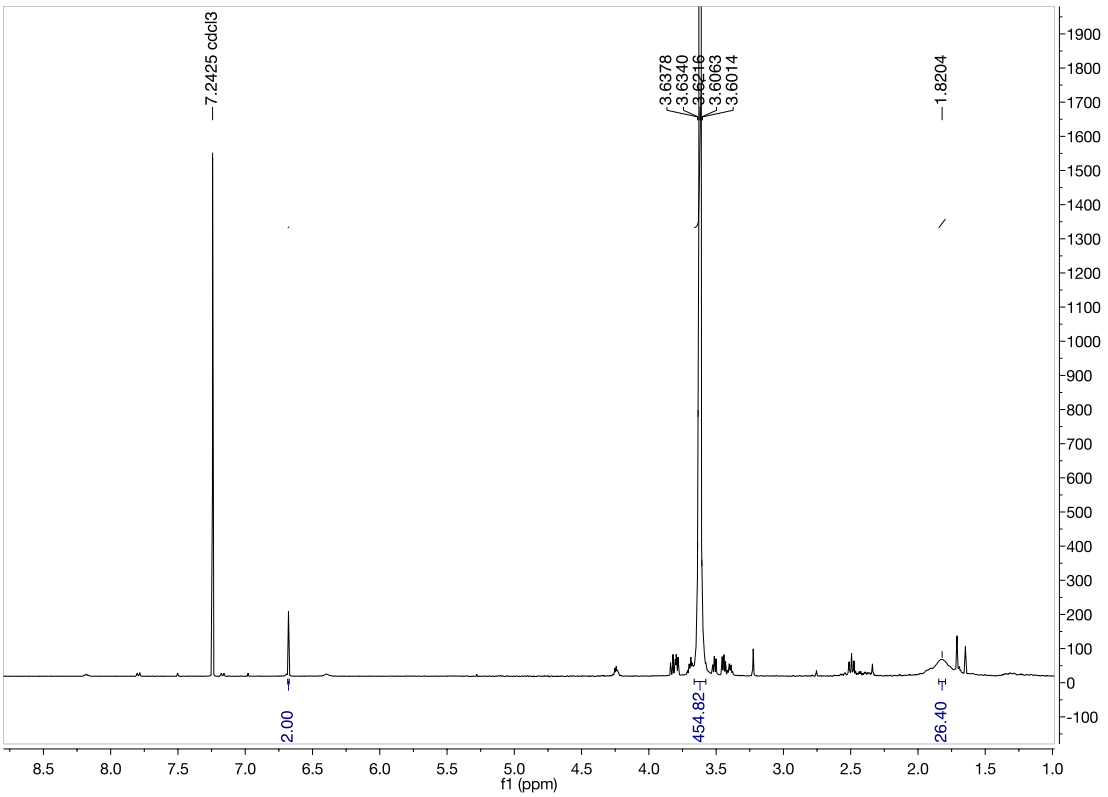

Fig. 14. ^{1}H NMR spectrum of mal-PEG macroinitiator in $CDCl_3$.

7.3.5 Characterization of polymeric micelles and conjugation of VLA-4 peptide to PDP/mPEG$_{5KDa}$-*b*-p(HPMAm-Bz)

PDP-PEG$_{5kDa}$-*b*-p(HPMA-Bz) micelles were prepared by introducing different amounts of mPEG$_{5kDa}$-*b*-p(HPMA-Bz) polymer to control the PDP density at the micelles surface (30mg/ml total polymers concentration). DLS measurement showed that 2.5% and 5% PDP-PEG$_{5kDa}$-*b*-p(HPMA-Bz) micelles had a Z-average size (Z_{ave}) of ~70 nm and a PDI of 0.1, comparable with that of mPEG$_{5kDa}$-*b*-p(HPMA-Bz) used as control. ZP was neutral (-1.3 ± 0.3 mV). ^{1}H NMR spectrum of the PDP-PEG$_{5KDa}$-*b*-p(HPMAm-Bz) micelles prepared in D_2O confirmed the formation of the typical core-shell micellar structure. The PEGylated corona was solvated in D_2O showing a clear ^{1}H NMR signal. On the other hand, the mobility of the solid core was significantly reduced, thus not showing any signal in the ^{1}H NMR spectrum. DTT assay performed on the PDP functionalized micelles showed that 88% of PDP groups were reduced by DTT releasing pyridine thione. These results clearly suggest that PDP groups are exposed on the micelles surface, available for coupling with VLA-4 peptide.

Preliminary experiments were performed to couple SATA-VLA-4 peptide to 5% PDP-PEG-*b*-p-(HPMA-Bz) by using a post micellar modification strategy. Moreover, deacetylation of SATA-peptide and coupling to the micelles surface were performed simultaneously in order preserve VLA-4 functionality and avoid disulphide formation. The micelles were characterized by determining size and zeta potential and no differences were observed before and after purification from the free peptide. The mean diameter was ~70nm and zeta potential was nearly neutral (- 2.6 ± 0.7 mV), in line with the uncoupled PDP/mPEG micelles. This is probably due to the low molecular weight of the peptide and the small percentage of PDP groups exposed on the surface that are not able to significantly influence the micelles size and surface charge respectively.

The conjugation reaction efficiency was investigated by measuring the Absorbance of pyridine thione released during the coupling reaction. The PDP concentration on the micelles surface was assessed by DTT assay before coupling and set as 100%. The percentage of coupling was determined as the ratio of pyridine thione released from the coupling reaction to the pyridine thione released after addition of DTT to PDP micelles. The coupling efficiency was estimated to be around 50 % but the conjugation reaction still needs to be optimized in terms of reaction conditions and coupling quantification. UPLC was also explored as technique to quantify the conjugation. To this end, a method to detect VLA-4 peptide was first developed. Coupling efficiency of 5% PDP micelles (2:1, SATA: PDP molar ratio) was

calculated to be around 50%. It has to be pointed out that further studies are needed to deeply investigate UPLC results.

7.4 Conclusions and discussions

The work reported in this chapter is part of a project that aims to develop actively targeted polymeric micelles based on mPEG-*b*-p-HPMA-Bz block copolymers to selectively associate with multiple myeloma cells in order to facilitate specific delivery of hydrophobic drugs. The research was initially focused on the rational design and functionalization of mPEG-*b*-p-(HPMA-Bz) block copolymer with an appropriate linker available for the coupling with VLA-4 peptide. To this end, appropriate bioconjugation techniques were studied. Initially maleimide chemistry was considered in order to use the double bond of the maleimide for alkylation reaction with sulphydryl group to finally form a stable thioether bond. The free radical polymerization using mal-PEG_2-ABCPA as macroinitiator and mHPMA-Bz produced a crosslinked product, reasonably resulting from the radical propagation on the double bond of the maleimide, highly reactive. Therefore, the inactivation of the double bond of the maleimide group hindered the coupling with the active target peptide. In order to obtain a functionalized block copolymer, an alternative strategy was exploited for the conjugation with the sulphydryl group of VLA-4 peptide. The heterobifunctional SPDP was selected due to its properties and the NHS ester was reacted with the amine group of NH_2PEG-OH.

PDP-PEG-*b*-p-(HPMA-Bz) functionalized block copolymer polymer was successfully synthetized and characterized.

The second step was the formulation of surface functionalized micelles by using PDP-PEG-*b*-p-(HPMA-Bz) and mPEG-*b*-p-(HPMA-Bz) block copolymers in different ratios. The presence of PDP groups available on the micelles surface is in fact a key factor to obtain a successful conjugation with the targeting peptide. An important aspect that needs to be considered is that PDP-PEG-*b*-p-(HPMA-Bz) and mPEG-*b*-p-(HPMA-Bz) block copolymers were synthetized by free radical polymerization by keeping the same MI / mHPMA-Bz ratio (1/200), in order to have final block copolymers with similar molecular weight characteristics and therefore obtain a comparable level of exposure on the micelles surface. In this system, PDP groups would be accessible for further derivatizations as it is located on the micelles surface. The rational of this novel design was to have in the same system both a PEGylated corona, able to satisfy the stealth requirements, and a specific linker available for coupling reactions with the targeting peptide.

Moreover, it is reasonably to consider such a system as a potential scaffold for several functionalisations with different ligands, thus allowing active targeting to specific cells types and tissues. Finally, the formulation combines the well-known advantages of polymeric nanocarriers and the innovative Π-Π stacking interactions for potential future application in active targeting.

A cyclic activated SH-VLA-4 peptide was used as targeting peptide for multiple myeloma cells, as the $\alpha_4\beta_1$ heterodimer is expressed on the surface of cancer cells of haematological origin. The low molecular weight of the SH-VLA-4 peptide makes it difficult to detect. Therefore, development of/deploying an appropriate technique is key to assess the coupling efficiency.

A post micellar modification strategy was explored to prepare vla-4 targeted polymeric micelles and preliminary experiments were conducted to assess the coupling efficiency of the employed peptide to the micelles surface.

7.5 Future perspectives

PDP-*b*-p-(HPMA-Bz) block copolymer was rationally synthetized using the PDP cross-linker. A post micellar modification strategy was then employed for the coupling of VLA-4 to the micelles surfaces.

Further studies need to be undertaken to optimize the formulation. An important aspect that will be considered in future studies with the aim of optimizing the formulation, is the introduction of higher density of the peptide on the micelles surfaces. Moreover, different molar ratios of SATA/PDP will also be exploited to increase the coupling efficiency.

Besides the optimization of the formulation, future research will focus on *in vitro* studies. Binding and uptake studies of VLA-4 targeted micelles by cells overexpressing $\alpha_4\beta_1$ integrin and cells lacking this receptor will be performed by using flow cytometry. Furthermore, to study the binding and uptake of targeted and untargeted micelles by different cells, confocal microscopy will be used. A perfusion method will be also developed to assess the binding/internalization of targeted nanoparticles. This method relies on the continuous flow of nanoparticles over a layer of cells of interest. In this way micelles with a targeted moiety will have higher affinity for binding to the $\alpha_4\beta_1$ integrin expressing cells when compared to untargeted micelles. Moreover, this method would be more realistic than conventional static conditions where the nanoparticles are added to cells and there is no dynamic circulation of fluids and the change of a specific uptake by cells is higher.

Supplementary data

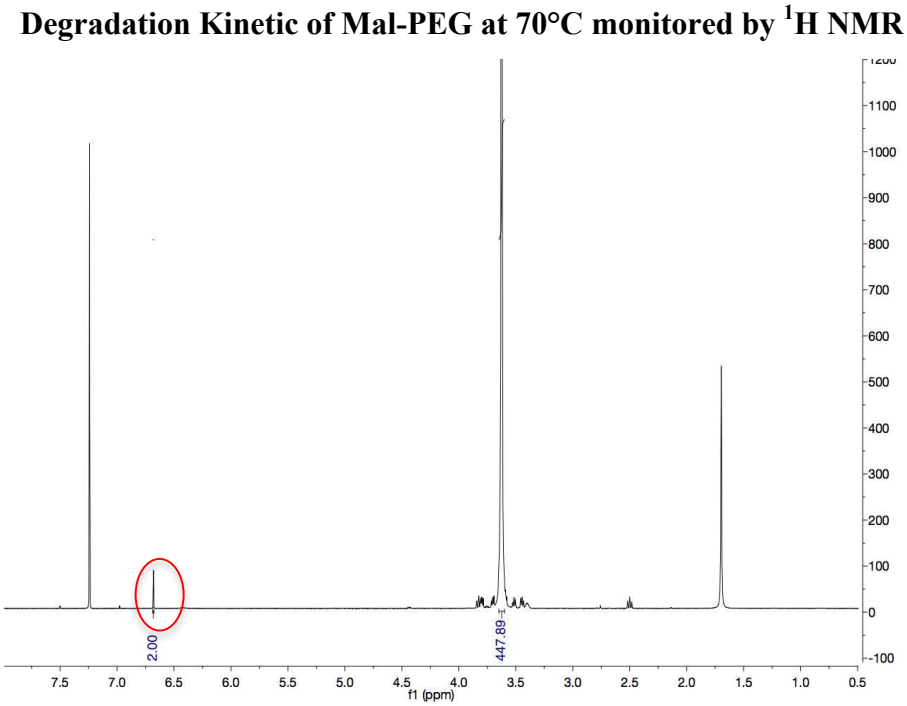

Fig. S1. ^{1}H NMR of mal-PEG-OH. The integral for methylene protons of the PEG chain is 448. The degradation kinetic is followed by monitoring the change in the value of the integral peak at 6.7 ppm (maleimide protons).

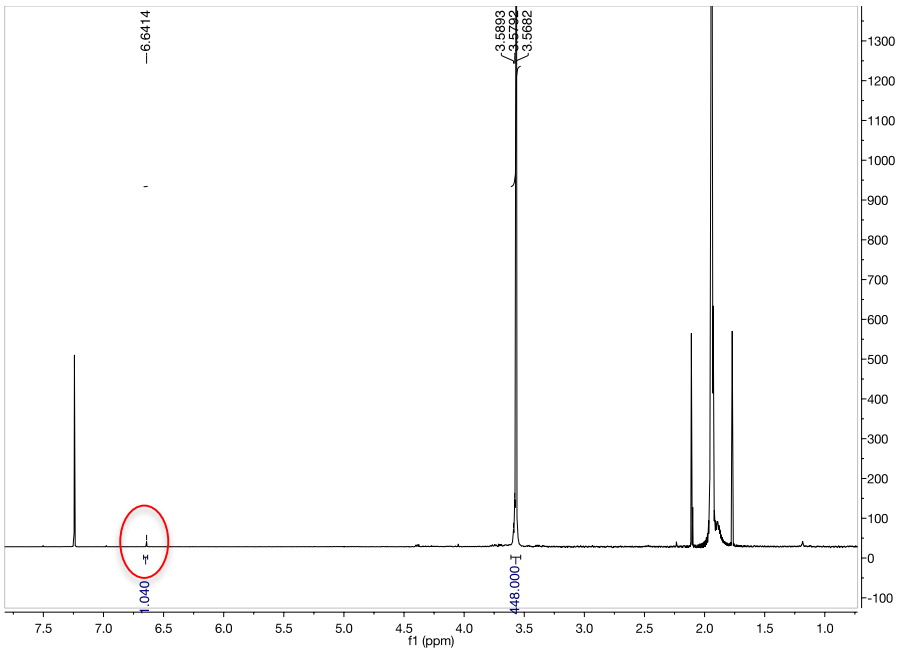

Fig. S2. ^{1} H NMR of mal-PEG-OH after 12h at 70°C. Example of calculation of the % of degradation after 12h. Percentage of maleimide preserved: (1.040/2)*100 = 52 %

Table S1. Mal-PEG-OH degradation kinetic at 70°C in ACN

Time points	% of mal preserved
1h	79%
2h	69%
3h	67%
4h	64%
6h	56%
8h	56%
10h	56%
12h	52%
24h	50%

Deacetylation of VLA-4 peptide

A calibration curve was designed for SATA-VLA-4 peptide with a typical elution time around 1.4 min. VLA-4 peptide was deacetylated by mixing 1/10 volume of deacetylation buffer to peptide solution in HBS and incubated 1.5h. A schematic representation of the deacetylation reaction is given in Fig.

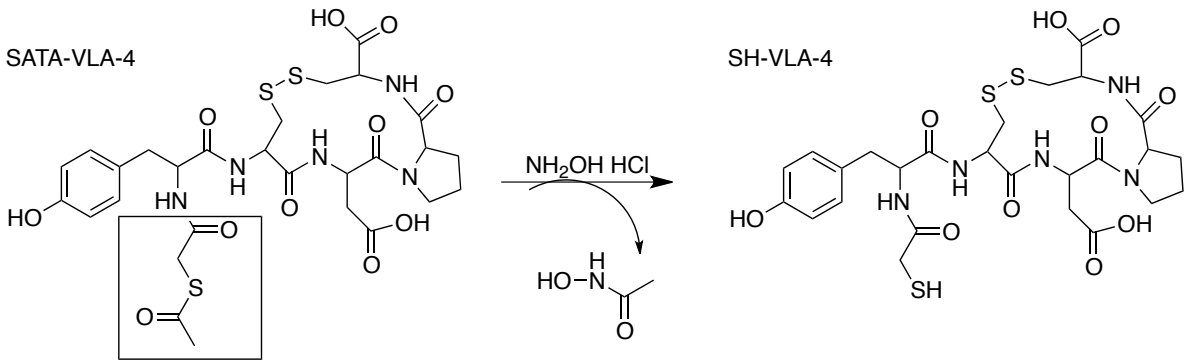

Fig. S3. Reaction scheme for the deprotection of SATA-modified VLA-4 peptide.

Deacetylation buffer was prepared as described above in section 7.2.10. The typical chromatogram is shown in fig. where two peaks at 1.2 min and 1.3 min are visible. Calibration curve is reported in Fig. S5.

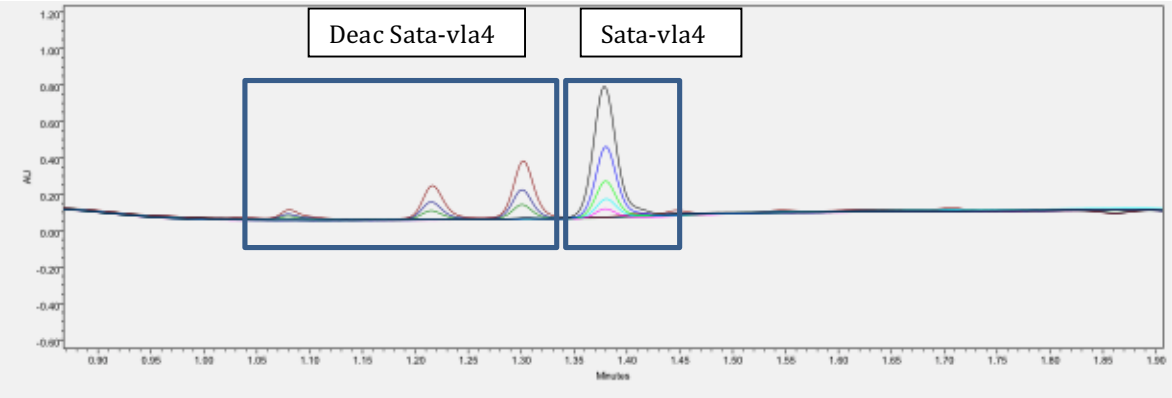

Fig. S4. UPLC chromatogram of SATA-VLA.4 and deacetylated VLA-4 peptide.

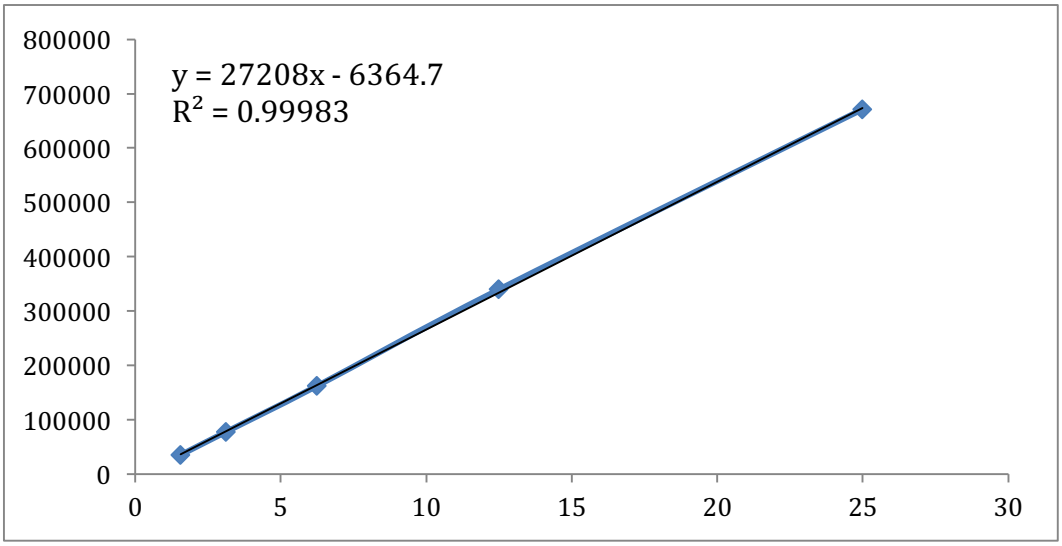

Fig. S5. Calibration curve of deacetylated SATA-VLA-4 peptide.

References

[1] T. Konno, H. Maeda, K. Iwai, S. Maki, S. Tashiro, M. Uchida, Y. Miyauchi, Selective targeting of anti-cancer drug and simultaneous image enhancement in solid tumors by arterially administered lipid contrast medium, Cancer. 54 (1984) 2367–2374.

[2] Y. Matsumura, H. Maeda, A new concept for macromolecular therapeutics in cancer chemotherapy: mechanism of tumoritropic accumulation of proteins and the antitumor agent smancs., Cancer Res. 46 (1986) 6387–92.

[3] K.S. Lee, H.C. Chung, S.A. Im, Y.H. Park, C.S. Kim, S.-B. Kim, S.Y. Rha, M.Y. Lee, J. Ro, Multicenter phase II trial of Genexol-PM, a Cremophor-free, polymeric micelle formulation of paclitaxel, in patients with metastatic breast cancer, Breast Cancer Res. Treat. 108 (2008) 241–250. doi:10.1007/s10549-007-9591-y.

[4] W.T. Lim, E.H. Tan, C.K. Toh, S.W. Hee, S.S. Leong, P.C.S. Ang, N.S. Wong, B. Chowbay, Phase I pharmacokinetic study of a weekly liposomal paclitaxel formulation (Genexol®-PM) in patients with solid tumors, Ann. Oncol. 21 (2010) 382–388. doi:10.1093/annonc/mdp315.

[5] T.-Y. Kim, D.-W. Kim, J.-Y. Chung, S.G. Shin, S.-C. Kim, D.S. Heo, N.K. Kim, Y.-J. Bang, Phase I and pharmacokinetic study of Genexol-PM, a cremophor-free, polymeric micelle-formulated paclitaxel, in patients with advanced malignancies., Clin. Cancer Res. 10 (2004) 3708–16. doi:10.1158/1078-0432.CCR-03-0655.

[6] H. Cabral, K. Kataoka, Progress of drug-loaded polymeric micelles into clinical studies, J. Control. Release. 190 (2014) 465–476. doi:10.1016/j.jconrel.2014.06.042.

[7] Y. Matsumura, K. Kataoka, Preclinical and clinical studies of anticancer agent-incorporating polymer micelles., Cancer Sci. 100 (2009) 572–9.

[8] A. Varela-Moreira, Y. Shi, M.H.A.M. Fens, T. Lammers, W.E. Hennink, R.M. Schiffelers, Clinical application of polymeric micelles for the treatment of cancer, Mater. Chem. Front. 1 (2017) 1485–1501. doi:10.1039/C6QM00289G.

[9] J.-Z. Du, L.-Y. Tang, W.-J. Song, Y. Shi, J. Wang, Evaluation of Polymeric Micelles from Brush Polymer with Poly(ε-caprolactone)- b -Poly(ethylene glycol) Side Chains as Drug Carrier, Biomacromolecules. 10 (2009) 2169–2174. doi:10.1021/bm900345m.

[10] T. Miller, A. Hill, S. Uezguen, M. Weigandt, A. Goepferich, Analysis of Immediate Stress Mechanisms upon Injection of Polymeric Micelles and Related Colloidal Drug Carriers: Implications on Drug Targeting, Biomacromolecules. 13 (2012) 1707–1718. doi:10.1021/bm3002045.

[11] G.S. Kwon, K. Kataoka, Block copolymer micelles as long- circulating drug vehicles, Adv. Drug Deliv. Rev. 16 (1995) 295–309. doi:10.1016/0169-409X(95)00031-2.

[12] Y. Bae, S. Fukushima, A. Harada, K. Kataoka, Design of Environment-Sensitive Supramolecular Assemblies for Intracellular Drug Delivery: Polymeric Micelles that are Responsive to Intracellular pH Change, Angew. Chemie Int. Ed. 42 (2003) 4640–4643. doi:10.1002/anie.200250653.

[13] R. Haag, Supramolecular Drug-Delivery Systems Based on Polymeric Core-Shell Architectures, Angew. Chemie - Int. Ed. 43 (2004) 278–282. doi:10.1002/anie.200301694.

[14] G.S. Kwon, Polymeric micelles for delivery of poorly water-soluble compounds., Crit. Rev. Ther. Drug Carrier Syst. 20 (2003) 357–403.

[15] M. Talelli, C.J.F. Rijcken, W.E. Hennink, T. Lammers, Polymeric micelles for cancer therapy: 3 C's to enhance efficacy, Curr. Opin. Solid State Mater. Sci. 16 (2012) 302–309. doi:10.1016/j.cossms.2012.10.003.

[16] E.S. Read, S.P. Armes, Recent advances in shell cross-linked micelles, Chem. Commun. (2007) 3021. doi:10.1039/b701217a.

[17] C.J. Rijcken, C.J. Snel, R.M. Schiffelers, C.F. van Nostrum, W.E. Hennink, Hydrolysable core-crosslinked thermosensitive polymeric micelles: Synthesis, characterisation and in vivo studies, Biomaterials. 28 (2007) 5581–5593. doi:10.1016/j.biomaterials.2007.08.047.

[18] C.F. van Nostrum, Covalently cross-linked amphiphilic block copolymer micelles, Soft Matter. 7 (2011) 3246. doi:10.1039/c0sm00999g.

[19] R.K. O'Reilly, C.J. Hawker, K.L. Wooley, Cross-linked block copolymer micelles: functional nanostructures of great potential and versatility, Chem. Soc. Rev. 35 (2006) 1068. doi:10.1039/b514858h.

[20] Y. Shi, R. van der Meel, B. Theek, E. Oude Blenke, E.H.E. Pieters, M.H.A.M. Fens, J. Ehling, R.M. Schiffelers, G. Storm, C.F. van Nostrum, T. Lammers, W.E. Hennink, Complete Regression of Xenograft Tumors upon Targeted Delivery of Paclitaxel via Π–Π Stacking Stabilized Polymeric Micelles, ACS Nano. 9 (2015) 3740–3752. doi:10.1021/acsnano.5b00929.

[21] D. Neradovic, C.F. Van Nostrum, W.E. Hennink, Thermoresponsive polymeric micelles with controlled instability based on hydrolytically sensitive N-isopropylacrylamide copolymers [6], Macromolecules. 34 (2001) 7589–7591. doi:10.1021/ma011198q.

[22] H. Maeda, T. Sawa, T. Konno, Mechanism of tumor-targeted delivery of macromolecular drugs, including the EPR effect in solid tumor and clinical overview of the prototype polymeric drug SMANCS, in: J. Control. Release, 2001: pp. 47–61. doi:10.1016/S0168-3659(01)00309-1.

[23] H. Maeda, J. Wu, T. Sawa, Y. Matsumura, K. Hori, Tumor vascular permeability and the EPR effect in macromolecular therapeutics: A review, J. Control. Release. 65 (2000) 271–284. doi:10.1016/S0168-3659(99)00248-5.

[24] S. Kumar, T.E. Witzig, M. Timm, J. Haug, L. Wellik, T.K. Kimlinger, P.R. Greipp, S.V. Rajkumar, Bone marrow angiogenic ability and expression of angiogenic cytokines in myeloma: evidence favoring loss of marrow angiogenesis inhibitory activity with disease progression, Blood. 104 (2004) 1159–1165. doi:10.1182/blood-2003-11-3811.

[25] A. Vacca, D. Ribatti, Bone marrow angiogenesis in multiple myeloma, Leukemia. 20 (2006) 193–199. doi:10.1038/sj.leu.2404067.

[26] M. Abe, Targeting the interplay between myeloma cells and the bone marrow microenvironment in myeloma, Int. J. Hematol. 94 (2011) 334–343. doi:10.1007/s12185-011-0949-x.

[27] J.S. Damiano, A.E. Cress, L.A. Hazlehurst, A.A. Shtil, W.S. Dalton, Cell adhesion mediated drug resistance (CAM-DR): role of integrins and resistance to apoptosis in human myeloma cell lines., Blood. 93 (1999) 1658–67.

[28] R. Schmidmaier, P. Baumann, ANTI-ADHESION Evolves To a Promising Therapeutic Concept in Oncology, Curr. Med. Chem. 15 (2008) 978–990. doi:10.2174/092986708784049667.

[29] F. Sanz-Rodríguez, J. Teixidó, VLA-4-dependent myeloma cell adhesion., Leuk. Lymphoma. 41 (2001) 239–245. doi:10.3109/10428190109057979.

[30] T. Kiziltepe, J.D. Ashley, J.F. Stefanick, Y.M. Qi, N.J. Alves, M.W. Handlogten, M.A. Suckow, R.M. Navari, B. Bilgicer, Rationally engineered nanoparticles target multiple myeloma cells, overcome cell-adhesion-mediated drug resistance, and show enhanced efficacy in vivo., Blood Cancer J. 2 (2012) e64. doi:10.1038/bcj.2012.10.

[31] P. Richardson, C. Mitsiades, J. Laubach, R. Schlossman, I. Ghobrial, T. Hideshima, N. Munshi, K. Anderson, Lenalidomide in multiple myeloma: An evidence-based review of its role in therapy, Core Evid. 4 (2009) 215–245. doi:10.2147/CE.S6002.

[32] G.T. Hermanson, Bioconjugate techniques, in: 2nd ed., Academic Press, San Diego, California, 2008: pp. 894–895.

[33] J. Carlsson, H. Drevin, R. Axén, Protein thiolation and reversible protein-protein conjugation. N-Succinimidyl 3-(2-pyridyldithio)propionate, a new heterobifunctional reagent., Biochem. J. 173 (1978) 723–37.

[34] G.T. Hermanson, Bioconjugate techniques 2ed, Elsevier Academic Press, 2008. doi:10.1007/s13398-014-0173-7.2.

[35] J.S. Moore, S.I. Stupp, Room Temperature Polyesterification, Macromolecules. 23 (1990) 65–70. doi:10.1021/ma00203a013.

[36] M. Talelli, C.J.F. Rijcken, S. Oliveira, R. Van Der Meel, P.M.P. Van Bergen En Henegouwen, T. Lammers, C.F. Van Nostrum, G. Storm, W.E. Hennink, Reprint of "nanobody - Shell functionalized thermosensitive core-crosslinked polymeric micelles for active drug targeting," in: J. Control. Release, Elsevier, 2011: pp. 93–102. doi:10.1016/j.jconrel.2011.06.003.

[37] G.T. Hermanson, Bioconjugate techniques., in: Academic Press, 2008: pp. 76–77.

[38] O. Soga, C.F. Van Nostrum, A. Ramzi, T. Visser, F. Soulimani, P.M. Frederik, P.H.H. Bomans, W.E. Hennink, Physicochemical characterization of degradable thermosensitive polymeric micelles, Langmuir. 20 (2004) 9388–9395. doi:10.1021/la048354h.

[39] Y. Shi, M.J. van Steenbergen, E.A. Teunissen, L. Novo, S. Gradmann, M. Baldus, C.F. van Nostrum, W.E. Hennink, Π–Π Stacking Increases the Stability and Loading Capacity of Thermosensitive Polymeric Micelles for Chemotherapeutic Drugs, Biomacromolecules. 14 (2013) 1826–1837. doi:10.1021/bm400234c.

[40] C. Li, W. Wang, Y. Xi, J. Wang, J.-F. Chen, J. Yun, Y. Le, Design, preparation and characterization of cyclic RGDfK peptide modified poly(ethylene glycol)- block -poly(lactic acid) micelle for targeted delivery, Mater. Sci. Eng. C. 64 (2016) 303–309. doi:10.1016/j.msec.2016.03.062.

[41] J.-C. Olivier, R. Huertas, H.J. Lee, F. Calon, W.M. Pardridge, Synthesis of pegylated immunonanoparticles., Pharm. Res. 19 (2002) 1137–43.

[42] C. Zhan, B. Gu, C. Xie, J. Li, Y. Liu, W. Lu, Cyclic RGD conjugated poly(ethylene glycol)-co-poly(lactic acid) micelle enhances paclitaxel anti-glioblastoma effect, J. Control. Release. 143 (2010) 136–142. doi:10.1016/j.jconrel.2009.12.020.

[43] M.-Y. Bai, S.-Z. Liu, A simple and general method for preparing antibody-PEG-PLGA sub-micron particles using electrospray technique: An in vitro study of targeted delivery of cisplatin to ovarian cancer cells, Colloids Surfaces B Biointerfaces. 117 (2014) 346–353. doi:10.1016/j.colsurfb.2014.02.051.

[44] N. Nasongkla, X. Shuai, H. Ai, B.D. Weinberg, J. Pink, D.A. Boothman, J. Gao, cRGD-Functionalized Polymer Micelles for Targeted Doxorubicin Delivery, Angew. Chemie Int. Ed. 43 (2004) 6323–6327. doi:10.1002/anie.200460800.

[45] Y. Nakayama, G. Smets, Radical and anionic homopolymerization of maleimide and N-n-butylmaleimide, J. Polym. Sci. Part A-1 Polym. Chem. 5 (1967) 1619–1633. doi:10.1002/pol.1967.150050712.

[46] H.C. Haas, Maleimide polymers. II. Radical polymerization kinetics, J. Polym. Sci. Polym. Chem. Ed. 11 (1973) 315–318. doi:10.1002/pol.1973.170110129.

[47] A.J. García, PEG–Maleimide Hydrogels for Protein and Cell Delivery in Regenerative Medicine, Ann. Biomed. Eng. 42 (2014) 312–322. doi:10.1007/s10439-013-0870-y.

[48] E.A. Phelps, N.O. Enemchukwu, V.F. Fiore, J.C. Sy, N. Murthy, T.A. Sulchek, T.H. Barker, A.J. García, Maleimide Cross-Linked Bioactive PEG Hydrogel Exhibits Improved Reaction Kinetics and Cross-Linking for Cell Encapsulation and In Situ Delivery, Adv. Mater. 24 (2012) 64–70. doi:10.1002/adma.201103574.

[49] R.M. Schiffelers, G.A. Koning, T.L.M. ten Hagen, M.H.A.M. Fens, A.J. Schraa, A.P.C.A. Janssen, R.J. Kok, G. Molema, G. Storm, Anti-tumor efficacy of tumor vasculature-targeted liposomal doxorubicin., J. Control. Release. 91 (2003) 115–22.

[50] R. Censi, W. Schuurman, J. Malda, G. di Dato, P.E. Burgisser, W.J.A. Dhert, C.F. van Nostrum, P. di Martino, T. Vermonden, W.E. Hennink, A Printable Photopolymerizable Thermosensitive p(HPMAm-lactate)-PEG Hydrogel for Tissue Engineering, Adv. Funct. Mater. 21 (2011) 1833–1842. doi:10.1002/adfm.201002428.

Chapter 8

Formulation and characterization of a Carbopol® hydrogel loaded with polymeric nanoparticles for vaginal drug delivery

8.1 Introduction

The vaginal cavity is a highly exposed site to bacteria and viruses responsible for several critical pathologies, including vaginal bacteriosis and sexually transmitted infections.

Vaginal drug delivery is commonly employed for the administration of antimicrobial and antiviral drugs. Moreover, this route has been recently exploited as a valid alternative to the parenteral and oral ones, to avoid undesirable systemic, hepatic or gastrointestinal side effects [1].

Vaginal drug delivery systems have been developed in a large variety of dosage forms, including tablets, capsules, films, foams and semi-solids preparations [2]. Semi-solids dosage forms, especially gels, have received an increasing attention over the past few years, due to their promising characteristics [3,4]. Gels present many advantages compared to other vaginal delivery systems including mucoadhesion and in situ retention, increased biovailability of the loaded drug, low costs, safety and feasibility [5–7]. Moreover, due to the mucoadhesion properties, the number of applications required can be potentially decreased, thus increasing the user compliance.

A drawback of vaginal administration is represented by the physiological removal mechanism, which reduces the in-situ residence time of the formulation, thus limiting drug distribution and absorption. Common strategies employed to overcome this limitation are represented by mucoadhesive and thermogelling systems [8]. Mucoadhesive formulations are able to interact with the vaginal mucosa through physical and chemical bonds with the secreted mucus, thus increasing drug permanence into the vaginal lumen. Mucoadhesion is commonly addressed through the use of specific polymers, such as polyacrilates (e.g. Carbopol), cellulose derivatives hydroxypropylcellulose (HPC), hydroxyethylcellulose (HEC), hydroxypropylmethylcellulose (HPMC), chitosan, natural gums, pectin, sodium alginate, hyaluronic acid, etc. [9]. As regard polyacrilic acid derivatives, they have been widely investigated both *in vitro* and *in vivo* for vaginal application, being included in various marketed products [4,10]. Interestingly, these polymers are acidic, thus providing a significant advantage in maintaining and eventually restoring the vaginal pH, generally altered in case of vaginal infections. Moreover their acid-buffering capacity was exploited as a strategy to treat vaginal bacteriosis, thus limiting the proliferation of pathogens [11–13].

A common limitation of the traditional dosage forms intended for vaginal delivery is represented by their poor ability to control the fate of the loaded drugs once they are released into the vaginal cavity.

Moreover, most of the antimicrobials and microbiocides suffer from poor water solubility, thus limiting their application in the vaginal lumen. Nanocarriers, particularly nanoparticles, have recently been proposed as a promising drug delivery system to overcome these limitations [14,15]. Nanosystems can ideally provide many advantages such as control of drug distribution, mucosal retention, cells uptake due to their nanoscale size, maintenance of drug integrity into the vaginal cavity and increase of drug availability. On the other hand, their application is limited by the liquid nature of the formulation. Therefore, a commonly exploited strategy to overcome such limitation, thus achieving an efficient intravaginal delivery, is the incorporation of nanosystems into the classical dosage forms, i.e. gels.

VivaGel® is an antiviral dendrimer-based carbomer gel developed by Starpharma (Melbourne, Australia) and currently in an advanced stage of the clinical trials [16–18].

Biocompatible and biodegradable polymers are commonly chosen for nanocarriers preparation including poly (DL-lactic acid), poly(lactic-*co*-glycolic acid) (PLGA), polycaprolactone (PCL), polyacrylates and poly(ethylene glycol) (PEG) derivatives, which have received the approval from the U.S. Food and Drug Administration (FDA) [19].

More importantly, previous studies have demonstrated the possibility of enhancing the efficacy of both antimicrobial and antiviral drugs by using vaginal gels and nanocarrier systems. Antimisiaris and Mourtas and Palmeira-de-oliveira et al., extensively revised the recent advances on anti-HIV and antimicrobials vaginal delivery systems, respectively [20,21].

The aim of the project was to develop a Carbopol-based hydrogel system loaded with polymeric nanoparticles, suitable as dosage forms for vaginal administration.

Methoxy poly(ethylene glycol)-poly(lactide-co-glycolide) mPEG-P(L)LGA di-block copolymers were employed to prepare nanoparticles, which were then incorporated into a 1.5% Carbopol® 974 hydrogel. Various di-block copolymers (with different mPEG/P(L)LGA ratio) were synthesized and screened for their ability to form stable nanoparticles. Different concentrations of nanoparticles were tested for their influence on the rheological properties of Carbopol hydrogels used as vehicles, by monitoring the storage modulus (G') and the loss modulus (G''). The presence of nanoparticles was found to cause a slight decrease in the strength of the hydrogel. Nevertheless, Carbopol®974 gives a hydrogel (from a rheological point of view) at any tested nanoparticles concentration. As a result, Carbopol®974 was demonstrated to be a suitable polymer for formulating a vaginal gel.

Metronidazole (MTZ) and Saquinavir mesylate (SQV) were then employed as model drugs to be loaded into the system. In fact, metronidazole has been widely employed for the treatment

of vaginal bacteriosis both for topical and oral formulations and different marketed products have been developed by combining metronidazole with acid polymers in order to increase its antimicrobial activity [13]. On the other hand, Saquinavir mesylate is the first protease inhibitor approved by the US Food and Drug administration and it has been recently studied as prophylaxis agent to control and reduce HIV infections.

Our formulation demonstrated the capacity to increase MTZ solubility in water while the encapsulation efficiency of SQV was 55%. Moreover, release studies showed an increased release of metronidazole from Carbopol® 974 hydrogel in presence of nanoparticles.

8.2 Material and methods

8.2.1 Materials

Methoxy poly(ethylene glycol) (number average molecular weight M_n = 5 kDa, mPEG $_{5kDa}$) was purchased from Polysciences; L-lactide and glycolide was kindly donated by PURAC Biochem (Gorinchem, Netherlands). Carbopol® 974 NF polymer and Carbopol® 940 NF polymer were obtained from Lubrizol. Sodium hydroxide (NaOH), ammonium acetate, methanol (MeOH), acetonitrile (CH_3CN), acetone were supplied by Carlo Erba. Stannous 2-ethylhexanoate ($Sn(Oct)_2$, Saquinavir mesylate (SQV) and all other reagents were purchased from Sigma-Aldrich (Milan, Italy) and used without further purification. Metronidazole (MTZ) was obtained from ACEF (PC, Italy).

8.2.2 Synthesis of mPEG$_{5kDa}$-P(L)LGA polymers

A ring opening polymerization (ROP) procedure was employed to synthesize methoxy poly(ethylene glycol)-poly(lactide-co-glycolide) (mPEG-P(L)LGA) diblock copolymers [22] as schematically reported in Fig. 1.

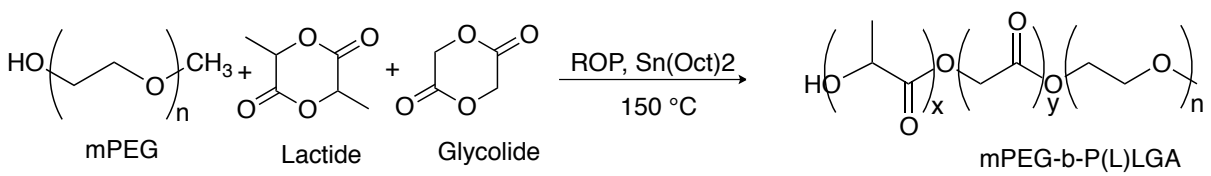

Fig. 1. Synthesis of mPEG-*b*-P(L)LGA block copolymers through a ring opening polymerization reaction (ROP).

In a round-bottom flask, mPEG 5kDa was melted at 80°C and flushed with nitrogen. L-lactide and glycolide were then added into the flask and the temperature was increased up to 150°C.

Different ratios of mPEG 5kDa, L-lactide and glycolide were employed for the synthesis of various copolymers and the percentage of the hydrophobic portion was progressively increased while the percentage of mPEG 5kDa was decreased from 74% wt to 50% wt (Table 1). Stannous 2-ethylhexanoate (1.25% wt) was then added into to the reaction as catalyst and the reaction was heated at 150°C for 2 to 3 hours under nitrogen, depending on the copolymer. Dichloromethane was added to the reaction mixture at room temperature, and the viscous solution was poured into cold diethyl ether, under stirring, to precipitate the copolymer and remove the impurities. The precipitated material was finally filtered and residual solvents were removed under vacuum. Copolymers were collected as white solids and characterized for their physicochemical properties by proton nuclear magnetic resonance (^{1}H NMR) and gel permeation chromatography (GPC).

Table 1. Experimental conditions

mPEG 5kDa-P(L)LGA copolymer	mPEG 5kDa (% wt)	L-lactide (%wt)	Glycolide (%wt)	Sn(Oct)2 (µl)	Time (h)
1	74	14	12	100	2
2	50	25	25	100	3

8.2.3 Proton nuclear magnetic resonance

Samples were dissolved in deuterium chloroform ($CDCl_3$) and ^{1}H-NMR spectra were recorded on a Bruker Advance 200 MHz spectrometer. Chemical shift values are reported in parts per million (δ) and referred to the solvent peak.

8.2.4 Gel permeation chromatography

GPC was performed to determine the number average molecular weight (M_n), weight average molecular weight (M_w) and the polydispersity index (M_w/M_n = PDI) of the polymers using an Agilent 1100 series system equipped with a TSKGel 2500HHR column (Tosoh Bioscience),
The column temperature was 35°C, tetrahydrofuran (THF) was used as eluent. The flow rate was 1ml/min and refractive index was used as detection method. Samples were prepared by solubilizing 7.5 mg of copolymer into 1.5 ml of THF at 40°C for 1 hour. The solution was filtered through a 0.45 µm syringe filter and 7.5 µl di CH_3CN (flow marker) was added. A calibration standard curve was achieved using a PEG calibration kit (PL2070-01000 by Varian) with molecular weight ranging from 106 to 21,300 M_p. Data were analyzed by the clarity software dataApex (DataApex Ltd, Prague, Czech Republic).

8.2.5 Preparation of polymeric nanoparticles $mPEG_{5kDa}$-P(L)LGA

mPEG-P(L)LGA polymeric nanoparticles (NPs) were prepared by the nanoprecipitation method by employing different copolymers at various concentrations. Morevover, various solvents were initially screened. Copolymer **1** and copolymer **2** were finally chosen for nanoparticles preparation and acetone was selected as the best solvent.

mPEG-P(L)LGA NPs were prepared at 5 mg/ml, 10 mg/ml, 20 mg/ml and 40 mg/ml final concentration. The copolymer was solubilized in the minimum amount of the required solvent (400 µl and 600 µl for 5mg/ml and 10, 20 and 40 mg/ml respectively) and then the polymer solution was added dropwise to 2 ml of distilled water under magnetic stirring. As regard NPs prepared using copolymer **1**, water was added dropwise to the acetone dispersion of the copolymer. Acetone was evaporated under vacuum before NPs characterization.

The Z-average particle size (Z_{ave}) and polydispersity index (PDI) of NPs were measured by dynamic light scattering (DLS) using a Malvern Zetasizer nanoS (Malvern instrument Worcestershire UK) equipped with a back-scattered light detector operating at 173°. 1 ml of the samples was loaded inside disposable cuvettes and the scattered signals were recorded after 180 s equilibration at 25°C.

8.2.6 Preparation of Carbopol® hydrogels

Carbopol® 940 NF and Carbopol® 974 NF polymers were tested for hydrogels preparation at the final concentration of 0.5 % wt, 1% wt and 1.5% wt. 30 gr of hydrogel were prepared by gradually dispersing the required amount of the selected polymer into distilled water and distilled water preserved with 0.2% wt nipagin respectively, under continuous stirring. The pH was monitored during the preparation (pH around 3) and then adjusted to 5 by adding NaOH. Hydrogels were kept overnight under stirring and then pH was measured.

8.2.7 Preparation of Carbopol ® hydrogels loaded with nanoparticles

Two different methods have been investigated for the preparation of 10 gr of Carbopol® hydrogel (final concentration 1.5% wt) loaded with NPs at different concentrations.

5 gr of NPs and 5 gr of Carbopol® hydrogel were initially prepared, as previously described, at a concentration double than the final sample; then NPs solution was added dropwise under stirring to the Carbopol® dispersion; finally the pH of the preparation was adjusted to 5 and gelation occurred. The hydrogel loaded with nanoparticles was kept overnight under stirring and the pH value was monitored.

According the second method, Carbopol® hydrogel loaded with nanoparticles was prepared as follow: 10 gr of samples were prepared by dispersing the required amount of Carbopol® polymer to 9.85 gr of nanoparticle solution. The gelation process occurred as the pH was adjusted to 5.

8.2.8 Rheological characterization of Carbopol® hydrogels

Carbopol® hydrogels and Carbopol® hydrogel loaded with nanoparticles were studied for their viscoelastic properties by rheological analysis using a stress control rheometer (Stress-Tech, Reologica) equipped with a cone-plate geometry (C 40/4) operating in the oscillation mode.
The following tests have been performed:

- Oscillation stress sweep: the samples were exposed to increasing stresses (0.5-20 Pa) at a constant frequency (1 Hz), at 25°C. This test allowed the determination of a linear viscolelastic regime (LVR).
- Frequency sweep: the samples were exposed to increasing frequencies (0.01-10 Hz) at a constant stress (5 Pa) in the field of linear viscoelasticity.

Storage modulus (*G'*) and loss modulus (*G''*) were monitored.

8.2.9 Preparation of nanoparticles to increase the solubility of metronidazole

Solubility of metronidazole in water and in presence of different concentrations of nanoparticles (5mg/ml, 10mg/ml, 15mg/ml and 20mg/ml) was measured using a UV-1800 Spectrophotometer (Shimadzu, JP) at 319.5 nm. The concentration of metronidazole employed was directly derived from the solubility study. Thus, metronidazole was employed at the concentration of 9.5 mg/ml in order to obtain a solution close to saturation. Copolymer **1** was solubilized at the desired concentration in acetone; then, nanoparticles were formed by adding a solution of metronidazole in water (9.5mg/ml). Next, organic solvent was removed by rotary evaporation. The aqueous dispersion of NPs and drug was then placed in contact with an excess of metronidazole for 24 hours. The supernatant was recovered after centrifugation (13000 rpm, 3 min) and filtered through a 0.22 µm cellulose filter to remove the excess of drug. UV absorbance was measured at 319.5 nm and the concentration of metronidazole was derived from the calibration curve.

8.2.10 Carbopol® 974 hydrogel loaded with metronidazole in presence of NPs

Carbopol® 974 hydrogels (final concentration 1.5% wt) loaded with NPs (10 mg/ml) was prepared as previously described using a saturated aqueous solution of metronidazole (final concentration 9.5 mg/ml). The NPs solution in metronidazole was added dropwise under stirring to the Carbopol® dispersion in metronidazole; finally the pH of the preparation was adjusted to 5 and gelation occurred. The hydrogel loaded with nanoparticles was kept overnight under stirring and the pH value was monitored before rheological characterization by frequency sweep test.

Release studies of metronidazole from Carbopol® 974 hydrogels both in presence and not of NPs, have been performed at 37°C using a USP dissolution apparatus (AT7 smart, Sotax, CH) equipped with Teflon enhancer cells (Agilent, USA) having a surface area of 4 cm^2 without membranes. 2 gr hydrogel sample were placed in the reservoir of the enhancer cell. The enhancer cell was left to equilibrate at 37°C for 10 min and then placed in the vessels containing 1000 ml of distilled water. The paddles were rotated at 50 rpm and their position was adjusted to remain 6 cm above the top of enhancer cells. 2 ml samples were collected at 0.5, 15, 30, 45, 60, 90, 120, 150, 180, 210, 240, 300 and 360 minutes. The absorbance of metronidazole released at each time-point was measured by UV-spectroscopy (UV 1800 spectrophotomer Shimadzu, JP) at 319.5 nm.

8.2.11 Preparation of saquinavir mesylate loaded nanoparticles

Copolymer **2** was used for the preparation of nanoparticles loaded with SQV, based on the results obtained from DLS measurements. 10 ml of NPs were prepared by a nanoprecipitation method. Briefly, 200 mg of mPEG-P(L)LGA copolymer (20mg/ml) were solubilized in 6 ml of acetone (sol. A), while SQV was dissolved in methanol, making a 2 mg/ml stock solution (sol. B). Solution A and 250 µl of solution B were then added dropwise to 10 ml distilled water and subsequently stirred for 1 hour; solvents were removed by rotary evaporation. The Z-average particle size (Z_{ave}) was measured by DLS and then the non-entrapped SQV was removed by ultracentrifugation (50000 rpm, 40 min, 20°C). SQV loaded NPs precipitated while non-entrapped SQV was recovered in the supernatant. A low concentration of SQV (that ensures drug solubilisation) was employed during NPs preparation to avoid drug precipitation with nanoparticles.

8.2.12 High-performance liquid chromatography method fo saquinavir mesylate quantification

The non-entrapped SQV was quantified by HPLC analysis using an Agilent HP1100 series system equipped with a photodiode array detector (DAD). A Spherisorb ODS2 Column (C18, 5 µm, 4.6 mm X 250 mm) (Waters, UK) was used and samples were filtered through a 0.45 µm filter before measure. The elution was made using 90% methanol and 10% (v/v) water with ammonium acetate (50 mM), adjusted to pH 4 with acetic acid. The chromatographic run was performed using an isocratic elution at a flow rate of 1 ml/min. The retention time was 3.7 min. Non-entrapped SQV was detected by quantifying the area under the curve measured at 238 nm (ChemStation software, Agilent Technologies).

8.2.13 Encapsulation efficiency of SQV NPs

The amount of unencapsulated SQV was quantified by HPLC and encapsulation efficiency (EE%) of SQV NPs was calculated as follow:

$$EE\% = \frac{total\ concentration\ of\ drug - concentration\ of\ drug\ in\ the\ supernatant}{total\ concentration\ of\ drug}\ X\ 100$$

8.3 Results and Discussion

8.3.1 ^{1}H NMR and GPC Characterization of mPEG$_{5kDa}$-P(L)LGA copolymers

The synthesized PEGylated polyesters have been characterized by ^{1}H NMR ($CDCl_3$) and GPC. Table 2 reports the molecular weight data of the synthesized copolymers, expressed as number average molecular weight (M_n) and weight average molecular weights (M_w), and the polydispersity index (PDI), resulting from both ^{1}H NMR and GPC analysis. Copolymer **1** is characterized by a higher hydrophilic character while copolymer **2** shows a higher PLGA/mPEG ratio.

Table 2. Characterization of the synthesized mPEG 5kDa-P(L)LGA di-block copolymers based on ^{1}H NMR and GPC.

Copolymers mPEG 5kDa-P(L)LGA	^{1}H NMR	GPC			PLGA/mPEG ratio*
	Mn (Da)	Mn (Da)	Mw (Da)	PDI	
Copolymer 1	6000	6735	9084	1.35	0.51
Copolymer 2	6800	7322	12076	1.65	1.01

* derived from GPC M_w

^{1}H NMR spectra (Fig. 2) showed typical peaks: 5.2 ppm referred to the methine proton of lactide (OC**H**CH_3CO), 4-62-4.92 ppm (methylene group of glycolide, -OC**H**$_2$CO), 3.6 ppm (PEG chain, -C**H**$_2$C**H**$_2$O), 3.4 ppm (methyl group of the methoxy PEG –CH_3), 1.5 ppm (methyl group of the lactide chain).

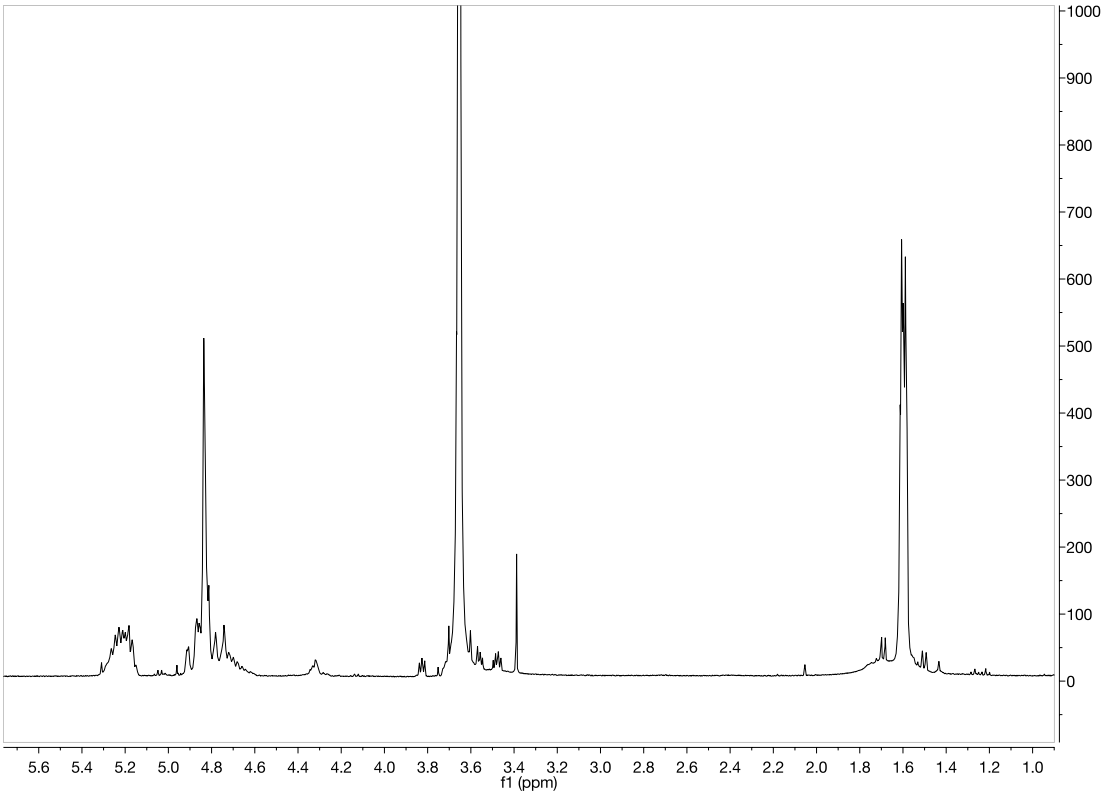

Fig. 2. ^{1}H NMR spectra of mPEG 5kDa-P(L)LGA di-block copolymer in $CDCl_3$. Chemical shift values are reported in parts per million (δ) and referred to the solvent peak.

8.3.2 Physicochemical characterization of nanoparticles

The different chemical composition of the employed copolymer was demonstrated to influence the physicochemical characteristics of the nanocarrier system.

Both the nanosystems made of copolymer **1** and copolymer **2** were characterized for their size and PDI using dynamic light scattering as reported in Table 3. Copolymer **1** was tested up to 40 mg/ml due to the high solubility, while copolymer **2** was screened in the concentration range of 5-20 mg/ml since aggregates were formed at higher concentrations.

Table 3. Physicochemical characterization by DLS of mPEG 5kDa-P(L)LGA nanoparticles prepared by copolymer **1** and copolymer **2** at different concentrations. Data are presented as mean ± SD (n = 3).

Concentration (mg/ml)	Z-average (d.nm)	PDI
Copolymer 1		
5	33.9 ± 0.11	0.17 ± 0.02
10	32.5 ± 0.52	0.25 ± 0.03
20	32.8 ± 0.16	0.20 ± 0.01
40	31.2 ± 0.07	0.23 ± 0.00
Copolymer 2		
5	58.9± 4.45	0.22± 0.05
10	63.8± 0.95	0.24±0.03
20	89.0± 9.03	0.34±0.06

Dynamic light scattering is a spectroscopic technique, based on the interaction between light and particles in order to measure particles size in the submicron region. The size of a particle in solution is calculated from the translational diffusion coefficient, which is a function of the velocity of the Brownian motion of dispersed particles when they possess a size comparable with the medium molecules. Hence, particles size is referred as hydrodynamic radius or diameter, that is the radius or diameter of a hypothetical sphere that diffuses with the same speed than the analysed particle [23].

Copolymer **1** was characterized by an increased hydrophilicity compared to copolymer **2**, due to the higher PEG/PLGA ratio. Moreover, particle size was independent from the concentration of copolymer **1**, with a single unimodal distribution centred at around 33 nm. On the contrary, insoluble nanoparticles formed by the partially soluble copolymer **2** demonstrated a size dependence upon concentration. In fact, the size of nanoparticles increases by increasing the copolymer concentration.

8.3.3 Characterization of Carbopol hydrogels and Carbopol hydrogels loaded with nanoparticles

Carbopol hydrogels and Carbopol hydrogels loaded with mPEG5kDa-P(L)LGA nanoparticles (made of copolymer **1** or copolymer **2)** were characterized for their viscoelastic properties by rheological analysis. Zidoval®, the marketed vaginal Carbopol® 974 hydrogel containing

metronidazole, was used as reference. Storage modulus (G') and loss modulus (G'') of Carbopol hydrogel and Carbopol hydrogel loaded with NPs were monitored. The cross over of G' and G'' indicates the transition from a polymeric dispersion to a gel system. When G'>G'', samples show a prevalent elastic behaviour [24,25].

Carbopol® 940 at 0.5% wt was initially screened in presence of different concentrations of nanoparticles, in order to obtain a system with rheological properties comparable to those of Zidoval®. Fig. 3 shows the influence of nanoparticles concentration on the final strength of the hydrogel. Carbopol® 940 hydrogels and Carbopol® 940 hydrogels loaded with 2.5 mg/ml NPs made of copolymer **1** showed G' values still acceptable, although lower than the reference Zidoval®. On the other hand, NPs at higher concentration (5-20 mg/ml) led to a drop of G' values significantly below the reference Zidoval® (Fig. 3a). Frequency sweep tests confirmed gel deconstruction. In fact, apart from Zidoval® which showed G'>G" independently from the frequency applied, for all the analysed samples a cross-over between G' and G" was observed. Although Carbopol® 940 loaded with the lowest concentration of nanoparticles showed G' values higher than G'' in the range of applied frequencies, a cross-over of G' and G'' moduli at lower frequencies (0.01 Hz) can be deduced from the graph. Furthermore, it is possible to observe a relation between gel deconstruction and nanoparticles concentration. As the nanoparticles concentration in the hydrogel is increased, the gel strength decreases. Gel deconstruction can be reasonably attributed to nanoparticles entrapped in the hydrogel matrix, which interfere with the three-dimensional network by weakening the interactions between carbomer polymeric chains, thus increasing their mobility.

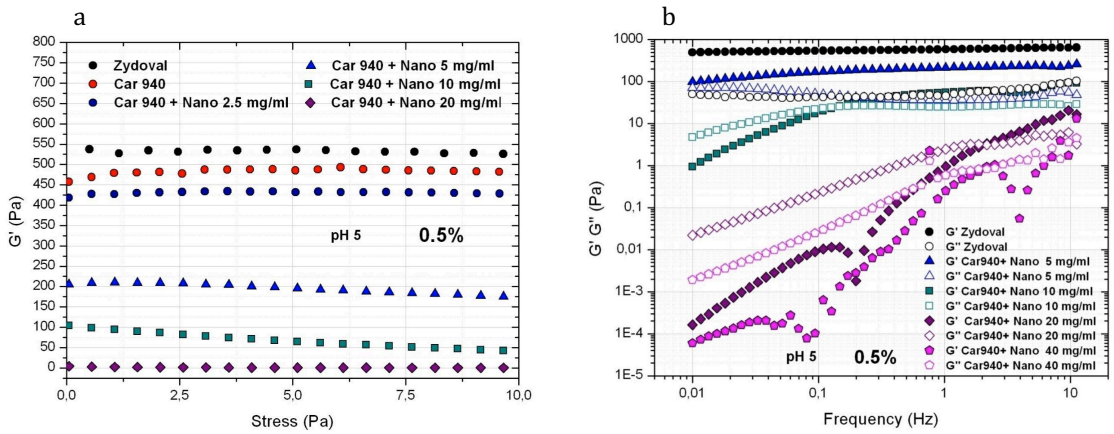

Fig. 3. Stress sweep test (a) and frequency sweep test (b) of Carbopol® 940 hydrogels in presence of different concentration of NPs.

Carbopol® 974 was then used for hydrogel preparation at 1% and 1.5% wt, to obtain a gel with a rheological behaviour comparable to Zidoval®. Carbopol® 974 hydrogels at 1% and

1.5%wt in presence of NPs (5-40 mg/ml) showed G' values higher than 0.5% Carbopol® 940 hydrogels. Fig. 4a and 4c show the results obtained from the stress sweep test of 1.5% Carbopol® 974 hydrogels loaded with NPs made of the two different copolymers, copolymer **1** and copolymer **2** respectively. Frequency sweep tests of Carbopol® 974 hydrogel loaded with NPs are reported in Fig. 4b and 4d.

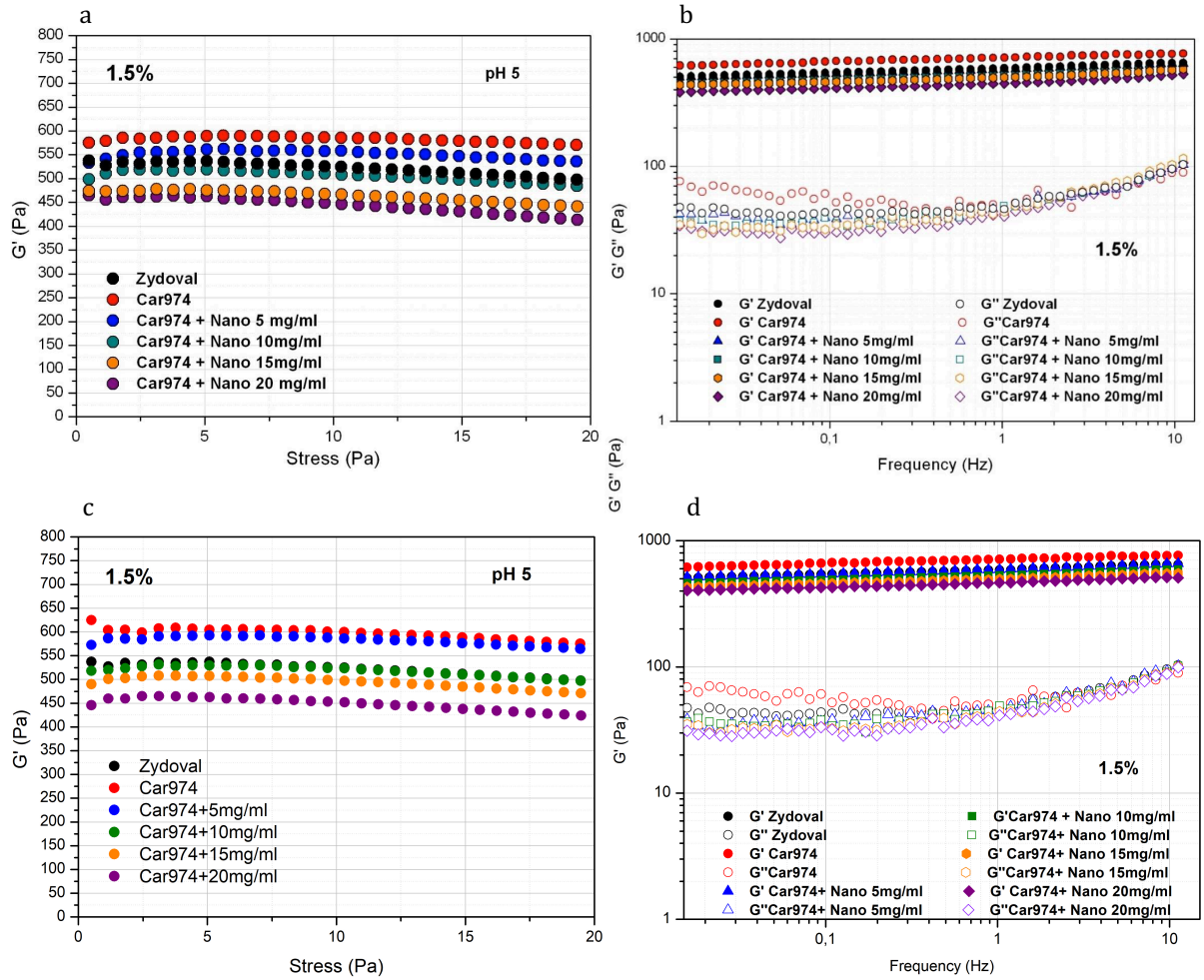

Fig. 4. a) Stress sweep test of Carbopol® 974 hydrogel loaded with different concentration of NPs made of copolymer **1**; b) Frequency sweep test of Carbopol® 974 hydrogel loaded with different concentration of NPs made of copolymer **1**; c) Stress sweep test of Carbopol® 974 hydrogel loaded with different concentration of NPs made of copolymer **2**; d) Frequency sweep test of Carbopol® 974 hydrogel loaded with different concentration of NPs made of copolymer **2**.

All samples demonstrated a typical viscoelastic behaviour with G' values higher than G'' and in the same range of magnitude of Zidoval®. This point out to a highly organized three-dimensional network which is not influenced by nanoparticles concentration conversely to Carbopol® 940. The concentration of carbomer polymer plays also a central role in defining the viscoelastic behaviour of Carbopol® 974 hydrogel, by affecting the gel strength. Thus, more concentrated polymer dispersions give stronger gels. In fact, as regards 1.5% wt

Carbopol® 974 hydrogel, G' and G'' moduli were less influenced by increasing nanoparticles concentrations, compared to 1% wt Carbopol® 974 hydrogel.

Based on these results it is reasonable to conclude that 1.5% Carbopol® 974 hydrogel possesses the best characteristics in terms of gel architecture.

8.3.4 Carbopol® 974 hydrogel loaded with metronidazole in presence of NPs

Various vaginal gels containing metronidazole have been studied in literature and their rheological and mucoadhesive properties have been compared with the marketed Zidoval® [26,27].

Fig. 5 show the solubility of metronidazole in water and in presence of nanoparticles made of copolymer **1** at different concentrations (5mg/ml, 10mg/ml, 15 mg/ml and 20mg/ml). The solubility of metronidazole in water is 9.96 mg/ml. In presence of nanoparticles the solubility of metronidazole is progressively increased, reaching a plateau at around 12.5 mg/ml in presence of 10 mg/ml, 15 mg/ml and 20 mg/ml NPs.

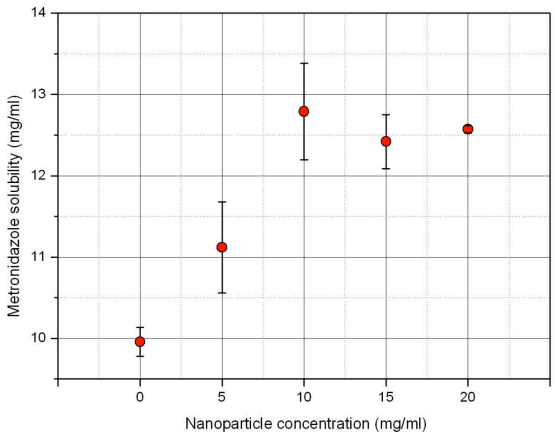

Fig. 5. Metronidazole solubility in water and in presence of nanoparticles made of copolymer 1 at 5 mg/ml, 10 mg/ml, 15 mg/ml and 20 mg/ml.

1.5% wt Carbopol® 974 hydrogels loaded with NPs (10mg/ml) in presence of metronidazole (9.5mg/ml) were studied for their rheological behaviour.

Results from frequency sweep test, show that metronidazole does not influence the rheological properties of the hydrogel and G' values are conserved (Fig. 6).

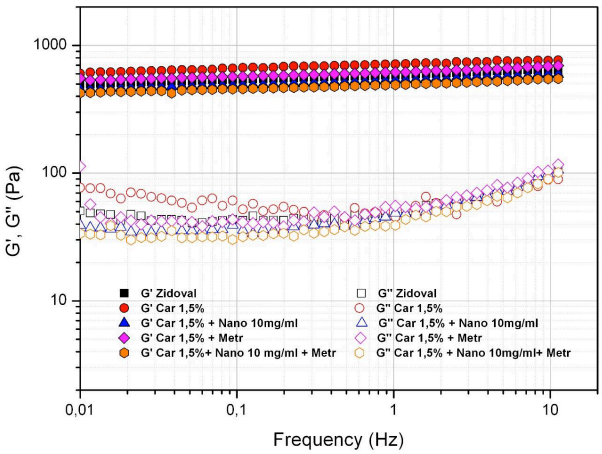

Fig. 6. Frequency sweep test of 1.5% Carbopol® 974 hydrogels with metronidazole and Carbopol® 974 hydrogels loaded with NPs (10mg/ml) in presence of metronidazole.

Moreover, release studies of metronidazole from 1.5% Carbopol® 974 hydrogels both in presence and absence of NPs (10mg/ml), have been performed in order to evaluate the influence of the nanocarrier system on the release of metronidazole from Carbopol® 974 hydrogels. Interestingly, results reported in Fig.7, show an increased solubility of metronidazole in presence of NPs. In fact, the amount of released metronidazole from the hydrogel loaded with NPs was found to be 1.5 mg higher than the hydrogel without NPs. Furthermore, the presence of NPs did not negatively affect the release of metronidazole from the hydrogel, showing a comparable release profile for both formulations.

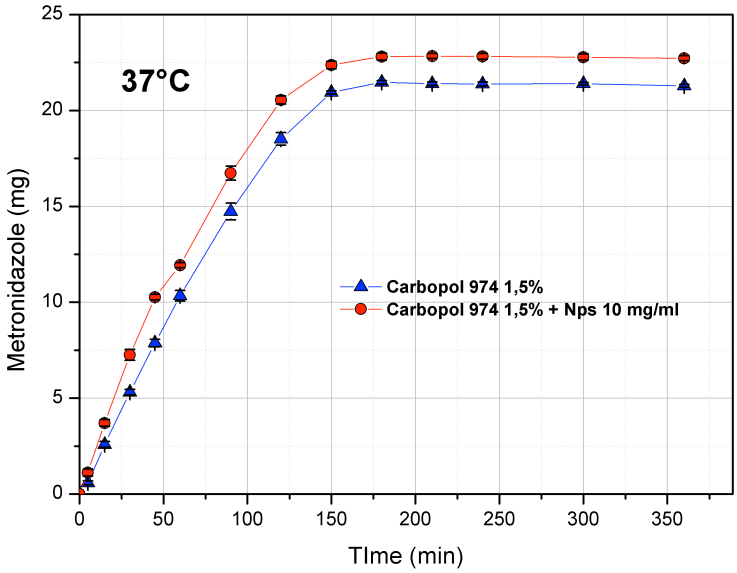

Fig. 7. Release studies of metronidazole from 1.5% Carbopol® 974 hydrogels both in presence and absence of NPs.

8.3.5 Saquinavir mesylate loaded nanoparticles

An increasing attention has been focused in recent years on the development of different nanomedicine intended for vaginal use, in particular for microbiocides administration to prevent or at least reduce HIV infection [28–31].

In the present work, Carbopol® 974 hydrogels were demonstrated to maintain its structure when loaded with nanoparticles. After assessing this important condition, nanoparticles were loaded with SQV and characterized in terms of EE%.

Based on the results obtained from the initial screening of different copolymers, copolymer 2 (20 mg/ml) was finally chosen to encapsulate SQV because it forms larger nanoparticles without affecting the rheological properties of the hydrogel. In fact, larger particles have a greater capacity to encapsulate drugs. A low concentration of SQV (that ensures drug solubilisation) was employed during NPs preparation to avoid drug precipitation with nanoparticles during ultracentrifugation. SQV loaded NPs precipitated while non-entrapped SQV was recovered in the supernatant and quantified by HPLC analysis (Fig. 8). In fact, the concentration of SQV was too low to be detected by UV-vis spectroscopy. EE% of SQV loaded NPs formulated in this study was 54.29 ± 2.4%.

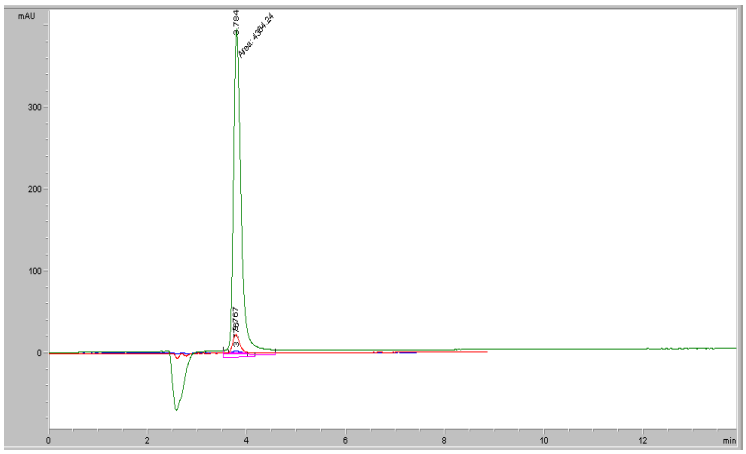

Fig. 8. Typical HPLC chromatogram of saquinavir mesylate.

Based on these promising results, SQV NPs will be loaded into 1.5% wt Carbopol® 974 hydrogel and the release studies of SQV loaded-NPs and Carbopol® 974 hydrogels loaded with SQV NPs will be performed in order to assess the release of SQV from both NPs and hydrogel formulations.

8.4 Conclusions

This study reports the formulation and an exhaustive rheological characterization of a Carbopol-based hydrogel loaded with polymeric nanoparticles intended for vaginal delivery. The rational of this design was to use a nanocarrier system that once loaded into the hydrogel matrix, could provide a sustained drug release over time, thus avoiding the limitations often associated with hydrogels. In fact, hydrogel can hardly control the fate of the loaded drug, which diffuse from the porous matrix.

Carbopol is an acidic-high molecular weight polymer extensively investigated in literature for vaginal administration. Two different Carbopol polymers (Carbopol® 940 and Carbopol® 974) were used in this study, with the main aim of selecting the hydrogel system with the best properties. Carbopol hydrogels were formulated at different concentrations, to obtain systems with rheological properties comparable to the commercial Zidoval®.

Various mPEG 5kDa-P(L)LGA di-block copolymers (differing for their PLGA/mPEG ratio) were screened for their ability to form nanoparticles with the desired characteristics. Nanoparticles at different concentrations were then incorporated into Carbopol® 974 and Carbopol® 940 matrices and their influence on the rheological behaviour of the system was studied. 1.5% wt Carbopol® 974 hydrogel exhibited the best rheological behaviour. The storage modulus G' and the loss modulus G'' were only slightly influenced by the presence of increasing concentration of nanoparticles, in contrast to Carbopol® 940 hydrogel. For this reason, 1.5% wt Carbopol® 974 hydrogel was selected for loading experiments using metronidazole and saquinavir mesylate. Nanoparticles were able to enhance metronidazole solubility in water while the encapsulation efficiency of SQV was 55%. Release studies were then performed to evaluate metronidazole release from the nanoparticles loaded into Carbopol® 974 hydrogel, showing a good release profile.

8.5 Future perspectives

The main objective of this study was to develop a platform for vaginal drug delivery, which combines the advantages of both gel and nanotechnology. Nanoparticles can potentially increase the drug efficacy, by enhancing drug solubility and eventually provide a protection against the vaginal adverse environment. The hydrogel matrix is intended to enhance the retention time of the formulation into the vaginal lumen, thus increasing the patient compliance. To this end, a mucoadhesive system is highly recommended, which can interact with the vaginal mucosa through physical and chemical bonds with the secreted mucus, thus

increasing drug permanence into the vaginal lumen. Carbopol polymer has often been employed for this purpose in vaginal formulations, due to its well-known muco-adhesion properties. Therefore, an important aspect that needs to be considered in future studies is the mucodhesion of the formulated system, that will be investigated through tensil strength method.

Carbopol® 974 based hydrogel was selected as matrix, due to its ability to support the loaded nanocarrier without loosing its structure, as showed by rheological studies. In the first step, nanoparticles were loaded with metronidazole and evaluated for their ability to increase metronidazole solubility. Moreover, release studies were performed to study the influence of nanoparticles on metronidazole release from the hydrogel matrix. A good release profile of metronidazole from both Carbopol® 974 hydrogel and Carbopol® 974 hydrogel loaded with nanoparticles was observed with a slightly higher metronidazole release than Carbopol® 974 hydrogel without nanoparticles.

Based on the results obtained with the model drug metronidazole, which suggest the potential application of the system as vaginal delivery system, saquinavir mesylate was then employed in the formulation as innovative drug. Nanoparticles were loaded with saquinavir mesylate and the encapsulation efficiency was calculated to be 55%. This study reports only partial results with the protease inhibitor saquinavir mesylate and future studies are needed to evaluate the formulation based on saquinavir mesylate. In particular, *in vitro* release of saquinavir mesylate from mPEG-PLGA nanoparticles will be initially assessed. Saquinavir mesylate nanoparticles will be then loaded inside the 1.5% Carbopol® 974 hydrogel matrix. The release profile of saquinavir mesylate from both nanoparticles and Carbopol® 974 hydrogel loaded nanoparticles will be studied in order to assess the effectiveness of the formulated system.

In vitro studies will finally evaluate the efficacy of both the formulated systems.

References

[1] G. Sandri, S. Rossi, F. Ferrari, M.C. Bonferoni, C. Caramella, Strategies to improve systemic and local availability of drugs administered via vaginal route, in: E. Touitou, B., Barry, BW (Ed.), Enhanc. Drug Deliv., 1 ed., 2007: pp. 441–470.

[2] K. Vermani, S. Garg, The scope and potential of vaginal drug delivery, Pharm. Sci. Technolo. Today. 3 (2000) 359–364. doi:10.1016/S1461-5347(00)00296-0.

[3] J. das Neves, R. Palmeira-de-Oliveira, A. Palmeira-de-Oliveira, F. Rodrigues, B. Sarmento, Vaginal Mucosa and Drug Delivery, in: Mucoadhesive Mater. Drug Deliv. Syst., John Wiley & Sons, Ltd, Chichester, United Kingdom, 2014: pp. 99–132. doi:10.1002/9781118794203.ch05.

[4] K. Edsman, H. Hägerström, Pharmaceutical applications of mucoadhesion for the non-oral routes, J. Pharm. Pharmacol. 57 (2005) 3–22. doi:10.1211/0022357055227.

[5] M. Justin-Temu, F. Damian, R. Kinget, G. Van Den Mooter, Intravaginal gels as drug delivery systems., J. Womens. Health (Larchmt). 13 (2004) 834–44.

[6] A. Hussain, F. Ahsan, The vagina as a route for systemic drug delivery, J. Control. Release. 103 (2005) 301–313. doi:10.1016/j.jconrel.2004.11.034.

[7] J. das Neves, M.F. Bahia, Gels as vaginal drug delivery systems, Int. J. Pharm. 318 (2006) 1–14. doi:10.1016/j.ijpharm.2006.03.012.

[8] C.M. Caramella, S. Rossi, F. Ferrari, M.C. Bonferoni, G. Sandri, Mucoadhesive and thermogelling systems for vaginal drug delivery, Adv. Drug Deliv. Rev. 92 (2015) 39–52. doi:10.1016/j.addr.2015.02.001.

[9] C. Valenta, The use of mucoadhesive polymers in vaginal delivery, Adv. Drug Deliv. Rev. 57 (2005) 1692–1712. doi:10.1016/j.addr.2005.07.004.

[10] F. Acartürk, Mucoadhesive vaginal drug delivery systems., Recent Pat. Drug Deliv. Formul. 3 (2009) 193–205. doi:10.2174/187221109789105658.

[11] J. Wilson, Managing recurrent bacterial vaginosis., Sex. Transm. Infect. 80 (2004) 8–11. doi:10.1136/STI.2002.002733.

[12] G.G. Donders, J. Zodzika, D. Rezeberga, Treatment of bacterial vaginosis: what we have and what we miss, Expert Opin. Pharmacother. 15 (2014) 645–657. doi:10.1517/14656566.2014.881800.

[13] S. Garg, R.A. Anderson, C.J. Chany, D.P. Waller, X.H. Diao, K. Vermani, L.J. Zaneveld, Properties of a new acid-buffering bioadhesive vaginal formulation (ACIDFORM)., Contraception. 64 (2001) 67–75.

[14] L.M. Ensign, R. Cone, J. Hanes, Nanoparticle-based drug delivery to the vagina: A review, J. Control. Release. 190 (2014) 500–514. doi:10.1016/j.jconrel.2014.04.033.

[15] J. das Neves, R. Nunes, A. Machado, B. Sarmento, Polymer-based nanocarriers for vaginal drug delivery, Adv. Drug Deliv. Rev. 92 (2015) 53–70. doi:10.1016/j.addr.2014.12.004.

[16] J. O'Loughlin, I.Y. Millwood, H.M. McDonald, C.F. Price, J.M. Kaldor, J.R.A. Paull, Safety, Tolerability, and Pharmacokinetics of SPL7013 Gel (VivaGel®): A Dose Ranging, Phase I Study, Sex. Transm. Dis. 37 (2010) 100–104. doi:10.1097/OLQ.0b013e3181bc0aac.

[17] I. McGowan, K. Gomez, K. Bruder, I. Febo, B.A. Chen, B.A. Richardson, M. Husnik, E. Livant, C. Price, C. Jacobson, MTN-004 Protocol Team, Phase 1 randomized trial of the vaginal safety and acceptability of SPL7013 gel (VivaGel) in sexually active young women (MTN-004), AIDS. 25 (2011) 1057–1064. doi:10.1097/QAD.0b013e328346bd3e.

[18] C.F. Price, D. Tyssen, S. Sonza, A. Davie, S. Evans, G.R. Lewis, S. Xia, T. Spelman, P. Hodsman, T.R. Moench, A. Humberstone, J.R.A. Paull, G. Tachedjian, SPL7013 Gel (VivaGel®) retains potent HIV-1 and HSV-2 inhibitory activity following vaginal administration in humans., PLoS One. 6 (2011) e24095. doi:10.1371/journal.pone.0024095.

[19] Inactive Ingredient Search for Approved Drug Products, (n.d.).

[20] S.G. Antimisiaris, S. Mourtas, Recent advances on anti-HIV vaginal delivery systems development, Adv. Drug Deliv. Rev. 92 (2015) 123–145. doi:10.1016/j.addr.2015.03.015.

[21] R. Palmeira-de-Oliveira, A. Palmeira-de-Oliveira, J. Martinez-de-Oliveira, New strategies for local treatment of vaginal infections, Adv. Drug Deliv. Rev. 92 (2015) 105–122. doi:10.1016/j.addr.2015.06.008.

[22] K.J. Zhu, L. Xiangzhou, Y. Shilin, Preparation, characterization, and properties of polylactide (PLA)–poly(ethylene glycol) (PEG) copolymers: A potential drug carrier, J. Appl. Polym. Sci. 39 (1990) 1–9. doi:10.1002/app.1990.070390101.

[23] R. Pecora, ed., Dynamic light scattering - applications of photon correlation spectroscopy, Springer Science & Business Media, 2013. doi:10.1002/bbpc.19870910455.

[24] J.Y. Chang, Y.K. Oh, H. gon Choi, Y.B. Kim, C.K. Kim, Rheological evaluation of thermosensitive and mucoadhesive vaginal gels in physiological conditions, Int. J. Pharm. 241 (2002) 155–163. doi:10.1016/S0378-5173(02)00232-6.

[25] P.B. Deasy, K.J. Quigley, Rheological evaluation of deacetylated gellan gum (Gelrite) for pharmaceutical use, Int. J. Pharm. 73 (1991) 117–123. doi:10.1016/0378-5173(91)90034-L.

[26] R.L. Sweet, New approaches for the treatment of bacterial vaginosis., Am. J. Obstet. Gynecol. 169 (1993) 479–82.

[27] L. Perioli, V. Ambrogi, L. Venezia, C. Pagano, M. Ricci, C. Rossi, Chitosan and a modified chitosan as agents to improve performances of mucoadhesive vaginal gels, Colloids Surfaces B Biointerfaces. 66 (2008) 141–145. doi:10.1016/j.colsurfb.2008.06.005.

[28] T. Mamo, E.A. Moseman, N. Kolishetti, C. Salvador-Morales, J. Shi, D.R. Kuritzkes, R. Langer, U. von Andrian, O.C. Farokhzad, Emerging nanotechnology approaches for HIV/AIDS treatment and prevention, Nanomedicine. 5 (2010) 269–285. doi:10.2217/nnm.10.1.

[29] R. Mallipeddi, L.C. Rohan, Nanoparticle-based vaginal drug delivery systems for HIV prevention, Expert Opin. Drug Deliv. 7 (2010) 37–48. doi:10.1517/17425240903338055.

[30] J. das Neves, M.M. Amiji, M.F. Bahia, B. Sarmento, Nanotechnology-based systems for the treatment and prevention of HIV/AIDS, Adv. Drug Deliv. Rev. 62 (2010) 458–477. doi:10.1016/j.addr.2009.11.017.

[31] S. Yang, Y. Chen, K. Gu, A. Dash, C.L. Sayre, N.M. Davies, E.A. Ho, Novel intravaginal nanomedicine for the targeted delivery of saquinavir to CD4+ immune cells., Int. J. Nanomedicine. 8 (2013) 2847–58. doi:10.2147/IJN.S46958.

SECTION THREE

RHEOLOGICAL STUDIES OF SELECTED HYDROCOLLOIDS

Chapter 9

General introduction

9.1 A general overview on polysaccharides

This third part of the thesis addresses an interesting rheological investigation of selected polysaccharides. Compared to the previous parts, focused on the synthesis of new materials then investigated for their properties, here the attention will be specifically focused on the rheological characterization of natural biopolymers. Rheology plays a central role in both pharmaceutical and food industries. Many products commonly employed, such as toothpaste and food products, display a rheological behaviour. To give an example, toothpaste which lies apparently unmoving on the toothbrush, is squeezed from the tube; similarly mayonnaise, that must break down its structure to flow from the tube and be spread on a sandwich. At this point it becomes clear that a detailed and exhaustive rheological analysis is a precondition required to evaluate the potential application of these materials.

Polysaccharides are versatile biopolymers made-up of different monosaccharide units, widely present in nature with different functions. They can be isolated from renewable sources, such as plants, marine sources and microorganisms. To give some well-known examples, starch and some plant seed polysaccharides such as guar gum and locust bean gum act as storage materials for plants; pectins and agar act as structural components of plants tissues while carrageenans and alginate play a similar role in marine species. As regards the polysaccharides derived from animals, chondroitin sulfate, hyaluronate and other biopolymers, play a fundamental role in physiological fluids and intercellular matrices.

Their attractive properties, which include biocompatibility, biodegradability and good toxicological profile, coupled with relatively low costs, high availability and extraordinary versatility, have contributed to establish their central role in the industrial field.

Their use has been widely exploited over the years for both biomedical, food and cosmetic applications. As regards the biomedical field, a highly investigated application of polysaccharides is in regenerative medicine and tissue engineering, as scaffolds for bone, cartilage and skin regeneration [1] [2]. For this purpose, a large variety of polysaccharides have been studied so far, including alginate, glycosaminoglycans, chitosan and hyaluronic acid. Another revolutionary application of polysaccharides is in the treatment of diabetes diseases. Polysaccharides-based hydrogel have been studied for transplantation of pancreatic islets in the treatment of type 1 diabetes [3].

Moreover, polysaccharides are nowadays the most widely studied polymers for the formulation of conventional or innovative drug delivery systems. An intense research has

been carried out in the field of nasal and ocular delivery, for the development of innovative polysaccharides-based systems [4–6]. Polysaccharides have also been studied for vaginal delivery, exploiting their gelling and bioadhesion properties [7].

Furthermore, polysaccharides have been used in the pharmaceutical field as laxative products, due to their swelling ability. Polysaccharides can act also as suspending agents, emulsifiers and stabilizers in many pharmaceutical formulations. Another interesting application of polysaccharides is as healing agents. Alginate fibers are employed to make surgical dressings. When applied to wounds, calcium ions from the fiber are exchanged with exudates, thus preventing microbial infections [8]. Hyaluronic acid is also widely applied as wound-healing agent [9,10].

Another important application of polysaccharides is in food industry, mainly as thickening and gelling agents to improve quality attributes and shelf-life of foods [11]. Furthermore, polysaccharides have been largely employed in cosmetics and personal care products [12].

The wide range of application is mainly related to their extraordinary structural diversity and versatility. Several monosaccharide units can be incorporated in the polysaccharide chain and different types of inter sugars glycoside linkages can be involved. Another important aspect that needs to be considered when studying polysaccharides is the derivatization of the hydroxyl groups, as they significantly affect the final properties of the polymer.

The molecular structure of polysaccharides has been well defined, despite the natural origin can sometimes represent an obstacle to the physicochemical characterization, especially on the basis of the complexity of the mixture. Polysaccharides possess different levels of structural organization: primary, secondary, tertiary and quaternary structure [13]. The primary structure is represented by the sequence of adjacent monomeric units that form the polymeric chain. The covalent linkages are not completely flexible, thus limiting the chain orientation to only certain shapes, the secondary structure, generally exemplified by helices and ribbons. Interactions between the secondary structured chains of a polysaccharides results in the tertiary structure, which can interact among themselves to give the quaternary structure.

Polysaccharides molecules can be linear, branched or cross-linked. The degree of ramification greatly affects their physicochemical properties, such as solubility, viscosity and gelling behaviour.

9.2 Hydrocolloids as thickening and gelling agents

Hydrocolloids are a heterogeneous group of polysaccharides characterized by their ability to form viscous dispersions and/or gels when dispersed in water. The reason of this behaviour is the large number of hydroxyl groups available in the polymer chain, which increase their affinity for water molecules.

Hydrocolloids have been widely applied in pharmaceutical, food and cosmetic industry due their ability to influence both the flow behaviour and the mechanical properties of the system in which they are employed. This introduces to the discussion of the two main roles of hydrocolloids. They have been extensively studied for their thickening properties, which involves the non-specific entanglement of polymeric chains, and structuring/gelation ability, which arises from the specific inter-chain association in ordered junction zones, also known as cross-linking [14].

Various thickening effects have been observed based on the nature and concentration of the hydrocolloid as well as the pH, temperature and composition of the system where the polymer is used. While most of the hydrocolloids give high viscosities at low concentrations, a few produce low viscosities, even when employed at high concentrations [15].

Besides the most commonly employed starch and xanthan gum, other hydrocolloids have been extensively studied as thickening agents, mainly in cosmetic and food industries. Guar gum and locust bean gum (LBG) are galactomannans widely applied as thickeners. They possess different water solubilities due to the degree of galactomannan substitution [16]. While guar gum, which possesses a higher galactose content than LBG, easily disperse in water, LBG needs to be heated to promote the complete dispersion. Moreover, guar gum is characterized by a higher viscosity than LBG, reasonably due to the higher molecular weight of guar gum [17]. Carboxymethyl cellulose (CMC), acacia gum and tragacanth gum have also been widely applied as thickening agents in food products.

Another important aspect that deserve a more detailed discussion is the ability of polysaccharides to form gels. Gel formation involves the chemical or physical cross-linking of polymer chains that organize themselves in a three-dimensional network able to entrap water in the spaces between the junction zones, i.e. hydrogels. Chemically cross-linked polymeric networks are based on covalent bonds among linear polymer chains. The definition “Physical gels”, introduced by de Gennes in 1979, is used to indicate all that systems non-covalently cross-linked, which are formed by ordered secondary structures, called junction

zones [18]. Hydrophobic interactions such as Van der Waals, dipole-dipole interactions and hydrogen bonds are involved in the gel formation.

Most of physical gels are weak gels. This type of gelation is most commonly observed in biological molecules, such as gelatin and starches.

Several definitions have been proposed to classify a gel over the years, and nowadays, an exhaustive definition is still lacking. A generally accepted definition of gels is: a system constituted by two components, namely a liquid (solvent) and a solid (gelling agent). As reported by Jordan Lloyd "a gel…is easier to recognize than to define" [19]. B. de Jong defined a gel as "a colloidal system of solid particles, interpenetrated by a liquid system" [20]. Later, Flory proposed a definition of gels based on their structural properties [21]. According to this definition, both covalent polymeric networks and physical polymeric networks were classified as gels. From the rheological point of view, a gel is defined as a viscoelastic system with the storage modulus (G') larger than the loss modulus (G") [22].

Several factors have been studied for their influence in the gelation process, in particular polymer structure, including molecular weight and degree of polymerization, polymer concentration, pH, temperature and ion density. In this regard, it is interesting to point out how, by carefully selecting conditions like pH, temperature, and ion concentration, gels with the desired characteristics can be obtained without requiring chemical crosslinking agents. This will reflect in a significantly improved biocompatibility of the final construct.

9.3 Considerations on the rheological behaviour of polysaccharides

The functional role of biopolymers is closely related to their structural organization. Therefore, many efforts have been focused over the years on their characterization, in particular from the physicochemical and rheological point of view. A detailed understanding of their properties plays in fact a crucial role in establishing their potential application for different purposes. Thus, several techniques have been used such as nuclear magnetic resonance, gel permeation chromatography, differential scanning calorimetry, microscopy and rheology. The latter, deserve a special mention, as it is recognized as the most relevant field to be investigated for a detailed characterization of polysaccharides.

In terms of rheological behaviour, hydrocolloids are classified as viscoelastic materials, which display a combination of viscous and elastic properties. Dynamic viscoelastic methods are employed to determine the viscoelastic coefficient. To this end, sinusoidal oscillational strain or stress is applied to the sample, and the induced stress or strain with the same frequency is

detected. Gelation kinetics have been monitored by observing the time dependence of storage and loss moduli of a polysaccharide solution at a constant temperature and frequency.

Different tests can be performed to determine the rheological behaviour of a sample. The most commonly employed rheological tests are: frequency sweep test, oscillation stress sweep test, viscometry test, temperature sweep test, time sweep test, yield stress, and creep/recovery test. In this context, various rheological parameters are generally considered to classify hydrocolloids, in particular, yield stress, shear modulus, storage and loss modulus, viscosity and loss angle.

In the oscillation stress sweep test, the sample is subjected to a range of stresses at a constant frequency (usually 1Hz). This test is performed for the determination of the viscoelastic regime (LVR) of the sample, within which a linear behaviour is observed independently from the shear stress. Measured parameters are the storage or elastic modulus (G'), the viscous or loss modulus (G''), the complex modulus G^* and the phase angle δ ($tg\ \delta = G''/G'$).

In the frequency sweep tests samples are exposed to increasing frequencies at a constant stress comprised in the LVR. This is important to study the viscoelastic behaviour of the sample in a non-disruptive way. This test is considered the "fingerprint" of the material, since it provides information about the energy dissipated by both the elastic and viscous components of the material [23]. Also in this case, the measured parameters are G', G'', G^* and δ. In a typical stress sweep test, the strain increased as the shear stress increased; in this case it increases as the frequency decreases, since low frequencies indicate that the stress is applied for a longer period of time to the sample. When G'> G'' the sample shows a prevalent elastic behaviour. The cross-over of the G' and G'' moduli indicates the relaxation time. A material with a low relaxation time shows a liquid-like behaviour [24,25].

From the frequency sweep test, it is possible to derive the classical definition of a gel. G' and G'' are frequency independent and the value of the phase angle is reduced. Instead, concentrated solutions show a frequency dependence of G' and G'' and δ is variable [26].

On the other hand, this definition holds some limits. In fact, it results difficult to measure G' and G'' at extremely low frequencies and as a consequence, it is not easy to visualize rheological behaviour on a very long-time scale. The well-known saying of the prophetess Deborah ''Even the mountains flow before the Lord'' can interpreted as follows: everything flow if you wait long enough. Therefore, all solid-like substances may flow if we continue to observe them for a very long time.

Chemical gels display higher mechanical resistance than physical gels and they further possess an equilibrium modulus of elasticity [27]. The mechanical breakage of this gel is

caused by the cleavage of the covalent bonds as a consequence of the application of an excessive stress.

On the other hand, physical gels have been classified by Ross-Murphy in "weak" and "strong" networks [27,28]. While both types of physical gels respond as solids at small deformations, the strong gels behave as solids also at large deformation. Conversely, weak gels may flow as liquids when submitted to high enough stress or long time.

Intermediate shear strain sweep measurements are not able to distinguish between strong and weak gels. In fact, when subjected to small deformations, both strong and weak gels present mechanical spectra typical of gels with G'>G''. Moreover, both G' and G'' are independent from the frequency (in the typical range of experimental frequencies 10^{-3} -10^{-2} Hz).

According to the transient network model first proposed by Green and Tobolsky [29] and then further developed by Lodge [30], permanent cross-links are replaced by transient junctions. The concept of transient is that junctions are able to break after a short lifetime to reform elsewhere, hence the system can flow. The total concentration of junctions always remains constant, therefore the elastic properties are constant.

Viscometry test studies the viscosity of materials. It is widely employed for the study of thick dispersions of polysaccharides. Different shear stresses are applied to the sample and shear rate is measured by the rotational rate.

Temperature sweep test measures the rheological behaviour of the sample as function of the temperature.

Time sweep test is used to study changes of the sample on time when predetermined conditions are applied.

Creep test studies the behaviour of a sample over the application of a constant stress for a finite time. The corresponding strain is measured as function of time. A gel, being a viscoelastic material responds to the creep test with nonlinear strain. On the other hand, a recovery test, studies the material behaviour when the shear stress is removed.

Even if it is not possible to establish a specific rule to distinguish strong and weak gels, some general consideration can be done. A strong gel, when subjected to large deformations, loose irreversibly its structure. On the contrary, a weak gel, can recover its initial structure on time [31].

References

[1] E. Alsberg, H.J. Kong, Y. Hirano, M.K. Smith, A. Albeiruti, D.J. Mooney, Regulating Bone Formation *via* Controlled Scaffold Degradation, J. Dent. Res. 82 (2003) 903–908. doi:10.1177/154405910308201111.

[2] N. Boucard, C. Viton, D. Agay, E. Mari, T. Roger, Y. Chancerelle, A. Domard, The use of physical hydrogels of chitosan for skin regeneration following third-degree burns, Biomaterials. 28 (2007) 3478–3488. doi:10.1016/J.BIOMATERIALS.2007.04.021.

[3] S. Schneider, P.J. Feilen, V. Slotty, D. Kampfner, S. Preuss, S. Berger, J. Beyer, R. Pommersheim, Multilayer capsules: a promising microencapsulation system for transplantation of pancreatic islets, Biomaterials. 22 (2001) 1961–1970. doi:10.1016/S0142-9612(00)00380-X.

[4] S. Cao, X. Ren, Q. Zhang, E. Chen, F. Xu, J. Chen, L.-C. Liu, X. Jiang, In situ gel based on gellan gum as new carrier for nasal administration of mometasone furoate, Int. J. Pharm. 365 (2009) 109–115. doi:10.1016/J.IJPHARM.2008.08.042.

[5] U.C. Galgatte, A.B. Kumbhar, P.D. Chaudhari, Development of *in situ* gel for nasal delivery: design, optimization, *in vitro* and *in vivo* evaluation, Drug Deliv. 21 (2014) 62–73. doi:10.3109/10717544.2013.849778.

[6] M. de la Fuente, M. Raviña, P. Paolicelli, A. Sanchez, B. Seijo, M.J. Alonso, Chitosan-based nanostructures: A delivery platform for ocular therapeutics, Adv. Drug Deliv. Rev. 62 (2010) 100–117. doi:10.1016/J.ADDR.2009.11.026.

[7] L.C. Rohan, A.B. Sassi, Vaginal Drug Delivery Systems for HIV Prevention, AAPS J. 11 (2009) 78–87. doi:10.1208/s12248-009-9082-7.

[8] S.E. Barnett, S.J. Varley, The effects of calcium alginate on wound healing., Ann. R. Coll. Surg. Engl. 69 (1987) 153–5.

[9] G. Abatangelo, M. Martelli, P. Vecchia, Healing of hyaluronic acid-enriched wounds: Histological observations, J. Surg. Res. 35 (1983) 410–416. doi:10.1016/0022-4804(83)90030-6.

[10] P.H. Weigel, S.J. Frost, C.T. McGary, R.D. LeBoeuf, The role of hyaluronic acid in inflammation and wound healing., Int. J. Tissue React. 10 (1988) 355–65.

[11] D. Saha, S. Bhattacharya, Hydrocolloids as thickening and gelling agents in food: a critical review., J. Food Sci. Technol. 47 (2010) 587–97. doi:10.1007/s13197-010-0162-6.

[12] P.A. Sandfornd, J. Baird, Industrial Utilization of Polysaccharides, in: The Polysaccharides, Elsevier, 1983: pp. 411–490. doi:10.1016/B978-0-12-065602-8.50012-1.

[13] R. Lapasin, S. Pricl, Rheology of Industrial Polysaccharides: Theory and Applications, Springer US, 1995.

[14] G. Philips, Wedlock David J., P.A. Williams, Molecular origin of hydrocolloids functionality, in: Gums Stab. Food Ind. vol.3, IRL Press, Oxford, 1986: pp. 3–5.

[15] M. Glicksman, Food hydrocolloids, CRC Publ, Boca Raton, Florida, 1982.

[16] M.S. Kök, S.E. Hill, J.R. Mitchell, Viscosity of galactomannans during high temperature processing: influence of degradation and solubilisation, Food Hydrocoll. 13 (1999) 535–542. doi:10.1016/S0268-005X(99)00040-5.

[17] J. Casas, A. Mohedano, F. Garcia-Ochoa, Viscosity of guar gum and xanthan/guar gum mixture solutions, J. Sci. Food Agric. 80 (2000) 1722–1727. doi:10.1002/1097-0010(20000915)80:12<1722::AID-JSFA708>3.0.CO;2-X.

[18] P.-G. de. Gennes, Scaling concepts in polymer physics, Cornell University Press, 1979.

[19] D.J. Lloyd, The problem of gel structure, J. Alexander Chemical Catalogue Company, New York, USA, 1926.

[20] B. de Jong H.G., A survey of the study objects in this volume, in: Colloid Sci. Vol. 2, Elsevier Publishing Company, Inc., Amsterdam, The Netherlands, 1949: pp. 1–18.

[21] P.J. Flory, Introductionary lecture. Disc Faraday Soc., (1974) 7–18.

[22] J. de Vries, G.O. Phillips, J. de Vries, Hydrocolloid gelling agents and their applications, in: Gums Stabilisers Food Ind. 12, 2004: pp. 23–31. doi:10.1039/9781847551214-00023.

[23] Stress Tech User's Manual, (n.d.).

[24] D.S. Jones, A.D. Woolfson, A.F. Brown, Textural, viscoelastic and mucoadhesive properties of pharmaceutical gels composed of cellulose polymers, Int. J. Pharm. 151 (1997) 223–233. doi:10.1016/S0378-5173(97)04904-1.

[25] T.H. Shellhammer, T.R. Rumsey, J.M. Krochta, Viscoelastic properties of edible lipids, J. Food Eng. 33 (1997) 305–320. doi:10.1016/S0260-8774(97)00030-7.

[26] J. Carlfors, K. Edsman, R. Petersson, K. Jörnving, Rheological evaluation of Gelrite® in situ gels for ophthalmic use, Eur. J. Pharm. Sci. 6 (1998) 113–119. doi:10.1016/S0928-0987(97)00074-2.

[27] G.M. Kavanagh, S.B. Ross-Murphy, Rheological characterisation of polymer gels, Prog. Polym. Sci. 23 (1998) 533–562. doi:10.1016/S0079-6700(97)00047-6.

[28] S.B. Ross-Murphy, Physical gelation of synthetic and biological macromolecules, in: E. De Rossi, D., Kajiwara, K., Osada, Y., and Yamauchi, A. (Ed.), Polym. Gels Fundam. Biomed. Appl., Plenum Press, New York, 1991: pp. 21–39.

[29] M.S. Green, A. V. Tobolsky, A New Approach to the Theory of Relaxing Polymeric Media, J. Chem. Phys. 14 (1946) 80–92. doi:10.1063/1.1724109.

[30] A.S. Lodge, A network theory of flow birefringence and stress in concentrated polymer solutions, Trans. Faraday Soc. 52 (1956) 120. doi:10.1039/tf9565200120.

[31] S.B. Ross-Murphy, Structure–property relationships in food biopolymer gels and solutions, J. Rheol. (N. Y. N. Y). 39 (1995) 1451–1463. doi:10.1122/1.550610.

Chapter 10

Rheological properties of selected polysaccharide gums as function of concentration, pH and temperature

Manuscript in preparation

10.1 Introduction

Polysaccharides have been intensively investigated in several industrial fields due to their attractive properties including biocompatibility, biodegradability, low cost and abundance in nature. They are derived from natural and renewable sources, mainly from plants, but also from microorganisms and animals, where they act as exudates, storage materials, cell wall or extracellular components [1]. Their physicochemical properties, that contribute to define the field of application, have been referred to the type of monosaccharide units and relative bonds involved, degree of polymerization, backbone substitutions and chain conformation.

Almost all the polysaccharides can absorb a large amount of water with a consequent swelling. In addition, those with high water solubility are characterized by the ability of giving viscous systems or gels when dispersed in aqueous media. Due to these characteristics, along with their high molecular weight that is responsible for their spatial conformations and interactions, they have been widely employed in both food, pharmaceutical and cosmetic industries, as thickeners, texture modifiers, emulsifiers, stabilisers and gelling agents [2–6]. In fact, they are able to modify the rheology of the formulated system, influencing the flow behaviour as well as the mechanical properties. For this purpose, an extensive and detailed characterization in terms of rheological properties has been required, in order to provide exhaustive information for industrial applications. It is generally recognized that polysaccharides are able to generate real gels, forming a three-dimensional network through physical or chemical cross-linking, as a function of their concentration, environmental conditions and presence of additive. Those requiring high concentration to build-up viscosity, as xanthan gum, guar gum, locust bean gum, arabic gum and starch are commonly defined thickening agents, while gellan, agar, pectin and carrageenan are generally recognized has gelling agents. Moreover, a synergistic effect has been reported from the blending of non-gelling hydrocolloids, resulting in more viscous systems [7–9].

While many researches have been conducted so far regarding the gelling properties of hydrocolloids, a limited literature is available about the influence of different environmental parameters such as pH and temperature on the final mechanical properties of the systems. Choppe et al. studied the rheological behaviour of xanthan gum solutions as function of concentration, temperature and ionic strength, while Horinaka et al. reported the effect of pH on gellan gum solutions [10,11].The influence of divalent cations on the mechanical properties of the anionic polysaccharide gellan gum, has also been studied by Thang et al.,

while Norton and colleagues showed the influence of pH on the gelation of gellan gum, discussing the influence of acidic environment to prolonged exposure [12,13].

The influence of the above-mentioned parameters would be useful for industrial manufacturers in selecting the polysaccharide with the desired mechanical properties, to be employed as additive in pharmaceutical, nutraceutical and cosmetic formulations. Moreover, these results are necessary to complete the large amount of information available in the literature concerning the rheological properties of these compounds.

The objective of the present work is a systematic investigation of the influence of pH, concentration and temperature on the rheological properties of water dispersions prepared with selected polysaccharides. Glucomannan, xanthan gum, tara gum, guar gum, konjac gum and gellan gum have been chosen among the most common thickening agents derived from plants and available with an organic certification, and the mechanical spectra of their water dispersions have been compared, with the aim of providing an extensive and comprehensive overview in terms of rheological properties.

10.2 Material and methods

10.2.1 Materials

The gums studied have been supplied by their respective manufacturers. Glucomannan (CEROKON Konjac Gum CKAA 1220 SO2), tara gum (Cerota Tara gum Type 5000), guar gum (CERAMEHL Guar Gum Type 166) and gellan gum (CEROGA Gellan 700 low acyl) and konjac gum (Idealblend KJ-MV GommaKonjac) were supplied by C.E. Roeper GmbH (Hamburg); xanthan gum (Ziboxan® F200-Xanthan Gum Food Grade) was obtained from Deosen Corporation Ltd (China).

The salts sodium chloride, sodium hydroxide, potassium dihydrogen phosphate, sodium acetate and hydrochloric acid and glacial acetic acid used for the buffers preparation were of analytical grade, purchased from Carlo Erba reagents.

10.2.2 Samples preparation

Acid solution at pH 1.2 (AS) with hydrocloridic acid and sodium chloride, acetate buffer at pH 5.5 (ABS) and phosphate buffer at pH 6.8 (PBS), were used as dispersing media. Samples were prepared at different concentrations based on the type of polysaccharide (from 0.5% to 1.5% w/w) by continuously dispersing the desired amounts of the dry powder in the selected buffer under constant stirring, until complete dispersion. Glucomannan, xanthan gum, tara

gum, guar gum and konjac gum samples were prepared at room temperature while gellan gum samples required heating (80°C) for a complete powder dispersion and then a gradual cooling of the hot solution for the gelation. Each dispersion was prepared and analysed in triplicate. In order to promote the complete hydration of the polymer, the prepared samples were stored overnight at 4°C and the pH was measured at ambient temperature prior the rheological characterization.

Table 1. Prepared samples

Polysaccharides	Acid solution (pH 1.2) (% w/w)		ACB (pH 5.5) (% w/w)		PBS (pH 6.8) (% w/w)	
Glucomannan	0.5	1.5	0.5	1.5	0.5	1.5
Xanthan gum	0.5	1.5	0.5	1.5	0.5	1.5
Tara gum	0.5	1.5	0.5	1.5	0.5	1.5
Guar gum	0.5	1.5	0.5	1.5	0.5	1.5
Konjac gum	1	1.5	1	1.5	1	1.5
Gellan gum	0.5	1.5	0.5	1.5	0.5	1.5

10.2.3 Rheological characterization

Rheological analyses were performed using a stress controlled rheometer (Stress Tech Rheologica Instruments, Lund, Sweden), equipped with a cone-plate (C 40/4) or a parallel-plate (P 20) geometries with radial grooves, based on the sample analysed, operating in the oscillation mode. More specifically P 20 geometry was used for the analysis of gellan gum samples in order to reduce the slippage phenomena related to the gel structure.

The analysis of flow behaviour was performed on 0.5% (w/w) samples at 37°C by increasing the shear stress from 0.1 to 10 Pa and then measuring the corresponding shear rate (*Viscometry test).* The flow curves were then modelled with the "Power-law" equation:

$$\sigma = K\gamma^n$$

where σ: shear stress, K: consistency index, γ: shear rate, n: power law index.

The Power law equation enables the analysis of the shearing properties of Newtonian and non-Newtonian fluids giving a unique value of viscosity (the K value) for each system. For *n* values equal to 1 a typical Newtonian behaviour is expected, while for shear thickening (dilatant) fluids $n>1$, and for shear thinning (pseudo-plastic) $n< 1$, with the viscosity resulting shear dependent.

All the samples were analysed also using oscillation tests to evaluate their viscoelastic properties. The following tests were performed:

• *Oscillation stress sweep*: samples were subjected to increasing stresses in the range 0.5-20 Pa at a constant frequency (1Hz). This test was performed for the determination of the linear viscoelastic regime (LVR) of the sample and consequently the choice of the stress value to use in all the other oscillation tests (1 Pa was chosen as stress value for glucomannan, xanthan gum, tara gum, guar gum and konjac gum while 10 Pa for gellan gum). All measurements were carried out at 25°C and 37°C.

• *Frequency sweep*: samples were exposed to increasing frequencies in the range 0.01-10 Hz at a constant stress (1 Pa or 10 Pa based on the results of the oscillation stress sweep above reported). All measurements were carried out at 25°C and 37°C. Then, selected samples were exposed to a continuous frequency increase (0.01-10 Hz) at a constant stress (1 Pa) in a range of temperature (5°-45°C). In this case each frequency sweep was preceded by a time sweep (1Pa,1Hz) with the aim to stabilize the sample at the tested temperature before the frequencies scan.

• *Temperature sweep*: samples were analysed in the temperature range 5°-50°C (heating rate 1°C/min) at a constant frequency (1Hz) and stress (1 Pa or 10 Pa).

10.3 Results

The objective of the present work was to compare the rheological behaviour of selected hydrocolloids dispersions in function of concentration, pH and temperature.

Storage modulus (G') and loss modulus (G'') were constantly monitored and used to describe the mechanical properties of the system. Stress sweep and frequency sweep tests performed at 25°C and 37°C showed comparable results. Thus, samples monitored at 25°C have been chosen as representative model for discussion and are analysed in the following section.

All the samples were preliminary analysed using stress sweep tests to determine the LVR. An example of the traces recorded at 25°C for xathan gum and glucomannan samples at different pH and concentrations is reported in Fig. 1. As expected, the LVR is dependent on the concentration of the system, other than on the nature of the polysaccharide. The temperature and the dispersion media had an almost negligible effect on the wideness of LVR.

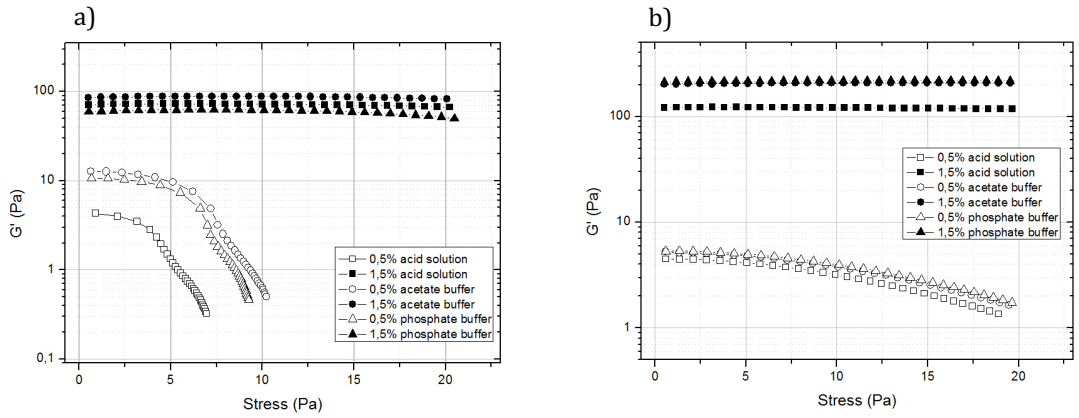

Fig. 1. Stress sweep traces of Xanthan gum (a) and glucomannan (b) dispersions at different concentration and pH values (25°C).

A more detailed characterization of the sample behaviour was performed analysing the change of the rheological parameters as a function of the oscillation frequency. Fig. 2 shows some representative frequency sweep traces for selected hydrocolloids prepared in different media at 1.5% (w/w). It is possible to identify two general rheological behaviours: glucomannan, tara gum, guar gum and konjac gum samples at 25°C showed a clear G' and G'' frequency dependence, with a typical liquid behaviour at low frequencies (G'' higher than G') and a crossover at high frequencies. Conversely, xanthan gum samples showed G' modulus higher than G'', over the whole range of applied frequencies. Samples prepared at the lowest concentration (0.5% w/w) demonstrated a similar trend of G' and G'', but lower values of both moduli were registered, thus indicating the influence of the concentration on the final rheological properties of the system.

Most of the gums were only slightly affected by the pH; however, gellan and konjac gums were characterized by a lower consistency at acid pH, especially at lower concentrations.

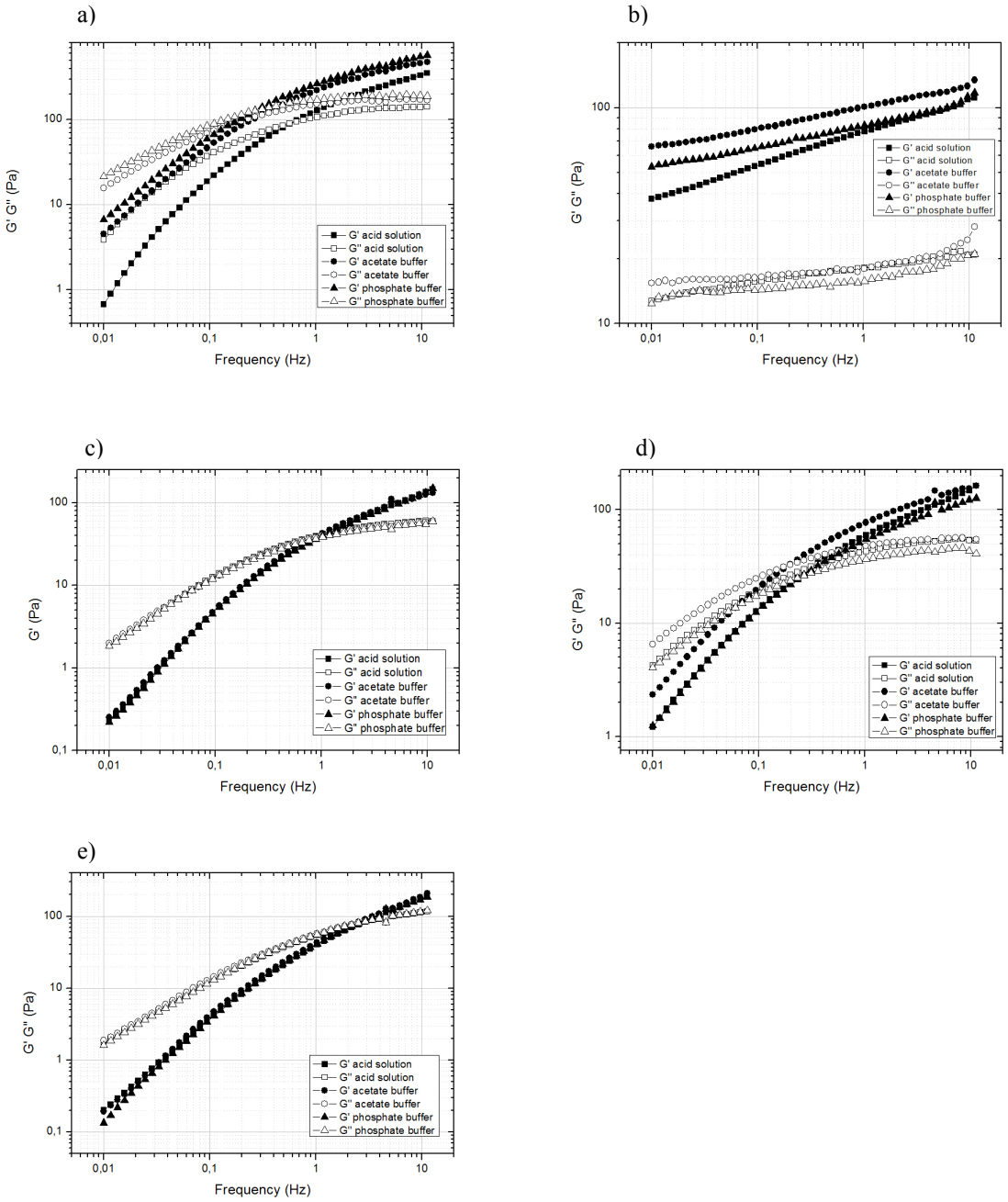

Fig. 2. Frequency sweep of glucomannan (a), xanthan gum (b), tara gum (c), guar gum (d), and konjac gum (e) at 1.5% (w/w) in different buffers.

The flow behaviour of samples prepared at 0.5% w/w was also investigated. The flow curves of tara gum in PBS and guar gum in AS obtained through viscometry test are reported in Fig. 3. A typical shear thinning behaviour was observed, with a viscosity of 0.37 and 0.12 Pa*s and a *n* value equal to 0.69 and 0.8. These values have been calculated by the power law equation.

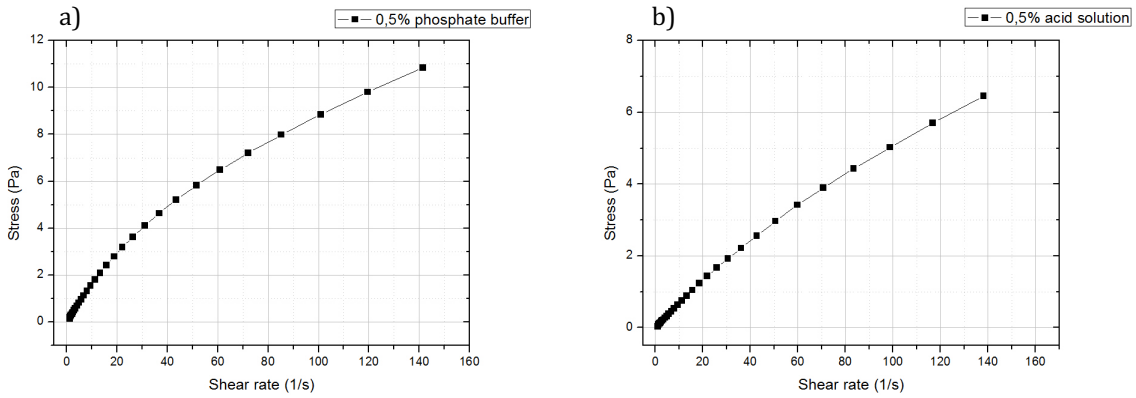

Fig. 3. Viscometry test of Tara(a) and Guar Gum (b) in PBS and AS respectively, at 0.5% (w/w).

Gellan gum samples deserve a special mention being highly influenced by pH and concentrations. In fact, samples prepared at pH 1.2 were not stable and therefore were not analysed. A conspicuous literature is reported about the acid gelation of gellan gum and its stability over a wide range of pH; however higher pH values have been usually employed when operating in acid conditions, in contrast with the strong pH used in the present work [11,14]. Moritaka et al. studied the effect of pH and electrolytes on the rheological properties of gellan gum samples. They reported that at pH 2, all samples became turbid with a phase separation and were not used [15]. In addition, Norton et al. showed that acid gels of gellan gum produced at pH 2 were weaker and not structured as the ones obtained at pH 4 and 5 [13]. This finding seems to be in agreement with our results. In fact, as the pH drops below certain values, also the capacity to form a stable gel decreases.

Moreover, gellan gum samples in PBS and ABS were analysed with a P20 geometry instead of the classical C 40/ 4, with the exception of the 0.5% sample in ABS, to avoid the wall slippage phenomena related to the highly organized structure.

Based on the results obtained from this initial screening, different samples were selected as the most promising for further investigations. Namely glucomannan, xanthan gum, tara gum and guar gum samples prepared in PBS at the concentration of 1.5% (w/w) were studied by temperature sweep and multi frequency tests, in order to deeply understand their rheological behaviour as function of temperature and frequency.

Temperature sweep, performed in the temperature range 5°C to 50°C, showed a strict dependence of the storage modulus G' of glucomannan and tara gum from the temperature. The decrease of these values demonstrates a deconstruction of the systems due to the heating.

On the contrary, the temperature did not influence the G' modulus of xanthan gum, while a slight decrease of the G' value of guar gum was observed (Fig. 4).

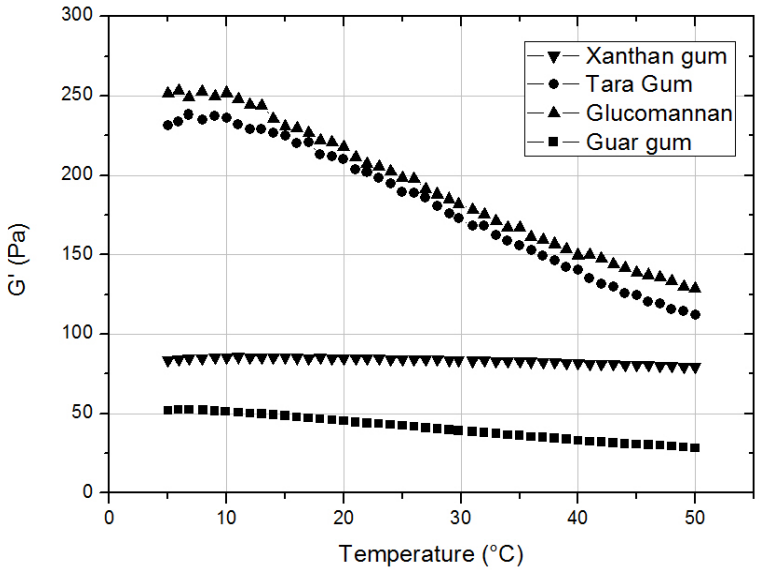

Fig. 4. Temperature sweep of the selected hydrocolloids samples in PBS at 1.5% w/w.

Multifrequency sweep of glucomannan, guar gum and tara gum samples performed at different temperatures showed a clear frequency dependence of G' and G'', with crossover shifted to higher frequencies as the temperature increases. On the other hand, xanthan gum samples showed a typical gel-like behaviour with G'>G''and a slight dependence of the storage modulus G' upon frequency over the whole range (Fig. 5).

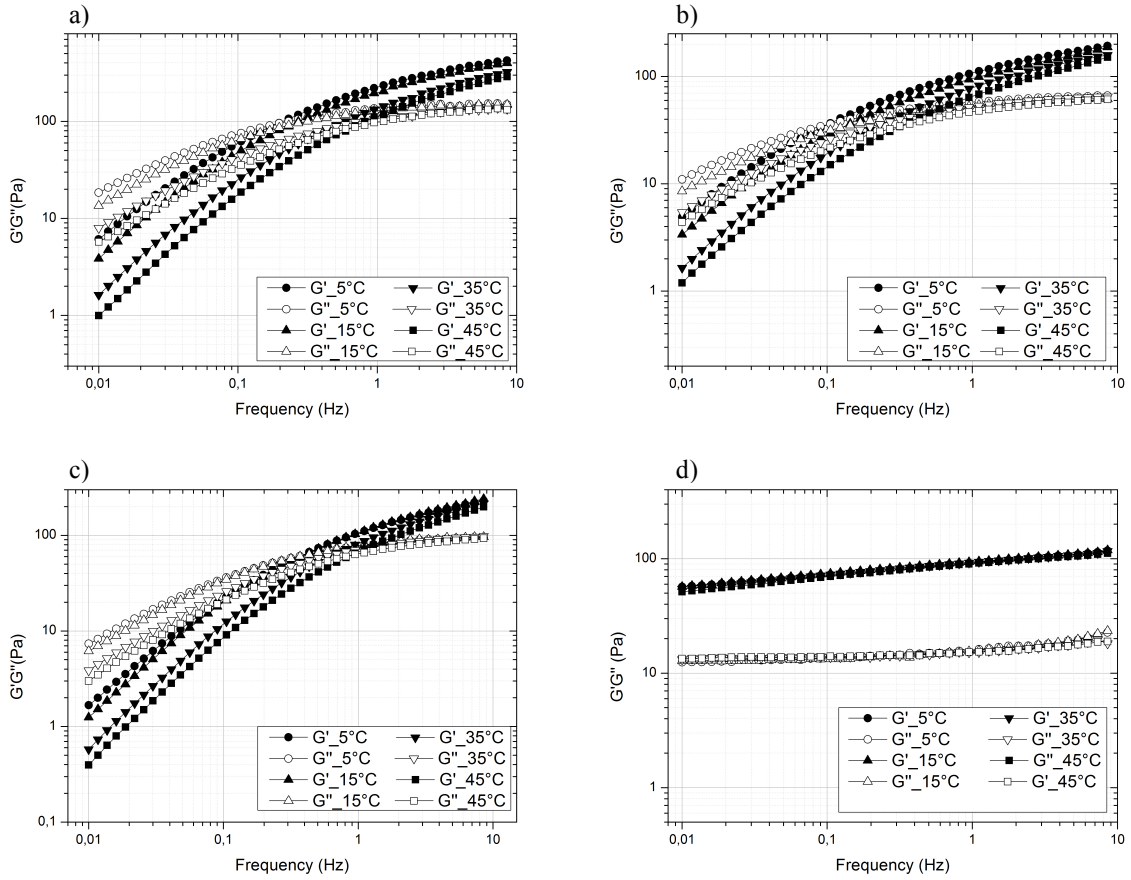

Fig. 5. Frequency sweep traces of (a) glucomannan, (b) guar gum, (c) tara gum and (d) xanthan gum (in PBS at 1.5% w/w) at different temperatures.

10.4 Discussion

The work described in this chapter was focused on the rheological characterization of polysaccharides derived from different natural sources, without any chemical modification. Physicochemical properties of polysaccharides are closely related to their chemical structure, carbohydrate units, type of glycosidic linkage, backbone composition and branching and chain conformation. Molecular weight is also an important factor governing the applicability of polymers. However, the molecular weight of the different polysaccharides has not considered in this work. On the other hand, it is interesting to correlate the rheological behaviour of the analysed polysaccharides with their chemical composition, molecular structure and functional properties.

Polysaccharides are widely employed in food, pharmaceutical and cosmetic industries as thickening and gelling agents [16]. Saha and Bhattacharya reviewed the use of hydrocolloids as food excipients, providing an exhaustive description of their properties and possible

applications. The authors extensively discussed the differences between thickening and gelling agents, focusing on the specific interactions between polymer chains [6]. While thickening agents involves physical entanglement of polymer chains, the gelling process is governed by the formation of junction zones through hydrogen bonds and hydrophobic interactions [17,18]. Gels systems, according to the most common definition, is a system characterized by a storage modulus G' higher than the loss modulus G'' [19].

Xanthan gum is a branched polysaccharide, characterized by a high molecular weight. It consists of a backbone chain of β linked D-glucose units with a trisaccharide side-chain of β-D-mannose-1,4-D-glucuronic acid-1,2-α-D-mannose, on alternating glucose units. The secondary structure of xanthan gum has been demonstrated to consist of 5-fold helical structure [20]. The extraordinary stability of xanthan gum over a wide range of temperature and pH has been attributed to its ordered conformational structure, where hydrogen bonds play a crucial role in maintaining the structure [21].

Data obtained from xanthan gum at the highest concentration (1.5% w/w) showed G' values higher than G'' over the whole range of applied frequencies regardless pH and temperature. These findings can be explained with the theory reported by Lim et al. and later by Choppe et al., according to which a transient network is formed through hydrogen bonds with a finite lifetime [22][10].

Gellan gum is a linear anionic polysaccharide consisting of β-D-glucose, β-D glucuronic acid, β-D-glucose and α-L-rhamnose repeating units, with a carboxyl side group. Two acyl substituents in position O(2) and O(6) are present on the glucose unit. Deacylation of gellan gum gives low acyl gellan gum, which give weaker gels compare to the high acyl gellan.

Low acyl gellan gum samples studied in this work, showed a typical gel behaviour, with a physical gelation occurring as the temperature is decreased after an initial heating. According to Miyoshi and Matricardi et al., ordered junction zones are formed in between double helices giving a thermo-reversible hydrogel [23,24]. Gellan gum samples were highly influenced by pH and concentration, demonstrating a typical gel-like behaviour at both concentrations. Although many studies reported the acid gelation of gellan gum describing its stability in a wide range of pH, acid gelation of gellan gum was not achieved in this study and this can be due to the strong conditions (pH 1.2), as described above.

Galactomannans are neutral polysaccharides which consist mainly of a high molecular weight hydrocolloids, composed of galactose and mannose units combined through glycosidic linkages. Galactomannans exist in dilute solutions as random-coils, associating each other

through hyperentanglements, as reported by Morris et al.[25]. Tara and guar gums with a mannose to galactose ratio 3:1 and 2:1 respectively, have been studied in the present work showing a typical pseudogel behaviour. The shear thinning behaviour demonstrated by viscometry test, has been then ascribed to the disruption of the polymeric interaction during shear. Wu et al. reported the rheological characterization of tara gum solutions showing a pseudoplastic behaviour without thixotropy. Mechanical spectra showed the typical viscoelastic behaviour of a macromolecular solution; in fact, tara gum solutions demonstrated viscous properties at low frequencies and acted more like a gel at high frequencies, while the pH did not affect the rheological properties [26]. Guar gum solutions exhibited a predominant viscous modulus at low frequencies, while storage modulus was predominant at high frequencies, as confirmed by previous investigations [27,28]. G' and G'' moduli were slightly influenced by pH with lower values registered for acid pH; the same behaviour was observed for glucomannan.

Konjac gum samples, which showed a crossover of G' and G'' moduli at high frequencies. Similarly to tara gum, pH did not influence the rheological properties.

10.5 Conclusions

Concentration, pH and temperature can significantly influence polysaccharide performance. In the present research two different concentrations, three different pH and two different temperatures have been considered.

Based on the information available in literature on the influence of polysaccharides concentration on the final rheological properties of the system, two different concentrations have been selected for samples preparation. The influence of pH has been investigated using three different pH conditions: acid (1.2), acetate buffer (pH 5.5) and phosphate buffer (pH 6.8). The reason for that was to mimic different body districts, namely stomach and intestine, to evaluate the potential influence of pH on the final rheological properties of the analysed polysaccharides. The mechanical spectra were recorded at two different temperatures, namely 25°C and 37°C, to reproduce room temperature and body temperature respectively, which need to be studied when evaluating the stability of a formulation.

The detailed screening reported in this work is really important as it provides both scientists and manufacturers with precious information about the applicability of the analysed polysaccharides in pharmaceutical as well as food formulations.

Results demonstrate a clear dependence of the rheological properties of the studied systems in

function of polymer concentration, with more concentrated samples showing improved rheological properties. The influence of pH on the hydrocolloids formulations has also been investigated. In general, it has been observed that most of the polysaccharides dispersions were less stable in acid conditions. This is evident from the values of the storage modulus G' and the loss modulus G'', which are generally lower for samples prepared in acid media. Conversely, temperature was not a critical parameter.

Glucomannan, xanthan gum, tara gum and guar gum samples prepared at 1.5% w/w in PBS (pH 6.8) have been finally selected as the most promising systems due to their favourable characteristics. Future studies will evaluate the synergistic effect of various polysaccharides mixtures on the rheological properties.

In conclusion, data collected from this study provide a useful tool for manufacturers operating in food and pharmaceutical fields, to select the hydrocolloid with the desired characteristics.

References

[1] M. Izydorczyk, W.Q. Cui, Q. Wang, Polysaccharide gums: structures, functional properties, and applications, FL: Taylor & Francis, 2005.

[2] A.M. Stephen, Food polysaccharides and their applications, second, CRC press, 1995.

[3] S.T. Osmałek, T., A. Froelich, Application of gellan gum in pharmacy and medicine, Int. J. Pharm. 466 (2014) 328–340. doi:10.1016/J.IJPHARM.2014.03.038.

[4] E.I. Yaseen, T.J. Herald, F.M. Aramouni, S. Alavi, Rheological properties of selected gum solutions, Food Res. Int. 38 (2005) 111–119. doi:10.1016/j.foodres.2004.01.013.

[5] K. Nishinari, H. Zhang, S. Ikeda, Hydrocolloid gels of polysaccharides and proteins, Curr. Opin. Colloid Interface Sci. 5 (2000) 195–201. doi:10.1016/S1359-0294(00)00053-4.

[6] D. Saha, S. Bhattacharya, Hydrocolloids as thickening and gelling agents in food: a critical review, J. Food Sci. Technol. 47 (2010) 587–597. doi:10.1007/s13197-010-0162-6.

[7] C. Schorsch, C. Garnier, J.-L. Doublier, Viscoelastic properties of xanthangalactomannan mixtures: comparison of guar gum with locust bean gum, Carbohydr. Polym. 34 (1997) 165–175. doi:10.1016/S0144-8617(97)00095-7.

[8] M. Tako, A. Asato, S. Nakumura, Rheological Aspects of the Intermolecular Interaction between Xanthan and Locust Bean Gum in Aqueous Media, Agric. Biol. Chem. 48 (1984) 2995–3000. doi:10.1271/bbb1961.48.2995.

[9] I.C.M. Dea, E.R. Morris, D.A. Rees, E.J. Welsh, H.A. Barnes, J. Price, Associations of like and unlike polysaccharides: Mechanism and specificity in galactomannans, interacting bacterial polysaccharides, and related systems, Carbohydr. Res. 57 (1977) 249–272. doi:10.1016/S0008-6215(00)81935-7.

[10] E. Choppe, F. Puaud, T. Nicolai, L. Benyahia, Rheology of xanthan solutions as a function of temperature, concentration and ionic strength, Carbohydr. Polym. 82 (2010) 1228–1235. doi:10.1016/j.carbpol.2010.06.056.

[11] J.I. Horinaka, K. Kani, Y. Hori, S. Maeda, Effect of pH on the conformation of gellan chains in aqueous systems, Biophys. Chem. 111 (2004) 223–227. doi:10.1016/j.bpc.2004.06.003.

[12] J. Tang, M.A. Tung, Y. Zeng, Mechanical properties of gellan gels in relation to divalent cations, J. Food Sci. 60 (1995) 748–752.

[13] A.B. Norton, P.W. Cox, F. Spyropoulos, Acid gelation of low acyl gellan gum relevant to self-structuring in the human stomach, Food Hydrocoll. 25 (2011) 1105–1111. doi:10.1016/j.foodhyd.2010.10.007.

[14] F. Yamamoto, R.L. Cunha, Acid gelation of gellan: Effect of final pH and heat treatment conditions, Carbohydr. Polym. 68 (2007) 517–527. doi:10.1016/j.carbpol.2006.11.009.

[15] H. Moritaka, K. Nishinari, M. Taki, H. Fukuba, Effects of pH, potassium chloride, and sodium chloride on the thermal and rheological properties of gellan gum gels, J. Agric. Food Chem. 43 (1995) 1685–1689.

[16] B. Katzbauer, Properties and applications of xanthan gum, Polym. Degrad. Stab. 59 (1998) 81–84. doi:10.1016/S0141-3910(97)00180-8.

[17] G.O. Phillips, Wedlock David J., P.A. Williams, Molecular origin of hydrocolloid functionality., in: G.O. Phillips, D.J. Wedlock, P.A. Williams (Eds.), Gums Stab. Food Ind. vol.3, IRL Press, Oxford, 1986: pp. 3–5.

[18] G.O. Phillips, P.A. Williams, eds., Introduction to food hydrocolloids, in: Handb. Hydrocoll., Woodhead Publ Ltd, New York, 2000: pp. 1–19.

[19] J. de Vries, Hydrocolloids gelling agents and their applications. In: Gums nd stabilizers for the food industry, in: P.A. Williams, P. G.O. (Eds.), RSC Publ, Oxford, 2004: pp. 22–30.

[20] R. Moorhouse, M.D. Walkinshaw, S. Arnott, Xanthan Gum—Molecular Conformation and Interactions, in: 1977: pp. 90–102. doi:10.1021/bk-1977-0045.ch007.

[21] B. Katzbauer, Properties and applications of xanthan gum, Polym. Degrad. Stab. 59 (1998) 81–84. doi:10.1016/S0141-3910(97)00180-8.

[22] T. Lim, J.T. Uhl, R.K. Prud'homme, Rheology of Self-Associating Concentrated Xanthan Solutions, J. Rheol. (N. Y. N. Y). 28 (1984) 367–379. doi:10.1122/1.549757.

[23] E. Miyoshi, Rheological and thermal studies of gel-sol transition in gellan gum aqueous solutions, Carbohydr. Polym. 30 (1996) 109–119. doi:10.1016/S0144-8617(96)00093-8.

[24] P. Matricardi, C. Cencetti, R. Ria, F. Alhaique, T. Coviello, Preparation and Characterization of Novel Gellan Gum Hydrogels Suitable for Modified Drug Release, Mol. . 14 (2009). doi:10.3390/molecules14093376.

[25] E.R. Morris, A.N. Cutler, S.B. Ross-Murphy, D.A. Rees, J. Price, Concentration and shear rate dependence of viscosity in random coil polysaccharide solutions, Carbohydr. Polym. 1 (1981) 5–21. doi:10.1016/0144-8617(81)90011-4.

[26] Y. Wu, W. Ding, L. Jia, Q. He, The rheological properties of tara gum (Caesalpinia spinosa), Food Chem. 168 (2015) 366–371. doi:10.1016/j.foodchem.2014.07.083.

[27] M. Hussain, S. Bakalis, O. Gouseti, T. Zahoor, F.M. Anjum, M. Shahid, Dynamic and shear stress rheological properties of guar galactomannans and its hydrolyzed derivatives, Int. J. Biol. Macromol. 72 (2015) 687–691. doi:10.1016/j.ijbiomac.2014.09.019.

[28] M. Oblonšek, S. Šostar-Turk, R. Lapasin, Rheological studies of concentrated guar gum, Rheol. Acta. 42 (2003) 491–499. doi:10.1007/s00397-003-0304-0.

Chapter 11

Conclusion and Perspectives

11.1 Conclusion and Perspectives

The work described in this thesis was focused on the synthesis, physicochemical characterization and biological evaluation of different materials for potential pharmaceutical applications. The thesis has been organized in three different parts, each of them referred to a specific research activity. The projects reported in each part, although independent of one another, are all related to a common theme, namely the study of specific materials for pharmaceutical drug delivery technologies.

A significant part of the work has been dedicated to the study of innovative surfactants, in particular sugar esters and biosurfactants produced by *Lactobacilli,* as attractive alternatives to the currently employed petroleum-based surfactants.

Surfactants are amphiphilic molecules widely applied in technological applications and industrial processes. Due to the environmental concerns derived from their massive use, recent research has been focused on the investigation of innovative biocompatible and biodegradable surfactants.

Natural surfactants have been recently proposed as promising candidates, being recognized as non-toxic and environmentally friendly compounds. They can be synthesized from renewable natural products and are generally characterized by a high biocompatibility and biodegradability. Among them, sugar-based derivatives are a broad class of non-ionic surfactants consisting of sugars as polar head groups and fatty acids or alcohols as hydrophobic tails. Their versatility and the increasing interest they are gaining in the scientific area, have mainly to be referred to their chemical structure, suitable for wide a range of modifications. As a result, physicochemical and biological properties of these compounds can be tailored by varying the polarity of the hydrophilic group and the length and degree of saturation of the hydrocarbon chain. A systematic investigation of the structure-activity relationship, which has rarely been conducted in the past, appears valuable for achieving a successfully rational design to select and combine suitable compounds for further developments and applications.

The aim of the project was to design a library of enzymatically synthesized lactose monoesters, that were then systematically investigated, through a multidisciplinary approach, for their physicochemical and biological properties.

Despite the conspicuous evidences derived from literature about the potential pharmaceutical application of sugar surfactants, a limited number of studies have been conducted on lactose-based surfactants.

Chapter 2 focuses on the investigation of two innovative lactose monoesters derivatives based on unsaturated fatty acids. Palmitoleic acid (C16:1 ω7) and nervonic acid (C24:1 ω 9) were selected as long-chain fatty acids and reacted with lactose. Lactose palmitoleate and nervonate were then investigated for their biological properties. The toxicological profile was evaluated *in vitro* on Caco-2 cells. The compounds were also studied as absorption enhancer agents through Transepithelial Electrical Resistance (TEER) measurements and permeability studies by using ovalbumin (OVA) as model protein of ~45 kDa. Permeability studies are extremely significant in the context of non-invasive delivery of biotherapeutics, such as proteins and peptides, as well as vaccine delivery. Significantly, a permeability enhancement ratio of 11.5 was achieved with lactose palmitoleate.

Lactose palmitoleate and lactose nervonate were also tested for their antimicrobial activity against various food-borne pathogens, by determining the minimum inhibitory concentration (MIC). MICs values of both compounds ranged from 64 to 128 µg/ml, thus highlighting a greater antibacterial activity compared to parabens, with MIC values > 1024 µg/ml.

These results are really promising and encourage further investigations in order to fully understand their mechanism of action and establish a potential application as food preservative.

Based on the results obtained with lactose palmitoelate and nervonate, oleic acid was then selected in **chapter 3** to expand the library of unsaturated fatty acid lactose derivatives. Oleic acid was chosen as unsaturated fatty acid for several reasons, including its intermediate acyl chain length (C18:1 ω 9) in between the previously investigated palmitoleic and nervonic acids and its absorption enhancing properties. The obtained lactose oleate was extensively characterized for its physicochemical properties. Further experiments were performed to evaluate its biocompatibility *in vitro*, and antimicrobial activity. Its applicability as absorption enhancing agent was also evaluated by TEER measurements and permeability studies on Caco-2 cell monolayers, by using dextran 4kDa as model for macromolecular drugs. The results obtained from both TEER and permeability studies demonstrated a concentration-dependent absorption enhancing effect, with increased permeability at the highest tested surfactant concentrations.

Chapter 4 was dedicated to the series of saturated lactose monoesters derivatives. Decanoic (C10), lauric (C12), myristic (C14) and palmitic (C16) acids have been selected as medium and long chain fatty acids and reacted with lactose using Lipozyme® as catalyst. The synthesized lactose monoesters were then investigated for their physicochemical properties

and toxicological profile in order to establish a correlation with the hydrocarbon chain length. The cytotoxicity profile was assessed by MTT and LDH assay on Calu-3 cell lines as model for the airway epithelium. Moreover, TEER experiments were also performed to evaluate their absorption enhancing properties.

Overall, this research demonstrated the potential application of lactose monoesters derivatives as absorption enhancers and antimicrobial agents.

Moreover, results obtained from the systematic investigation of the designed library of lactose esters highlight the close relationship between the chemical structure and the biological activity of the tested compounds. These findings are really promising, leading future research to the investigation of different sugars as polar head groups, with the final aim of evaluating also the influence of the carbohydrate moiety on the final properties of the sugar surfactants while keeping unchanged the fatty acid chain length.

Another important aspect that needs to be considered in the future is the comparison with commercially available sugar surfactants, to further investigate the potential benefits with respects to the traditional surfactants.

Finally, besides the in-depth characterization of sugar surfactants for their biological properties, their application in drug delivery systems such as solid lipid nanoparticles (SLNs) is an important aspect to be considered toward potential pharmaceutical applications, mainly for transdermal and intestinal administration of biotherapeutics.

A second goal of the project was to characterize biosurfactants produced by lactic acid bacteria (LAB) for their surface-active properties and anti-biofilm activity against oral Streptococci biofilms. Promising results are reported in **Chapter 5**, while on-going studies are evaluating the complex chemical structure of the biosurfactants mixture.

Due to the increasing demand for sustainable and environmentally friendly processes, the extraction of sugar-based fractions from natural resources and industrial/agricultural waste biomasses will be also exploited as source of molecules in alternative to the commonly employed synthetic techniques.

In the second part of this thesis complex polymeric materials have been synthesized and then employed in the formulation of drug delivery systems (DDS) intended for the treatment of different diseases.

Recent years have witnessed an intense research on polymeric materials for biomedical applications, mainly applied in the nanomedicine field for the formulation of innovative nanocarrier systems. Among the large variety of available polymers, only a limited number

have received so far regulatory approval for biomedical application. Among them, poly(ethylene glycol) (PEG), poly(lactic-*co*-glycolic acid), poly(DL-lactic acid) (PDLLA), polyacrilates and polymethacrilates, are few examples of the polymers approved by the US Food and Drug Administration (FDA). As results, an extraordinary variety of nanocarrier systems with different properties can be easily obtained by selecting the polymer with the desired characteristic.

Nanotechnology has been extensively applied to medicine for therapeutic, diagnostic and theranostic purposes.

Chapter 7 is dedicated to the design of an actively targeted nanocarrier system based on the methoxy poly(ethylene glycol)-b-(N-(2-benzoyloxypropyl) methacrylamide)) (mPEG-*b*-p-HPMA-Bz) block copolymer, to actively target multiple myeloma cells via a specific VLA-4 antagonist peptide. To this end, two different bioconjugation techniques were studied to synthetize a functionalized polymer available for the coupling with the VLA-4 peptide. In the first step maleimide chemistry was exploited, but an unexpected crosslinked product was obtained during the polymerization process, thus hindering the coupling with the sulphydryl group of VLA-4 peptide. Therefore, the heterobifunctional N-succinimidyl-3-(2-pyridyldithio)-propionate (SPDP) crosslinker was employed in the successful synthesis of PDP-PEG-*b*-p-(HPMA-Bz) functionalized block copolymer. PDP-PEG-*b*-p-(HPMA-Bz) polymer was then mixed with mPEG-*b*-p-(HPMA-Bz) block copolymer to prepare surface functionalized micelles, fully characterized for particle size and percentage of PDP group exposed on the micelles surface. The PDP group exposed on the micelles surface was therefore available for the conjugation with the VLA-4 targeting peptide. A preliminary targeted micellar system was developed and characterized in term of particle size and coupling efficiency.

Future studies will be focused on the optimization of the micellar system to increase the coupling efficiency. The optimized system will be then evaluated *in vitro* for its targeting efficiency on multiple myeloma cells.

Chapter 8 reports the formulation and characterization of a Carbopol-based hydrogel loaded with polymeric nanoparticles for vaginal delivery with prophilaxis purposes. Methoxy poly(ethylene glycol)-*block*-poly(lactide-*co*-glycolide) (mPEG-PLGA) based nanoparticles were incorporated into a 1.5% Carbopol 974 hydrogel at different concentrations and their influence of the rheological properties of the vehicle was studied by monitoring the storage modulus (G') and the loss modulus (G''). The strength of the gel was only slightly influenced

by the presence of nanoparticles. Metronidazole, widely employed for the treatment of vaginal bacteriosis, and Saquinavir mesylate, the first protease inhibitor FDA approved, were then selected to be loaded into the system. Release studies were performed with the model drug metronidazole, showing an increased solubility of metronidazole in presence of nanoparticles. At the same time the presence of nanoparticles did not negatively affect the release of metronidazole from the hydrogel.
Based on the preliminary results obtained in this study with metronidazole, employed as model drug, future studies will be focused on the evaluation of the release profile of saquinavir mesylate from both nanoparticles and Carbopol hydrogel loaded with nanoparticles. Moreover, the mucoadhesion properties of the system will be investigated.

The third part of this thesis, more specifically **Chapter 10**, focuses on the study of the rheological behaviour of selected polysaccharide dispersions, in function of various physiological parameters, such as concentration, pH and temperature. For this purpose, glucomannan, xanthan gum, tara gum, guar gum, konjac gum, and gellan gum were selected among the most commonly employed thickening agents derived from natural sources. The mechanical spectra of the different polysaccharides dispersions were then compared with the final aim of providing a comprehensive overview of their rheological properties, which can potentially help manufacturers operating in food and pharmaceutical fields in selecting the polysaccharides with the desired characteristics.

Appendix A

Curriculum vitae and list of Publications

Curriculum vitae

Laura Fagioli was born on the 11th of November 1990 in Fermo, Italy. She attended the high school "Liceo Scientifico T. C. Onesti" in Fermo, and she graduated with 100/100 in 2009. During the summer she participated at various English courses organized by certificated English schools in Malta (2007), Dublin (2008) and England (2010).

She received her master degree *cum laude* in Chemistry and Pharmaceutical Technology at University of Urbino in 2014, with a master thesis in Pharmacology. She obtained the licence to practise as pharmacist in 2014. In the same year, she started a PhD program in Pharmaceutical Technology at Univerity of Urbino, under the supervision of Dr. Luca Casettari. Her research focused on the synthesis and characterization of new materials for innovative pharmaceutical applications. In 2016, she was a visiting PhD student at the Department of Pharmaceutics, Utrecht University (The Netherlands), under the supervision of Prof. Dr. W.E. Hennink. During these nine months she worked on the development of targeted micelles for the treatment of haematological malignancies.

She participated in several educational courses and international conferences and schools. In 2017, she was awarded with a travel grant from EUCHIS Society to attend the XIII EUCHIS, VIII SIAQ (Seville, Spain).

During her PhD program, she acquired new personal skills in the field of innovative drug delivery systems (e.g. nanoparticles, micelles, microemulsions, capsules and films), polymer science (Ring opening polymerization (ROP) and Free radical polymerization (FRP)), rheology and several analytical techniques including HPLC, GPC, DLS, DSC, NMR and cell culture.

List of Publications

Publications included in this thesis

Perinelli D.R., Lucarini S., Fagioli L., Campana R., Vllasaliu D., Duranti A. and Casettari L. Lactose oleate as new biocompatible surfactant for pharmaceutical applications. *European Journal of Pharmaceutics and Biopharmaceutics* March **2018**, *124*, 55–62.

Lucarini S., Fagioli L., Campana R., Cole H., Duranti A., Baffone W., Vllasaliu D. and Casettari L. Unsaturated fatty acids lactose esters: cytotoxicity, permeability enhancement and antimicrobial activity. *European Journal of Pharmaceutics and Biopharmaceutics* **2016**, *107*, 88–96.
doi: 10.1016/j.ejpb.2016.06.022

Ciandrini E., Campana R., Casettari L., Perinelli D.R., Fagioli L., Manti A., Palmieri G.F., Papa S. and Baffone W.
Characterization of biosurfactants produced by Lactobacillus spp. and their activity against oral streptococci biofilm. *Applied Microbiology and Biotechnology* **2016**, *100,* 6767-6777.
doi: 10.1007/s00253-016-7531-7

Lucarini S., Fagioli L., Cavanagh R., Perinelli D.R., Campana M., Stolnik S., Lam J.K.W., Casettari L. and Duranti A.
Fatty acid lactose monoesters: synthesis, chemico-physical characterization and cytotoxicity studies. *Manuscript in preparation*

Rheological properties of selected polysaccharide gums as function of concentration, pH and temperature. *Manuscript in preparation*

Other publications

Campana R., Casettari L., Fagioli L., Cespi M., Bonacucina G. and Baffone W.
Activity of essential oil-based microemulsions against Staphylococcus aureus biofilms developed on stainless steel surface in different culture media and growth conditions. *International Journal of Food Microbiology* **2017**, *241*, 132-140.
doi: 10.1016/j.ijfoodmicro.2016.10.021

Martarelli D., Casettari L., Shalaby K.S., Soliman M.E., Cespi M., Bonacucina G., Fagioli L., Perinelli D.R., Lam J.K.W. and Palmieri G.F.
Optimization of melatonin dissolution from extended release matrices using artificial neural networking. *Current Drug Delivery* **2016**, *13, Issue 4,* 565-573.
doi: 10.2174/1567201812666150608101528

Perinelli D.R., Fagioli L., Campana R., Lam J.K.W; Baffone W.; Palmieri G.F., Casettari L. and Bonacucina G.
Chitosan and its exploited antimicrobial activity. *Submitted for publication.*

Oral presentation

Fagioli L., Perinelli D.R., Lucarini S., Duranti A., Jenny K.W. Lam, Stolnik S., Vllasaliu D. and Casettari L.
Lactose fatty acid monoesters: synthesis, characterization and toxicological evaluation
25-28 September 2017 – Advanced School in Nanomedicine – Pula, Sardinia (Italy)

Conference proceedings

Fagioli L., Campana R., Casettari L., Ciandrini E. and Baffone W.
Antimicrobial and anti-biofilm properties of different molecular weight chitosan on urinary catheters
31 May – 3 June 2017 – XIII EUCHIS, VIII SIAQ – Seville (Spain)

Casettari L., Fagioli L., Lucarini S., Lam J.K.W., Cavanagh R. and Stolnik S.
Sustainable sugar-based-surfactants for innovative drug delivery systems
FIP PSWC 2017, 6th Pharmaceutical Sciences World Congress, 21-24 May 2017

Fagioli L., Perinelli D. R., Logrippo S., Bonacucina G., Cespi M., Palmieri G.F. and Casettari L.
Mucoadhesive hydrogel loaded with nanoparticles for the vaginal release of saquinavir mesylate
8-13 April 2017 - International School of Nanomedicine-Course: New trend in Nanomedicine - Erice, Sicily (Italy)

Sestili M., Logrippo S., Cespi M., Ferrara L., Ganzetti R., Bonacucina G., Blasi P., Perinelli D.R., Fagioli L., Casettari L. and Palmieri G.F.
Clinical risk management related to drug therapy in dysphagic patients
June 2016 – 56° Simposio AFI - Rimini (Italy)

Perinelli D.R., Berardi A. , Bisharat L., Logrippo S., Fagioli L., Pavoni L., Ceccarelli G. and HlKhatib H.S.
Controlling tramadol release using zein based matrices
May 2016- A.It.U.N. Annual Meeting - Parma (Italy)

Casettari L., E. Soliman M., S.Shalaby K., Bonacucina G., Cespi M., Fagioli L., Perinelli D.R. and Palmieri G.F.
Noscapine loaded biodegradable nanoparticles to treat breat cancer
April 2016 - 10 th World Meeting on Pharmaceutics, Biopharmaceutics and Pharmaceutical Technologies – Glasgow (UK)

Perinelli D.R., Fagioli L., Logrippo S., Bonacucina G., Cespi M., Palmieri G.F. and Casettari L.
Formulation and characterization of a mucoadhesive hydrogel loaded with nanoparticles for the vaginal administration of metronidazole
Dicember 2015 - School of Nanomedicine – Bari (Italy)

Sestili M., Logrippo S., Palmieri G.F., Ganzetti R., Bonacucina G., Cespi M., Perinelli D.R., Casettari L. and Fagioli L.
Confronto fra le cinetiche di rilascio della pravastatina sodica in compresse semplici e in compresse disperse in acqua gelificata
October 2015 – XXXVI Congresso Nazionale SIFO – Catania (Italy)

Ciandrini E., Campana R., Manti A., Casettari L., Fagioli L., Papa S., Baffone W.
Activity of "excreted biosurfactants" of several lactic acid bacteria against streptococci oral biofilm
September 2015 - 33° Conferenza Nazionale di Citometria – Lucca (Italy)

Perinelli D.R., Bonacucina G., Pucciarelli S., Cespi M., Casettari L., Canala E., Logrippo S., Fagioli L. and Palmieri G.F.
Protein loading capacity, effect of pH and storage temperature on the stability of a water/ethyl oleate/span80-tween80 ternary system
June 2015 - 55° Simposio AFI – Rimini (Italy)

Cespi M., Bonacucina G., Casettari L., Perinelli R.F., Perinelli D.R., Logrippo S., Fagioli L. and Palmieri G.F.
Experimental factors affecting drug release from gel using VanKel (enhancer®) cells

June 2015 - 55° Simposio AFI – Rimini (Italy)

Grants

Travel grant from EUCHIS Society to attend the XIII EUCHIS, VIII SIAQ (Seville, Spain).

Acknowledgements

Caro Luca, sarebbe impossibile riassumere in poche righe questo percorso, potrei dire che è stata un'avventura straordinaria e ricca di emozioni. Urbino, Camerino, Utrecht e poi di nuovo Urbino, per completare il cammino lì dove tutto è iniziato. Grazie! Grazie per questi tre anni faticosi ma ricchi di soddisfazioni, grazie per aver creduto in me, grazie per i tuoi insegnamenti, grazie per le tue idee sempre propositive, grazie per il tuo entusiasmo e per la tua positività, grazie per la fiducia e l'autonomia che ci hai sempre lasciato nel laboratorio e infine grazie per avermi fatta crescere come persona e come "ricercatrice".

Vorrei ringraziare il Prof. Spadoni per avermi dato questa possibilità e per la disponibilità sempre dimostrata.

Ringrazio il Prof. Duranti e al Dr. Simone Lucarini per il supporto fornito con le loro conoscenze nel corso di questi anni.

I would also like to thank Dr. Diego Romano Perinelli, Dr. Raffaella Campana, Prof. Jenny K. W. Lam, Prof. Snjezana Stolnik, Dr. Campana, Dr. Driton Vllasaliu e Hannah Cole for the works done in collaboration. All of them have contributed to the realization of this PhD thesis.

I would like to acknowledge Prof. W.E. Hennink for giving me the opportunity to work at the Department of Pharmaceutics, Utrecht University, for nine months. Thank you for all the inspiring meetings and constructive discussions. You have been an extraordinary mentor for me.

A special thank goes to Aida, for the collaboration during the period spent at the Department of Pharmaceutics. Thank you for all the lunches together and thank you for sharing your bench with me.

I would also thank Prof. Schiffelers, Dr. Marcel Fens and Anil for all their support and their precious suggestions.

Cara nonna, sei stato il mio portafortuna più grande. La mia seconda mamma e la mia migliore amica. Grazie per avermi saputo ascoltare, sempre e comunque, anche a centinaia di chilometri di distanza; grazie per le lunghe chiacchierate su Skype, le sere d'inverno, quando riuscivi con un semplice sorriso ad incoraggiarmi. "Dai Laura, forza! Che diceva nonno? Mai arrendersi nella vita!", poche parole, ma preziose.

Un ringraziamento speciale va alla mia famiglia, per avermi supportata durante questo percorso. Caro babbo, grazie per avermi insegnato a rischiare e ad essere coraggiosa; cara mamma grazie per la tua ragionevolezza e la tua discrezione. Caro Francesco, grazie per avermi fatta arrabbiare nei momenti meno opportuni e avermi così fatto dimenticare per qualche istante le mie preoccupazioni.

Caro Claudio, semplicemente GRAZIE! Grazie per l'amore che mi regali ogni giorno. Grazie per essermi stato vicino quando ne avevo più bisogno, grazie per avermi sempre appoggiata in ogni decisione, grazie per aver condiviso con me i miei sogni. Questo traguardo lo stiamo tagliando insieme. Sei stato tu a suggerirmi di cambiare marcia quando era necessario, a rallentare quando mi vedevi stanca perché la salita era troppo ripida e ad approfittare delle discese per tirare un sospiro di sollievo. Con te vicino questo viaggio è stato più colorato.